EFFECT OF EPOXY COATING ON BOND AND ANCHORAGE OF REINFORCEMENT IN CONCRETE STRUCTURES

APPROVED BY
DISSERTATION COMMITTEE:

Dr. James O. Jirsa

Dr. John E. Breen

Dr. Ramon L. Carrasquillo

Dr. Michael E. Kreger

Dr. Harovel G. Wheat

EFFECT OF EPOXY COATING ON BOND AND ANCHORAGE OF REINFORCEMENT IN CONCRETE STRUCTURES

by

Bilal Salim Hamad, B.E.C.E., M.S.C.E.

DISSERTATION

Presented to the Faculty of the Graduate School of

The University of Texas at Austin

in Partial Fulfillment

of the Requirements

for the Degree of

DOCTOR OF PHILOSOPHY

THE UNIVERSITY OF TEXAS AT AUSTIN

December 1990

To my wife, Rouba
whose love and patience made this possible,
and to my parents.

ACKNOWLEDGEMENT

The author would like to express his deepest thanks to Dr. James O. Jirsa, chairman of the supervising committee, for his invaluable friendship, constructive criticism, continuous guidance, and helpful suggestions in planning, conducting, and reporting this research effort. The author will be always thankful to God for the good luck and great honor to have worked with such a fine professor and good man.

Sincere thanks are extended to Professors John Breen, Ramon Carrasquillo, Michael Kreger and Harovel Wheat for serving on the supervising committee.

The author would also like to express his gratitude for the assistance and willing cooperation of all the staff of the Phil M. Ferguson Structural Engineering Laboratory. Very special thanks are expressed to Jean Gehrke, who prepared all the drawings, and Sharon Cunningham, who typed the entire manuscript and brought it to its present form.

The assistance of Alan Dean, Alfredo E. Santolamazza, and Julio Jimenez in the preparation and testing of the specimens is greatly acknowledged. Appreciation is expressed for the very helpful advise, friendship, and assistance of all fellow graduate students, especially Hakim Bouadi and Sergio Alcocer.

The friendship and support of the Jirsas and the Burns throughout the time the author and his wife spent in Austin will be always remembered. Although the author and his wife passed through difficult and painful experiences in Austin (losing a baby in May 1989, getting burnt out of their apartment on July 4, 1990, and almost getting killed in a car accident by a reckless driver on

July 28, 1990), they will be always grateful to the University of Texas where the author fulfilled his father's dream.

There are no words the author could use to thank his father for his encouragement to come back to Austin, and his wife for making his father's dream a reality.

The study described herein was conducted at the Phil M. Ferguson Structural Engineering Laboratory and was sponsored by the Texas State Department of Highways and Public Transportation and the Federal Highway Administration under study number 3-5-88-1181.

Bilal Salim Hamad

The University of Texas at Austin
September, 1990

EFFECT OF EPOXY COATING ON BOND AND ANCHORAGE OF REINFORCEMENT IN CONCRETE STRUCTURES

Publication No. _____

Bilal Salim Hamad, Ph.D.
The University of Texas at Austin, 1990

Supervisor: James O. Jirsa

The objective of the research program was to assess the influence of epoxy coating on the bond characteristics of reinforcing bars and to develop or revise the existing recommendations for the design of splices and anchorage of straight and hooked epoxy-coated reinforcement.

In one phase of the study, eighty pullout specimens were tested to determine differences in stress transfer between normal mill scale uncoated and epoxy-coated bars using different bar sizes, coating thicknesses, bar deformation patterns, rib face angles, concrete strengths, and different levels of restraint to splitting. Results indicated that coating reduced the bond strength of reinforcing bars. However, the magnitude of the reduction in bond strength of coated bars relative to uncoated bars was independent of the level of the variables investigated.

In the second phase of the program, twelve beams with splices in a constant moment region were tested in negative bending. All bars were cast in a top bar position with more than 12 in. of concrete below the bars. Variables included bar size, bar spacing, and amount of transverse

reinforcement crossing the splitting plane in the splice region. Failure of all beams was governed 11by splitting of the concrete cover. The presence of ties in the splice region increased the deflection capacity of the beams and improved the bond strength of coated bar splices relative to uncoated bar splices. The improvement was independent of bar size or bar spacing.

In the third phase of the program, twenty-four specimens simulating typical beam-column joints in a structure were tested to compare the anchorage capacities of uncoated and epoxy-coated hooked bars. Variables included bar size, concrete strength, concrete cover, hook geometry, and the amount of transverse reinforcement through the beam-column joint. Epoxy-coated hooked bars consistently developed lower anchorage capacities and greater slips than uncoated hooked bars.

Using the results of this study and results of other tests on coated bars in the literature, the most comprehensive review of the effect of epoxy coating on structural aspects of coated bars was performed. Design equations were recommended for coated straight and hooked bars.

TABLE OF CONTENTS

LIST OF FIGURES

Figures **Page**

LIST OF TABLES

CHAPTER 1

OBJECTIVE AND SCOPE

1.1 Introduction

Since 1973, the use of epoxy-coated bars, in most types of reinforced concrete structures, has been steadily increasing as designers utilize coated bars to reduce or eliminate problems with structures in corrosive environments. Because of concern for the bond properties of epoxy-coated bars, several research studies were conducted that resulted in a basic understanding of the effect of epoxy coating on bond strength of reinforcing bars. Results of the previous studies led to modifications of the 1989 ACI Code (ACI 318-89)[1] for basic development length of an epoxy-coated deformed bar. For epoxy-coated bars with cover less than $3d_b$ or clear spacing between bars less than $6d_b$, the development length of an uncoated deformed bar is multiplied by a factor of 1.5. The factor is 1.2 for all other conditions. The product of the factor for top reinforcement, 1.3, and the factor for epoxy-coated reinforcement should not be greater than 1.7.

1.2 Objective

Previous research on the effect of epoxy coating on the bond strength of reinforcing bars, raised several questions concerning the bond behavior of epoxy-coated bars. The need for further research to give a better and more complete understanding of the bond problem of epoxy-coated bars was apparent. Of primary concern was the effect of bar deformation pattern, rib face angle, and epoxy-coated transverse reinforcement on the bond strength of coated bars.

1.3 Scope of the Test Program

To address questions concerning the bond behavior of epoxy-coated bars, the study reported here was divided into four phases.

1.3.1 Phase One - Fundamental Bond Studies. To study the fundamental bond characteristics of epoxy-coated bars, eighty pullout specimens were tested. In one group of specimens, to simulate the confining effect of concrete cover and transverse reinforcement, only the bottom surface of the anchored bar was embedded in the concrete and a uniformly distributed load was applied to the exposed half of the bar. The "confining" load was held constant until pullout failure occurred. In a second group of pullout specimens, the bar was fully embedded in the concrete.

The unit bond strength or the load-slip behavior of epoxy-coated bars was compared with that of companion uncoated bars. The following variables were considered:

(1) Bar Size: Two bar sizes, #6 and #11, reflect the range of coated bars most commonly used in corrosive environments. In bridge decks and slabs, where deicing salts may be used, #6 bars are common. Large bars, such as #11, are routinely used in supporting members located in marine or other corrosive environments.

(2) Coating Thickness: Bars were either uncoated (normal mill scale surface) or coated with epoxy of 5-, 8-, or 12-mil thicknesses. Five and 12 mils are the minimum and maximum coating thicknesses specified by ASTM A 775/A 775M-88a "Standard Specification for Epoxy-coated Reinforcing Steel Bars"[2]. Two pullout specimens had bars coated with latex paint to compare bond behavior of fusion bonded epoxy-coated bars with that of painted bars under identical conditions.

(3) Bar Deformation Pattern: Diamond, parallel (bamboo), and crescent patterns were studied.

(4) Rib Face Angle: The rib face angle is the angle that the bar rib or lug face makes with the longitudinal axis of the bar. Most reinforcing bars have an average rib face angle of 30 degrees regardless of the bar deformation pattern. Round bar stock (7/8-in. diameter) was machined to simulate #6 bars with parallel deformation pattern and three different rib face angles: 30, 45, and 60 degrees. A two-part liquid epoxy system, provided by the epoxy coating fabricator, was used to coat the bars.

(5) Degree of Confinement: In the pullout specimens, where the anchored bar was confined by a lateral load applied directly to the bar, lateral loads ranged from 5 to 20 kips. In other specimens, concrete covers of 2 and 3 in. were considered, and in some specimens additional restraint was provided by a #2 or 3# tie at the middle of the embedment length.

(6) Concrete Strength: Two nominal concrete strengths were used, 4000 and 8000 psi.

1.3.2 Phase Two - Effect of Transverse Reinforcement. To determine the effect of epoxy-coated transverse reinforcement on splices of epoxy-coated bars, twelve beams were tested with multiple splices in a constant moment region at the center of the beam. It has been well established that the bond strength of uncoated bars is substantially improved by adding transverse reinforcement. However, in previous studies of epoxy-coated bars, the effect of transverse reinforcement was not investigated.

Companion specimens were identical except for bar coating. The prime variable was the amount of transverse reinforcement in the splice region. Other variables included bar spacing and bar size (#6 and #11).

1.3.3 Phase Three - Hooked Bars. To determine the anchorage characteristics of epoxy-coated hooked bars, twenty-four specimens simulating typical beam-column joints in a structure were tested. The 1989 ACI Code (ACI 318-89)[1] does not address this subject, and there is no information in the literature.

The test specimen was designed to simulate the anchorage of two hooked beam bars in a reinforced concrete column. Companion uncoated and epoxy-coated hooked bars were tested. The variables included: bar size (#7 and #11), concrete strength (3000, 4000, and 8000 psi), amount of side concrete cover normal to the plane of the hook (2-7/8 in. in most specimens, 1-7/8 in. in two tests), hook geometry (90- and 180-degree hooks), and amount of transverse reinforcement (column ties) in the beam-column joint.

1.3.4 Phase Four - Design Recommendations. The objective of this phase was to develop (or revise the existing) design recommendations for splice length and development length of straight and hooked epoxy-coated bars.

It is important to note that the analysis of the test results of the research program was done with reference to:

(1) Other research on epoxy-coated bars;

(2) Procedures for determining the ultimate bond capacity of coated and uncoated bars; and,

(3) Existing ACI design procedures for epoxy-coated bars in anchorage or development conditions.

CHAPTER 2

CORROSION PROTECTION METHODS FOR REINFORCING BARS

2.1 Introduction

Corrosion of reinforcing steel in concrete is the most common cause of premature deterioration of reinforced concrete structures. The corrosion problem continues to drain resources of owners of reinforced concrete structures in both the public and private economic sectors in the United States and throughout the world.

Reinforced concrete is inherently a durable and maintenance free material under normal conditions. The calcium hydroxide solution in set cement is an alkaline solution with a pH of 12.5. In this alkaline solution a protective iron oxide film forms over the reinforcing steel rendering it passive and well-protected against corrosion. The stability of the film depends on the maintenance of a certain minimum pH value and under such conditions, access of oxygen will not cause corrosion.

In the northern tier of states, contemporary society's demands for a "dry pavement" for highway travel requires heavy and continual application of chloride salts on highway and bridge surfaces to hasten the thawing of ice and snow and to prevent moisture from freezing. In coastal states, the salt spray from the ocean covers concrete highways, bridge decks and substructures, and marine structures. The process of corrosion in a bridge deck begins with the deicing salt, in solution as ice melts, penetrating to the level of the reinforcing bars. The presence of the chloride ions reduces the alkalinity of the solution and raises the pH value required to stabilize the passive oxide film on the reinforcing bars to a value which may exceed that of a saturated calcium hydroxide

solution. The protective film is then disrupted leading to corrosion of steel by electrochemical action.

2.2 Corrosion Mechanism

Corrosion is an electrochemical process associated with the presence of anodic and cathodic areas arising from inhomogeneities in the steel surface or non-uniformities in the chemical or physical environment afforded by the surrounding concrete. For corrosion to occur three things must be available, including an anode-cathode couple, the maintenance of an electric circuit where the contaminated salt water solution is the electrolyte, and the presence of moisture and oxygen. The flow of current in the steel from an anodic to a cathodic area, in the presence of moisture and oxygen, results in the production of hydroxyl ions at the cathode. As the hydroxyl ions migrate to the anode, they react with ferrous iron and form hydrous iron oxide:

At the anode: $4Fe + 4Cl^- \rightleftharpoons 2Fe^{++} + 4Cl^- + 4e^-$

At the cathode: $2H_2O + O_2 + 4e^- \rightleftharpoons 4OH^-$

Then at the anode: $2Fe^{++} + 4OH^- \rightarrow 2Fe(OH)_2$

This is followed by the oxidation of the ferrous ion to ferric state and the formation of expansive rust products:

$$2Fe(OH)_2 + H_2O + \frac{1}{2}O_2 \rightarrow 2Fe(OH)_3$$

The overall reaction of conversion of iron to rust may be stopped by retarding the cathodic process and the rate at which oxygen reaches the cathode therefore controls the velocity of the anodic reaction. Therefore, any factors which control the cathodic reactions will likewise control the overall corrosion process.

Upon expansion, rust products occupy a greater volume than the original steel and large pressures build up between the concrete and steel surface. As a result, the concrete-steel bond will be broken and spalling starts. With concrete cracking, more chloride ions enter to attack the bars and facilitate the formation of Fe^{++} ions and deterioration of the reinforced concrete structure is accelerated.

2.3 Corrosion Protection Methods

There are several methods to protect reinforced concrete structures against corrosion.

2.3.1 Increased Concrete Cover. The purpose for increasing the depth of the concrete cover over the reinforcing steel is based upon the theory that it takes longer for the chlorides to seep through a greater distance. However, if the chlorides are present in the concrete, then increased depth does not help against corrosion. Also, the susceptibility of steel reinforcement to corrosion is independent of concrete cover in cracked concrete since corrosion initiates at crack locations and corrosive agent (chloride) penetration is more a function of crack width than cover[3]. Another problem is that increasing the thickness of the slab is costly and requires change in the structural design.

2.3.2 Membranes and Overlays. The function of membranes and overlays is to provide an impervious layer through which the chlorides cannot pass. One technique is to place a water-proof membrane on the concrete deck which is then covered by a thin, asphalt wearing course. Another technique is to add a special, high quality, impermeable, and properly consolidated low water-cement ratio concrete topping overlay on a new deck.

The problem with membranes and overlays is that if the concrete contains chlorides, corrosion attack will not be prevented. Also, membranes are installed at the construction site and are weather dependent. Any cracks, breaks, or bubbles in the membrane will allow the chloride bearing waters to seep into the concrete and allow the corrosion to proceed.

2.3.3 Sealers. Sealing the concrete surface by a proper surface coating such as linseed oil or bituminous coating is another method to prevent the absorption of exterior salts and other aggressive substances into the concrete. Furthermore, the sealing will reduce the access to oxygen and will reduce the absorption and evaporation of moisture during changes in the weather conditions and thus promote more uniform moisture content in the concrete. Bituminous coatings are usually not effective unless they are preceded by applications of some kind of primer coat. Primers such as coal tar or asphalt base impregnate the pores and hairline cracks. A bituminous solution or a hot bituminous membrane is then applied over the primer followed by a coat of white wash for thermal protection.

Although impervious surface coatings have displayed a certain degree of effectiveness, they have a tendency to maintain high moisture contents within the concrete and thereby reduce the electrical resistivity[4]. These coatings also seem to somehow increase the ratio of cathodic areas to anodic areas and as a result, localize and intensify corrosion. Therefore, the effectiveness of surface coatings is certainly questionable and in many cases may do more harm than good.

2.3.4 Anodic Inhibitors. Anodic inhibitors contain materials such as alkalies, phosphates and chromates which form either iron salts or a ferric oxide film on the anodic surface of the reinforcing bar thus preventing ferrous ions from entering the solution[5]. Such anodic inhibitors are effective only in high concentrations. If they are added in insufficient quantities, the corrosion reaction may be locally intensified. On the other hand, high concentrations may adversely affect the concrete.

2.3.5 Polymer Concrete. The function of the polymer in concrete is to form a dense impermeable material which will prevent the movement of chlorides through concrete. The polymer is applied at the construction site and is weather dependent. Moisture and temperature are critical to the success of the system. Any cracks in the concrete structure or voids in the concrete itself will lead to failure of the protection system and to corrosion attack.

2.3.6 Cathodic Protection. Cathodic protection is a preventative maintenance procedure which uses electrochemical principles to reduce the corrosion rate in an existing structure. In cathodic protection an external current is supplied to the corroding metal. The current makes all the reinforcing bar cathodic and eliminates electrolytic attack of the steel and repels dissolved corrosion salts such as chlorides. Two methods are used to supply the external current[6]. In the first method the protected metal is made the cathode (current acceptor) by connecting it to a more active metal, the anode (a sacrificial metal, such as zinc or magnesium, with a more negative open circuit potential). The method requires that the anodes be replaced as they are deteriorated. In the second and more common method, an external direct current power source supplies the current. The first method is the sacrificial anode system and the second is the impressed current system.

Cathodic protection has been applied to relatively few existing ordinary reinforced and prestressed concrete structures installed in severely corrosive environments. Applications include reinforced concrete pipelines, prestressed concrete tanks, and reinforced concrete foundations for storage tanks.

Although the method has proven effective, there are many problems involved in applying it to reinforced concrete structures. One problem is that the entire system of reinforcement must be electrically continuous for effective protection. A lack of complete electrical connection of one or more bars would set up isolated corrosion systems causing intensified attack under the action of impressed current[4]. Electrical continuity can be accomplished by bonding the steel reinforcement together. To provide bonding of a complex reinforcing steel network geometry after construction can be expensive and difficult to accomplish. Another problem is that the cathodic metallic circuit should have a low uniform resistivity so that large potentials are not required to provide adequate currents[5]. It is doubtful then if cathodic protection can be used more economically than a program of routine repair of the structure as corrosion defects appears[4,5].

2.3.7 Galvanized Bars. Galvanizing the reinforcing steel is a hot dipping process where the reinforcing bar is immersed in an aqueous preflux solution of zinc ammonium chloride at a controlled temperature between 840 and 850° F. A metallurgical bond of zinc-iron alloy is developed between the zinc coating and the steel product which it protects. The galvanized coating is tough due to its layered structure. Galvanizing provides cathodic protection to the base steel. The zinc sacrifices itself to protect any exposed steel.

Hot dip galvanized steel has been used in northern bridge decks, southern bridge decks, wharves and piers, off-shore oil drilling and storage structures, water conduits, building facades, and many other applications. Many installations have been made which mix untreated and galvanized reinforcing steel. However, laboratory results, reported by Clear[7], indicate that such mixing does not enhance the sacrificial life of the galvanized bar. Clear indicated that galvanizing the top mat of reinforcing steel in reinforced concrete slabs, exposed to corrosive environments, was very detrimental and resulted in corrosion rates twice as high as those for all untreated steel slabs. Undesirable galvanic cells between dissimilar metals are established at every point the different bars are in contact. It is more economical to consider galvanizing all the reinforcing bars in the structures rather than to go to the extra time, work and cost required to isolate the dissimilar metals. Even bar supports should be either galvanized or plastic coated.

One very important disadvantage to the use of galvanized bars is that since galvanizing is sacrificial, it has a finite life. Kobayashi and Takewaka[8] reported on experimental studies carried out over a period of four years to compare the performance of epoxy-coated bars with galvanized bars and uncoated bars subjected to severely corrosive environments. The exposure tests were carried out using small reinforced concrete beam specimens set in an environment subject to salt water spray at all times and may be considered as a splash zone which is extremely severe with respect to corrosion of reinforcing bars. Exposure was started at concrete ages of 30 to 50 days and continued for a maximum of three years. Before exposure, flexural cracks at the tension fiber were

induced at midspan of the beam specimens and the crack width was about 0.2 to 0.3 mm. Test results of the galvanized bar specimens showed that the zinc corrosion protection layer over the reinforcing steel was reduced considerably by chloride corrosion. Specimens with concrete cover of 20 mm, after one year of exposure, showed white zinc hydroxide precipitate $Zn(OH)_2$ covering roughly the entire surface of the reinforcing bar. Scattered locations of red rust could be seen. It appeared that the zinc coating continued to decrease roughly in proportion to the exposure period. After three years of exposure for specimens with concrete cover of 20 mm, it was clearly seen that where cracks were largest in width, practically all of the zinc coatings disappeared due to corrosion.

Kobayashi and Takewaka's tests indicate that the zinc coating of galvanized reinforcing bars is reduced in a chloride environment and that corrosion protection using galvanizing can be maintained only for a certain limited length of time.

2.3.8 Fusion-Bonded Epoxy Coating. Of all the methods of corrosion protection possible, fusion-bonded epoxy coating often offers the best combination of protection, ease of use, and economy. The purpose of the epoxy coating is to prevent chlorides from reaching the steel surface. The material is applied to the reinforcing bar at a coating plant away from the job site. Therefore, it is not weather dependent and will not cause construction delays. Cracking in the concrete, allowing penetration of chloride bearing water, should not be a factor because the coating provides a barrier at the bar surface where corrosion is initiated.

2.3.8.1 Experimental and Field Investigations. In the early 1970's, the Federal Highway Administration officials determined through field evaluation, as well as other testing, that the premature deterioration of concrete bridge decks was caused primarily by the corrosion of reinforcing steel in chloride contaminated concrete. In quest of a solution, FHWA launched a comprehensive research program and the National Experimental and Evaluation Program (NEEP) Project No. 16 was born. The first step in this project was to contract the National Bureau of Standards to evaluate the feasibility of using nonmetallic organic coating materials, especially

epoxies, to protect steel reinforcing bars from corrosion. The program included the selection of promising coating materials, evaluation of physical and chemical durabilities of coatings, assessing the potential protective qualities of the coatings, and determining the bond strength between coated reinforcing bars and concrete.

Epoxy powder coatings, studied in the NBS project, showed low permeability to chloride ions, flexibility, and abrasion and impact resistance[9]. The bond strength of coated reinforcing bars was determined from pullout tests. With average film thicknesses between 5 and 11 mils, powder epoxy-coated bars developed bond strengths which were only slightly less than bond strengths for uncoated bars. The NBS study indicated that the electrostatic spray method was the most effective application method in producing thin films free of defects and uniform in thickness. The study concluded that powder epoxy-coated reinforcing bars could be incorporated in bridge design without compromising the structural integrity of the bridges[9].

A lengthy program of investigations followed the NBS study. This involved in-house slab research, experimental installations joint-ventured with states, field evaluations, and verification of the practicality of epoxy-coated reinforcing bars. The results demonstrated the effectiveness of epoxy coatings. Rapid implementation on a nation-wide basis followed. Epoxy-coated reinforcing bars have since had full status FHWA approval as a cost-effective corrosion prevention system for concrete bridge deck construction. In 1983, the FHWA final report on accelerated testing of epoxy-coated reinforcing bars in chloride contaminated slabs proved the long-term effectiveness of epoxy-coated bars in preventing corrosion[10]. In comparing concrete slabs having upper and lower mats of bare steels with slabs having an upper mat of epoxy-coated steel and a lower mat of bare steel, and assigning a life of one year to the all-bare steel slabs, twelve years of exposure of the epoxy-coated steel would be required to consume an equal amount of the epoxy-coated iron. For slabs having upper and lower mats of epoxy-coated steel, forty-six years of exposure would be required

to consume an equal amount of iron in the upper mat of the epoxy-coated steel compared to slabs that have both mats of bare steel[10].

In the Kobayashi and Takewaka corrosion tests[8], epoxy-coated reinforcing steel demonstrated far superior corrosion protection effects compared with galvanized reinforcing steel in a marine splash zone. In beam specimens having bars with epoxy coating thickness of 100 μm ($\cong$ 4.0 mils), the bars were not completely protected against corrosion. There were several locations along the reinforcing bars where the steel bases were corroded. At the corroded locations the coating films separated slightly. However with coating thickness of 200 μm($\cong$ 8.0 mils) the condition of the reinforcing bars was more or less sound after three years of exposure. The corroded areas were very small and corrosion losses were so slight that they could be ignored compared with untreated bars and galvanized bars. Kobayashi and Takewaka concluded that a coating thickness of at least about 200 μm ($\cong$ 8.0 mils) was necessary for complete corrosion protection of reinforcing bars.

In December 1984, Poston[3] reported on a durability test program intended to study the performance of transversely prestressed slabs relative to nonprestressed slabs when subjected to an aggressive corrosion-producing environment. Sixteen prestressed and eight nonprestressed slab specimens were cracked before exposure to saltwater solution. The nonprestressed reinforcement in all slabs was either uncoated or epoxy-coated. Exposure testing consisted of subjecting each specimen to one wet-dry test cycle every fourteen days. The number of cycles ranged from eight to fourteen for the different specimens. Test results indicated that transverse prestressing reduced corrosion risk by limiting crack width. Also, visual inspection of the reinforcement after testing indicated that corrosion of nonprestressed reinforcement initiated and occurred at the location of flexural cracks. The extent of corrosion was much greater for uncoated than for epoxy-coated reinforcement. Epoxy coating provided the reinforcement with satisfactory protection from chloride-

induced corrosion up to a threshold level of 12 lbs. Cl^- per cubic yard of concrete. However, in some specimens with very heavy chloride levels at crack locations, it appeared that the epoxy coating chipped off the bar deformations which resulted in very light surface corrosion at these locations. As a result of his study, Poston[3] recommended the use of epoxy-coated reinforcement in conventially (nonprestressed) reinforced concrete bridge decks exposed to deicing salts or located in marine environments.

In January 1987, Weyers and Cady[11] reported on a study undertaken to evaluate the corrosion protection performance afforded by epoxy-coated reinforcing steel in concrete bridge decks after approximately ten years of service in the state of Pennsylvania. Twenty-two concrete bridge decks, eleven constructed with bare reinforcing steel and eleven constructed with epoxy-coated reinforcing steel, were visually inspected. In addition, an in-depth evaluation of two decks containing bare steel and two decks containing epoxy-coated steel from the eleven decks was conducted. The visual inspection indicated that 40% of the decks containing bare reinforcing steel were in the initial stage of deterioration, but none of the decks containing epoxy-coated reinforcing steel were deteriorated because of corrosion of the steel. The in-depth study revealed more extensive deterioration of the decks containing bare steel, but no deterioration in those containing epoxy-coated steel.

To date, there are no public reports of significant corrosion failure of epoxy-coated reinforcing bars in applications within the northern states. There has been, nevertheless, increasing evidence that epoxy-coated reinforcing steel is corroding and creating structural damage in the substructure of bridges in the Florida Keys[12, 13]. The Florida Department of Transportation underwent a two-year program to thoroughly inspect four bridges in 1986 out of concern about the area's salinity level. The bridges were built between seven and ten years ago, for service in an environment with high average temperatures and unusually saline sea water containing typically 2.6% chlorides. The bridges have epoxy-coated bars in both the superstructures and the

substructures. The two-year program was completed in July 1988 and inspectors found corrosion in three out of the four structures. The bridge that did not exhibit corrosion had a thicker concrete cover over the reinforcing bar, from 4-6 in., compared to 2-3 in. on the others. The results raised questions about corrosion in epoxy-coated reinforcing bars bent after coating.

Because of the severity of the deterioration observed, the Florida agency has been sponsoring a research project at the University of Southern Florida on corrosion in high chloride environments. The investigation was established to determine the effect of different surface and mechanical conditions on the corrosion behavior of reinforcing steel, namely, the degree of bending, epoxy damage, surface condition of the steel, presence of cracks in the concrete, and the manufacturing process[14]. The results of experiments in progress proved that fabrication bending resulted in loss of adherence of the epoxy, and corrosion was observed in the resulting debonded areas. Cracking of the concrete cover appeared to accelerate the initiation of active corrosion but there was not enough evidence to determine its long-term effect on the corrosion of epoxy-coated bars. The effect of other variables tested necessitates longer exposure times. The tests are still in progress.

The Florida Department of Transportation decided to specify coating after fabrication for the new Dodge Island bridge in Miami. The additional cost should be "negligible", about 2-3% of the total cost, according to Florida DOT. Many coaters now have the capability of coating prefabricated reinforcement steel and the problems of cracked coatings in the bent areas could be eliminated.

2.3.8.2. Applications. During 1973, the first bridge deck was constructed with the use of epoxy-coated reinforcing bars. The 15-span, steel multi-girder and plate girder bridge is located in West Conshohocken, a suburb of Philadelphia, in the state of Pennsylvania. Four of the fifteen spans were constructed with epoxy-coated reinforcing steel and the remaining spans were constructed with conventional untreated reinforcing steel. One by one, more states started

specifying and using epoxy-coated bars. As of 1988, forty-six of the fifty state highway agencies have specified the usage of epoxy-coated bars for new and replacement bridge decks.

Initially, almost all of the epoxy-coated bars were used in bridge decks in the snow belt states of the North. Their problem was directly related to the increasing amounts of deicing chemicals being used in conjunction with the "dry pavement" policy. Eventually, states in coastal areas, such as Florida, began using large quantities of coated reinforcing bars in all bridge elements exposed to sea water or sea spray. Their problem was related to the marine environment and perhaps, to some degree, chlorides present in the aggregates.

Use of epoxy-coated reinforcing bars has spread to nearly all types of structures where concrete is exposed to a corrosive environment. Epoxy-coated bars are used in decks, shafts and foundations, piers, bent caps, and other bridge supporting elements. Other applications include sewage and water treatment plants, cooling towers and other parts of power plants, chemical plants, parking garages, refineries, subways, reinforcement for earth retention, and in continuously reinforced concrete pavements. Total usage of epoxy-coated bars in the United States in 1987 was an estimated 180,000 tons (approximately 5% of total reinforcing bar consumption).

Since its first usage, and despite tremendous inflation, the price of epoxy powder coatings applied to reinforcing bars has dropped considerably and the quality of the product has been improving. The cost-benefit ratio is now more attractive than ever before. With respect to parking garages, for example, the cost of epoxy-coated bars is estimated to be 1% or less of the entire project cost. Needless to say, the cost of reconstruction within the confines of a parking garage is considerable. Higher control construction costs are rapidly offset by reduced maintenance and repair. In "frost belt" states using deicing salts, current practice is to coat the top mat of bars only (top two orthogonal layers of bars). This practice is mainly responsible for the cost-effective advantage of using epoxy-coated bars as a corrosion protection system in a bridge deck. In a salt-

water sea coast location, all of the bars in the deck, as well as those in the other parts of the bridge, might have to be epoxy-coated.

2.3.8.3 Materials and Coating Process. An epoxy coating is formed by combining an epoxy resin with the appropriate curing agent, pigments, catalysts, flow control agents, etc., to achieve the desired application and performance characteristics. Fusion bonded means that the coating achieves adhesion as a result of a heat-catalyzed chemical reaction. The reaction is irreversible. Unlike thermoplastic coatings, if heated after the coating is cured, fusion bonded epoxy coating will not soften.

The epoxy coatings that were first tested and approved by the Federal Highway Administration for use on reinforcing steel were materials designed and used to protect pipelines in chloride environments[9]. It was not until 1976 that a fusion bonded epoxy coating specifically designed for reinforcing steel was put on the market. The epoxy material and the coating process involved with the first bridge in Pennsylvania in 1973 were required to meet the "Interim Specification for Epoxy Coated Reinforcing Steel" which was distributed by the Federal Highway Administration for the NEEP Project No. 16[15]. The specification, which was based on the results of the NBS study[9], included the FHWA acceptance requirements for epoxy coating materials and epoxy-coated bars. After several years of use, these requirements evolved into ASTM A775-81, "Standard Specification for Epoxy-Coated Reinforcing Bars"[16]. The 1981 ASTM specification has been modified to reflect changes in the state-of-the-art of the coating process. Many sates have written individual specifications to meet their own needs. Currently, the generally requirement for epoxy-coated reinforcing bars are covered under ASTM A775/A775M-88a specification[2].

The approved coating system consists of the following four stages:

(1) Surface Preparation: The surface of the bar is cleaned by abrasion blasting with steel grit or steel shot to a near-white metal finish where 95% of the surface is

white metal. The abrasive blasting develops an anchor pattern on the bar which will provide physical adhesion of the coating in addition to the chemical adhesion.

(2) Material Application: The clean bar is heated with a non-contaminating heat source to approximately 450° F. The heat source should be clean and even. After the bar has been raised to the proper temperature, it is automatically conveyed through preheating and powder application units where the powdered coating is electro-statically sprayed evenly on the bar surface at a controlled temperature. Normally the product is applied to a thickness of 5 to 12 mils. After the powdered coating melts, it flows into the anchor pattern of the bar surface and solidifies again after a given period of time, called the gel time.

(3) Material Curing: After the epoxy product becomes a solid, it must continue to be exposed to heat until proper cross-linking of the coating system has been achieved. The time from melting to final cross-linking is called the cure time. After the cure time has been reached, the coated bar is passed through a cooling process, typically a water quench bath.

(4) Material Inspection: The coating surface of the reinforcing bar is electrically inspected for cracks and pinholes by using a 67.5-volt D.C. holiday detector and a wet search electrode. Holidays are repaired using a two-part liquid epoxy system.

The ASTM A775/A775M-88a[2] requirements for acceptance of the epoxy coating material include tests for chemical resistance, resistance to applied voltage, chloride permeability, bond strength to concrete, abrasion resistance, impact and hardness. Acceptance is also based upon evaluations of the coating thickness, continuity, and adhesion to the bar. Coating thickness is required to be 5 to 12 mils. Thickness tests are required on a minimum of two bars of each size from each production shift. A minimum of fifteen measurements are taken approximately evenly

spaced along the test bar. At least 90% of the measurements are to be within the specification limits for acceptance. The maximum amount of coating damage due to fabrication is limited to 2% of the surface area of each bar. Damaged areas larger than 0.1 sq. in. must be repaired with a compatible patching material.

CHAPTER 3

THE BOND PROBLEM OF EPOXY-COATED REINFORCING BARS

3.1 Review of Bond

3.1.1 General. Bond is the interaction of the two materials, steel and concrete. It is one of the most important prerequisites of reinforced concrete construction. It is necessary for composite action of the two materials.

In reinforced concrete structures, the external load is very rarely applied to the reinforcement. Forces are transformed to the steel only through the surrounding concrete. The transfer of load or stress from the concrete to the steel is made possible by the shear stresses along the surface between the concrete and the embedded steel bar. The higher the surface shear or resistance to relative motion or slippage under stress, the more effective will be the interaction between the concrete and the steel. The resistance to slippage is called bond or bond stress. Without any bond stress the embedded steel would be practically useless. Inherent in the analysis of a reinforced concrete section is the assumption that the strain in the concrete and the steel is equal at the location of the steel. This implies perfect bond between the concrete and steel.

To ensure ductility, bond between the steel and concrete must be maintained until the bars develop yield. ACI Building Code Requirements for Reinforced Concrete (ACI 318-89)[1] ensure ductility by specifying a required development length or splice length for all bars. The development length required is based on the bond strength the bars are capable of developing. Bond strength is dependent on bar size, depth of cover, spacing between bars, transverse reinforcement surrounding the bar, concrete strength, and position of the bars when cast.

Two modes of failure are commonly recognized: a splitting failure and a pullout failure. In both cases it is assumed that the main component of bond is the reaction of the bar deformations

against the surrounding concrete. The reaction force is inclined at an angle β to the axis of the bar, as shown in Figure 3.1. If the stress component parallel to the axis of the bar is u, then the stress component of the bond force perpendicular to the axis of the bar is u tan β. The stress component u tan β exerts a radial pressure on the surrounding concrete. If the cover on the bars or the spacing between bars is relatively small, then the radial pressure will cause splitting (Figure 3.2). The restraint against splitting is dependent on the tensile capacity of the concrete across the splitting plane. Additional restraint may be provided by transverse reinforcement across the splitting plane.

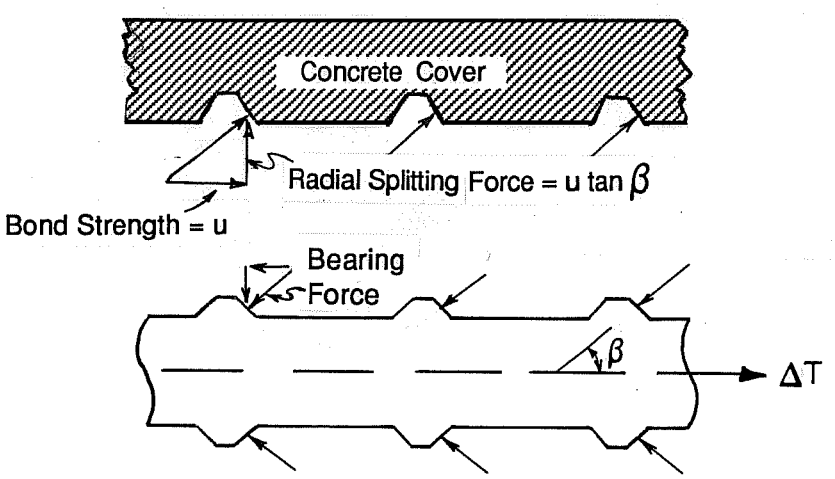

Figure 3.1 Inclination of bond stresses

If the cover and spacing between bars is great enough, or if enough transverse reinforcement is provided, a splitting failure cannot develop and a pullout failure will occur or the bar will yield. In a pullout failure, the concrete between bar deformations is sheared from the surrounding concrete (Figure 3.3). The bond strength for a pullout failure is primarily dependent on the strength of concrete in direct shear. A pullout failure is more likely for small bars or large bars where the depth of cover is large or transverse reinforcement is provided around the bars.

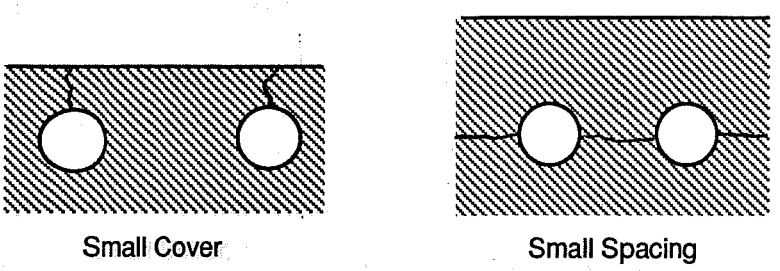

Figure 3.2 Splitting failure

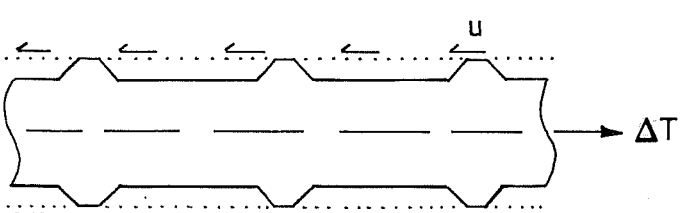

Figure 3.3 Bond stresses in pullout failure

In both splitting and pullout failure modes the contribution of adhesion to the bond between the bars and concrete is ignored.

3.1.2 Previous ACI Code Bond Provisions. The 1963 ACI Code (ACI 318-63)[17] computed the bond strength for a splitting failure as $u = 9.5\sqrt{f'_c}\ /d_b$. The bond strength was considered independent of the depth of cover. The bond strength for a pullout failure was taken

as 800 psi. In 1971, the ACI Code (ACI 318-71)[18] requirements were changed to specifying a required development or splice length. The required length was based on the same bond strengths outlined above. The 1983 ACI Code (ACI 318-83)[19] provisions for bond and development length used the same basic development length, ℓ_{db}, as the 1971 code where:

$$\ell_{db} = 0.04\, A_b f_y / \sqrt{f'_c} \geq 0.0004\, d_b f_y \tag{3.1}$$

The basic development length, ℓ_{db}, was derived from the 1963 provisions for bond strength by equating the bond strength over the surface of the bar to the total force in the bar at yield.

$$u\, \pi\, d_b\, \ell_{db} = A_b f_y$$

The actual strength of steel is usually greater than the nominal strength. To ensure a ductile failure rather than a splitting failure, the development length was required to develop 125% of the nominal yield strength. If the bond strength for a splitting failure is $u = 9.5\sqrt{f'_c}\,/d_b$, then:

$$(9.5\sqrt{f'_c} / d_b)\, \pi\, d_b\, \ell_{db} = A_b(1.25 f_y)$$

$$\ell_{db} = 0.04 A_b f_y / \sqrt{f'_c}$$

For a pullout failure the bond strength was taken as 800 psi:

$$(800)\, \pi\, d_b \ell_{db} = A_b(1.25 f_y)$$

$$\ell_{db} = 0.0004 d_b f_y$$

For splices in tension, ACI 318-83 Section 12.15 provided for lap splice lengths in terms of ℓ_{db}. The development length was modified by a factor of 1.0 to 1.7 depending on the percentage of steel to be spliced and the stress to be developed.

3.1.3 Orangun, Jirsa and Breen Empirical Approach. The 1971 ACI code value of ℓ_{db} was independent of cover and spacing between bars. However, it has been recognized for some

time that the bond strength is dependent on the depth of cover and the spacing between adjacent bars or splices in addition to the transverse reinforcement crossing the splitting plane.

Orangun, Jirsa and Breen, in a research project conducted for the Texas State Department of Highways and Public Transportation in 1974, used a nonlinear regression analysis of over 500 available and well-documented tests on bond[20]. The analysis was based on a failure hypothesis which assumes that the bond strength is controlled by the lesser of the minimum cover or one-half the clear spacing. The three modes of failure shown in Figure 3.4, which are copied from Ref. [20], were described previously[21].

The radial stress component of the reaction of the bar deformations against the surrounding concrete, u tan β (Figure 3.1), can be regarded as water pressure against a thick-walled cylinder having an inner diameter equal to the bar diameter and a thickness c, the smaller of the clear bottom cover c_b, or one-half the clear spacing, c_s, between two adjacent bars or splices. The capacity of the cylinder depends on the tensile strength of the concrete. When this is exhausted, splitting cracks form in the concrete. With $c_b > c_s$, splitting will occur through the side cover and the plane of the bars or splices and will result in a "side split failure." If $c_s > c_b$, then splitting will occur through the bottom (or top) cover followed by splitting across the plane of the bars or splices and through the side cover. The result is a "face-and-side split failure." If $c_s >> c_b$, a "V-notch failure" forms with longitudinal cracking through the bottom (or top) cover followed by inclined cracking (see Figure 3.4).

As a result of their study, Orangun, et al.[20], developed an empirical equation to compute the bond strength of an anchored deformed bar or a splice. The equation accounts for the variation in depth of cover, the spacing between adjacent bars or splices, and the transverse reinforcement:

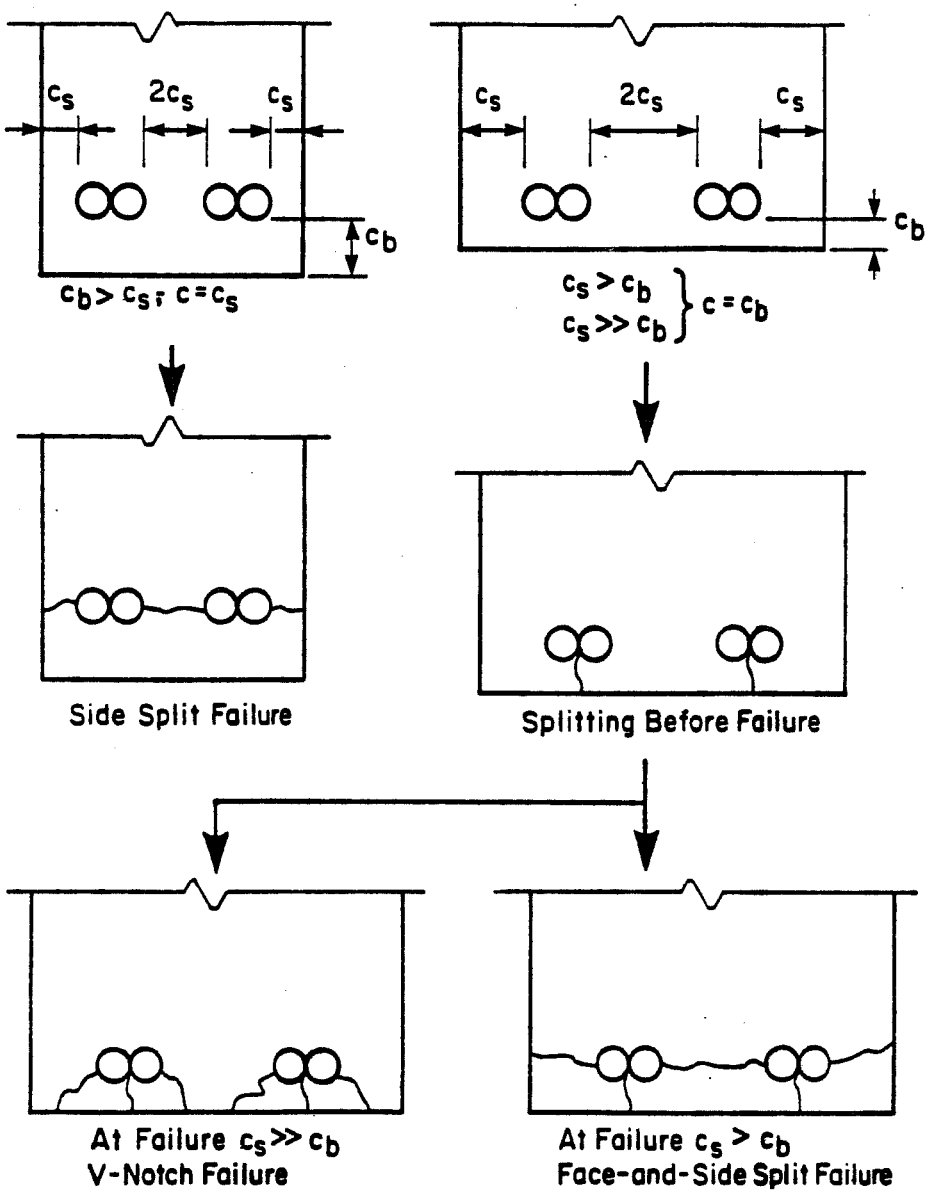

Figure 3.4 Splitting bond failures, Orangun et al.[20]

$$u = u_c + u_{tr}$$
$$= \left[1.2 + 3\frac{c}{d_b} + 50\frac{d_b}{\ell_s} + K_{tr}\right]\sqrt{f'_c}, \qquad K_{tr} = \frac{a_{tr}f_{yt}}{500sd_b} \tag{3.2}$$

Assuming a uniform distribution of bond stress along a bar with area A_b, the length needed to develop a steel stress f_s is determined in the following manner. Equating the tensile force on the bar with the total bond force on the surface area of the bar yields:

$$\ell_s \pi d_b u = A_b f_s$$

Combining this with Eq. (3.2) and solving for ℓ_s:

$$\ell_s = \frac{d_b\left[\frac{f_s}{4\sqrt{f'_c}} - 50\right]}{1.2 + 3\frac{c}{d_b} + \frac{a_{tr}f_{yt}}{500sd_b}} \tag{3.3}$$

In Eq. (3.2) the bond strength of the anchored bar or splice increases as the cover to bar diameter ratio increases. However, it is obvious that at some cover to diameter ratio the mode of failure will not involve splitting. For large c/d_b values, direct pullout could occur with the bar deformation shearing off the concrete between the lugs. Orangun, Jirsa, and Breen agreed that since most of the data on which the empirical equation, Eq. (3.2), was based were limited to c/d_b values of 2.5 or less, they suggested that c/d_b be limited to 2.5.

Moreover, Orangun, et al.[20], indicated that a "V-notch" type of failure was observed in tests with large bar spacings. This is due to the fact that with large side or clear spacing, the concrete outside the "minimum" cylinder surrounding the bar tends to restrain splitting across the plane through the anchored bars or splices. Based on the available data, Orangun et al. proposed

for $c_s/(c_b d_b)$ values exceeding 6 a reduction factor of 0.7 on the development length required by Eq. (3.3).

The factor reflecting the effect of transverse reinforcement in Eq. (3.2) is $K_{tr} = a_{tr} f_{yt}/(500sd_b)$ where $a_{tr} f_{yt}$ represents the force that can be developed at a stirrup location. The effectiveness of a stirrup is inversely proportional to the spacing of the stirrups and diameter of the bar enclosed. The area of transverse reinforcement, a_{tr}, was defined as shown in Figure 3.5. Orangun, et al., stated that the available test results indicated that when a number of bars were contained within a single hoop, the transverse reinforcement, as expected, would not be as effective in restraining the splitting at interior bars. The transverse reinforcement factor also shows that the greater the transverse restraint relative to the bar diameter, the greater the strength or increment of stress over that provided by the concrete cover alone. However, beyond a certain point transverse reinforcement will no longer be effective since the mode of failure will not then involve splitting. Based on examination of tests with extremely heavy transverse reinforcement, Orangun, et al., suggested that K_{tr} be limited to 3.

3.1.4 Current ACI Code Bond Provisions. To reflect recent research, the 1989 ACI Code (ACI 318-89)[1] contains revised specifications for computing the development length of deformed bars. The changes consider the factors of clear cover and clear spacing which have been shown to influence bond. The basic development length was copied from the 1971 Code[18]. A limitation on the value of concrete strength, $\sqrt{f'_c} \leq 100$ psi, was added because "research on development of bars in high strength concretes is not sufficient to substantiate a reduction beyond the limit imposed."

$$\ell_{db} = 0.04 A_b f_y / \sqrt{f'_c} \geq 0.03 d_b f_y / \sqrt{f'_c}, \quad \sqrt{f'_c} \leq 100 \tag{3.4}$$

The basic development length is modified by several factors "to reflect the influence of cover, spacing, transverse reinforcement, casting position, type of aggregates, and epoxy coating."

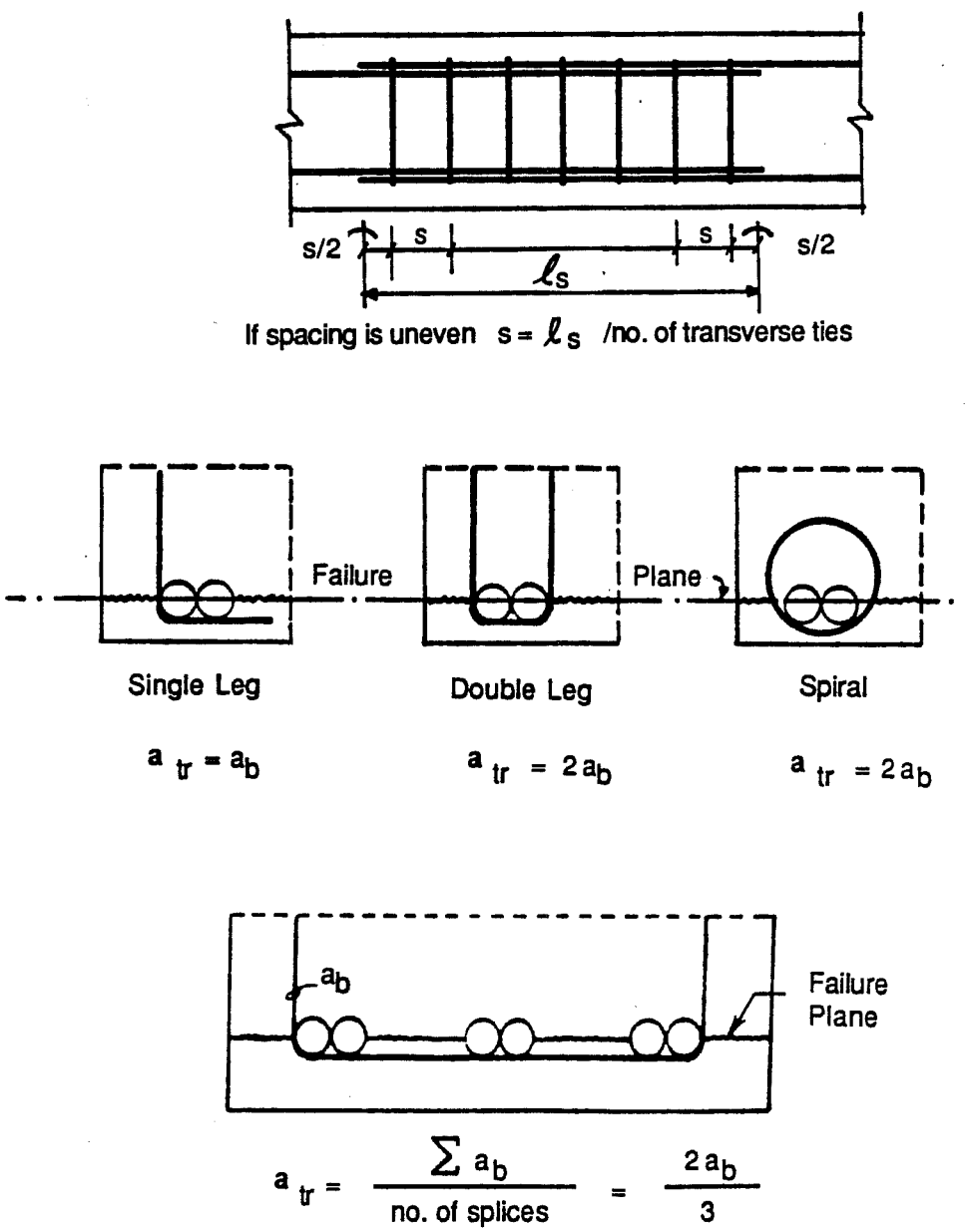

Figure 3.5 Definition of transverse reinforcement, a_{tr}, Orangun et al. [20]

Again a lower limit is imposed on the modified development length, ℓ_d, to cover the possibility of a pullout failure if restraint to splitting is provided. The limit, $0.03\, d_b f_y \sqrt{f'_c}$ with $\sqrt{f'_c} \leq 100$ psi, different from the one provided by the 1971 Code, is "the minimum length required to yield a bar that is subject to pullout."

For splices in tension, ACI 318-89 Section 12.15 provides for lap splice lengths in terms of the modified development length ℓ_d. The modification factor of excess reinforcement given by Section 12.2.5 is excluded in computing ℓ_d since the splice specifications already reflect any excess reinforcement at the splice location. To obtain the splice length, the modified development length, ℓ_d is multiplied by a factor of 1.0 or 1.3 depending on the percentage of steel to be spliced and the stress to be developed.

3.2 Current Code Specifications for Epoxy-Coated Reinforcement

Due to the importance of development and splices of reinforcement in analysis and design of reinforced concrete structures, bond between concrete and steel is essential. A very important consideration in the use of epoxy-coated reinforcing bars is the effect of epoxy coating on the strength of bond between reinforcing bars and concrete.

Most codes prohibit any non-metallic coatings from being applied to reinforcing bars which may decrease the bond capacity by preventing adhesion between the bar and the concrete. ACI 318-89, Section 7.4.1[7], states that bars should be free from non-metallic coatings, mud, or oil which may decrease the bond capacity. Epoxy coatings, however, are permitted by Section 7.4.1. Also, Section 3.5.3.7 states that epoxy-coated reinforcing bars should comply with "Specifications for Epoxy-Coated Reinforcing Steel Bars" (ASTM A 775).

Before the Federal Highway Administration approved the use of epoxy-coated bars in the early 1970's, little attention was devoted to epoxy materials as protective coating for reinforcing bars because of the supposition that the coated bars had unacceptable bond strength[22]. However, since

1973 epoxy-coated reinforcing bars have been used in nearly all types of structures to provide protection against corrosion which leads to premature deterioration of concrete structures. Before the 1989 ACI Code (ACI 318-85)[1] was issued, epoxy coating was used without much concern about the bond characteristics of epoxy-coated bars. The available test data then indicated that the reduction in bond strength of epoxy-coated bars was not excessive[23, 24].

Based on more recent studies of the bond strength of epoxy-coated bars [25], the 1989 ACI Code, Section 12.2.4.3[1], modified the basic development length ℓ_{db} of a deformed bar to account for epoxy coating. For bars with cover less than $3d_b$ or clear spacing between bars less than $6d_b$, the development length is multiplied by a factor of 1.5. The factor is 1.2 for all other conditions. The Commentary to Section 12.2.4.3 argues that "when the cover or spacing is small, a splitting failure can occur and the anchorage or bond strength is substantially reduced. If the cover and spacing between bars is large, a splitting failure is precluded and the effect of epoxy coating on anchorage length is not as large." Moreover, Section 12.2.4.3 specifies that in the case of a top bar, defined as a horizontally cast bar with more than 12 in. of concrete cast below the bar, the product of the factor for top reinforcement, 1.3, and the factor for epoxy-coated reinforcement should not be greater than 1.7.

The available test data, on which the current ACI Code specifications are based, are limited. Because of the extensive use of epoxy-coated bars in highway structures and other reinforced concrete applications, there is an immediate need to clarify bond and anchorage requirements for such bars in design codes.

3.3 Previous Research

3.3.1 National Bureau of Standards Tests. The first study on epoxy-coated bars was done at the National Bureau of Standards by Mathey and Clifton[23] and was reported in 1976. A total of twenty-three epoxy-coated bars with varying thicknesses and different methods of coating

application were compared to five uncoated bars in concentric pullout tests. The reinforcing bars tested were all #6, Grade 60 bars with two deformation patterns, barrel and diamond. The majority of the coating thicknesses ranged from 1 to 11 mils with two bars having a coating thickness of 25 mils.

The pullout specimens were concrete prisms (10-in. x 10-in. x 12-in.) with a reinforcing bar embedded concentric with the longitudinal axis. Therefore, the bars had an embedment length of 12 in. The average concrete compressive strength was 6170 psi. To minimize splitting, the concrete was reinforced with a cylindrical cage of 2-in. x 2-in. - 12/12 welded wire fabric. Instrumentation included one dial gage to measure free-end slip and two dial gages to measure loaded-end slip versus applied load.

The specimens were tested in a 200,000-lb. capacity universal electro-mechanical testing machine which placed the concrete prism in compression on the face at which the bar was pulled. Loads were applied in increments of 2000 pounds to the reinforcing bars until failure occurred either by yielding of the steel or excessive slip between the bar and concrete was attained. A schematic view of the pullout specimen is shown in Figure 3.6.

The values of all calculated bond stresses were adjusted for the differences in concrete strength by multiplying them by the ratio of the square root of the average concrete strength, 6170 psi, to the square root of the specimen's concrete strength.

Based on the comparison of critical bond strengths, it was concluded that the bars with a coating thickness from 1 to 11 mils developed acceptable bond strengths. "The average value of applied load corresponding to the critical bond strength in the nineteen pullout specimens with the bars having epoxy coatings 1 mil - 11 mils thick was 6% less than for the pullout specimens containing the uncoated bars." No relationship was observed between the bar deformation pattern and bond behavior. The critical bond strength refers to the lesser of the bond stress corresponding to a loaded-end slip of 0.01 in. or that corresponding to a free-end slip of 0.002 in. This critical

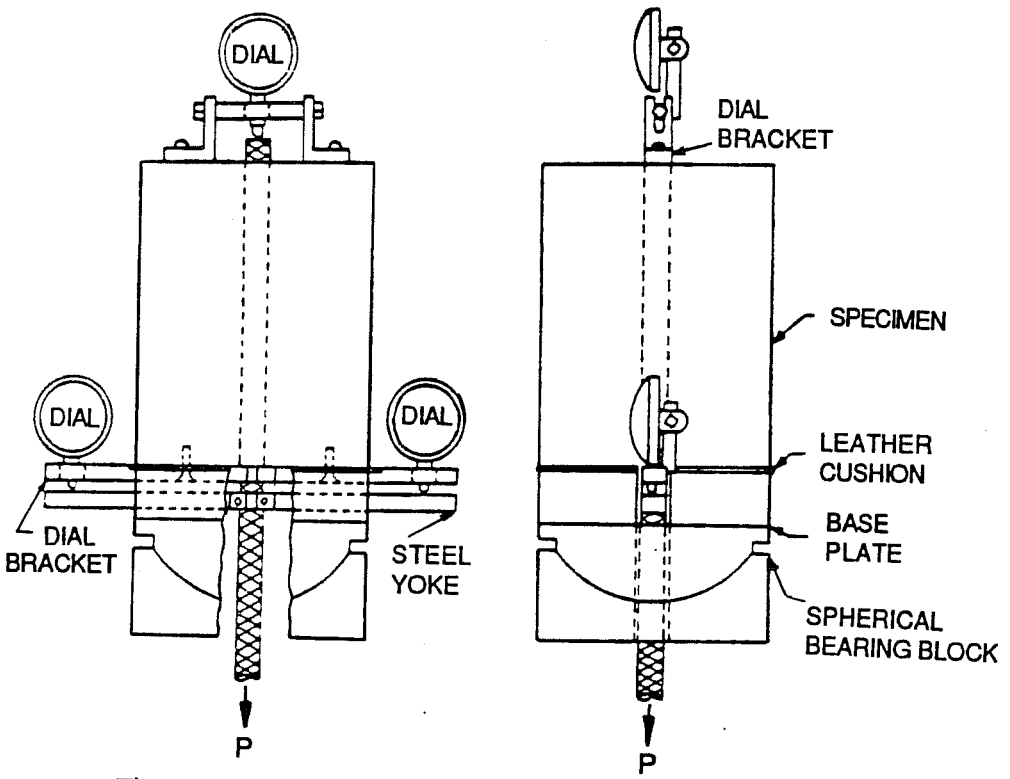

Figure 3.6 Schematic of pullout specimen, Mathey and Clifton [23].

bond strength does not give the actual bond capacity of the bar. Another conclusion of the NBS study was a recommendation that additional tests of flexural members be carried out to confirm results of the pullout tests.

The method by which coated bars were compared to uncoated bars is questionable. The critical bond strengths of the coated bars with a coating thickness from 1 mil to 11 mils were averaged and compared to the average critical bond strength of the uncoated bars. The bars used had two different deformation patterns and were not necessarily from the same heat of steel. Therefore the comparisons made were not between identical bars, but between two groups of randomly selected bars.

All of the uncoated bars as well as the coated bars with 1- to 11-mil coating thicknesses yielded in the tests. Based on this it was again concluded that bars with a coating thickness of

approximately 10 mils or less have essentially the same bond strength as uncoated bars. A bond failure occurred in only two of the epoxy-coated bars: those with a coating thickness of 25 mils. Based on this it was recommended that bars with an epoxy coating thickness greater than 10 mils not be used.

Without a bond failure, the actual bond strength capable of being developed cannot be determined. As stated in the article[23], when the stress in the steel exceeded yield considerably, the test was halted. It is not known at what steel stress a bond failure would have occurred. Certainly if the embedment length was long enough or if enough cover was provided, a bar with any coating thickness could develop yield. However, this would give no information as to the relative bond strengths between coated and uncoated bars.

Requirements for bond strength of epoxy-coated bars in ASTM A 775/A 775M-88a "Standard Specification for Epoxy-Coated Reinforcing Steel Bars"[2], were based on the NBS study. The bond strength to concrete is evaluated using two coated and two uncoated, uncleaned #6 bars in pullout test with concrete prisms identical to those used in the NBS study. For acceptance of the coating, ASTM A775/A 775M-88a requires that the mean critical bond strength for epoxy-coated bars be not less than 80% of the mean strength for uncoated bars.

3.2.2 North Carolina State University Tests. Another study was conducted at North Carolina State University and reported by Johnston and Zia[24] in August 1982. Epoxy-coated bars were compared to uncoated bars with companion specimens under different criteria. Six slab specimens, three with coated and three with uncoated #6 bars, were used to compare strength, crack width, and crack spacing. Forty beam end specimens were used to compare strength under both static and fatigue loadings. The beam end specimens contained either #6 or #11 bars. Three different embedment lengths were investigated for each bar size. Constants for the tests included reinforcing steel grade and production heat, concrete mix, and epoxy coating type and thickness.

The slab specimens were 6 ft. long, 2 ft. wide and 8-1/2 in. deep. Longitudinal reinforcement consisted of two layers of three #6 bars at 8 in. The slab details are shown in Figure 3.7. The slab specimens were tested basically as simply supported beams with the tensile surface on top to simplify measurement of cracks. The loading details provided a development length of 35 in.

Results of the slab specimens showed little difference in crack width and spacing, deflections or ultimate strengths between coated and uncoated bar specimens. The epoxy-coated bar specimens failed at approximately 4% lower loads than the uncoated bar specimens.

The simple support setup of the slab specimens may have influenced the crack width and stiffness comparisons. The moment gradient was very steep and cracks could not form randomly as they would within a constant moment region. Also, the 35-in. development length, provided for the #6 bars, is more than two times the required length by the current ACI Code Specifications. Consequently, the tests resulted in flexural failures rather than in bond failures so the actual bond strengths could not be measured.

The beam end specimens were flexural type specimens in which the load was applied directly to the reinforcing bar. The specimens were supported in such a way as to simulate beam behavior (Figure 3.8). The beams contained either a #6 bar with a cover to bar diameter ratio of 3.10, or a #11 bar with a cover to bar diameter ratio of 1.46. Transverse reinforcement was provided by #3 stirrups spaced at 3 in. or at 6 in. as shown in Figure 3.9. Loads were generally applied in increments of 2.0 kips to the #6 bars and in increments of 7.5 kips to the #11 bars until failure occurred. After application of each load increment, slip measurements were recorded using 0.0001-in. dial gages. Loading was terminated either upon pullout, in the case of short embedment specimens, or upon reaching 125% to 140% of the bar yield stress in the case of long embedment lengths.

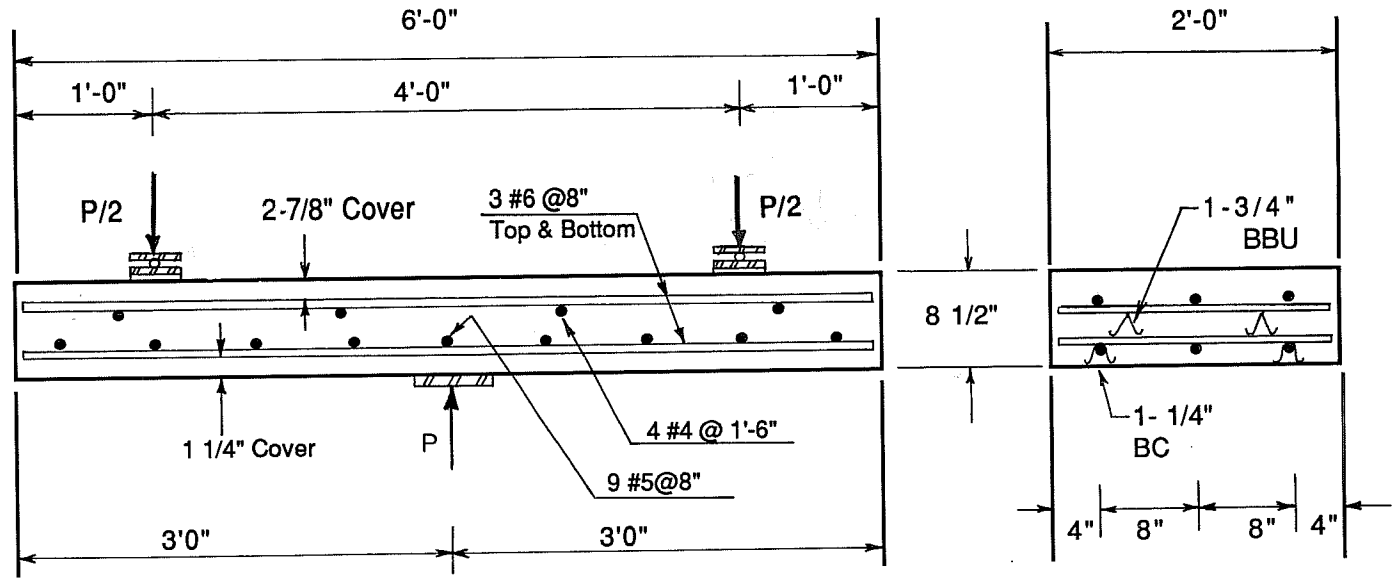

(a) Longitudinal Section

(b) Transverse Section

Figure 3.7 Slab specimen test setup and reinforcement details, Johnston and Zia [24].

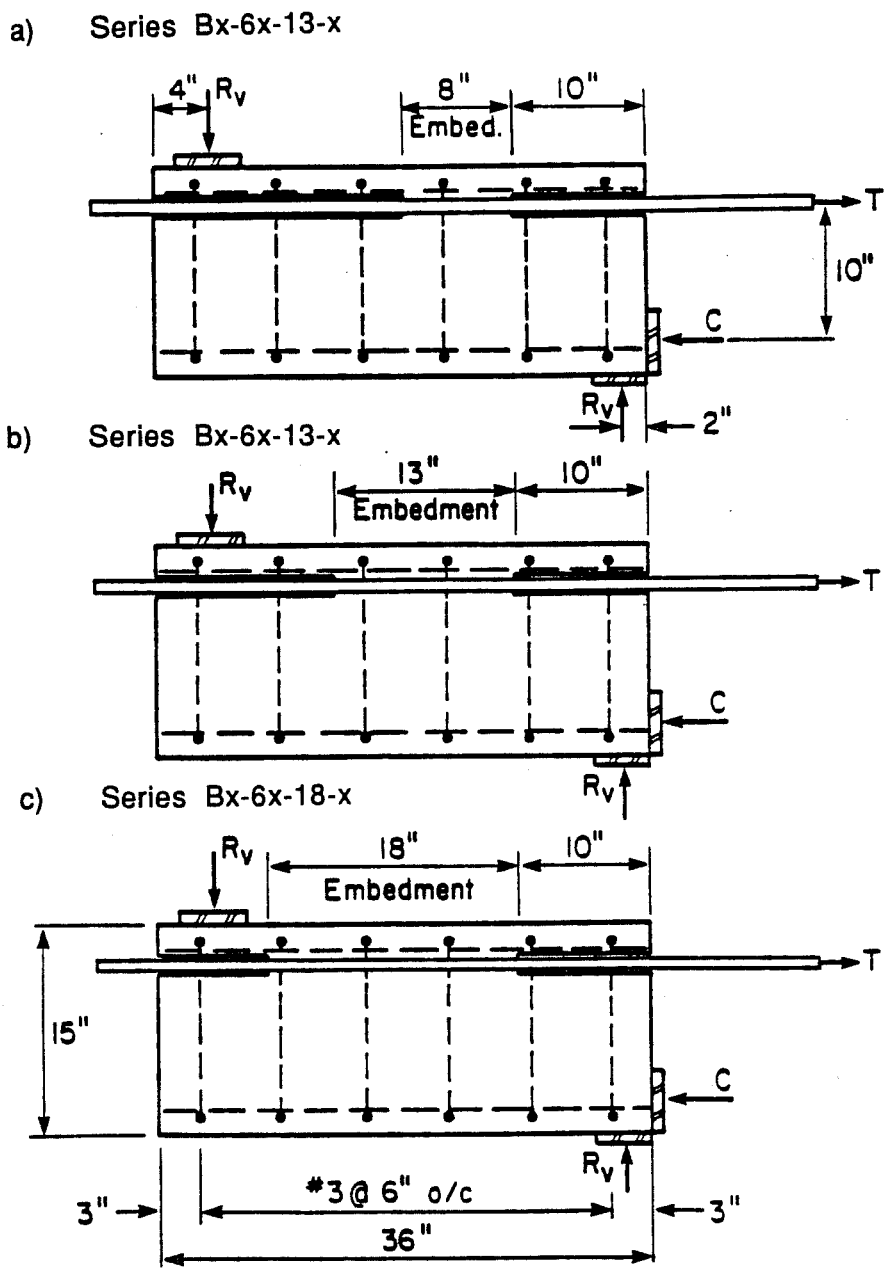

Figure 3.8 Beam end specimens, Johnston and Zia[24].

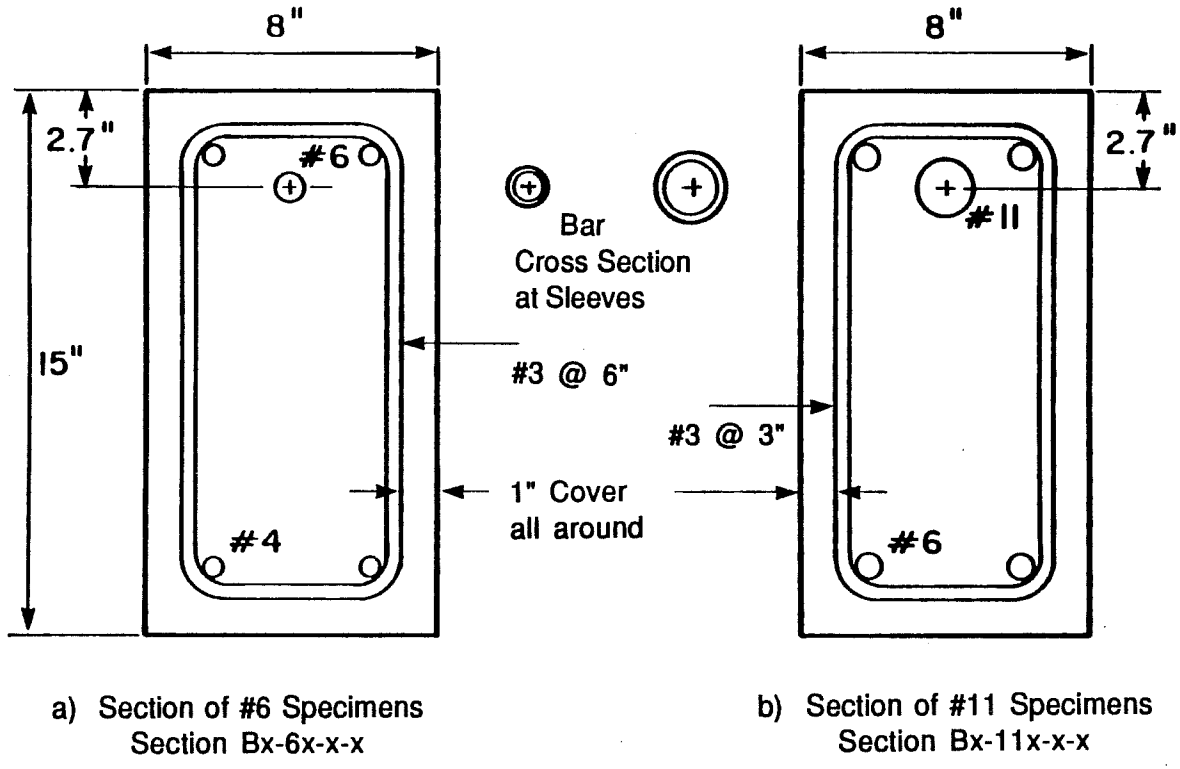

Figure 3.9 Beam cross sections, Johnston and Zia [24].

Two primary types of cracks occurred during the beam tests. The first was flexure shear cracking and the second was bond splitting where a longitudinal crack formed in the cover of the top face directly above the test bar. However, the modes of failure were modified because splitting was restrained by transverse reinforcement. Specimens with epoxy-coated bars developed bond splitting cracks at significantly lower load levels and flexural cracking at somewhat lower load levels than comparable specimens with uncoated bars. Larger slips were recorded for epoxy-coated bar specimens than uncoated bar specimens for the same level of stress. As the embedment length increased, the free-end and loaded-end slip corresponding to a given bar stress decreased in all beam specimens tested. The performance of epoxy-coated bar specimens relative to uncoated bar specimens was not influenced by changing the embedment length. The relative performance was also not affected by changing the bar size from #6 to #11.

Based on the few beam tests which ended in a pullout bond failure, the uncoated bar developed 17% more bond strength than epoxy-coated bars. This corresponds to the epoxy-coated bars developing about 85% of the bond strength of uncoated bars. Results of the fatigue tests showed similar results as for the static tests. To account for the reduction in bond strength due to epoxy coating, it was recommended that the development length be increased by 15% when using epoxy-coated reinforcing bars.

3.3.3 The University of Texas Exploratory Studies. In an exploratory research program at the University of Texas[25], sponsored by the Reinforced Concrete Research Council and the Concrete Reinforcing Steel Institute, twenty-one beam specimens were tested to determine the bond strength of epoxy-coated bars. The influence of epoxy coating on member stiffness and on the spacing and width of cracks was also studied. The variables were bar size, concrete strength, casting position, and coating thickness. In each of nine series, a different combination of variables was examined, but the only variable within a series was the coating thickness on the bars.

Each series included a control specimen with uncoated bars and a specimen with bars having a 12-mil coating. In some series a third specimen with bars having a coating thickness of 5 mils was cast. The minimum (5-mil) and maximum (12-mil) coating thicknesses are specified by ASTM A775/A 775M-88a[2]. Specimens were cast with either #6 or #11 bars. Three nominal concrete strengths (4, 8 and 12 ksi) were used. Seventeen specimens were cast with bars in the top position (more than 12 in. of concrete cast below bars) and four specimens were bottom cast.

Test specimens were beams with three bars in tension, all spliced at the center. The splice lengths were selected so that the bars would fail in bond before reaching yield. Lengths were based on the empirical equation developed by Orangun, et al.[20]. The beams were tested in negative bending with a constant moment region in the middle of the specimen. With the tensile surface at top, marking and measuring cracks was easier. All the bars of each size were from the same heat of steel and had a diamond deformation pattern. No transverse reinforcement was provided in the splice region so that splitting rather than a pullout would govern failure. Beam dimensions and details are shown in Figures 3.10 and 3.11. Test parameters and results for each specimen are shown in Table 3.1

Load increments of about 1 kip were applied until the beam was cracked along the length of the constant moment region. Thereafter load was applied at increments of approximately 2 kips. At each load stage deflections were read using 0.001-in. dial gages at the load point and at the center of the beam. Also, cracks were marked and crack widths were measured.

In each test, the mode of failure was a splitting failure at the splice region. Test results showed that epoxy-coated bars with average coating thicknesses above 5 mils, developed 67% of the bond strength of uncoated bars with a standard deviation of 9% (see Table 3.1). The reduction in bond was consistent for the range of variables considered in the study. Therefore, epoxy coating was the only variable which caused reduction in bond strength.

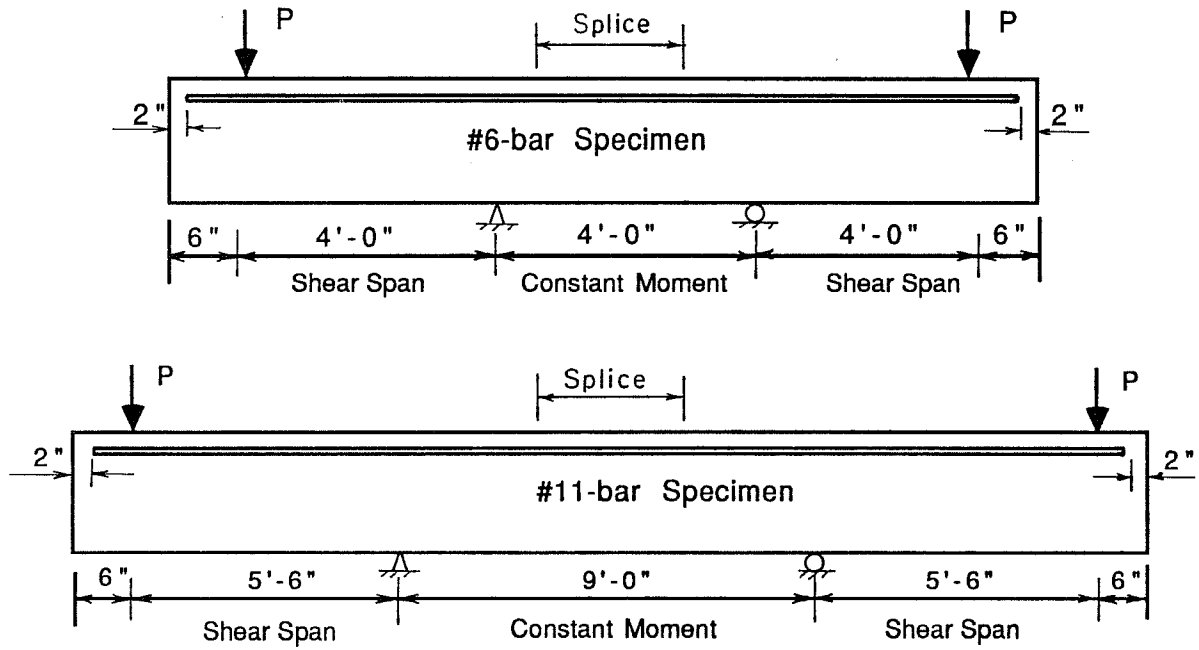

Figure 3.10 Test setup and beam dimensions, Treece [25].

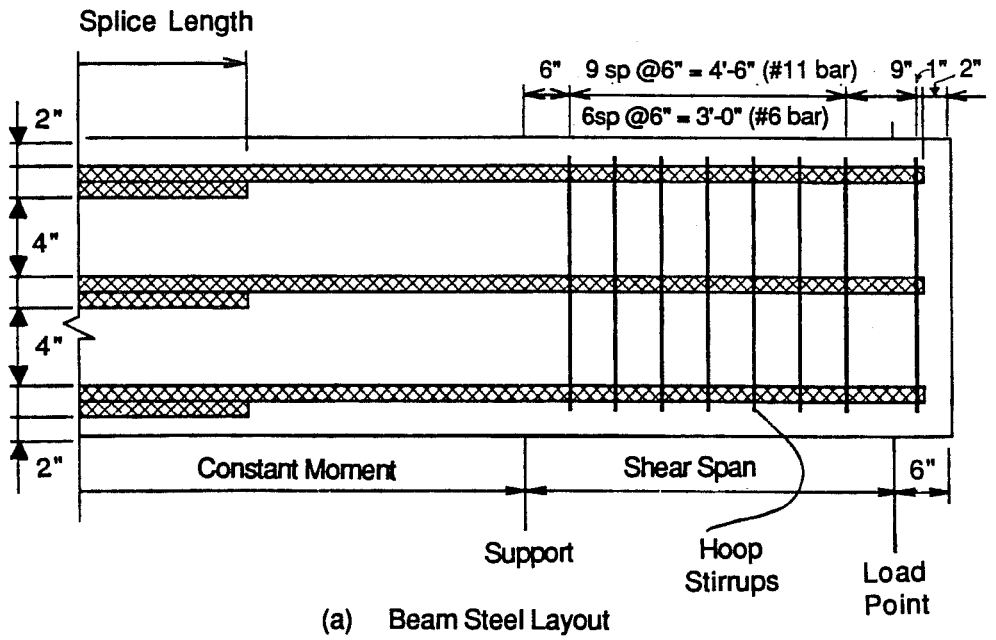

(a) Beam Steel Layout

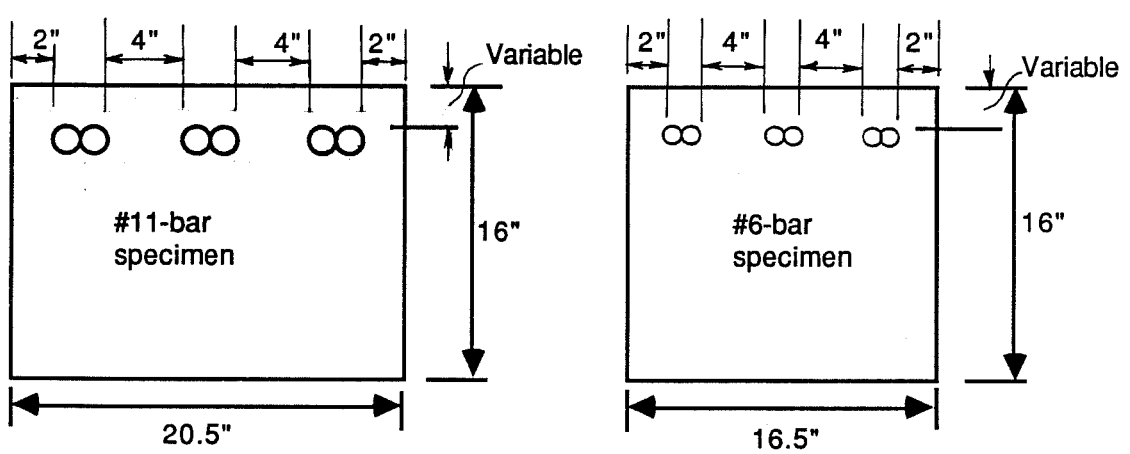

(b) Beam Cross-sections

Figure 3.11 Beam reinforcement details, Treece[25].

Treece compared the test results with the predicted theoretical bond stresses using the empirical equation (3.2) developed by Orangun, et al.[20]:

$$u = \left[1.2 + 3\frac{c}{d_b} + 50\frac{d_b}{\ell_s} + K_{tr}\right]\sqrt{f'_c}, \qquad K_{tr} = 0$$

Comparison was also made with the predicted bond stresses using Eq. (3.1) of the 1983 ACI Code (318-83)[19] assuming $\ell_s = \ell_{db}$:

$$\ell_s = 0.04A_b f_y / \sqrt{f'_c} \geq 0.0004 d_b f_y$$

combining the above equation with $u\pi d_b \ell_s = A_b f_y$:

$$u = 7.96\sqrt{f'_c} / d_b \leq 625 \text{ psi} \tag{3.5}$$

The measured bond strength, u_t, for each specimen was divided by its theoretical or ACI predicted bond strengths, Eq. (3.2) and Eq. (3.5), to obtain bond efficiencies. The computed bond efficiencies are shown in Table 3.2.

By plotting the end deflection versus the load for each specimen, Treece proved that little difference in flexural behavior was noted between specimens with uncoated and coated bars. The cracks outside the splice length in the constant moment region were compared. Specimens with epoxy-coated bars had fewer cracks but the width of the cracks was greater than in uncoated bar specimens.

Based on the test results, Treece recommended a 50% increase in basic development length in situations where the concrete cover is less than $3d_b$ or bar spacing is less than $6d_b$ where splitting failure is likely. For all other situations, Treece recommended a 15% increase in basic development length. The 15% increase was based on Johnston and Zia's pullout bond tests[24].

Table 3.1 Test parameters and results, Treece [25].

Specimen Notation[+]	Average Coating Thickness (mils)	Bar Size	Concrete Strength f'_c (psi)	Splice Length (inch)	Depth of cover c_b (inch)	Steel Stress f_{su} (Ksi)	Bond Stress u_t (psi)	Bond Ratio coated/uncoated
12-6-4	10.6	#6	4250	12	2.0	33.0	516	0.62
5-6-4	4.8	#6	4250	12	2.0	46.2	722	0.87
0-6-4	0	#6	4250	12	2.0	53.1	830	1.00
12-6-4r*	9	#6	3860	24	0.875	44.8	350	0.71
5-6-4r	4.5	#6	3860	24	0.75	47.9	374	0.76
0-6-4r	0	#6	3860	24	1.0	66.3 Y++	495	1.00
12-11-4	9.1	#11	5030	36	2.0	28.3	277	0.65
5-11-4	5.9	#11	5030	36	2.0	30.4	298	0.7
0-11-4	0	#11	5030	36	2.0	43.3	424	1.00
12-11-4b**	11	#11	4290	36	2.0	24.9	244	0.54
0-11-4b	0	#11	4290	36	2.0	45.9	449	1.00
12-6-8	14	#6	8040	16	0.75	35.0	410	0.55
0-6-8	0	#6	8040	16	0.875	63.2 Y	742	1.00
12-11-8	7.4	#11	8280	18	2.25	25.3	495	0.63
0-11-8	0	#11	8280	18	2.125	40.3	789	1.00
12-6-12	10.3	#6	12600	16	0.625	41.1	482	0.65
0-6-12	0	#6	12600	16	0.75	63.2 Y	742	1.00
12-11-12	9.7	#11	10510	18	2.0	33.8	662	0.72
0-11-12	0	#11	10510	18	2.0	46.9	918	1.00
12-11-12b	8.7	#11	9600	18	2.0	27.5	539	0.64
0-11-12b	0	#11	9600	18	2.0	43.0	842	1.00

Average of all coated bars: **0.67**
Standard deviation: **0.09**

[+] The first number is the nominal coating thickness, the second is bar size, and the third is the nominal concrete strength in Ksi.

++Y = Yielded bar.

* r = Replicate.

**b = Bottom cast, all other specimens are top cast.

Table 3.2 Bond efficiencies[+], Treece [25].

Specimen Notation	Measured Bond Stress* u_t (psi)	Predicted Bond Strength(psi)* ACI 318-83 Eq. (3.5)	Predicted Bond Strength(psi)* Orangun Eq. (3.2)	Bond Efficiency u_t/u(ACI)	Bond Efficiency u_t/u(Orangun)
12-6-4	520	690**	800	0.83	0.64
5-6-4	720	690**	800	1.15	0.90
0-6-4	830	690**	800	1.33	1.03
12-6-4r	350	660**	390	0.56	0.90
5-6-4r	370	660**	360	0.59	1.05
0-6-4r	500	660**	420	0.80	1.18
12-11-4	280	400	530	0.70	0.53
5-11-4	300	400	530	0.75	0.57
0-11-4	420	400	530	1.05	0.81
12-11-4b	240	370	490	0.65	0.50
0-11-4b	450	370	490	1.22	0.93
12-6-8	410	960**	590	0.66	0.70
0-6-8	740	960**	630	1.18	1.17
12-11-8	500	520	850	0.96	0.59
0-11-8	790	520	850	1.52	0.93
12-6-12	480	1200**	680	0.77	0.71
0-6-12	740	1200**	740	1.18	1.01
12-11-12	660	580	960	1.14	0.69
0-11-12	920	580	960	1.58	0.96
12-11-12b	540	560	920	0.99	0.59
0-11-12b	840	560	920	1.52	0.92

[+] The modification factor for top cast bars was not included in this comparison.
* Bond stress values are rounded to the nearest 10 psi.
** Upper limit on bond stress is 625 psi.

Treece also suggested that the combined factor for top reinforcement and epoxy-coated bars be limited to 1.7.

Treece's design recommendations were later adopted by ACI-318 in the 1989 Building Code[1] with the exception that a 20% increase in development length was recommended for cases where splitting is prevented.

Treece indicated the need to study in detail the influence of transverse reinforcement on the bond strength of epoxy-coated bars.

3.3.4 Purdue University Tests. In 1989, Cleary and Ramirez[26] reported on an experimental program designed to evaluate the bond strength of splices of epoxy-coated reinforcement in constant moment regions of slab specimens representative of bridge deck slabs. The effect of epoxy coating on member stiffness and on the spacing and width of cracks was also studied. The variables were splice length and concrete strength.

In each of four series of specimens, a 13-ft. x 2-ft. x 8-in. slab reinforced with epoxy-coated bars and a companion slab with uncoated bars were tested. Each slab contained three #6 bars spaced at 8 in. and spliced at midspan. All the bars were from the same heat of steel and had a parallel deformation pattern. The average coating thickness was 9.0 mils with a standard deviation of 2.1 mils. No transverse reinforcement was included. Three series of specimens had a nominal concrete strength of 4 ksi and were designed with 16-in., 14-in., and 12-in. splice lengths consecutively. The fourth series had a 10-in. splice length and an 8-ksi nominal concrete strength.

The slab specimens were loaded at the ends and supported at the third points. The loading arrangement resulted in negative bending with a constant moment region in the middle of the specimen. The arrangement also provided for convenient observation and measurements of cracks. Slab specimens and load setup are shown in Figure 3.12. The load was gradually applied in 500 pound increments. At each increment the load was held while the dial gages, measuring deflections, were read and cracks marked and measured.

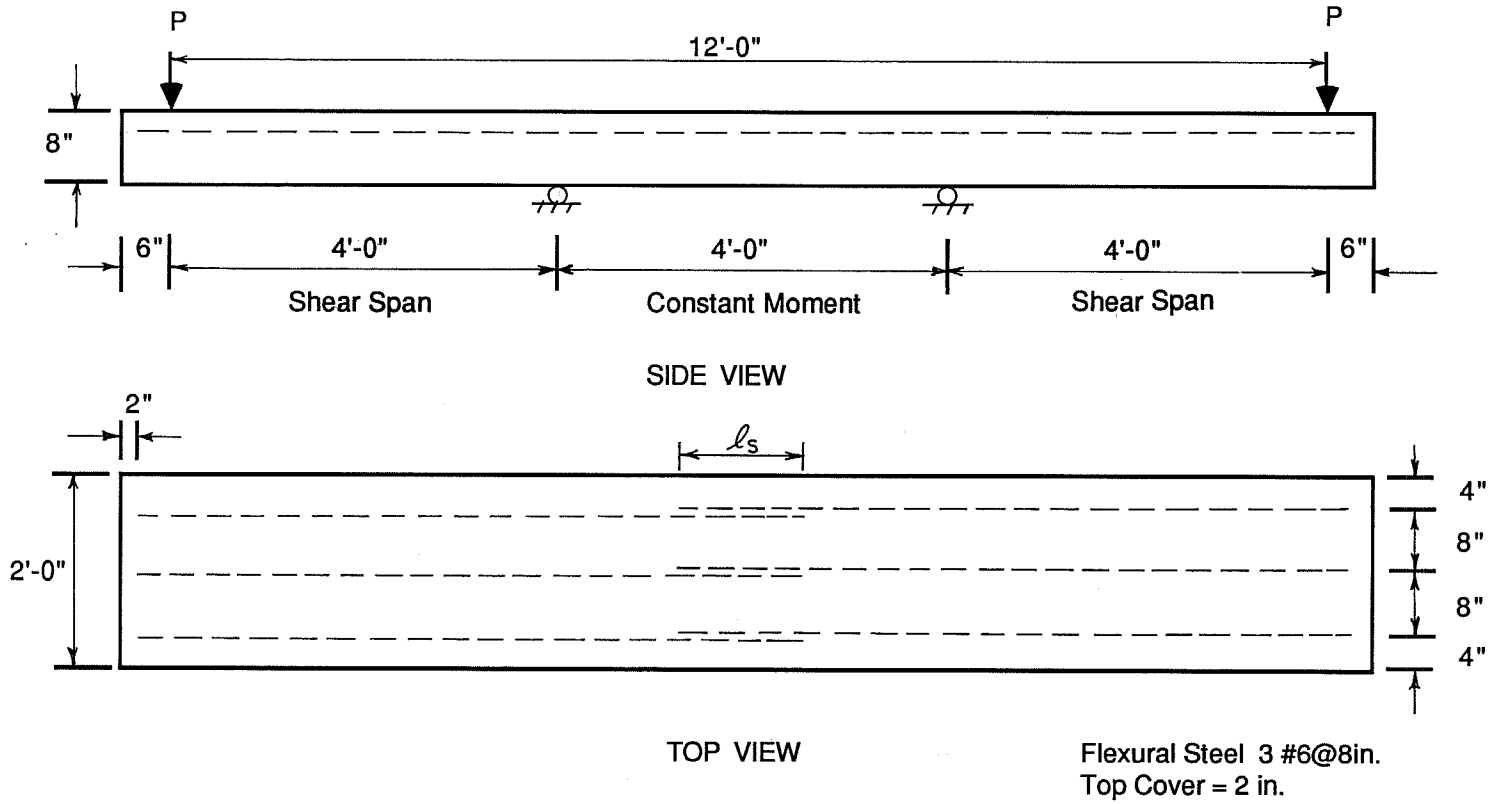

Figure 3.12 Slab specimen details and load setup, Cleary and Ramirez [26].

Table 3.3 Test parameters and results, Cleary and Ramirez [26].

Specimen Notation	Concrete Strength f'_c (psi)	Splice Length (inch)	Steel Stress f_{su} (Ksi)	Bond Stress u_t (psi)	Bond Ratio coated/uncoated
U16*	5620	16	65.2 Y+	761	-
E16**	5520	16	58.8	686	0.91
U14	5380	14	65.2 Y	870	-
E14	5840	14	53.6	715	0.79
U12	3990	12	49.0	763	-
E12	3990	12	47.3	736	0.97
U10	8200	10	63.5	1186	-
E10	8200	10	41.5	775	0.65

* U = Uncoated.
** E = Epoxy-coated.
+ Y = Yielded specimen.

The steel bars yielded in the uncoated slab specimens designed with 16-in. and 14-in. splices. Test parameters and results are shown in Table 3.3. Based on the 12-in. and 10-in splice series which resulted in bond splitting failure prior to steel yielding, epoxy-coated bar specimens developed lower bond strength than uncoated bar specimens. The reduction in bond strength was 3% for the 12-in. splice with a 4-ksi nominal concrete strength, and 35% for the 10-in. splice series with an 8-ksi nominal concrete strength. Cleary and Ramirez attributed this large difference in reduction percentages to the concrete strength and the number of flexural cracks. They argued that with higher strength concretes, the contribution of adhesion and friction to the bond between the concrete and uncoated reinforcement is larger than in lower strength concrete. Cleary and Ramirez concluded that the loss of adhesion between the concrete and epoxy-coated bars causes a greater reduction in bond strength relative to uncoated bars when used in high strength concrete. The number of flexural cracks in the splice region added to the greater reduction of bond strength of the epoxy-coated bar slab in the 10-in. splice series. The uncoated bar specimen had three flexural cracks in the splice region whereas the coated specimen had only two. A large portion of the bar force is transferred at crack locations where slip and bearing are greatest. This portion of the bar force was distributed over three points in the uncoated bar specimen compared to only two points in the epoxy-coated bar specimen.

Test results also showed that there was no loss of slab stiffness due to epoxy coating. Also, there were fewer cracks in the epoxy-coated bar specimens but the width of the cracks was greater than in uncoated bar specimens.

Based on the test results, Cleary and Ramirez concluded that there appeared to be no significant difference in the behavior of slabs relative to beams designed with epoxy-coated bars to fail in a splitting mode of failure. They used their data and results of previous research to conclude that with increasing splice length, the reduction in bond strength of epoxy-coated bars relative to uncoated bars was larger. Cleary and Ramirez stated that as splice length increased the possibility

of an uncoated bar specimen having more cracks across the splice than an epoxy-coated bar specimen increased. This would lead to fewer cracks but larger stress concentrations in the case of epoxy-coated bar specimens. Another reason was that the longer splice length would allow the friction and adhesion mechanism of bond, which is lost by epoxy coating, to act over a larger area of the uncoated bar.

Cleary and Ramirez accepted Treece's design recommendations[25], but pointed out the need to account for the effect of concrete strength and provided anchorage or splice length in the recommendations. Like Treece, they raised the need to do further research on the role of transverse reinforcement on the bond strength of epoxy-coated bars.

Cleary and Ramirez' conclusions were based on eight slab tests, two of which ended with the yielding of the steel reinforcement. The wide range of the test results could be due to the slab specimen design. With very short splice lengths, the location of flexural cracks along the splice could have a significant effect on the bond strength. Treece had to repeat a few of his beam tests using longer splice length to overcome the effect of short splice lengths on the test results[25]. Moreover, only two slab specimens with high strength concrete (8200 psi) designed with 10-in. splice length were used to draw conclusions on the role of concrete strength on the reduction in bond strength of epoxy-coated bars relative to uncoated bar specimens. More data would be needed to make such conclusions.

3.3.5 University of California at Berkeley Tests. In 1989, DeVries and Moehle[27] reported an experimental study designed to examine the effects of concrete strength, casting position, epoxy coating, and the presence of an anti-bleeding agent on the bond strength of splices.

Nine series of four beams each were tested. In each series two beams were cast with bottom bars and two with top bars. The pilot series did not include epoxy-coated bars, but each of the next eight series included two epoxy-coated bar specimens one with bottom cast bars and one with top cast bars. The pilot series and four others used concrete with an anti-bleeding agent

present. The remaining four series did not. Three nominal concrete strengths of 8, 10 and 15 ksi were tested. Two groups of eight beams were tested with 8-ksi concrete. One had #6 reinforcing bars and one had #9's. All other beams had #9 bars. All the bars of each size came from the same heat of Grade 60 steel and had a bamboo deformation pattern except the pilot series which had a chevron pattern. The epoxy coating was nominally 8 mils thick. The test parameters are shown in Table 3.4.

The beams were 14 ft. in length with a nominal depth of 16 in. and a nominal width of 11 in. The 16-in. depth ensured at least 12 in. of concrete below the reinforcing bars for the top bar specimens. The concrete cover to the reinforcing bars was 1-1/8 in. on both the side and tension faces for all beam specimens. Each beam had two longitudinal bars spliced at the center. The splice lengths were the same for all four beams in a series except for the four beams of the pilot series. The transverse reinforcement consisted of three #3 stirrups along the splice length for all but the pilot series. For the pilot series the number of stirrups varied with the splice length. The splice lengths were designed to cause a splitting failure before yielding of the bar.

The beams were loaded with the tension face up and a region of constant moment over the middle of the beam. The test setup facilitated the marking and measure of cracks. The beam dimensions and test setup are shown in Figure 3.13. The load on each end was increased by 2-kip increments until the beam cracked, after which the load increment was 1 kip until failure. At each load stage cracks were marked and crack widths were measured.

The mode of failure was a splitting failure at the splice region for all beams tests. The failures were sudden but not explosive. It was observed that the eight beams with 15-ksi nominal concrete strength were noticeably louder when they cracked.

DeVries and Moehle compared the measured bond stress, u_t, for each specimen with the predicted bond stresses using the following four equations:

(1) Eq. (3.2) developed by Orangun, et al.[20]:

Table 3.4 Test parameters, DeVries and Moehle [27].

Batch	BEAMS				Concrete strength(psi)
	Bot. uncoated	Bot. uncoated	Top uncoated	Top uncoated	
8G9(Pilot)	8G-16B-P9	8G-22B-P9	8G-22T-P9	8G-28T-P9	7460
	Bot. coated	Bot. uncoated	Top coated	Top uncoated	
8G9	8G-18B-E9	8G-18B-P9	8G-18T-E9	8G-18T-P9	8610
8N9	8N-18B-E9	8N-18B-P9	8N-18T-E9	8N-18T-P9	7660
8G6	8G-9B-E6	8G-9B-P6	8G-9T-E6	8G-9T-P6	8850
8N9	8N-9B-E6	8N-9B-P6	8N-9T-E6	8N-9T-P6	8300
10G9	10G-12B-E9	10G-12B-P9	10G-12T-E9	10G-12T-P9	9680
10N9	10N-12B-E9	10N-12B-P9	10N-12T-E9	10N-12T-P9	9780
15G9	15G-12B-E9	15G-12B-P9	15G-12T-E9	15G-12T-P9	16100
15N9	15N-12B-E9	15N-12B-P9	15N-12T-E9	15N-12T-P9	13440

BATCH CODE ##X#

= Nominal f'c, Ksi
X = N for no anti-bleeding agent present
G for anti-bleeding agent present
= Bar size, #9 or #6

e.g. Batch 8G6 is 8 Ksi concrete with the anti-bleeding agent and the beams have #6 bars.

BEAM CODE ##X-##Y-Z#

= Nominal f'c, Ksi
X = N for no anti-bleeding agent present
G for anti-bleeding agent present
= Splice Length, in.
Y = B for bottom cast, T for top cast
Z = E for epoxy-coated bars, P for uncoated bars
# = Bar size, #9 or #6

e.g. Beam 15N-12B-E9 has 15 Ksi concrete without the anti-bleeding agent, a 12 inch splice length and bottom cast epoxy-coated bars.

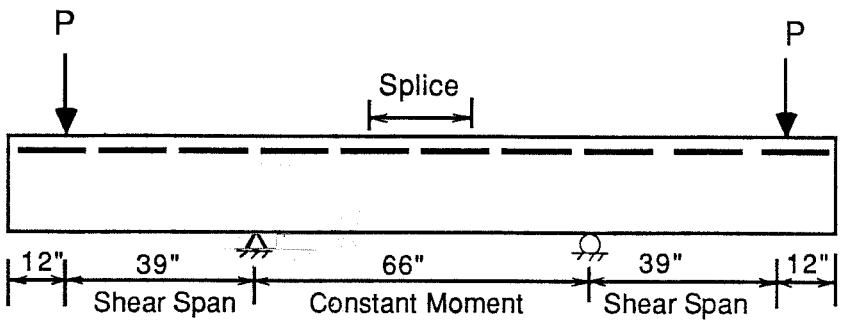

(a) Test Setup

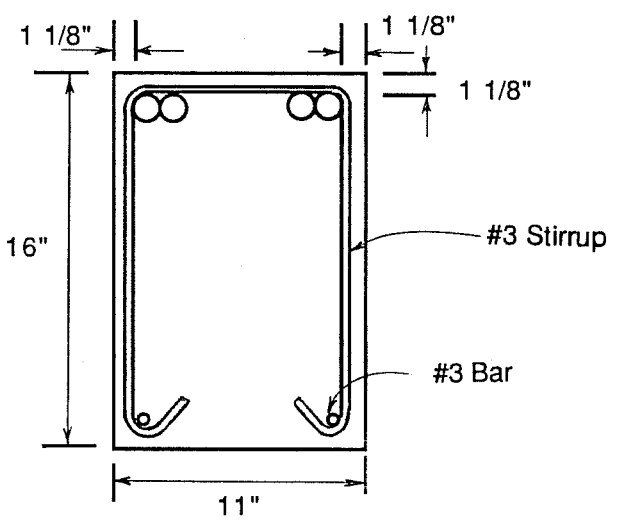

(b) Beam Cross-section

Figure 3.13 Beam dimensions and test setup, DeVries and Moehle[27].

$$u = \left[1.2 + 3\frac{c}{d_b} + 50\frac{d_b}{\ell_s} + K_{tr}\right]\sqrt{f'_c}, \qquad K_{tr} = \frac{a_{tr}f_{yt}}{500sd_b}$$

(2) The ACI Committee 408[26] design recommendation for development length assuming $\ell_s = \ell_{db}$:

$$\ell_s = \frac{5500A_b}{\phi K\sqrt{f'_c}} \tag{3.6}$$

which can be rewritten, using $u\pi d_b\ell_s = A_b f_y$ and equating f_y to 60,000 psi and ϕ to 0.8, as

$$u = 2.8K\sqrt{f'_c} / d_b \tag{3.7}$$

where K is the confinement parameter as defined by Committee 408.

(3) Eq. (3.5) developed from the 1983 ACI Code (ACI 318-83)[19] excluding the upper limit of 625 psi:

$$u = 7.96\sqrt{f'_c} / d_b$$

(4) The 1989 ACI Code (ACI 318-89)[1] specification for development length, Eq. (3.4), assuming $\ell_s = \ell_{db}$:

$$\ell_s = 0.04A_b f_y / \sqrt{f'_c} \geq 0.03d_b f_y / \sqrt{f'_c}$$

Combining the above equation with $u\pi d_b\ell_s = A_b f_y$ and modifying ℓ_s by a factor of 1.4 according to Section 12.2.3.3 of the code:

$$u = 5.7\sqrt{f'_c} / d_b \leq 8.33\sqrt{f'_c}, \qquad \sqrt{f'_c} \leq 100 \text{ psi} \tag{3.8}$$

The upper limits on u and on $\sqrt{f'_c}$ were excluded from the comparison. Also, the modification factors for top bars and epoxy-coated bars were ignored.

The measured bond strength, u_t, for each beam specimen was divided by the predicted values from equations (3.2), (3.7), (3.5), and (3.8) to obtain bond efficiencies. A listing of the test results and bond efficiencies is given in Table 3.5.

The test results showed that the casting position and epoxy coating adversely affected the bond strength. However, the effects of casting position and epoxy coating were not cumulative. The bond strength of top cast uncoated bars, bottom cast epoxy-coated bars, and top cast epoxy-coated bars was approximately 3/4 the bond strength of a bottom cast uncoated bar. DeVries and Moehle concluded that the modification for top cast epoxy-coated bars relative to bottom cast epoxy-coated bars, given in Section 12.2.4.3 of the 1989 ACI Code (ACI 318-89)[1], was not needed.

DeVries and Moehle observed that the presence of an anti-bleeding agent apparently stopped the bleeding of the concrete. However, the test results proved that anti-bleeding agent did not significantly alter the bond stress of the splice for either top or bottom cast bars. DeVries and Moehle concluded that while the agent stopped bleeding, plastic settlement of the concrete would still lower the bond strength of a top cast bar.

Based on the data of the thirty-six beams shown in Table 3.5, DeVries and Moehle made the following two observations:

(1) Eq. (3.8) developed from the 1989 ACI Code (318-89)[1] specifications for bond strength was over conservative for the cases considered.

(2) The proposed ACI Committee 408[28] design equation (3.6) was appropriately conservative for the cases considered.

Based on the above observations, DeVries and Moehle suggested the use of equation (3.6) with a modification factor of 1.3 for top bars and epoxy-coated bars regardless of casting position. Figure 3.14 is a bar graph of the measured bond stress divided by the predicted bond strength using

Table 3.5 Test results and bond efficiencies*, DeVries and Moehle [27].

Beam Notation	K_{tr}	Measured Bond Stress u_t (psi)	Bond Ratio	Bond Efficiency Relative To Orangun et al. Eq.(3.2)	ACI Comm. 408 Eq.(3.7)	ACI 318-83 Eq.(3.5)	ACI 318-89 Eq.(3.8)
8G-16B-P9	2.87	753	-	0.82	1.37	1.24	1.73
8G-22B-P9	2.79	682	-	0.83	1.21	1.12	1.56
8G-22T-P9	2.79	685	-	0.82	1.13	1.12	1.57
8G-28T-P9	2.74	587	-	0.76	0.97	0.96	1.34
8G-18B-P9	2.55	826	-	0.90	1.30	1.26	1.76
8G-18B-E9	2.55	628	0.76	0.69	1.09	0.96	1.34
8G-18T-P9	2.55	758	-	0.83	1.19	1.16	1.62
8G-18T-E9	2.55	663	0.87	0.72	1.00	1.01	1.41
8N-18B-P9	2.55	814	-	0.94	1.30	1.32	1.84
8N-18B-E9	2.55	607	0.75	0.70	0.88	0.68	1.37
8N-18T-P9	2.55	652	-	0.75	1.00	1.06	1.47
8N-18T-E9	2.55	647	0.99	0.75	0.99	1.05	1.46
8G-9B-P6	7.68	1458	-	1.20	1.86	1.46	2.04
8G-9B-E6	7.68	1057	0.72	0.87	1.35	1.06	1.48
8G-9T-P6	7.68	1339	-	1.11	1.71	1.34	1.87
8G-9T-E6	7.68	1019	0.76	0.84	1.33	1.02	1.43
8N-9B-P6	7.68	1167	-	1.00	1.54	1.21	1.69
8N-9B-E6	7.68	896	0.77	0.76	1.18	0.93	1.29
8N-9T-P6	7.68	1026	-	0.88	1.35	1.06	1.48
8N-9T-E6	7.68	814	0.79	0.69	1.10	0.84	1.18
10G-12B-P9	3.83	887	-	0.76	1.24	1.28	1.78
10G-12B-E9	3.83	732	0.83	0.63	1.05	1.05	1.47
10G-12T-P9	3.83	771	-	0.66	1.06	1.11	1.55
10G-12T-E9	3.83	747	0.97	0.64	1.03	1.08	1.50
10N-12B-P9	3.83	885	-	0.75	1.26	1.27	1.77
10N-12B-E9	3.83	806	0.91	0.69	1.10	1.15	1.61
10N-12T-P9	3.83	729	-	0.62	1.02	1.04	1.46
10N-12T-E9	3.83	682	0.94	0.58	0.95	0.98	1.36
15G-12B-P9	3.83	1155	-	0.77	1.28	1.29	1.80
15G-12B-E9	3.83	897	0.78	0.59	1.02	1.00	1.40
15G-12T-P9	3.83	1062	-	0.70	1.06	1.19	1.66
15G-12T-E9	3.83	939	0.88	0.62	0.96	1.05	1.46
15N-12B-P9	3.83	1191	-	0.86	1.42	1.46	2.03
15N-12B-E9	3.83	850	0.71	0.62	1.05	1.04	1.45
15N-12T-P9	3.83	1044	-	0.76	1.17	1.28	1.78
15N-12T-E9	3.83	1021	0.98	0.74	1.12	1.25	1.74

*Modification factors for top bars and coated bars were not included in the comparison.

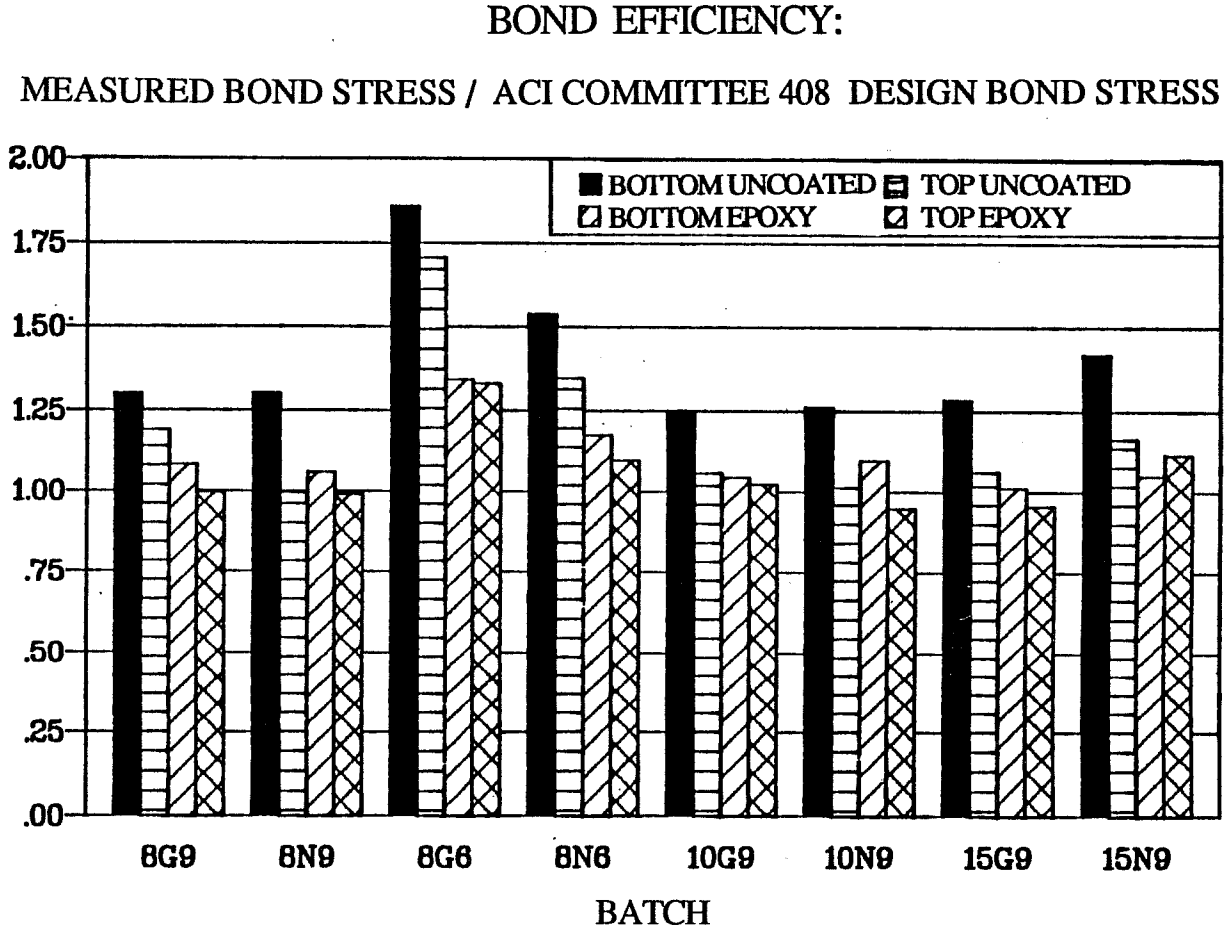

Figure 3.14 Bond efficiencies relative to ACI Committee 408 design bond stress, DeVries and Moehle[27].

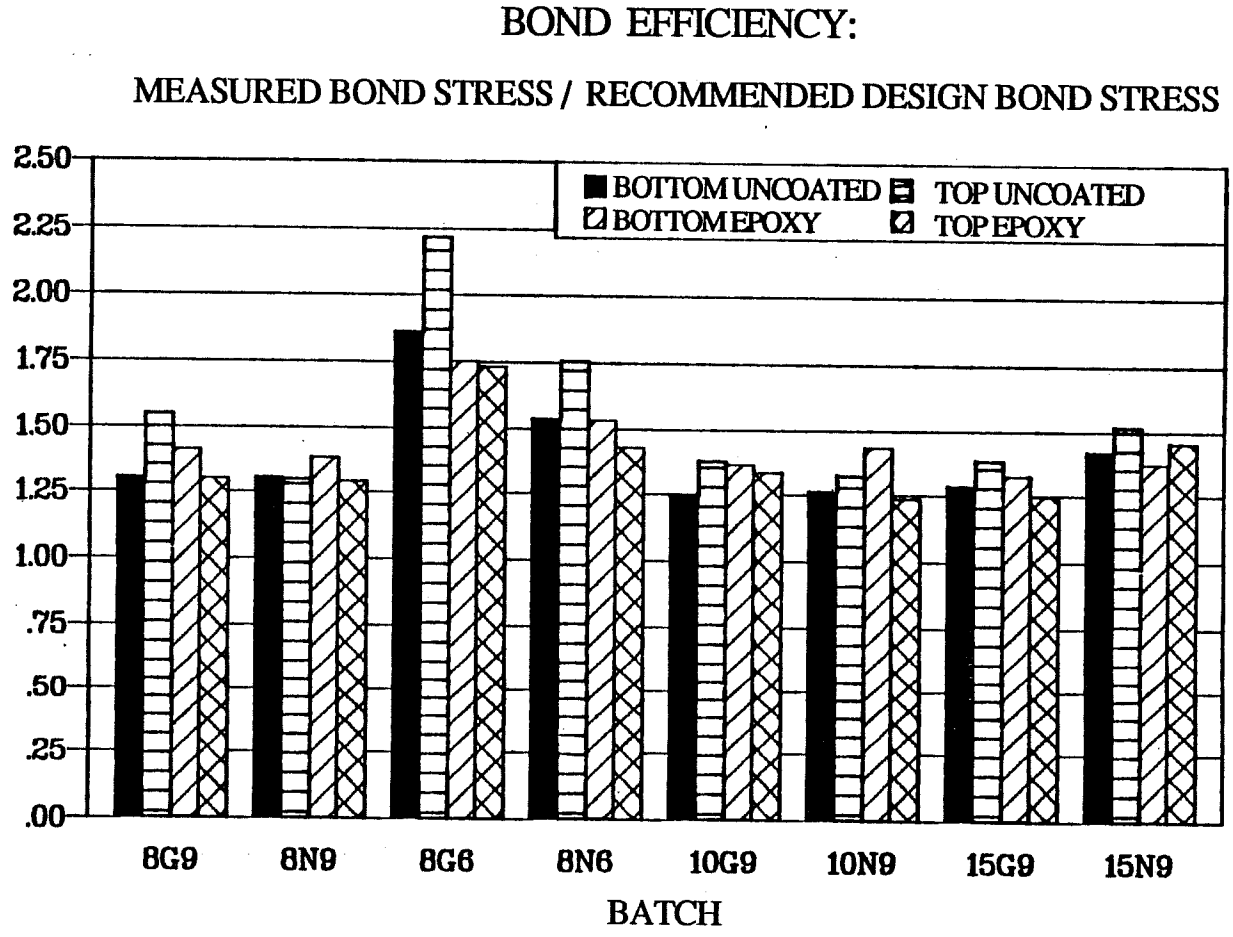

Figure 3.15 Bond efficiencies relative to the recommended design bond stress, DeVries and Moehle [27].

Eq. (3.7), developed from the ACI Committee 408 design equation (3.6), for the eight series with epoxy-coated bars reported by DeVries and Moehle. Figure 3.15 is a similar graph which includes in Eq. (3.7) the suggested modification factor of 1.3. The average value of the bond efficiencies shown in Figure 3.15 for all thirty-six beams is 1.43 with a standard deviation of 0.21. The recommended design approach was also conservative for series 15G9 with concrete strength of 16,100 psi, which is near the current practical limit for concrete strength. Therefore, DeVries and Moehle concluded that it was unnecessary to place an upper limit on the value of $\sqrt{f'_c}$ in the recommended design equation as is done by the ACI Code (318-89)[1] development length specifications.

All the beams in DeVries and Moehle's tests had transverse reinforcement crossing the splitting plane in the splice region. Since there were no companion beams without such transverse reinforcement, no conclusions could be drawn on the effect of transverse reinforcement on the bond strength of epoxy-coated bars relative to uncoated bars.

3.4 Failure Hypothesis of Epoxy-Coated Bars

Previous studies of epoxy-coated bars indicate a reduction in the bond strength relative to uncoated bars. Strength comparisons in the NBS study[23] showed that epoxy-coated bars developed 94% of the bond of uncoated bars. The results of the NBS study were influenced by the test specimen used as well as the fact that most of the coated and uncoated bars yielded. Bond strength comparisons in the North Carolina State University study[24] showed that epoxy-coated bars developed 85% of the bond of uncoated bars. The comparisons were based on tests which ended with a pullout bond failure. In the University of Texas tests[25], all the failures were caused by splitting of the cover in the splice region. Epoxy-coated bars, with average coating thickness above 5 mils, developed 67% of the bond strength of uncoated bars with a standard deviation of 9%.

Purdue University slab tests[26] and the University of California beam tests[27] tend to agree with the University of Texas test results.

After presenting the results of his beam tests, Treece[25] presented the following failure hypothesis of epoxy-coated bars. Treece argued that the the primary reason for the reduction in bond strength appeared to be the loss of adhesion between the concrete and epoxy-coated bars. The epoxy coating destroyed the adhesion between the steel bars and the surrounding concrete. However, the uncoated bars showed evidence of good adhesion with the concrete. The epoxy coating breaks the bond between the steel and concrete causing most or all of the friction capacity to be lost. Friction between the concrete and steel has not been considered an important component of bond strength. The major component of bond is considered to be bearing of the deformations against the concrete. However, it was recognized by Lutz, Gergely and Winter[29] that the friction between the concrete and steel at the deformations is very important in developing bond strength.

When the rib of the reinforcing steel bears against the surrounding concrete, the concrete key tends to slide up and over the face of the rib causing splitting of the concrete cover. Friction between the concrete and steel along the face of the rib acts to prevent the concrete key from sliding relative to the rib. The force due to the friction between the steel and concrete at the rib adds vectorially to the component of bond acting perpendicular to the rib (Figure 3.16). If the friction between the concrete and steel is lost, the only component of the bond strength is the force perpendicular to the face of the rib.

The magnitude of the bond force is controlled by the amount of radial pressure the concrete cover can resist before splitting. This is the vertical component of the resultant bond force in Figure 3.16. The horizontal component of the resultant is the effective bond strength. If the resistance to splitting of the cover is the same for either case, then the bar with no friction will have

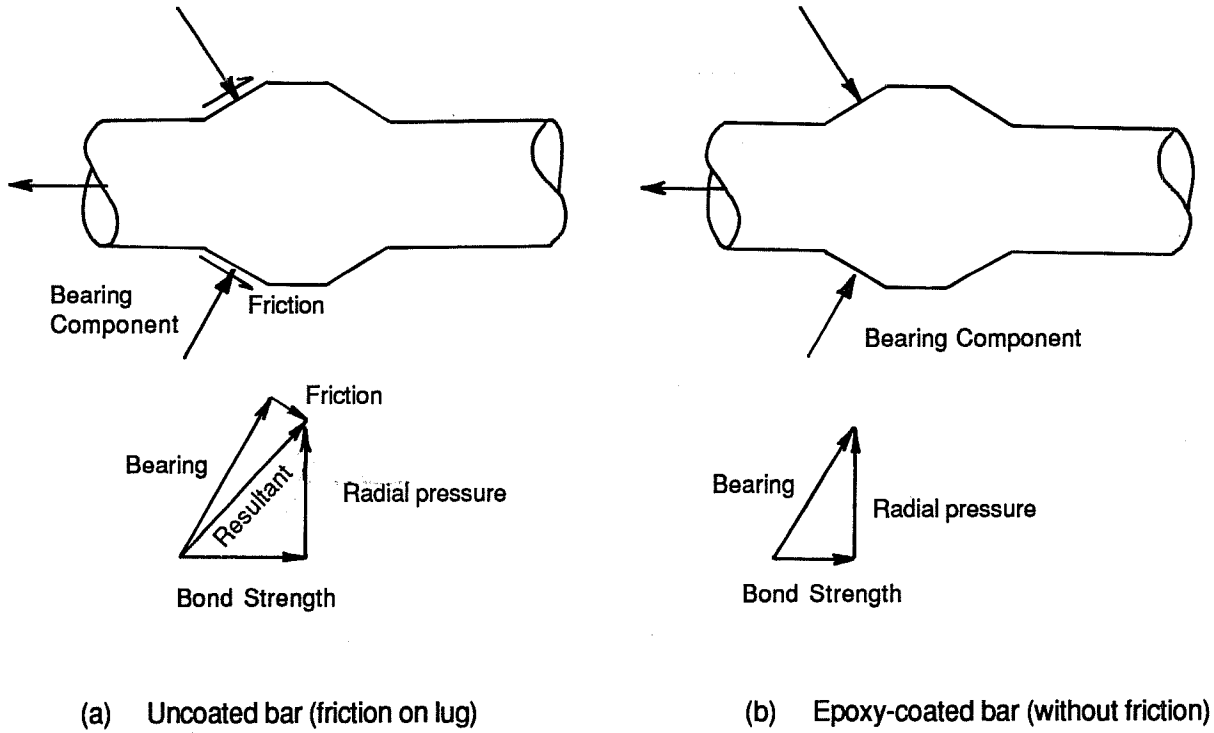

Figure 3.16 Bond Strength components, Treece [25].

a much smaller bond capacity than the bar which develops friction between the concrete and the bar lug.

In a pullout failure, the friction between the concrete and steel is much less important than in a splitting failure. A pullout failure occurs when the steel is well confined by concrete cover or transverse steel, preventing a splitting failure. In this case, the bond strength is controlled by the capacity of the concrete in direct shear. The bearing of the ribs against the concrete causes the key between ribs to shear from the surrounding concrete. Since the bar is well confined, friction between the rib and concrete is not necessary to prevent sliding of the concrete key relative to the rib.

Lutz, Gergely, and Winter[29] predicted that bars with a larger rib face angle would be less affected by grease or other friction reducing agents than bars with a flatter rib face angle. If the face of the rib formed an angle of 90° with the axis of the bar, all of the bond strength would be produced by direct bearing of the rib against the concrete key. In this case friction between the concrete and steel would be unnecessary. However, for a plain bar (a rib face angle of 0°), friction caused by adhesion between the concrete and steel would be the only component of bond. Loss of adhesion between the concrete and steel would completely destroy the bond. As the rib face angle becomes larger, the contribution of the friction component, parallel to the face of the rib, to the bond strength becomes smaller. Therefore, the loss of adhesion becomes less significant. Research work is needed to clarify the importance and effect of rib face angle on bond strength.

The loss of adhesion may cause an additional reduction in bond strength by reducing the tensile capacity across the plane of splitting. Normally only concrete across the failure plane is considered to resist splitting, as shown in Figure 3.17. However, the adhesion between uncoated bars and the surrounding concrete may cause tensile forces to develop which would increase the capacity of the cover. When the adhesion between the steel and concrete is lost due to the epoxy coating, this added splitting capacity is also lost.

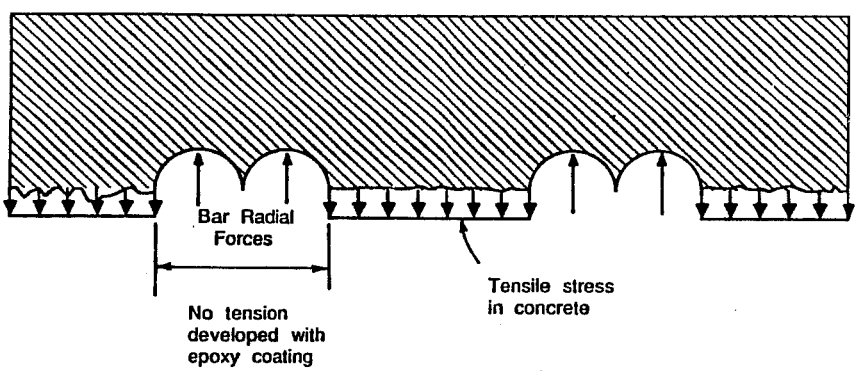

Figure 3.17 Tensile stresses across splitting plane, Treece[24].

CHAPTER 4

FUNDAMENTAL BOND STUDIES OF EPOXY-COATED BARS - EXPERIMENTAL PROGRAM

4.1 Design of Specimens

In this phase of the test program, fundamental bond properties of epoxy-coated reinforcing bars were examined. The variables included bar size, coating thickness, bar deformation pattern, rib face angle, degree of confinement of the anchored bar, and concrete strength.

Eight series with a total of eighty specimens were tested. The series were numbered in the sequence they were tested. Some series included replicates to check the reliability of the test setup and the scatter of test results. The specimens consisted of a reinforcing bar embedded in a 12-in. x 12-in. x 10-in. concrete block. The bar had an anchorage length of 10 in. The short embedment length was chosen to avoid yielding of the reinforcing bar. Two types of pullout specimens were tested, A and B. A schematic of both types is shown in Figure 4.1.

In Type A tests, the reinforcing bar was anchored in the specimen at 3 in. below the top surface. The specimen was cast with a styrofoam wedge (removed after casting) which allowed only the bottom half surface of the bar to be embedded in the concrete. A uniformly distributed lateral or confining load was applied directly to the exposed portion of the bar. The lateral load was held constant while the bar was pulled in the longitudinal direction until failure occurred. The confining load, described later as "top load", simulated the confining effect of concrete cover and transverse reinforcement. The Type B test specimen was a rectangular eccentric pullout specimen with no wedge. The bar was completely embedded in the concrete. Confinement for the anchored bar was provided by concrete cover and transverse reinforcement.

In each of the first five series, twelve Type A pullout specimens were tested. In the first series #11 bars with diamond deformation pattern were tested. The nominal concrete strength was

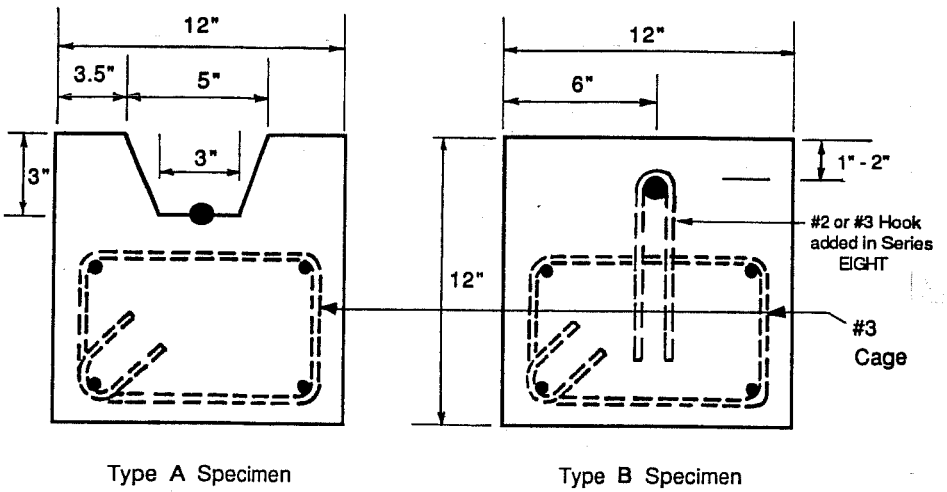

Figure 4.1 Schematic drawing of the pullout specimens.

4000 psi. Four levels of top load (5, 10, 15 and 20 kips) were examined. For each level, an uncoated bar and two epoxy-coated bars with nominal coating thicknesses of 5 and 12 mils were tested and compared. In the second series #11 bars with parallel and crescent deformation patterns were tested. The nominal concrete strength was 4000 psi. The nominal coating thickness of the coated bars was 8 mils. For each one of the four levels of top load, an uncoated bar specimen and an epoxy-coated bar specimen, both with parallel deformation pattern, were tested and compared. For two levels of top load, an epoxy-coated bar specimen with crescent deformation pattern was included in the comparison. Two replicates were included and tested in the second series. The third series had #11 bars but the nominal concrete strength was 8000 psi. Again, for each one of four levels of top load (5, 10, 15 and 20 kips), an uncoated bar specimen and an epoxy-coated bar specimen, both with parallel deformation pattern, were tested and compared. For two levels of top load, an uncoated bar specimen and an epoxy-coated bar specimen, both with crescent deformation pattern, were included in the above comparison. The fourth and fifth series were similar to the

second and third series, respectively, with the exception that #6 bars were used instead of #11 bars. The nominal coating thickness of the #6 epoxy-coated bars was 8.0 mils.

Type A pullout specimens of the first five series are identified in Table 4.1. A four-part notation system was used to identify the variables of each test specimen. The first part of the notation indicates the bar deformation pattern (D = diamond, P = parallel, and C = crescent) and the bar size (#11 or #6). The second part indicates whether the bar is uncoated (U) or epoxy-coated (C). The third part is the nominal concrete strength in ksi. The fourth part is the top load: 1 = 5 kips, 2 = 10 kips, 3 = 15 kips and 4 = 20 kips.

The objective of the seventh series was to investigate the effect of the rib face angle on the bond performance of epoxy-coated bars relative to uncoated bars. The rib face angle for the #11 and the #6 bars used in the project was around 30 degrees regardless of the deformation pattern. This coincides with the rib face angle of most reinforcing bars in the industry. Therefore, to achieve the objective, 7/8-in. diameter plain round bars were machined to simulate #6 bars with parallel deformation pattern and a rib face angle of 30, 45, or 60 degrees. For each rib face angle an uncoated bar specimen and an epoxy-coated bar specimen were tested and compared. A two-part liquid epoxy system, provided by the manufacturer for patching purposes, was used to coat the manufactured bars. The same top load, 10 kips, was used in all tests in series SEVEN. The nominal concrete strength was 4000 psi. A three-part notation system was used to identify the variables of each specimen in the seventh series (see Table 4.2). The first part, M, refers to the fact that the bar is manufactured. The second part indicates whether the bar is uncoated (U) or epoxy-coated (C), and the third part is the rib face angle in degrees.

Six type B pullout specimens were tested in the sixth series. The bars were #6 with a parallel deformation pattern and the nominal concrete strength was 4000 psi. For each of two concrete covers, 1 in. and 2 in., the bond performance of an epoxy-coated bar was compared to that of an uncoated bar and that of a latex painted bar. The effects of fusion bonded epoxy coating and

Table 4.1 Test parameters of Type A pullout specimens.

SERIES NUMBER	Specimen Notation	Bar Size	Deformation Pattern	Coating Thickness Nominal (mils)	Coating Thickness Average (mils)	Nominal Concrete Strength (psi)	Top* Load (Kips)
	D11-U-4-1	#11	Diamond	-	-	4000	5
	D11-U-4-2	#11	Diamond	-	-	4000	10
	D11-U-4-3	#11	Diamond	-	-	4000	15
	D11-U-4-4	#11	Diamond	-	-	4000	20
	D11-C5-4-1	#11	Diamond	5	6.2	4000	5
SERIES ONE	D11-C5-4-2	#11	Diamond	5	4.8	4000	10
	D11-C5-4-3	#11	Diamond	5	5.2	4000	15
	D11-C5-4-4	#11	Diamond	5	4.8	4000	20
	D11-C12-4-1	#11	Diamond	12	13.4	4000	5
	D11-C12-4-2	#11	Diamond	12	12.9	4000	10
	D11-C12-4-3	#11	Diamond	12	12.2	4000	15
	D11-C12-4-4	#11	Diamond	12	11.5	4000	20
	P11-U-4-1	#11	Parallel	-	-	4000	5
	P11-U-4-2	#11	Parallel	-	-	4000	10
	P11-U-4-3	#11	Parallel	-	-	4000	15
	P11-U-4-4	#11	Parallel	-	-	4000	20
	P11-C-4-1	#11	Parallel	8	8.8	4000	5
SERIES	P11-C-4-2	#11	Parallel	8	8.3	4000	10
TWO	P11-C-4-2r**	#11	Parallel	8	9.2	4000	10
	P11-C-4-3	#11	Parallel	8	8.5	4000	15
	P11-C-4-4	#11	Parallel	8	9.0	4000	20
	P11-C-4-4r	#11	Parallel	8	8.3	4000	20
	C11-C-4-2	#11	Crescent	8	9.5	4000	10
	C11-C-4-4	#11	Crescent	8	10.1	4000	20

* "Top load" refers to the uniformly distributed confining load applied directly to the top surface of the anchored bar.
**r = Replicate.

Table 4.1 (Continued)

SERIES NUMBER	Specimen Notation	Bar Size	Deformation Pattern	Coating Thickness Nominal (mils)	Coating Thickness Average (mils)	Nominal Concrete Strength (psi)	Top* Load (Kips)
	P11-U-8-1	#11	Parallel	-	-	8000	5
	P11-U-8-2	#11	Parallel	-	-	8000	10
	P11-U-8-3	#11	Parallel	-	-	8000	15
	P11-U-8-4	#11	Parallel	-	-	8000	20
	P11-C-8-1	#11	Parallel	8	9.0	8000	5
SERIES	P11-C-8-2	#11	Parallel	8	7.8	8000	10
THREE	P11-C-8-3	#11	Parallel	8	8.7	8000	15
	C11-C-8-4	#11	Parallel	8	7.1	8000	20
	C11-U-8-1	#11	Crescent	-	-	8000	5
	C11-U-8-3	#11	Crescent	-	-	8000	15
	C11-C-8-1	#11	Crescent	8	9.4	8000	5
	C11-C-8-3	#11	Crescent	8	9.9	8000	15
	P6-U-4-1	#6	Parallel	-	-	4000	5
	P6-U-4-2	#6	Parallel	-	-	4000	10
	P6-U-4-3	#6	Parallel	-	-	4000	15
	P6-U-4-4	#6	Parallel	-	-	4000	20
	P6-C-4-1	#6	Parallel	8	7.8	4000	5
SERIES	P6-C-4-1r**	#6	Parallel	8	6.7	4000	5
FOUR	P6-C-4-2	#6	Parallel	8	6.6	4000	10
	P6-C-4-3	#6	Parallel	8	6.4	4000	15
	P6-C-4-3r	#6	Parallel	8	7.1	4000	15
	P6-C-4-4	#6	Parallel	8	7.0	4000	20
	C6-C-4-1	#6	Crescent	8	8.5	4000	5
	C6-C-4-3	#6	Crescent	8	8.6	4000	15

* "Top load" refers to the uniformly distributed confining load applied directly to the top surface of the anchored bar.
**r = Replicate.

Table 4.1 (Continued)

SERIES NUMBER	Specimen Notation	Bar Size	Deformation Pattern	Coating Thickness Nominal (mils)	Coating Thickness Average (mils)	Nominal Concrete Strength (psi)	Top* Load (Kips)
	P6-U-8-1	#6	Parallel	-	-	8000	5
	P6-U-8-2	#6	Parallel	-	-	8000	10
	P6-U-8-3	#6	Parallel	-	-	8000	15
	P6-U-8-4	#6	Parallel	-	-	8000	20
	P6-C-8-1	#6	Parallel	8	6.4	8000	5
SERIES	P6-C-8-2	#6	Parallel	8	5.9	8000	10
FIVE	P6-C-8-3	#6	Parallel	8	6.3	8000	15
	P6-C-8-4	#6	Parallel	8	6.4	8000	20
	C6-U-8-1	#6	Crescent	-	-	8000	5
	C6-U-8-3	#6	Crescent	-	-	8000	15
	C6-C-8-1	#6	Crescent	8	8.0	8000	5
	C6-C-8-3	#6	Crescent	8	8.0	8000	15

* "Top load" refers to the uniformly distributed confining load applied directly to the top surface of the anchored bar.

Table 4.2 Test parameters of series SEVEN of Type A pullout specimens.

Specimen Notation	Nominal Concrete Strength (psi)	Average Coating Thickness (mils)	Rib Face Angle (degrees)	Top Load (Kips)
M-U-30	4000	-	30	10
M-U-45	4000	-	45	10
M-U-60	4000	-	60	10
M-C-30	4000	6.6	30	10
M-C-45	4000	7.2	45	10
M-C-60	4000	6.5	60	10

ordinary painting on the bond behavior of a reinforcing bar were compared. In Table 4.3, a three-part notation system is used to identify the variables of each test specimen in the sixth series. The first part refers to the #6 bar with parallel deformation pattern. The second part indicates whether the bar is uncoated (U), epoxy-coated (C), or painted (P). The third part is the nominal concrete strength in ksi, and the fourth part is the concrete cover to the anchored bar.

In the eighth series, eight Type B pullout specimens were tested. As in the sixth series, the bars were #6 with parallel deformation pattern and the nominal concrete strength was 4000 psi. The concrete cover to the anchored bar was 2 in. in all test specimens. The objective of the series was to investigate the effect of adding transverse reinforcement on the bond performance of epoxy-coated bars relative to uncoated bars. The transverse reinforcement consisted of one #2 or #3 Grade 60 uncoated deformed bar hooked over the anchored bar at the middle of the 10-in. embedment length. The variables of the test specimens of the eighth series are identified in Table 4.3. The notation system is similar to that of the sixth series with the addition of a suffix indicating the presence of a #2 or #3 transverse hook bar. Two replicates were included in the eighth series to check the scatter of the test results.

In all test specimens of the first phase of the research program, the total length of the reinforcing bars was controlled by providing a suitable length of the bar extending out of the concrete block. This length was required to provide room for a compression steel plate, a center-hole hydraulic ram, and a gripping wedge assembly. A longer extension out of the concrete block was needed for the #11 bars than for the #6 bar because of the use of a larger hydraulic ram (60 ton relative to 20 ton) and a larger gripping wedge. The overall length was 30 in. for the #11 bar and 24 in. for the #6 bar.

Table 4.3 Test parameters of series SIX and series EIGHT of Type B pullout specimens.

SERIES NUMBER	Specimen Notation	Coating Thickness Nominal (mils)	Coating Thickness Average (mils)	Concrete Cover (inch)	Transverse Reinforcement*
SERIES SIX**	P6-U-4-1"	-	-	1	-
	P6-C-4-1"	8	7.2	1	-
	P6-P-4-1"	8	6.1	1	-
	P6-U-4-2"	-	-	2	-
	P6-C-4-2"	8	6.4	2	-
	P6-P-4-2"	8	6.4	2	-
SERIES EIGHT**	P6-U-4-2"	-	-	2	-
	P6-U-4-2"-#2	-	-	2	#2
	P6-U-4-2"-#2r+	-	-	2	#2
	P6-U-4-2"-#3	-	-	2	#3
	P6-C-4-2"	8	5.3	2	-
	P6-C-4-2"-#2	8	7.5	2	#2
	P6-C-4-2"-#2r	8	6.5	2	#2
	P6-C-4-2"-#3	8	8.5	2	#3

* Transverse reinforcement, if provided, consisted of one Grade 60 deformed bar hooked over the anchored bar at the middle of the 10-in. anchorage length.

** All the bars in series SIX and series EIGHT were #6 with parallel deformation pattern. The nominal concrete strength was 4000 psi for both series.

+ r = Replicate.

4.2 Materials

4.2.1 Reinforcing Steel. Bars of each size were from the same heat of steel to ensure that both uncoated and epoxy-coated bars in companion specimens had identical rib geometry and mechanical properties. The #6 and #11 bars were Grade 60 and met ASTM A615-87a specifications[30]. Samples of #11 and #6 bars with the different deformation patterns investigated are shown in Figure 4.2. In Table 4.4, measured reinforcing bar properties are compared with ASTM A615-87a values.

For the series in which machined bars were tested, hot rolled carbon steel Grade 1045 was used. Parallel deformations were produced with rib face angles of 30, 45, and 60 degrees. The round stock met ASTM A576-87a[31]. The deformation characteristics of the manufactured bars were designed to duplicate those listed in Table 4.4 for #6 bars. Two manufactured bars with rib face angles of 30 and 60 degrees are shown in Figure 4.3.

Two coupons of each bar size in a given lot were tested to confirm the mill test report obtained from the fabricator. The stress-strain curves are shown in Figures 4.4, 4.5, and 4.6.

A micro-test thickness gage was used to measure the coating thickness of the epoxy-coated bars. The gage and the measuring procedure are shown in Figures 4.7 and 4.8, respectively. Prior to casting, each bar was measured at six places along the marked anchorage length on each side of the bar, a side being considered the area between longitudinal ribs. The average coating thickness for each epoxy-coated bar is shown in Tables 4.1, 4.2 and 4.3. For bars with a nominal coating thickness of 5 mils, the average measured coating thickness ranged from 4.8 to 6.2 mils. The corresponding ranges for bars with 8-mil and 12-mil nominal coating thicknesses were 5.9 to 10.1 mils and 11.5 to 13.4 mils, respectively.

4.2.2 Concrete. Two non air-entrained concrete mixes were ordered from a local ready-mix company and were designed to provide a minimum 28-day compression strength of 4000 and 8000 psi. The maximum size aggregate in both mixes was 3/8 in. Assuming saturated surface dry

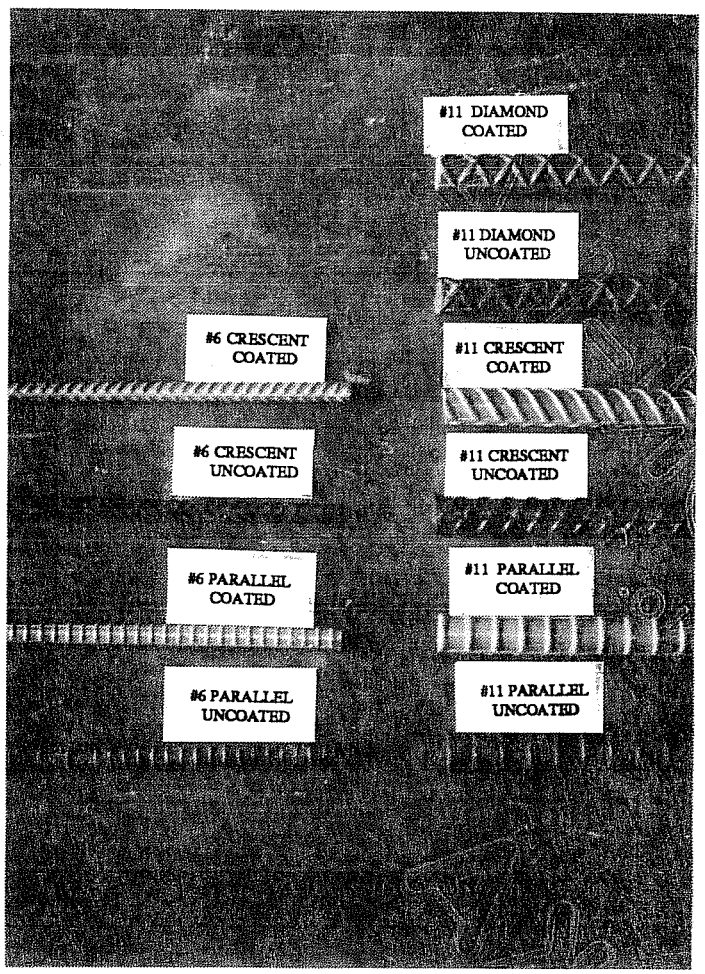

Figure 4.2 Reinforcing bars with different deformation patterns investigated in the test program.

conditions for the aggregates, the mix proportions per cubic yard are shown in Table 4.5. However, the proportions of the mixes delivered varied from the design according to the moisture content of the aggregates. The amount of water was always less than the mix design. Before casting, additional water was added in small increments until a slump of 3.0 to 4.0 in. was reached. The variation of the concrete compression strength with time for the eight series included in the first phase of the project, is shown in Table 4.6.

Table 4.4 Measured properties of #6 and #11 reinforcing bars compared with ASTM A615-87a specifications.

Deformation Properties	#11 Deformed Bars			#6 Deformed Bars	
	Diamond	Parallel	Crescent	Parallel	Crescent
Average Spacing (inch)	0.759(≤0.987)*	0.938(≤0.987)	0.863(≤0.987)	0.490(≤0.525)	0.469(≤0.525)
Average Height (inch)	0.095(≥0.071)	0.075(≥0.071)	0.080(≥0.071)	0.040(≥0.038)	0.038(≥0.038)
Gap (inch)	0.344(≤0.540)	0.234(≤0.540)	0.250(≤0.540)	0.156(≤0.286)	0.125(≤0.286)
Average Rib-Face Angle	26.5°	27.0°	29.5°	36.0°	32.5°

Strength Properties	#11 Deformed Bars			#6 Deformed Bars	
	Diamond	Parallel	Crescent	Parallel	Crescent
Yield Strength (Ksi)	62.8(≥60)	64.0(≥60)	68.1(≥60)	68.2(≥60)	74.7(≥60)
Yield Strain (%)	-	0.22	0.23	0.23	0.25
Ultimate Strength (Ksi)	99.7(≥90)	103.0(≥90)	103.8(≥90)	107.2(≥90)	110.9(≥90)
Ultimate Strain (%)	-	14.4	16.2	15.4	9.6

*Number in parenthesis is ASTM A615-87a specification.

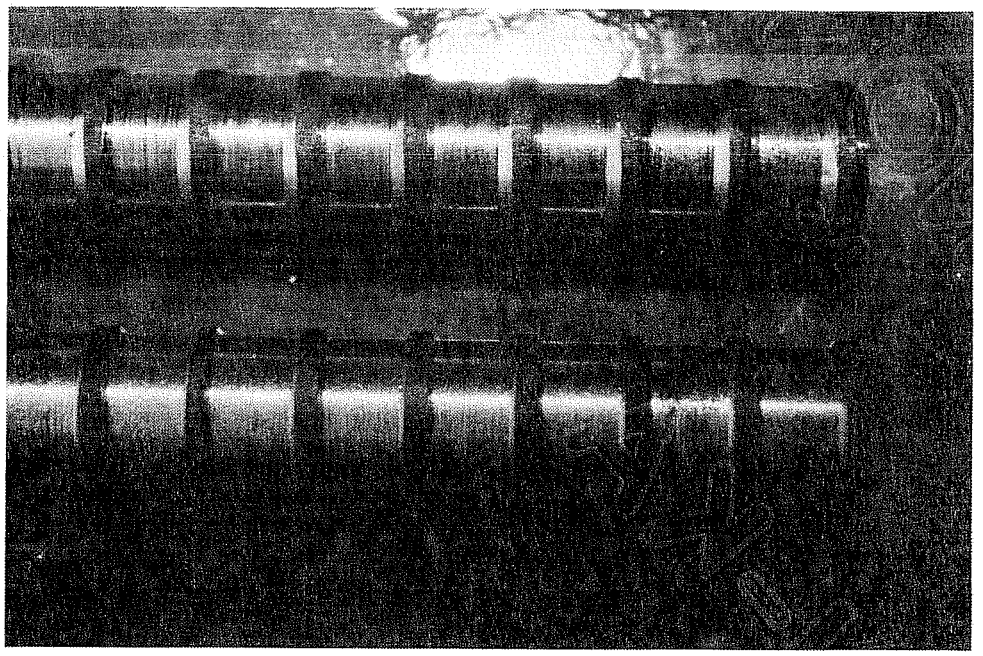

Figure 4.3 Manufactured bars with rib face angles of 30 and 60 degrees.

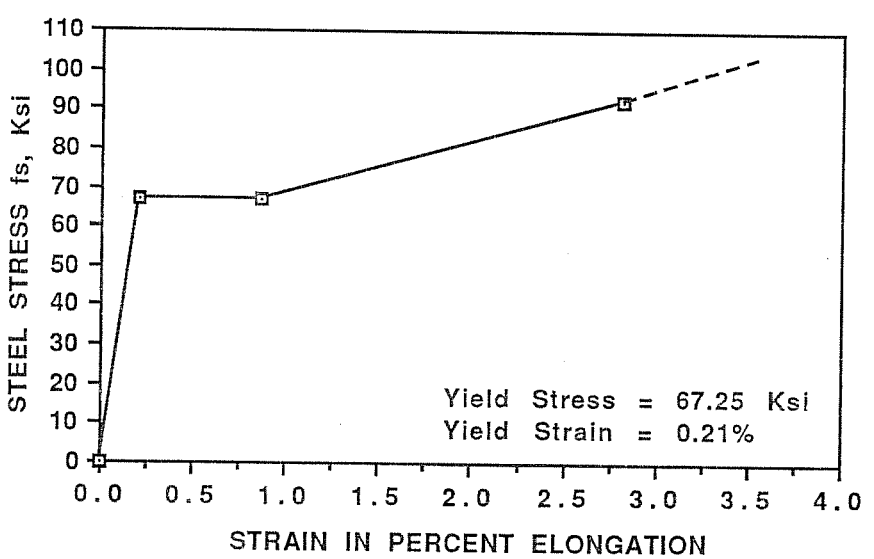

Figure 4.4 Stress-strain curve for the #7 plain round bars.

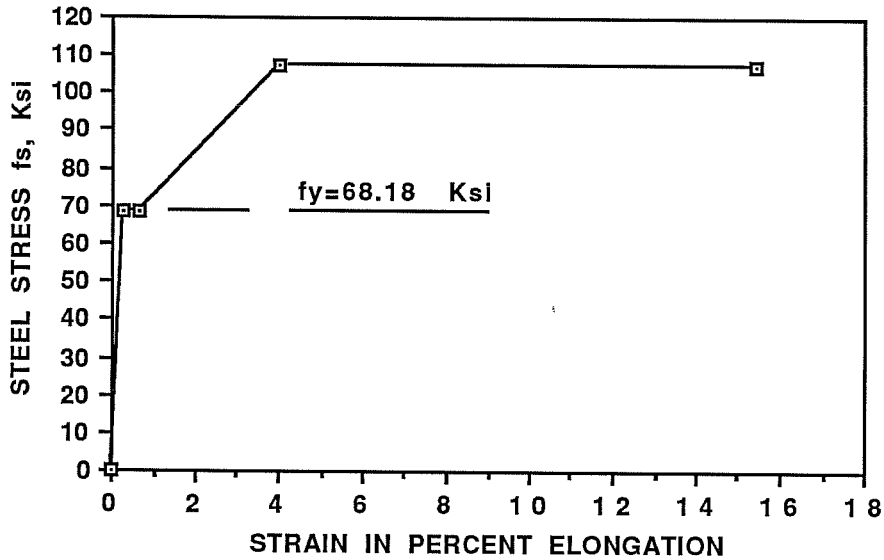

(a) Parallel deformation pattern

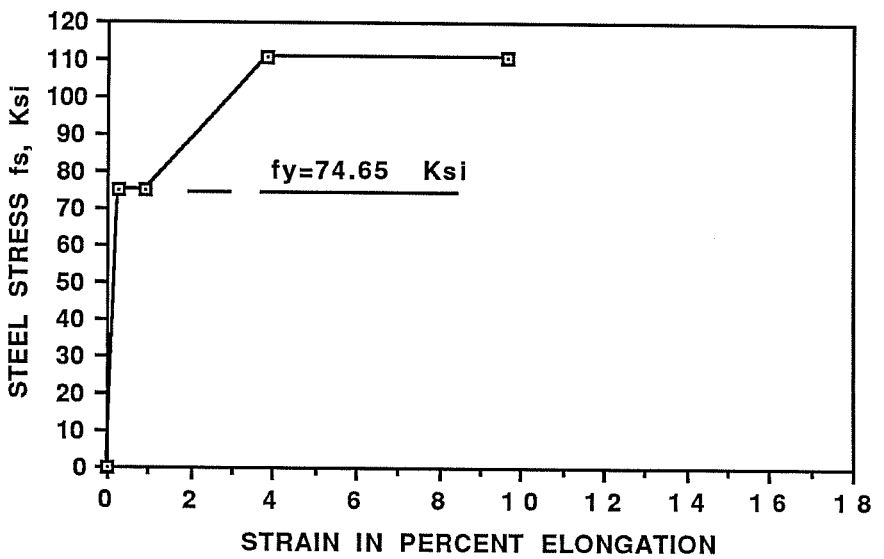

(b) Crescent deformation pattern

Figure 4.5 Stress-strain curves for the #6 bars.

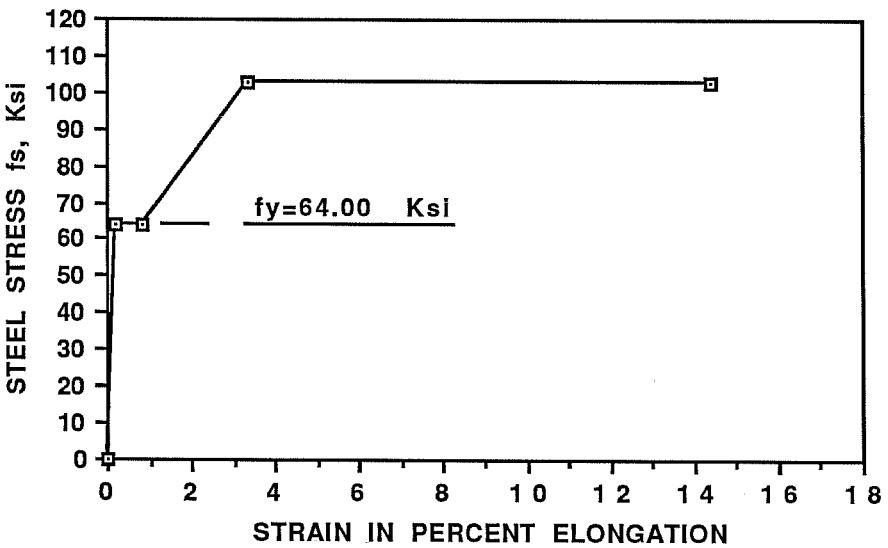

(a) Parallel deformation pattern

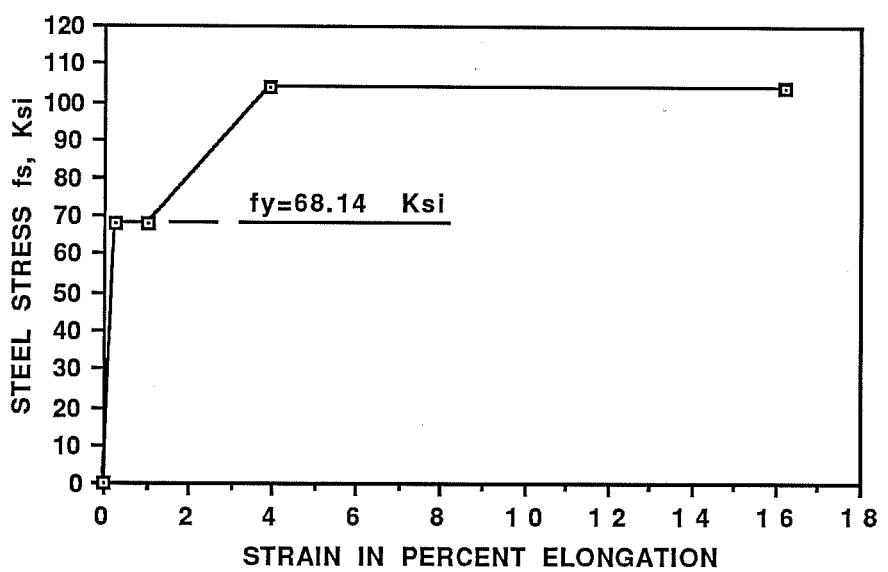

(b) Crescent deformation pattern

Figure 4.6 Stress-strain curves for the #11 bars.

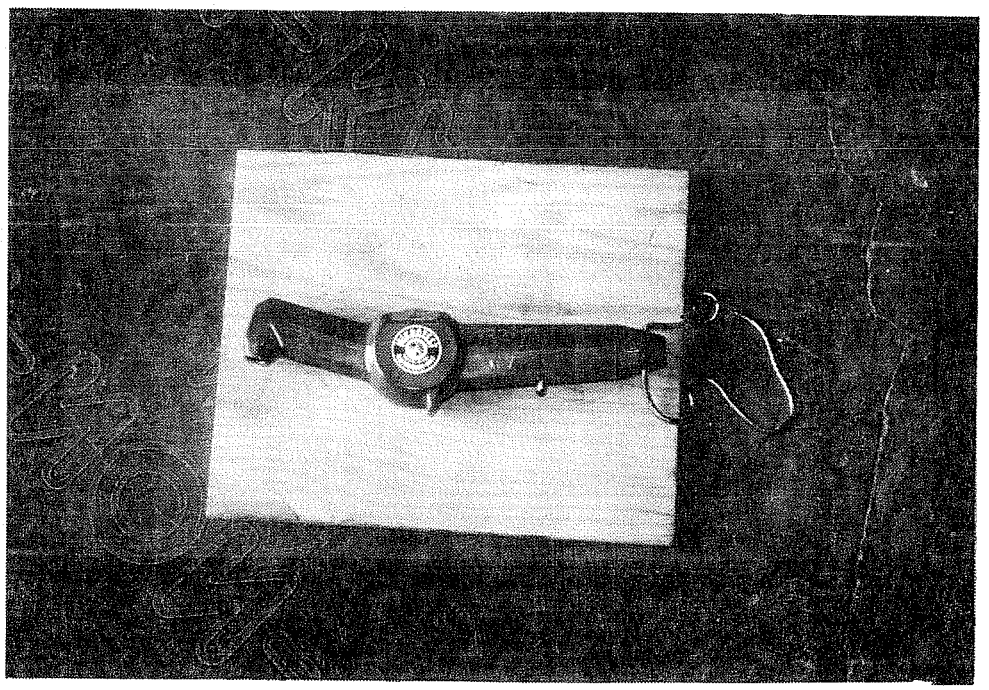

Figure 4.7 Microtest thickness gage used to measure the epoxy coating thickness.

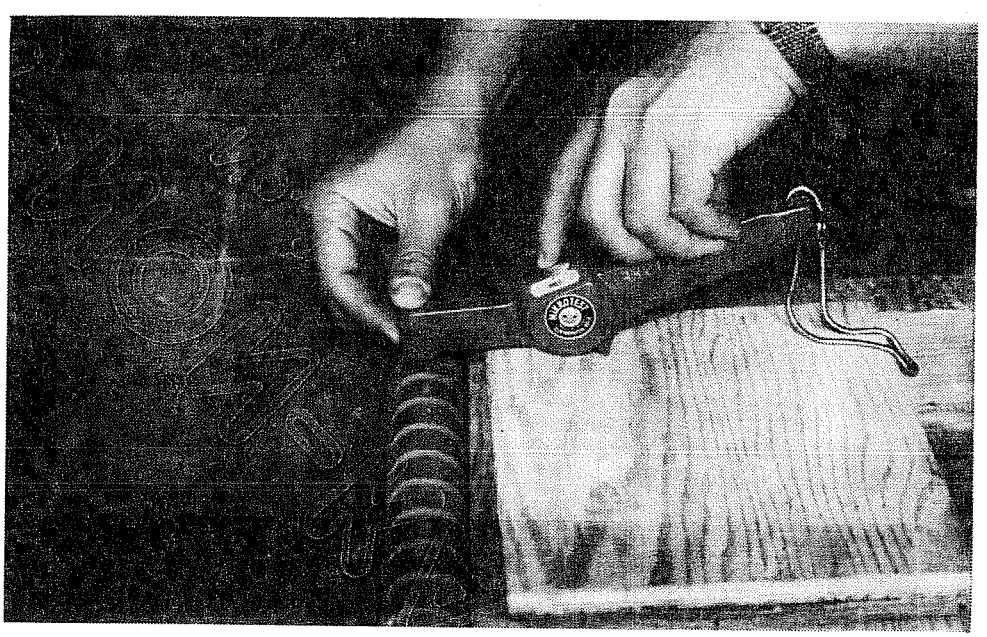

Figure 4.8 Measuring the epoxy coating thickness.

Table 4.5 Concrete mix proportions per cubic yard for the pullout specimens.

	Nominal Concrete Strength	
	4000 psi	8000 psi
Max. Size Aggregate, in.	3/8	3/8
Cement(Type 1), lb.	470	525
Fly Ash, lb.	-	225
Coarse Aggregate, lb.	1625	1790
Sand, lb.	1655	1131
Water, lb.	250	295
Water Reducer Retarder, oz.	20.0	22.5

Table 4.6 Variation of concrete compression strength with time for the pullout specimens.

SERIES NUMBER	CONCRETE COMPRESSION STRENGTH, psi			
	Age=2 days	Age=7 days	Age=14 days	Age=28 days*
ONE	-	3880	4550	5300
TWO	-	3940	4600	5200
THREE	4400	7690	8920	9400
FOUR	-	4360	5090	5400
FIVE	5225	6880	7930	8750
SIX	-	3720	4175	4500
SEVEN	-	4750	5200	5825
EIGHT	-	4300	4900**	5400

* The first six series were tested at 28 days, series SEVEN was tested at 7 days, and series EIGHT was tested at 11 days.

** Strength at 11 days.

4.3 Construction of Specimens

4.3.1 Formwork. The formwork was designed so that twelve specimens could be cast simultaneously from the same batch of concrete. Six formwork bases were built, each with the capacity of holding two #6 or #11 specimens. In general, each formwork unit consisted of a 22-in. x 36-in. base form, two side forms 36-in. wide and 12-in. high, and four end forms 12-in. wide and 12-in. high. This gave each of the two specimens in the unit a 12-in. x 12-in. end cross-section. The end forms were sandwiched between the two side forms in positions that gave each specimen a length of 10 in.

Holes were drilled in the end forms at the required positions. The diameter of the hole was slightly larger than that of the test bar to simplify stripping the form after casting and curing. However, to hold the bar rigidly in place before and during casting, the extra space around the bar in the hole was filled with styrofoam. Also, a small 2 x 2 piece of lumber was bolted to the end forms to act as a seat for the test bar and to keep the cover and height of the bar constant along the anchorage length. A 6-in. long 3/8-in. diameter threaded rod was inserted in the end form at the back of each specimen in the formwork unit. This rod was used later to mount a potentiometer to measure the free-end slip of the bar relative to the concrete block. Three threaded tie-rods provided rigidity and reasonable water-tightness to each formwork unit. The lines of contact of any two form pieces were also sealed with silicon.

Before placing the test bar in the forms, a #3 cage was placed inside the form at about 1 in. below the test bar. The purpose was to provide the concrete block with restraint against splitting due to the compression force applied on the block while pulling the bar during the test. The cage consisted of three #3 stirrups spaced at 4-in. on centers and hooped around four 8-in. long #3 bars at the corners (refer to Figure 4.1).

Details of one formwork unit, built for two Type A pullout specimens, are shown in Figure 4.9. The test bar was placed in the form with the longitudinal ribs in a horizontal plane and no mill

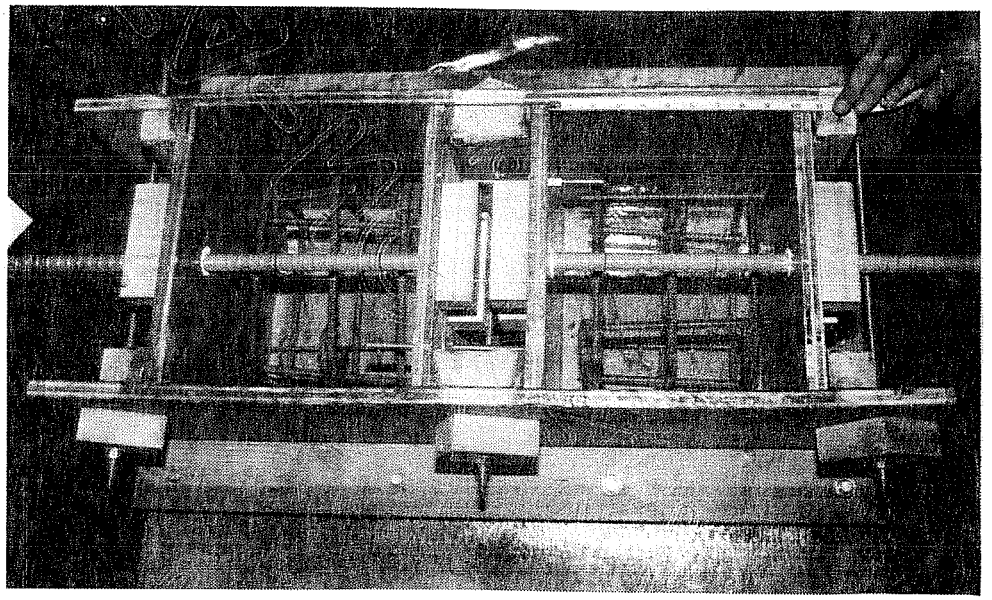

(a) Top view

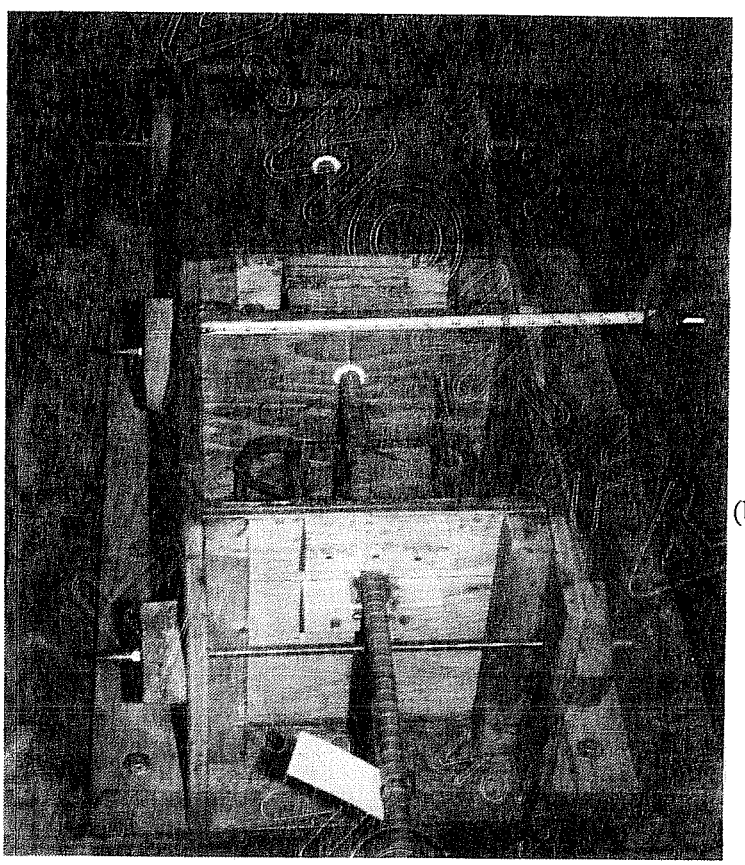

(b) End view

Figure 4.9 Formwork details of Type A pullout specimen.

markings along the anchorage length. Also, two steel wires were hooked on the test bar and anchored inside the core of the specimen. Their purpose was to prevent the bar, which had only the bottom half surface embedded in the concrete, from getting loose during stripping of the form after casting and curing. This problem was especially critical in the case of epoxy-coated bars which have no adhesion with the concrete.

To form the desired wedge in the formwork of Type A pullout specimens, a 2-in. deep styrofoam block was snugged on top of the test bar. A groove was formed at the bottom surface of the block so that it would cover the top surface of the test bar. The details of the styrofoam block are shown in Figure 4.10. An overall view of the six formwork units designed for Type A pullout specimens, with the styrofoam blocks in place, is shown in Figure 4.11. To protect the styrofoam block while casting, a 5 in. x 16 in. piece of plywood was placed on top as shown in Figure 4.12.

Details of one formwork unit built for two Type B pullout specimens are shown in Figure 4.13. No steel wires or styrofoam blocks were required for this type of specimens. In the sixth series, the top concrete cover was either 2 in. or 3 in. In the eighth series, the cover was held at 2 in. and a #2 or #3 Grade 60 deformed bar was hooked over the bar at the middle of the anchorage length as shown in Figure 4.13.

4.3.2 Casting. All specimens of the same series were cast from the same batch of concrete. After a slump of 3.0 to 4.0 in. was achieved, concrete was poured from the ready-mix truck into wheelbarrows. Shovels were used to place the concrete properly in the forms. Concrete was cast in two lifts in each specimen. One person was assigned the compaction and vibration to ensure that the concrete placed in each specimen was of the same consistency. Care was taken in the insertion and removal procedures of the vibrator and in the duration of the insertion to avoid as much as possible the formation of air bubbles around the anchored bar which would hurt the bond.

As the specimens were cast, concrete was also placed in 6 x 12 cylinder molds. At the end of the casting procedure, the top surface of each specimen was screeded and trowelled smooth, and lifting hooks were inserted (see Figure 4.12). The specimens were then covered with wet burlap and plastic sheets. The 6 x 12 cylinders were also covered with plastic caps. The forms were stripped three to seven days after casting except for the two series with high strength concrete which were cured for seven days by keeping the burlap continuously wet. The 6 x 12 cylinders were stripped on the same day as the specimens.

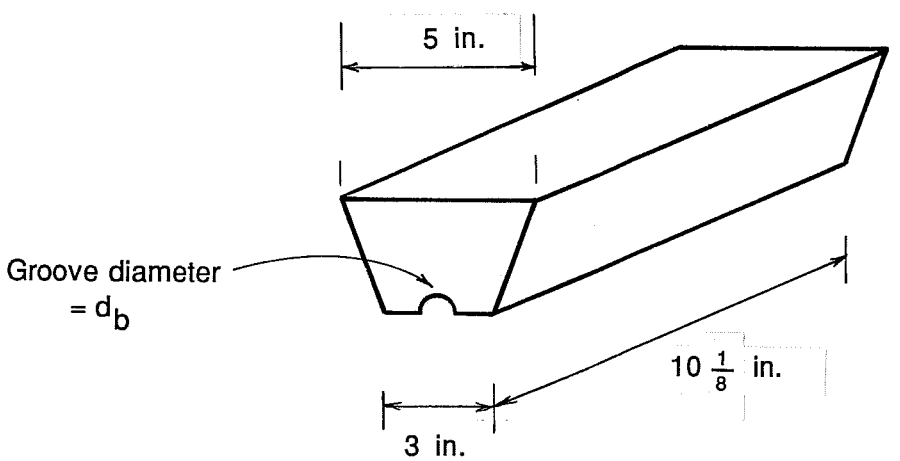

Figure 4.10 Geometry of the styrofoam block used to form a wedge in Type A pullout specimens.

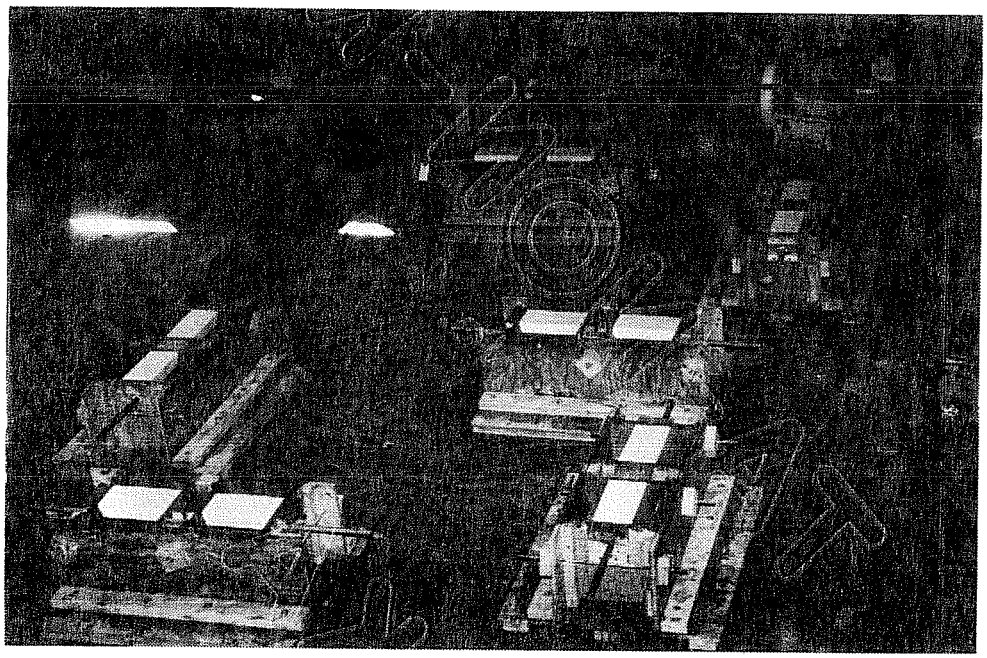

Figure 4.11 Overall view of the formwork built for Type A pullout specimens.

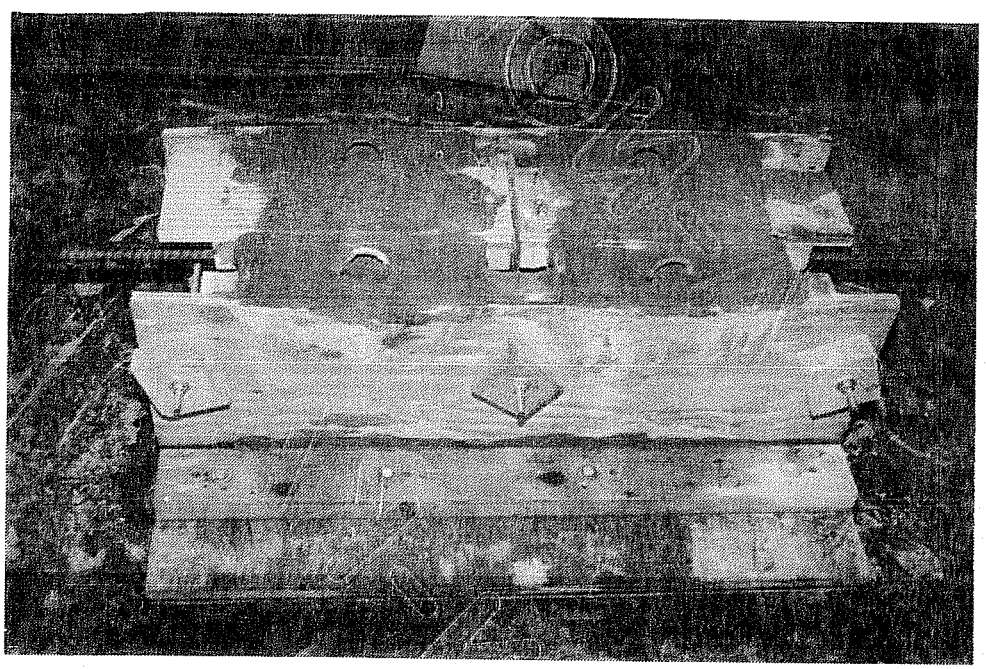

Figure 4.12 Concrete cast in a Type A pullout specimen formwork unit.

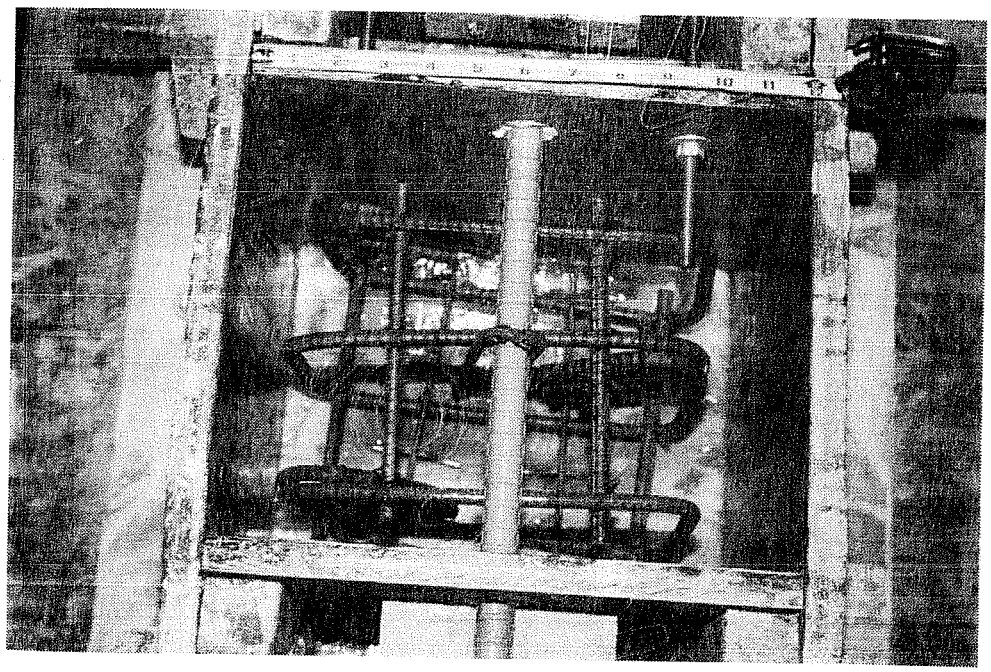

(a) Top view

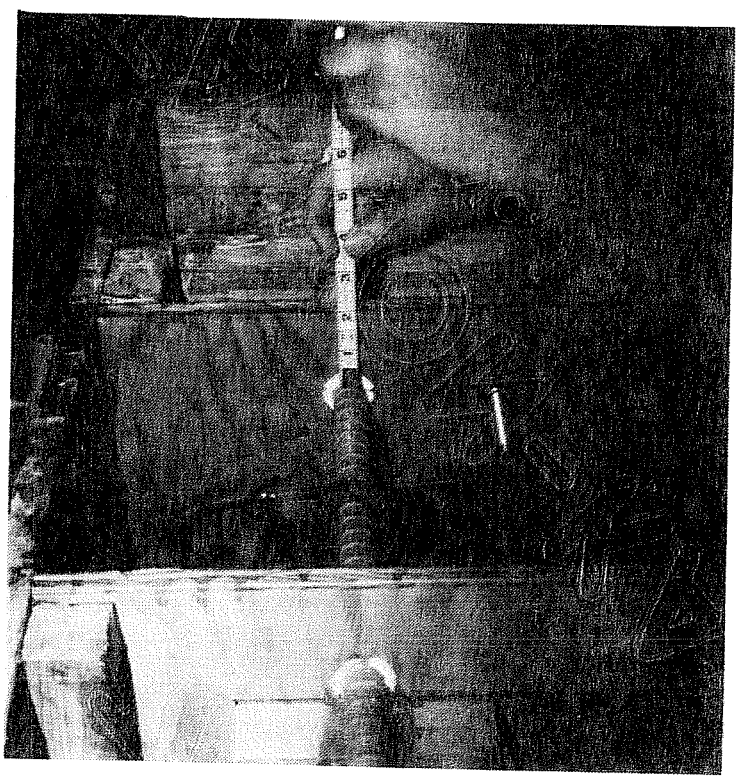

(b) End view

Figure 4.13 Formwork details of Type B pullout specimens used in the eighth series.

4.4 Test Frame

Schematic front and side view of the test frame used for Type A pullout specimens are shown in Figures 4.14 and 4.15. Before placing the specimen in the test frame, the styrofoam wedge block was removed. Care was taken not to harm the bar which had only the bottom surface embedded in the concrete. The test specimen was then seated in the frame on a 1-in. thick base plate. The plate was supported on three steel beams laid on the reaction floor. A test specimen placed in the test frame is shown in Figure 4.16.

The confining top load was applied before the pulling load setup was mounted on the anchored bar. This would eliminate the danger of loosening the bar and breaking the bond by cantilever action. A small layer of hydrostone was placed on top of the exposed surface of the anchored bar to secure the uniformity of the confining distributed top load. The top load was applied by means of a 20-ton, single-action, spring-return hydraulic ram operated by a hydraulic pump. The ram had a 4.72-sq. in. effective area and a 2.0-in. stroke. The transfer of load from the ram to the bar was done through a 1-in. thick 10-in. x 3-1/2-in. steel plate. The plate had a 5-in. long 7/8-in. diameter steel handle bar welded to it and inserted inside the center hole of the ram. The ram was bolted to a 3/4-in. thick steel plate which was welded to the bottom of two 5 x 3 structural steel tubes. Each tube was fitted over two 1-in. diameter threaded rods and held in the required position by means of threaded nuts. Four springs with a stiffness of 2 kips/inch were fitted over the threaded rods and seated over the structural tubes. Threaded nuts were positioned over the springs. The role of the springs was to maintain the confining top load constant while the bar rode over the concrete during pullout.

The top load was monitored by an electronic 5000 psi pressure transducer read in micro-strains with a portable, solid state digital strain gage indicator. Hydraulic hose pressure was also measured at the pump by a 5000 psi pressure gage. The calibrations of the pressure transducer and

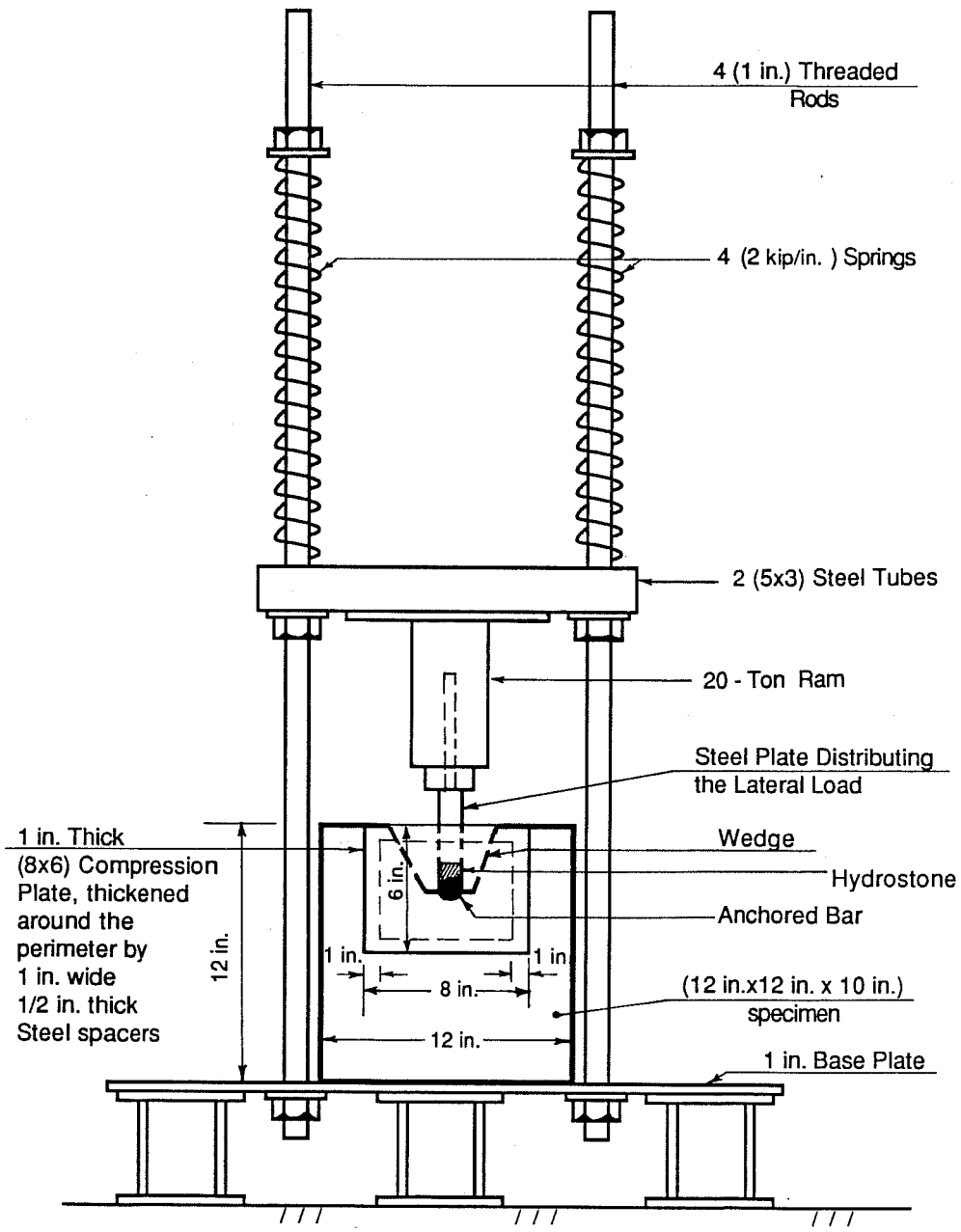

Figure 4.14 Schematic of the test setup of Type A pullout specimens, front view.

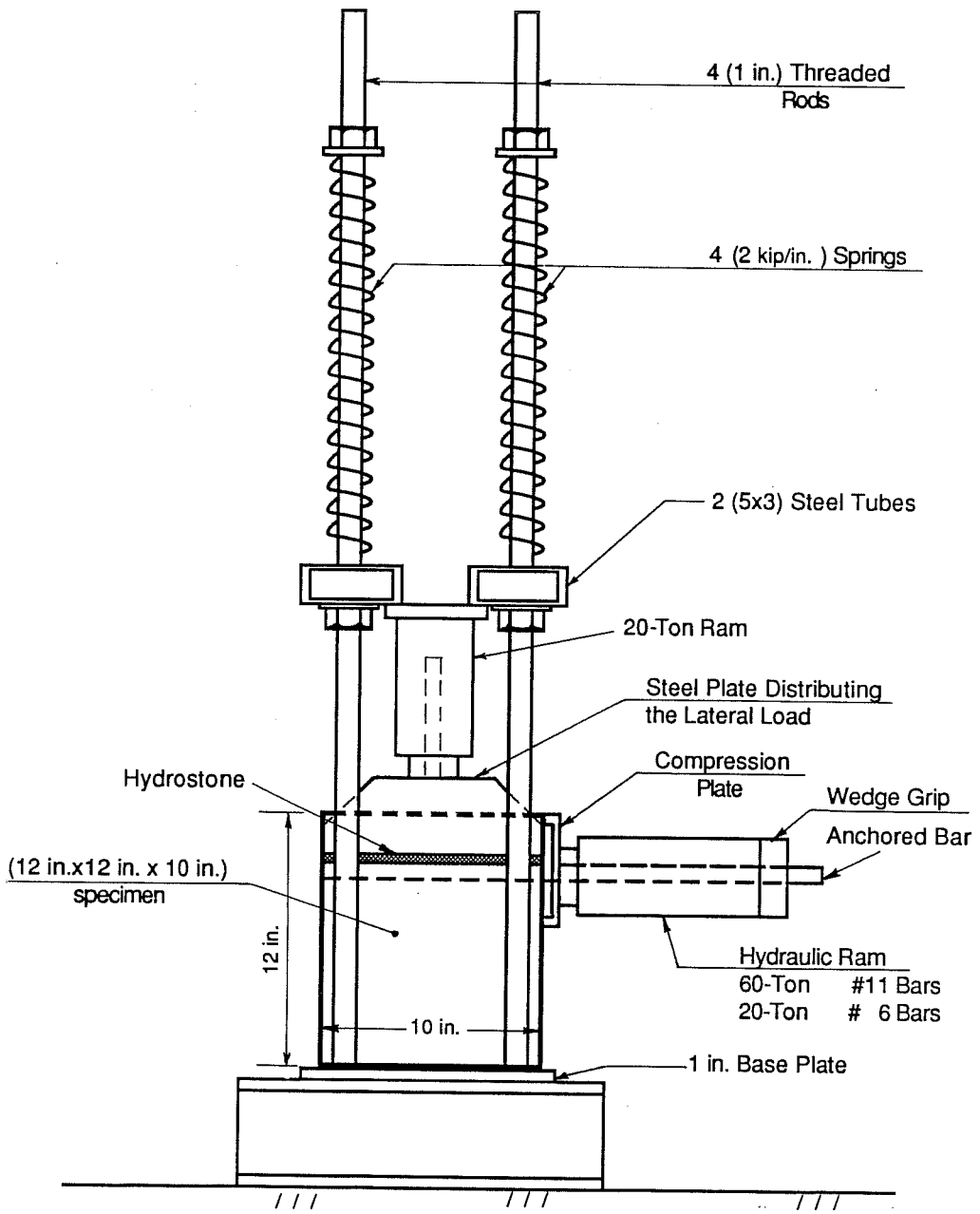

Figure 4.15 Schematic of test setup of Type A pullout specimens, side view.

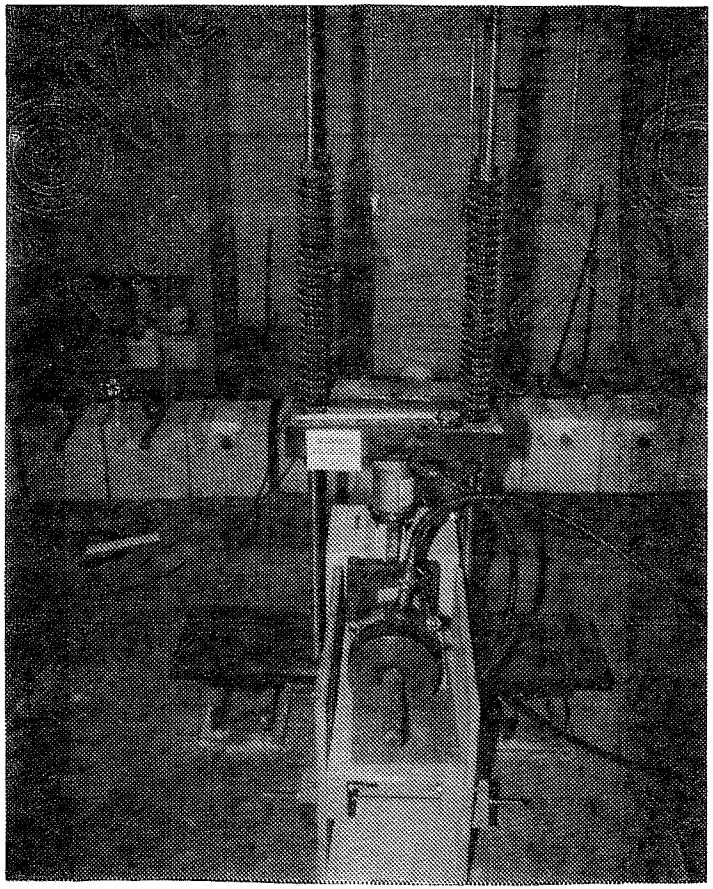

(a) Front view

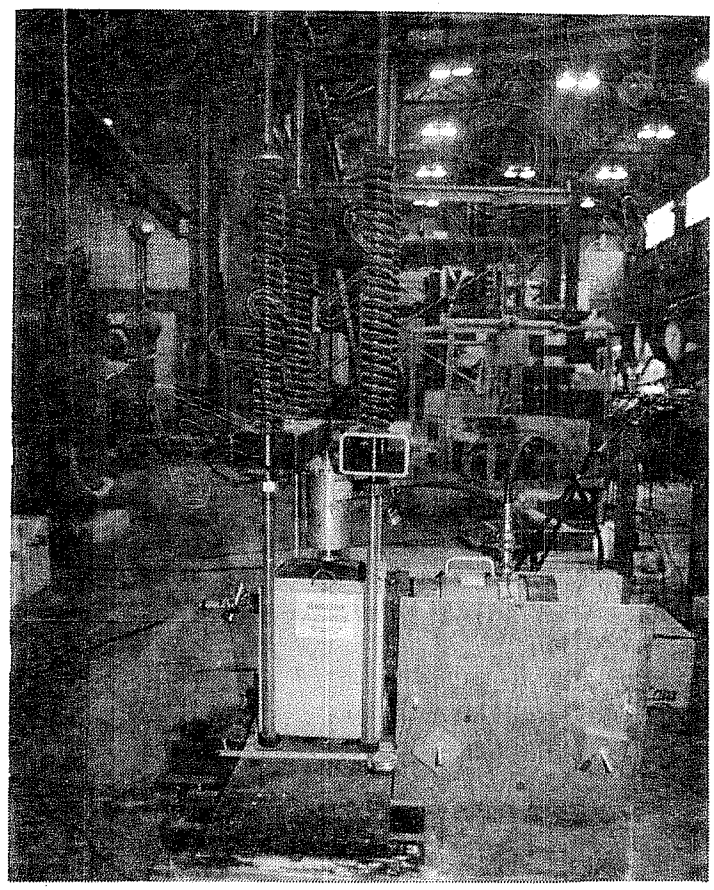

(b) Side view

Figure 4.16 Test frame used to test the Type A pullout specimens.

pressure gage were done in a 60 kip universal testing machine. A flow chart of the top load setup is shown in Figure 4.17.

After the application of the top load, which would be held constant throughout the test of Type A pullout specimens, the pulling load setup was mounted on the anchored bar and seated on a wood frame. The setup consisted of a hydraulic ram through which the tensile load was applied. The ram was centered on the test bar and operated by a hydraulic pump. The ram load was transferred to the test bar by means of a wedge grip assembly. The assembly is shown in Figure 4.18 mounted in the test frame with wedges gripping the bar. The wedge grips used for the #6 and #11 bars are shown in Figure 4.19. While pulling on the bar, the ram was designed to bear against the concrete block through a 1-in. thick 8-in. x 6-in. steel plate. To keep the compression zone in the concrete as far away from the test bar as possible, the plate was thickened all around its perimeter, in contact with the concrete, by 1-in. wide and 1/2-in. thick steel spacers (see Figures 4.14 and 4.15).

The same test frame, excluding the top load setup, was used for the Type B pullout specimens. The top load was not needed since confinement to the anchored bar in Type B specimens was provided by concrete cover and transverse reinforcement.

In all test specimens, Type A and Type B, a plunger-type precision potentiometer was used to measure the free-end slip of the anchored bar relative to the concrete block. The potentiometer was mounted on the 3/8-in. threaded rod which was inserted into the back of the concrete block as shown in Figure 4.20. The plunger of the potentiometer rested against the end cross-section of the bar.

4.5 Test Procedure

The hydraulic ram used to test the #11 bar specimens had a 60-ton capacity, a 6.0-in. stroke, and a 13.75-sq.in. effective area. On the other hand the ram used to test the #6 bar

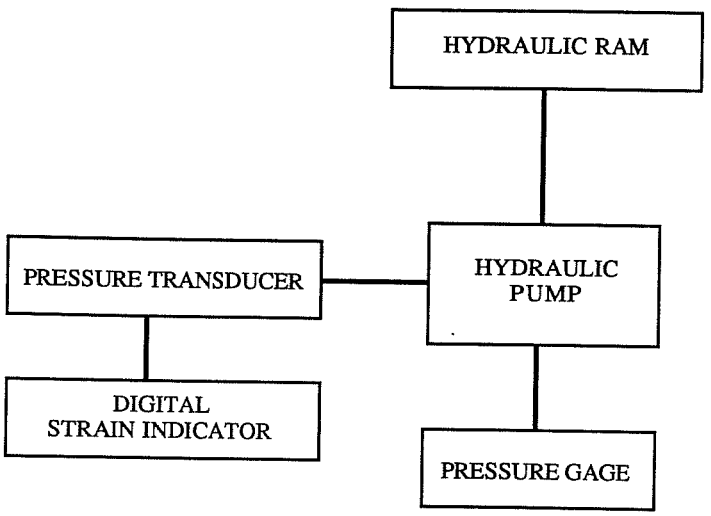

Figure 4.17 Flow chart of the top load setup for Type A pullout specimens.

specimens had a 20-ton capacity, a 2-in. stroke, and a 4.72-sq.in. effective area. Both hydraulic rams were of the single-action, spring-return type.

The tensile-load applied by the hydraulic ram was monitored by an electronic pressure transducer read in micro-strains with a portable solid state digital strain gage indicator. Hydraulic hose pressure was measured at the pump by a pressure gage. The pressure transducer and pressure gage used to test the #11 bar specimens had a 5000-psi capacity whereas those used to test the #6 bar specimens had a 10,000-psi capacity. The instrumentation was calibrated in a 60 kip universal testing machine.

The tensile load was gradually applied in 1.0-kip increments until bond failure occurred. At each load stage, the maximum load was read. A constant voltage was maintained across the potentiometer which allowed the change in resistance to be converted into deformation. The

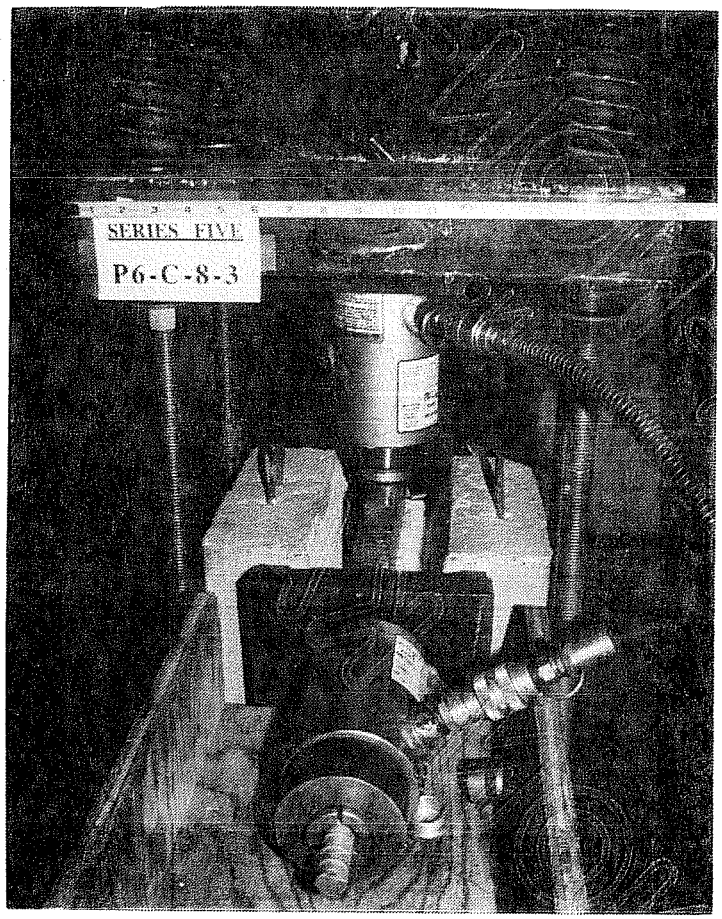

Figure 4.18 Wedge grip assembly mounted in the test frame.

potentiometer voltage was measured at every load stage and read by a digital voltmeter to 0.0001 volts.

During each test, the pullout load was plotted against the free-end slip using an X-Y plotter. The load was monitored by a calibrated electronic 10,000 psi pressure transducer connected to the pressure line. The potentiometer, the voltage of which was read by a digital voltmeter, was also connected to the X-Y plotter to monitor the slip.

After the ultimate load was reached, the test was not halted. Further deformation was imposed and corresponding values of load and free-end slip were recorded at various stages.

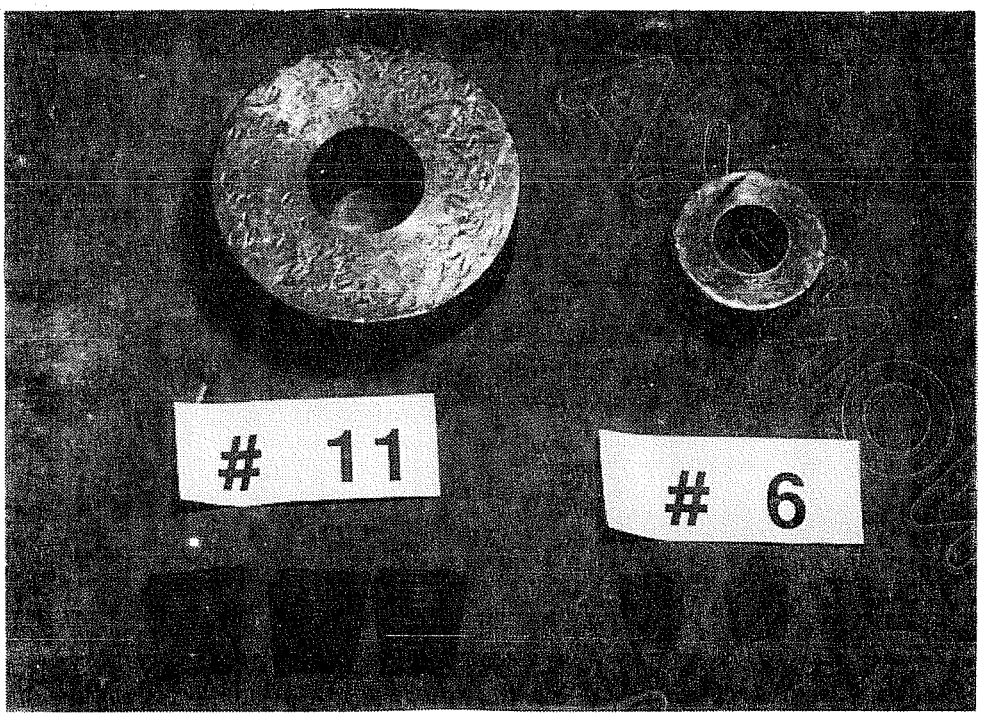

Figure 4.19 Wedge grips used for the two bar sizes investigated.

However, in the case of Type B pullout specimens, failure was brittle and the load dropped completely.

It is important to note that during the testing of Type A pullout specimens, the pressure line of the hydraulic ram applying the confining top load was closed. However, due to the tendency for this load to drop slightly, continuous observation of the load level was exercised during the test. At any drop the pressure line was opened, deformation was increased to achieve the required level, and the line would be closed again.

An overall view of the test setup and the instrumentation used is shown in Figure 4.21. A flow chart of the tensile loading and slip potentiometer setup is shown in Figure 4.22.

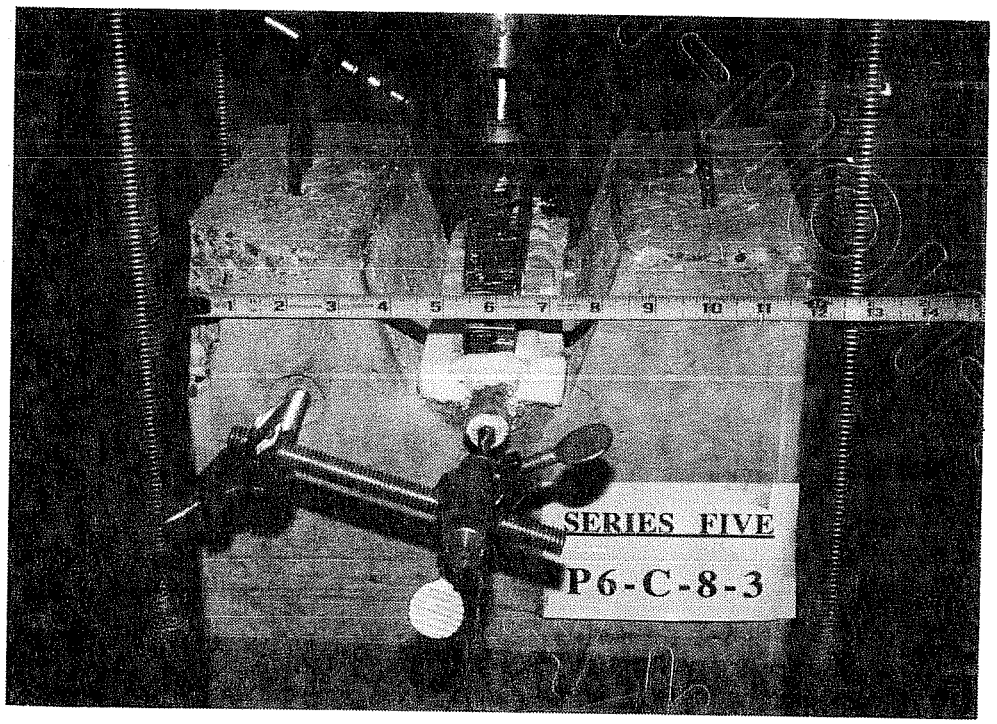

Figure 4.20 Slip potentiometer setup at the free end of the bar in Type A pullout specimen.

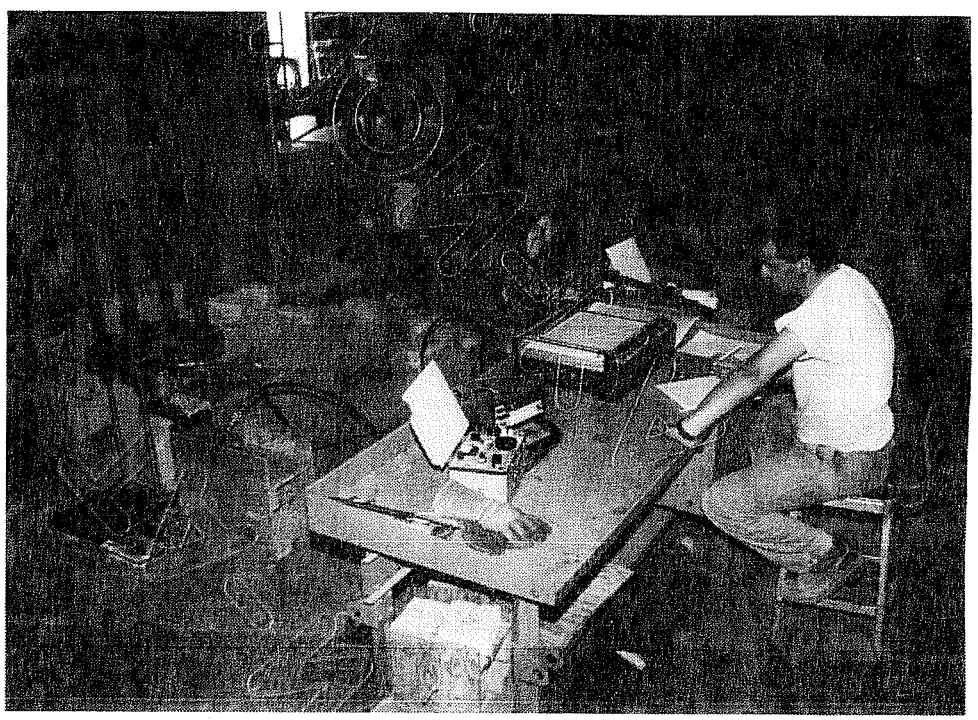

Figure 4.21 Overall view of the test setup of the pullout specimens.

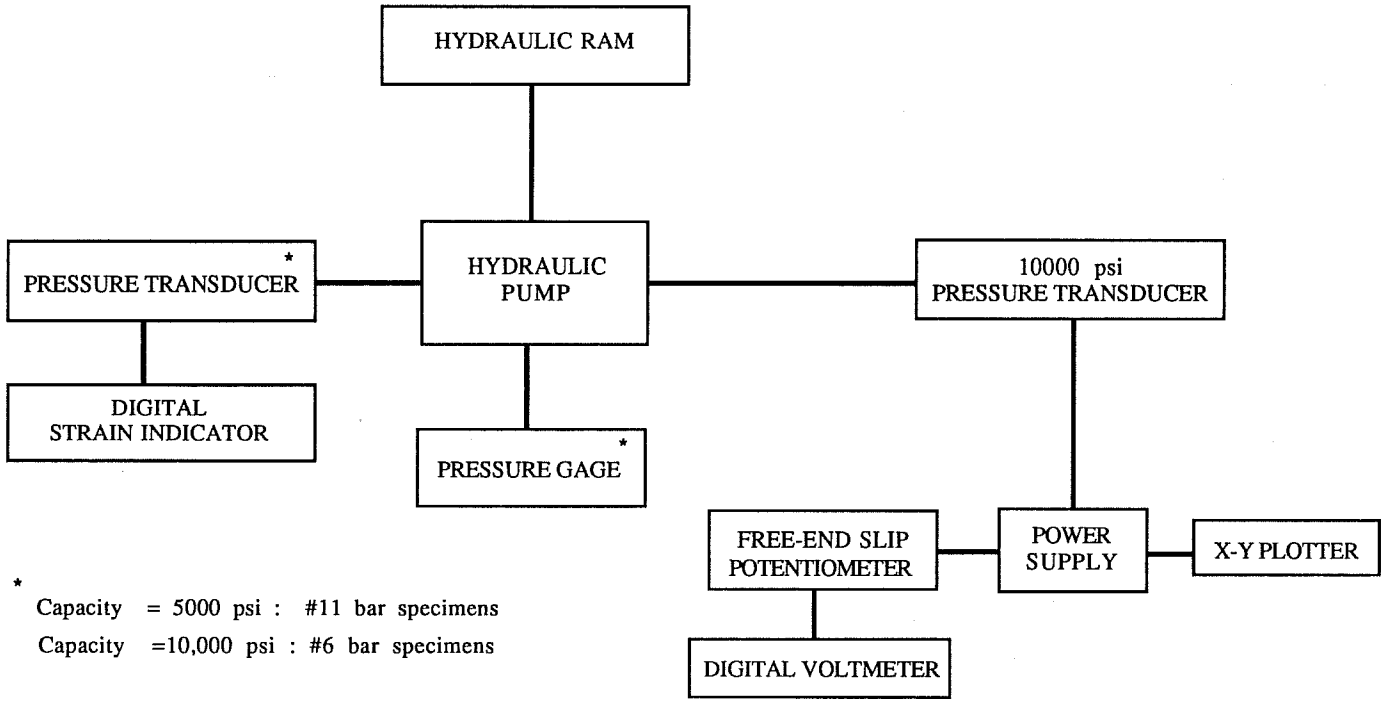

Figure 4.22 Flow chart of the tensile load and slip potentiometer setup of Type A and Type B pullout specimens.

CHAPTER 5

FUNDAMENTAL BOND STUDIES OF EPOXY-COATED BARS - SPECIMEN BEHAVIOR AND ANALYSIS OF TEST RESULTS

5.1 Introduction

The results of pullout tests are presented, compared, and evaluated in this chapter. Since the general mode of failure was similar, the results can be compared directly. The primary variables for Type A tests (only half the bar was embedded in concrete) were the level of the confining top load, coating thickness, bar deformation pattern, bar size, concrete strength, and bar rib face angle. For Type B tests, the bar was completely embedded in concrete. The primary variables were the amount of concrete cover above the reinforcing bar, transverse reinforcement, and coating versus painting application. The transverse reinforcement took the form of a #2 or #3 tie at the middle of the embedment length.

The effect of each one of the variables on the bond performance of epoxy-coated bars relative to uncoated bars is discussed and assessed. The bond performance is studied in terms of ultimate steel stresses, free-end slips at ultimate, steel stresses at a critical level of free-end slip (0.002 in.) and load-slip behavior.

It is important to note that in each of the first five series, it took about one week to test all twelve specimens cast from the same batch of concrete. Since testing was done after the concrete was at least twenty-eight days old, the change in concrete compression strength from one specimen to another was minimal. The specimens in the remaining three series were all tested on the same day. Therefore, no adjustment for changes in concrete strength in a given series was needed.

5.2 General Load-Slip Behavior

5.2.1 Type A Pullout Specimens. In earlier trial specimens, both loaded-end and free-end slip of the reinforcing bar were monitored. In tests with long embedment lengths, slip at the free end coincides with bond deterioration and indicates that the bar is close to failure and the stress transfer mechanism is no longer effective. However, very little difference was noted between the loaded- and free-end slip mainly due to the short embedment length, 10 in. Therefore, only the free-end slip was measured.

For most specimens in the first five series, the free end slipped at an early stage after only a few increments of tensile loading. At higher levels of loading (50 to 60% of ultimate), the bar began to ride over the concrete keys between the lugs and the stiffness of the load-slip curve decreased. Large free-end slip values were then measured in each load increment. Typical load-slip curves of #6 and #11 uncoated and epoxy-coated bars are shown in Figures 5.1 and 5.2. The loss of stiffness was noted earlier and was larger for epoxy-coated bars than for uncoated bars, and for bars with a crescent deformation pattern as opposed to parallel or diamond deformation patterns. The above trend was noticed for both #11 and #6 bars regardless of the concrete strength or the level of the top load.

After reaching ultimate, the load dropped rapidly. The drop in the load, as a percentage of ultimate, was larger for #6 bars than for #11 bars regardless of the deformation pattern, concrete strength, or top load level. This is probably due to the smaller height of the #6 bar lug above the bar surface (see Table 4.4), which would make it easier for the bar to ride over the concrete key. The test was not stopped after reaching the ultimate load level. An increase in deformation (slip) was accompanied by a more gradual drop in the tensile load. For the #6 bars, the load increased again at slip values of 0.4 in. as indicated in Figure 5.1. The slip increment between the first ultimate peak and the second peak was approximately equal to the average spacing between the bar ribs (about 0.5 in.). For the #11 bars, the test was stopped just when the stiffness

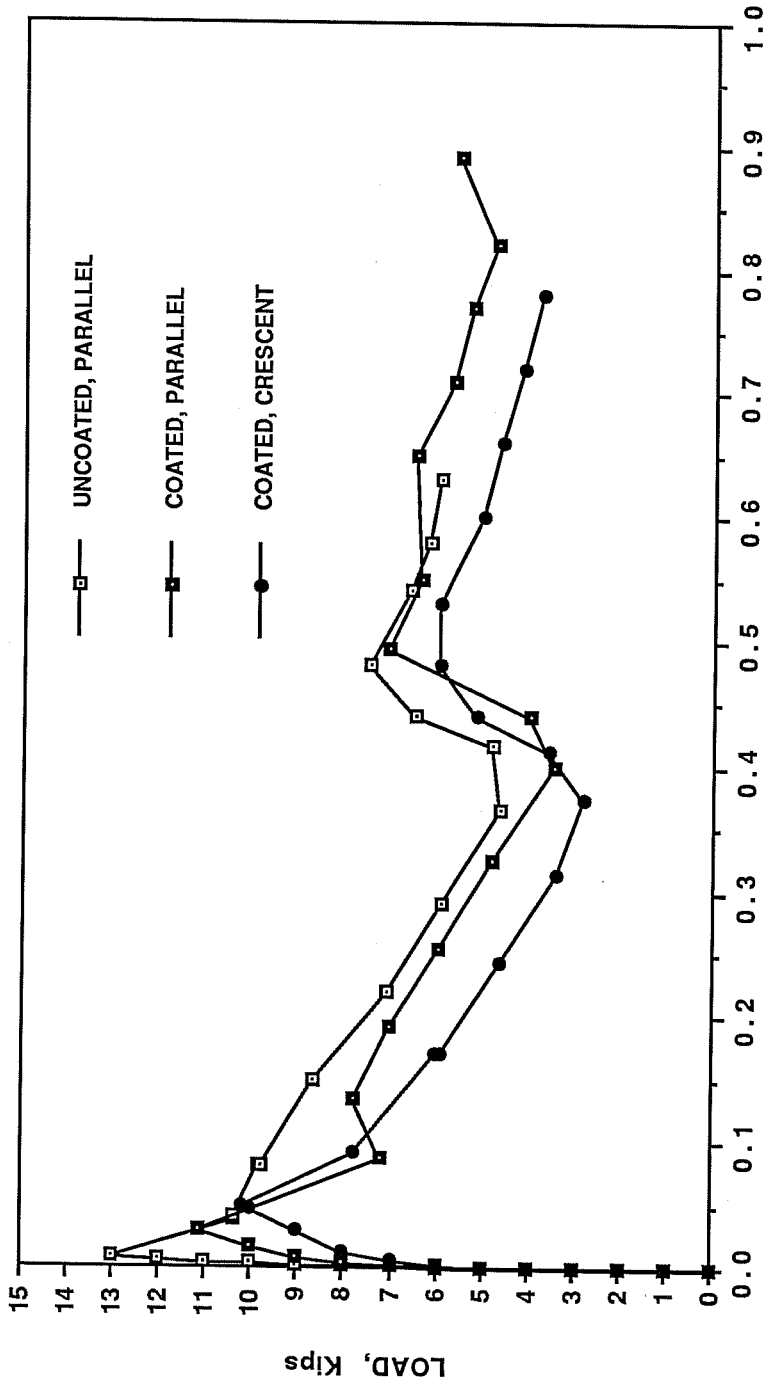

Figure 5.1 Comparison of load-slip curves for #6 bars, top load = 5 kips, f'_c = 5400 psi.

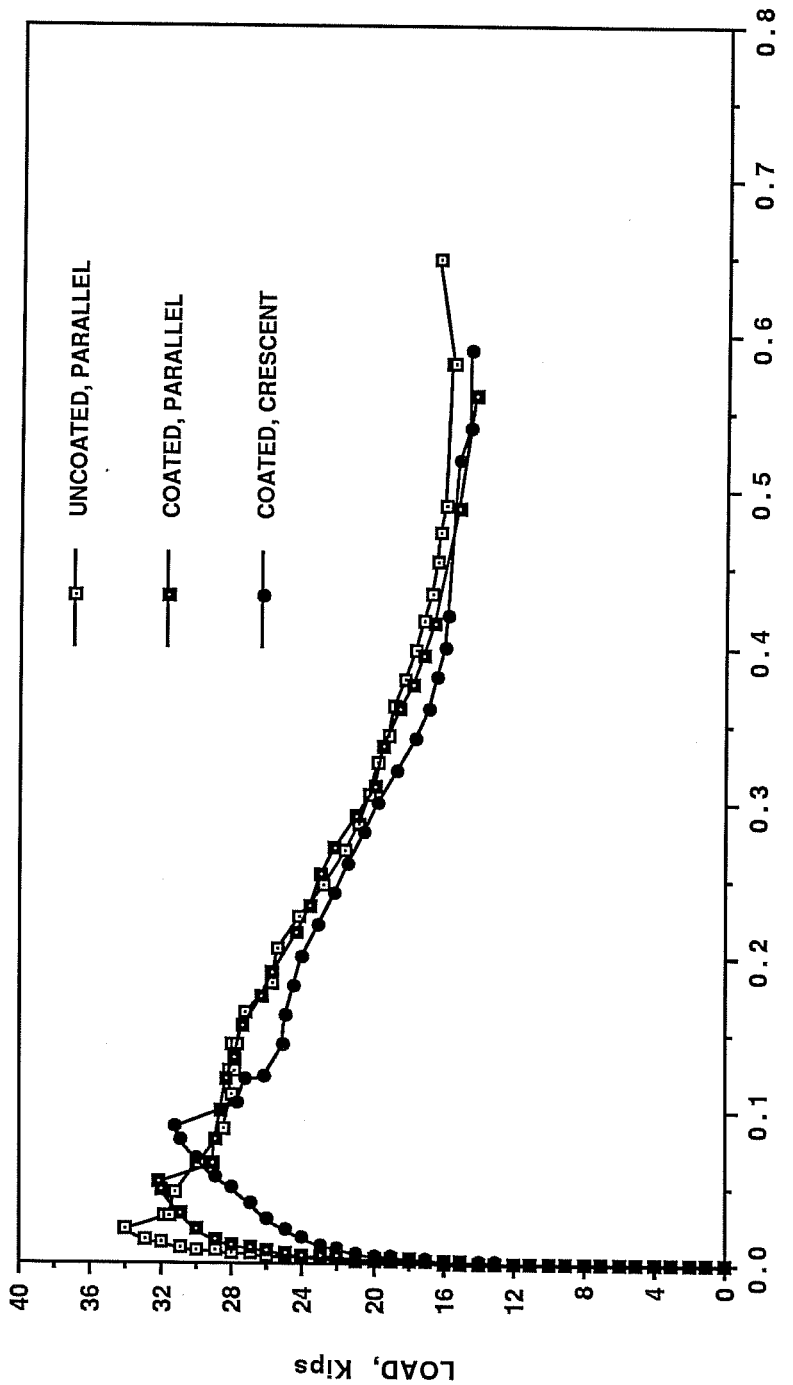

Figure 5.2 Comparison of load-slip curves for #11 bars, top load = 20 kips, f'_c = 5200 psi.

increased slightly (see Figure 5.1). Had large deformations been imposed, it is likely a second peak would have been reached at about 1.0-in. slip. It should be noted that the measured slips are much greater than the slip values which would be expected under any severe loading on a structure or even at regions of distress in a typical subassemblage tested to failure.

In the Type A specimens with bars machined to different rib face angles (30, 45 and 60 degrees), the load-slip history and behavior of all uncoated and epoxy-coated manufactured bars were similar to those of the #6 deformed bars discussed before. The only exception is that the loss of load-slip stiffness of the uncoated bars did not start until just before failure. Typical load-slip curves of one uncoated and one epoxy-coated manufactured bars are shown in Figure 5.3.

It is important to note that throughout any Type A test, the top load was maintained at a constant level. Even when the reinforcing bar was riding over the concrete keys, the four springs kept the top load level almost constant.

5.2.2 Type B Pullout Specimens. The free-end slip of all #6 bars in Type B specimens started at very early stages of loading. Typical load-slip curves of uncoated, epoxy-coated, and painted #6 bars are shown in Figure 5.4. The load-slip stiffness started decreasing at 10 to 40% of the ultimate load with larger amounts of slip recorded per load increment than at the beginning of loading. For painted bars, free-end slip even started with the very first load increment and progressed at a faster rate than epoxy-coated bars. This is due to the softness of the latex painting as compared to the hardness of the fusion-bonded epoxy coating. In all Type B tests the load dropped completely after reaching ultimate.

5.3 Mode of Failure

5.3.1 Type A Pullout Specimens. After a Type A test was halted, the tensile loading frame mounted on the reinforcing bar was removed and the cracking or failure pattern was

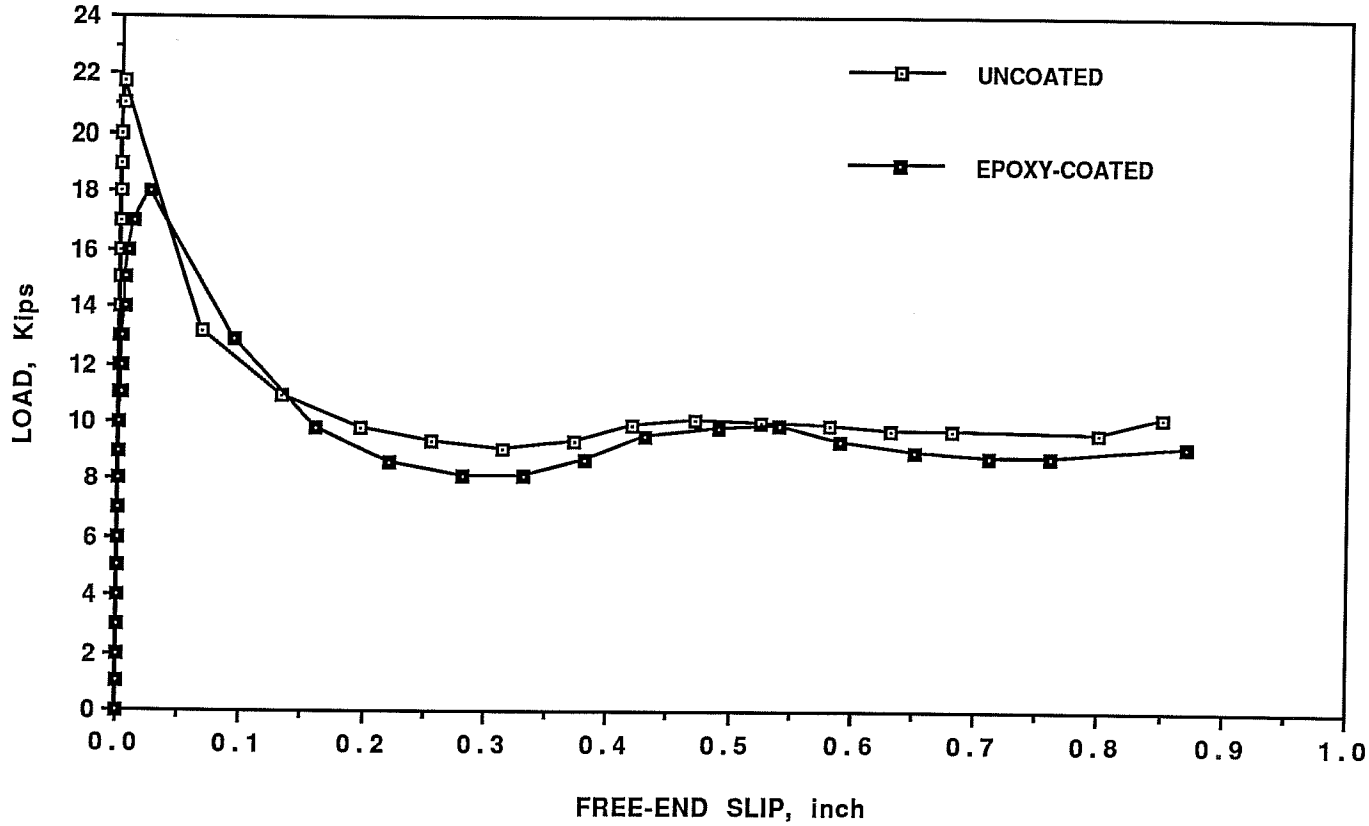

Figure 5.3 Comparison of load-slip curves for the manufactured bars of series SEVEN, rib face angle = 60°, top load = 10 kips, concrete strength = 4750 psi.

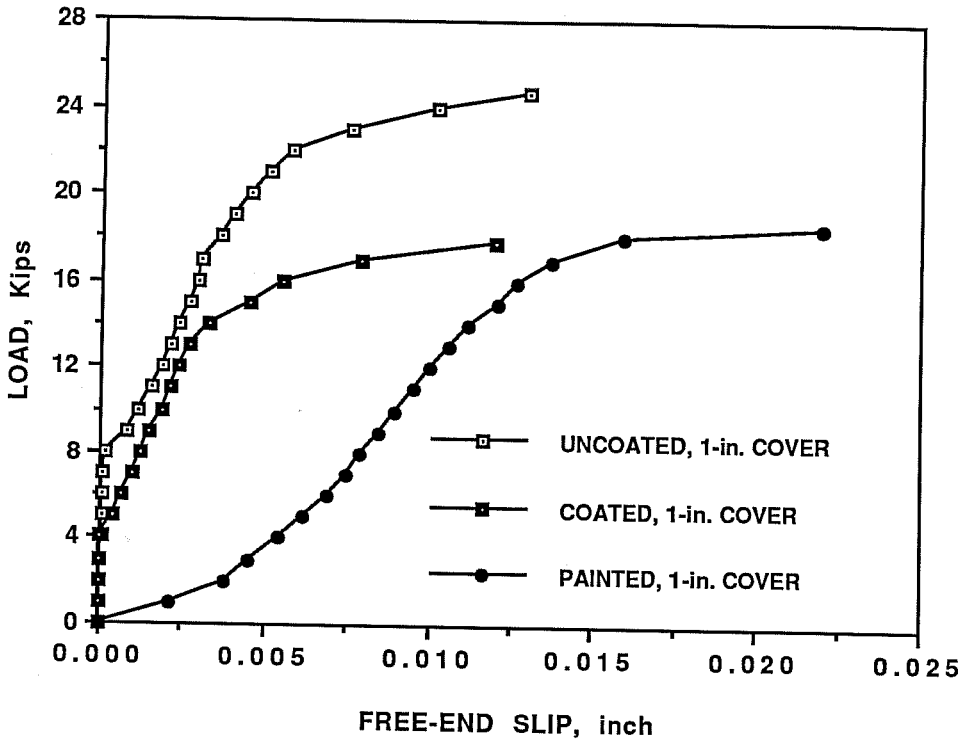

Figure 5.4 Comparison of load-slip curves for #6 bars, parallel deformation pattern, Type B specimens, f'_c = 4500 psi.

examined. In all Type A specimens the bars pulled out a cone of concrete which was defined by the edges of the loading plate as shown in Figure 5.5

After the specimen was removed from the test frame, the bar was carefully removed from the specimen to examine the appearance of the interface between the concrete and the bar. In Figure 5.6, the bottom surfaces of #11 bars with different deformation patterns are shown after failure.

The following observations can be made on the effect of various variables on the failure pattern and appearance of Type A pullout specimens of the first five series:

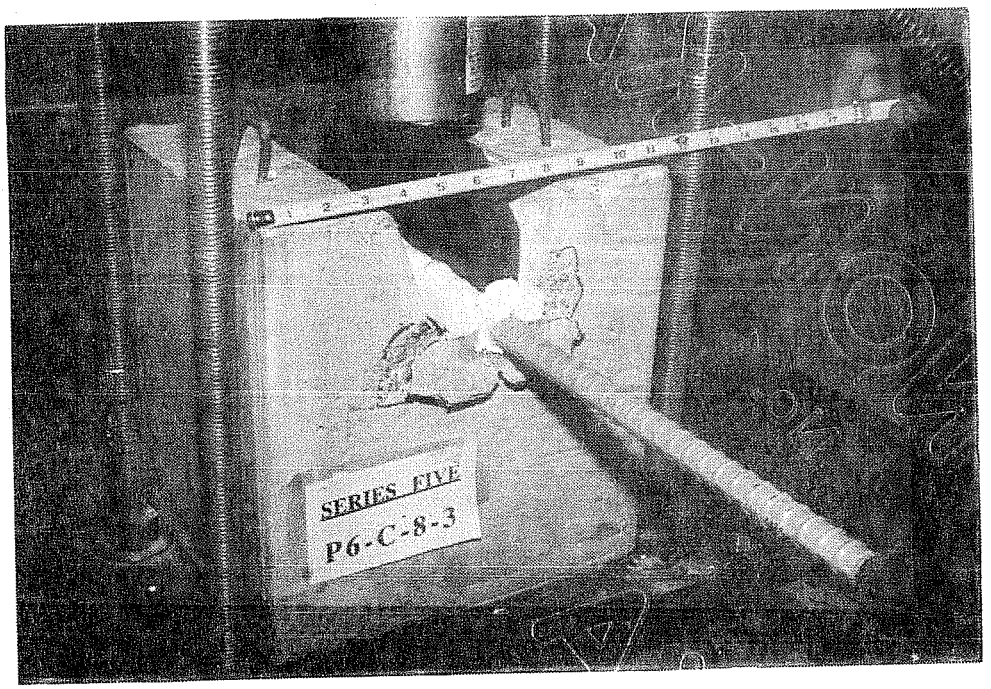

(a) Front view

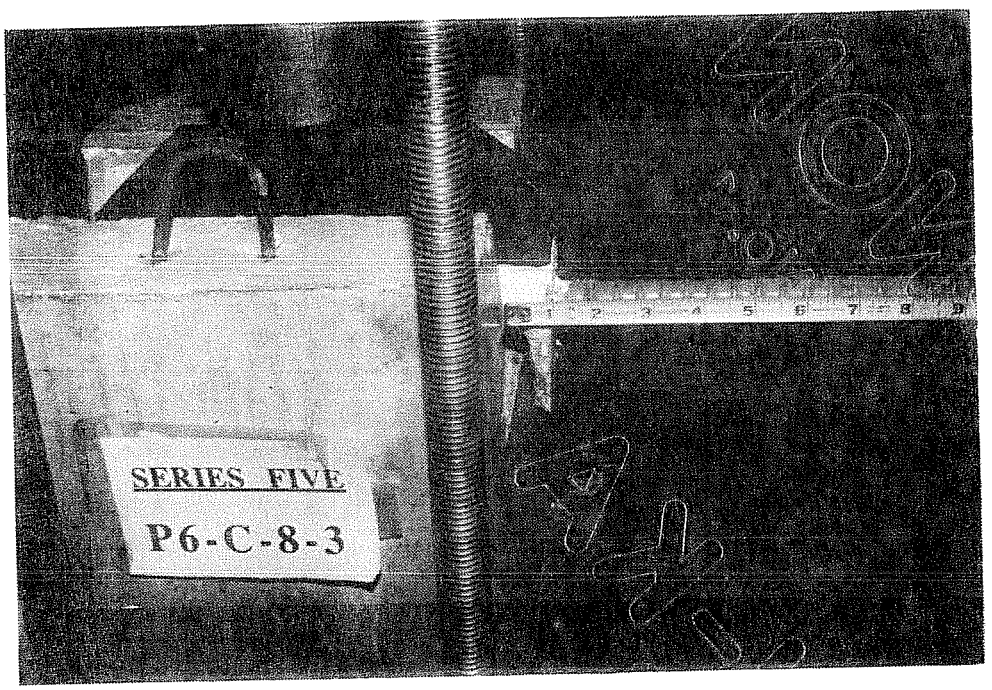

(b) Side view

Figure 5.5 Mode of failure of Type A pullout specimens.

(1) Concrete adhered to the deformations of all uncoated bars whereas no concrete was found to adhere to epoxy-coated bars (see Figure 5.6). The only exception was the #11 diamond pattern coated bars as shown in Figures 5.6 and 5.7, probably due to the geometry of the deformation pattern itself.

(2) The concrete interface around uncoated bars was rough, whereas the concrete in contact with coated bars had a smooth, glassy surface with no evidence of adhesion between the bar and the concrete.

(3) More concrete adhered to the uncoated bars as the lateral (top) load increased. At high levels of confinement, the reinforcing bar tended to fail in a "pullout" mode, shearing off the concrete keys between the ribs, instead of the bar riding over the concrete as in a splitting mode of failure. Figures 5.8 and 5.9 show normal strength concrete, #11 parallel and crescent deformation pattern bar specimens (10 kips lateral load) after failure.

(4) The amount of concrete adhering to uncoated bars was larger in the case of high strength concrete than normal strength concrete. The reason is that adhesion between the embedded uncoated bar and the concrete increases with concrete strength. Figures 5.10 and 5.11 show large amounts of concrete retained on embedded surfaces of uncoated #6 parallel and crescent deformation pattern bars tested in high strength concrete specimens with a top load of 15 kips. For the corresponding epoxy-coated bars, no concrete was observed to adhere to the bar.

(5) A more extensive cracking pattern was observed in a few of the specimens with high strength concrete. A wedge of concrete tended to split from the concrete specimen. In Figure 5.12, the typical cracking pattern of specimen P11-C-8-3 is compared with the extensive cracking pattern of specimen P11-C-8-4. However,

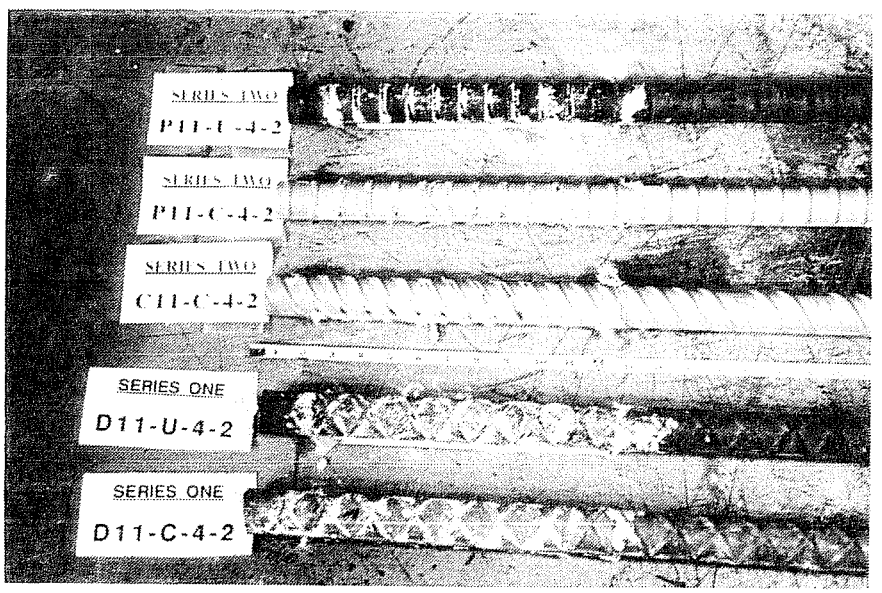

Figure 5.6 Appearance of #11 bars with different deformation patterns after failure.

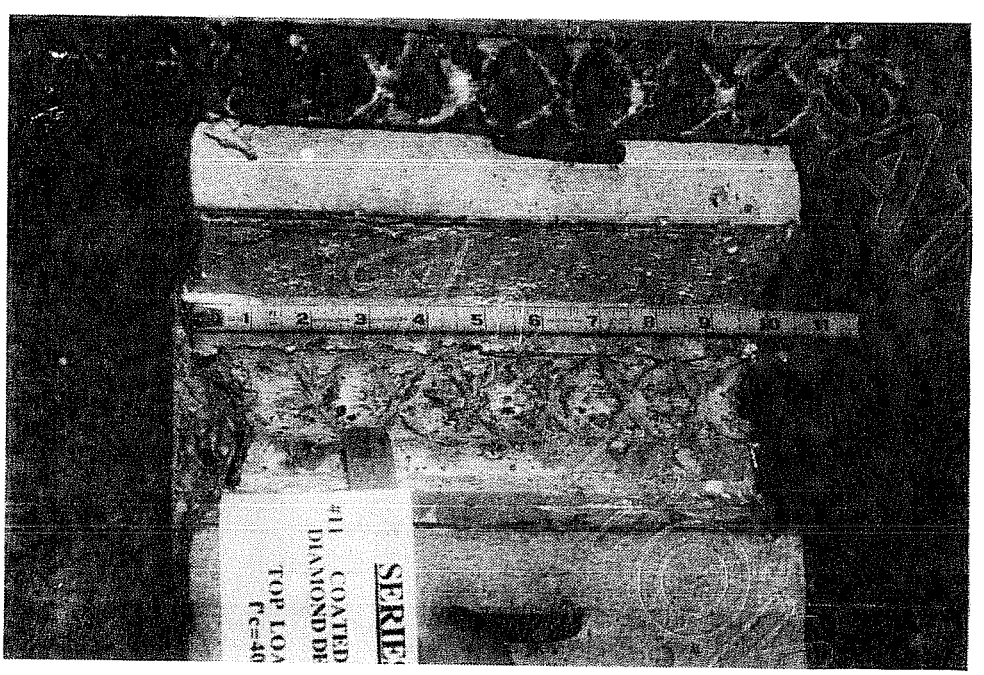

Figure 5.7 Epoxy-coated diamond pattern #11 bar after failure.

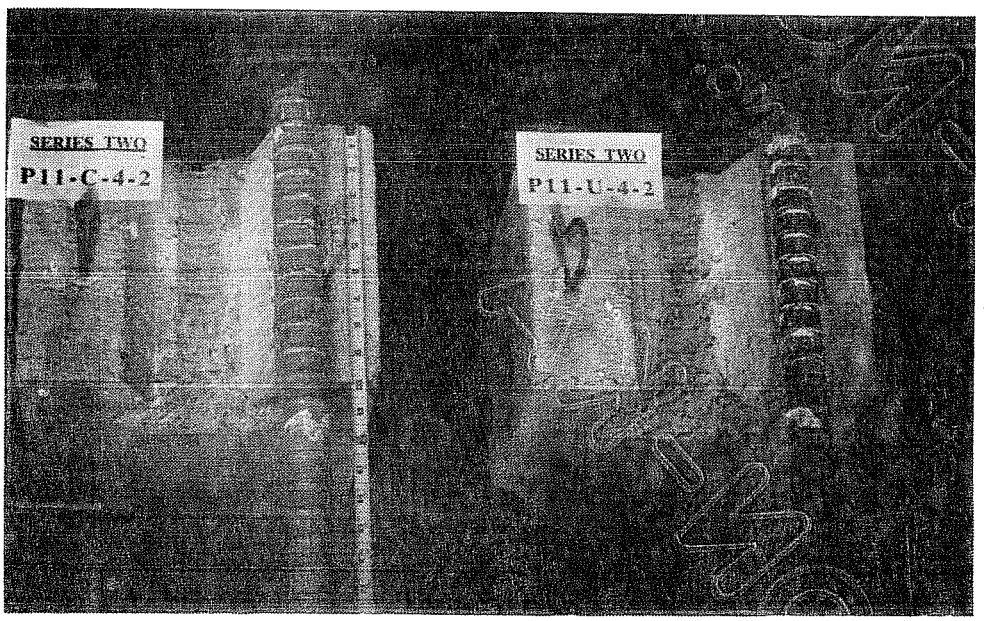

Figure 5.8 Parallel deformation pattern #11 bar Type A pullout specimens after failure, top load = 10 kips, normal strength concrete.

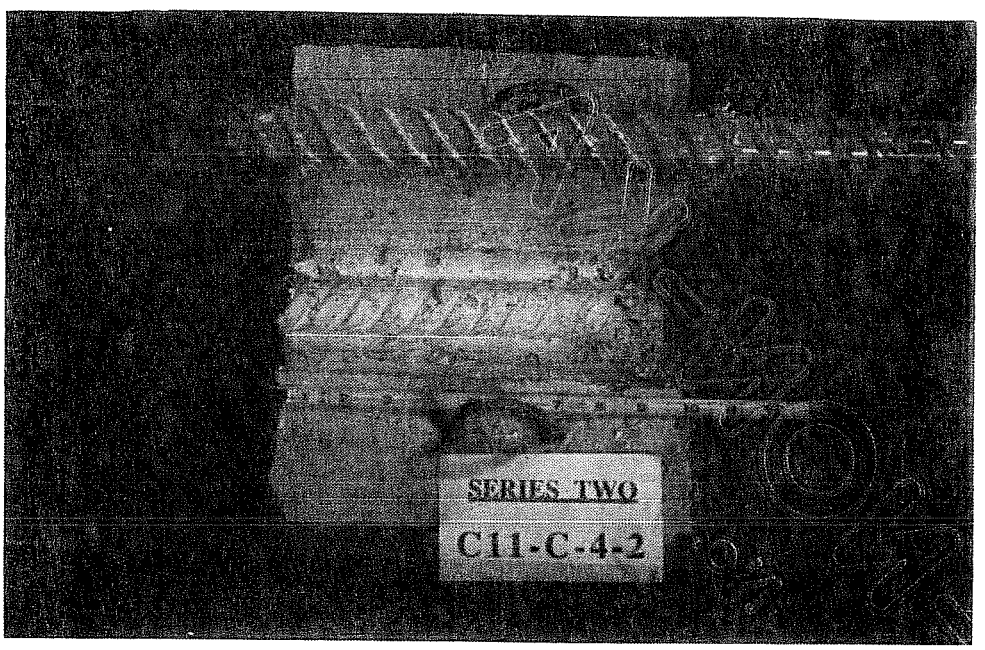

Figure 5.9 Epoxy-coated crescent deformation pattern #11 bar Type A pullout specimen after failure, top load = 10 kips, normal strength concrete.

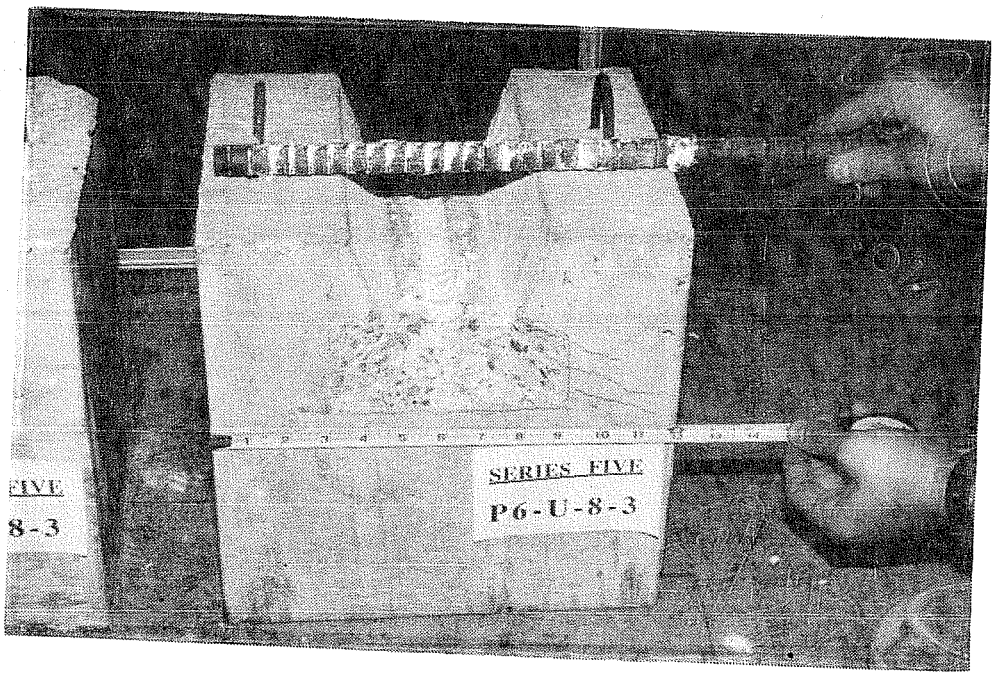

(a) Uncoated bar specimen

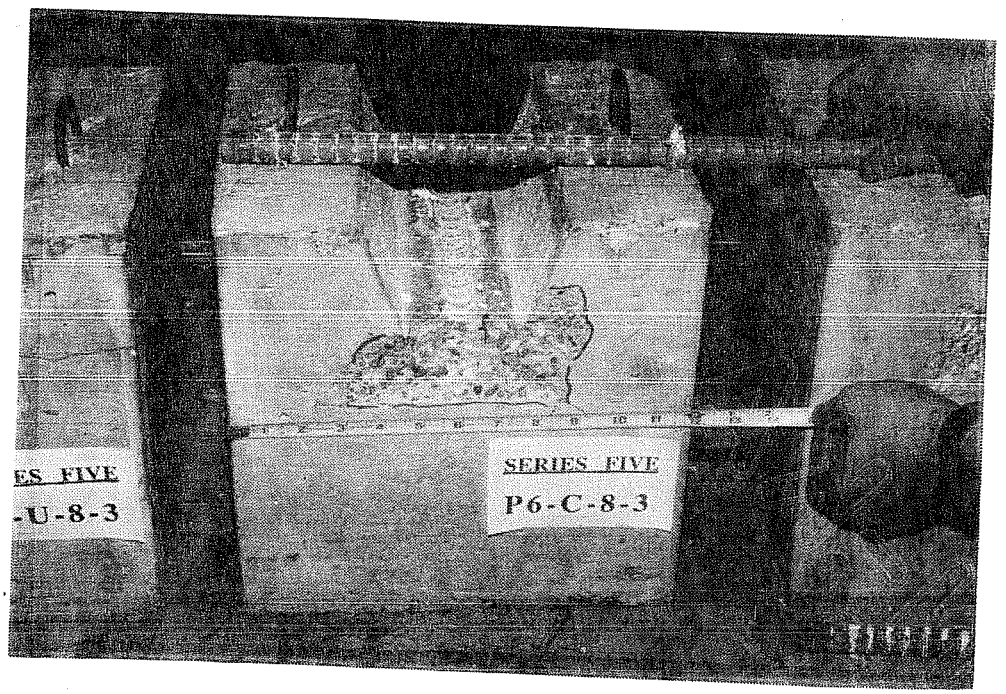

(b) Epoxy-coated bar specimen

Figure 5.10 Parallel deformation pattern #6 bar Type A pullout specimens after failure, top load = 15 kips, high strength concrete.

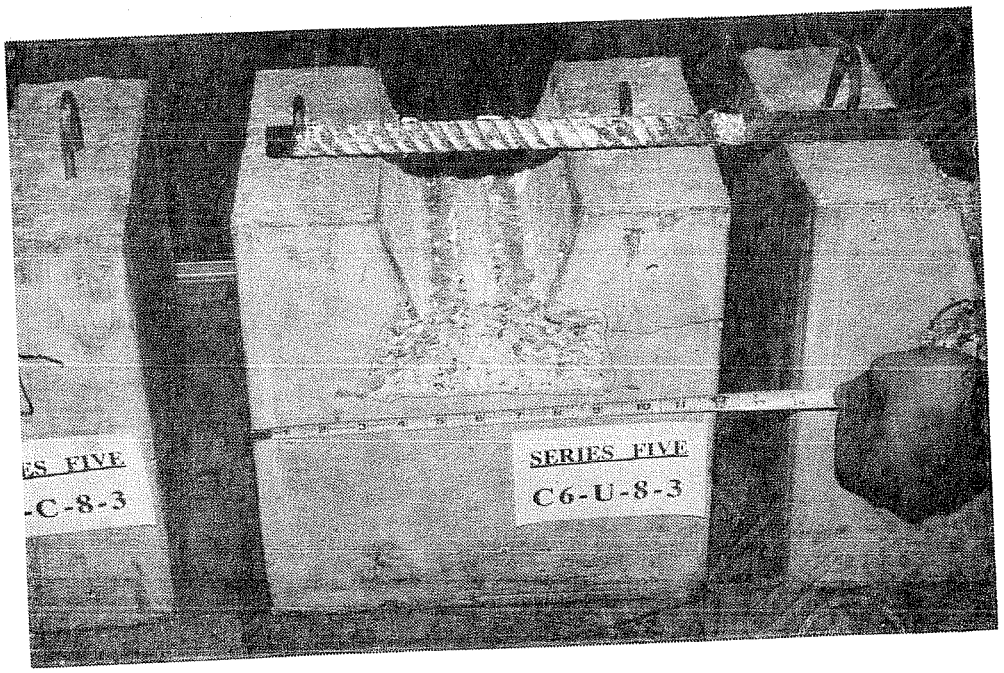

(a) Uncoated bar specimen

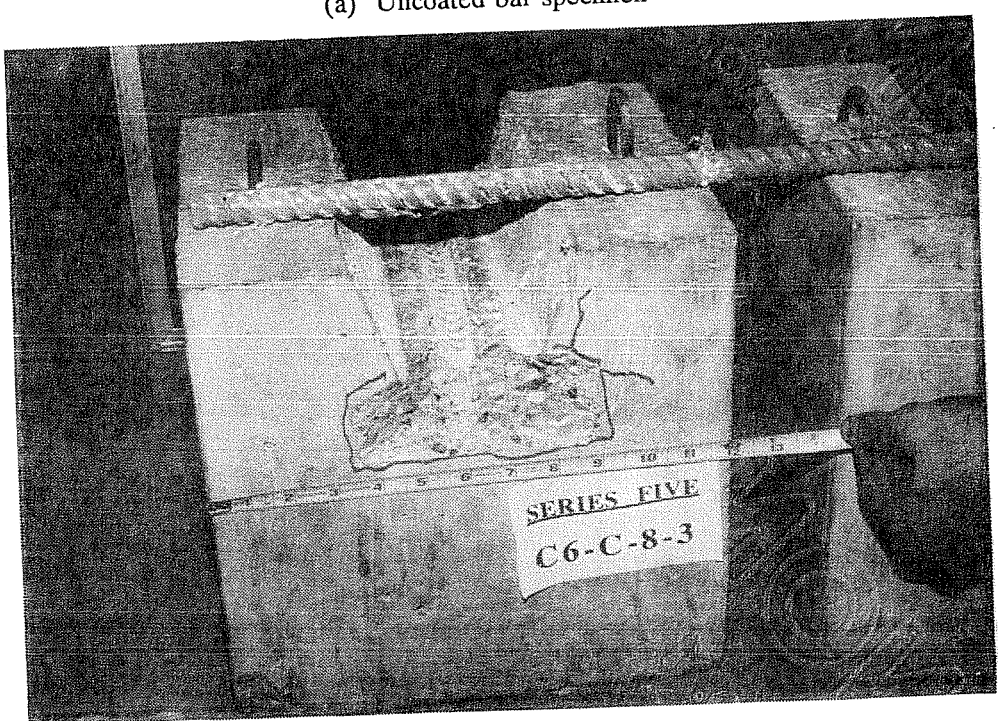

(b) Epoxy-coated bar specimen

Figure 5.11 Crescent deformation pattern #6 bar Type A pullout specimens after failure, top load = 15 kips, high strength concrete.

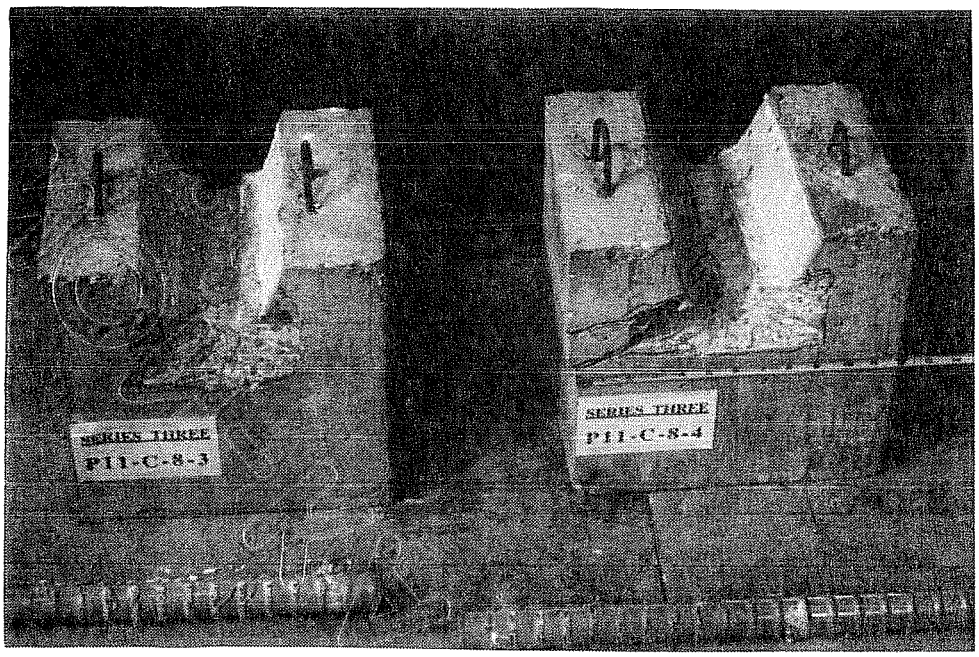

Figure 5.12 Different cracking patterns of parallel deformation pattern #11 bar Type A pullout specimens with high strength concrete.

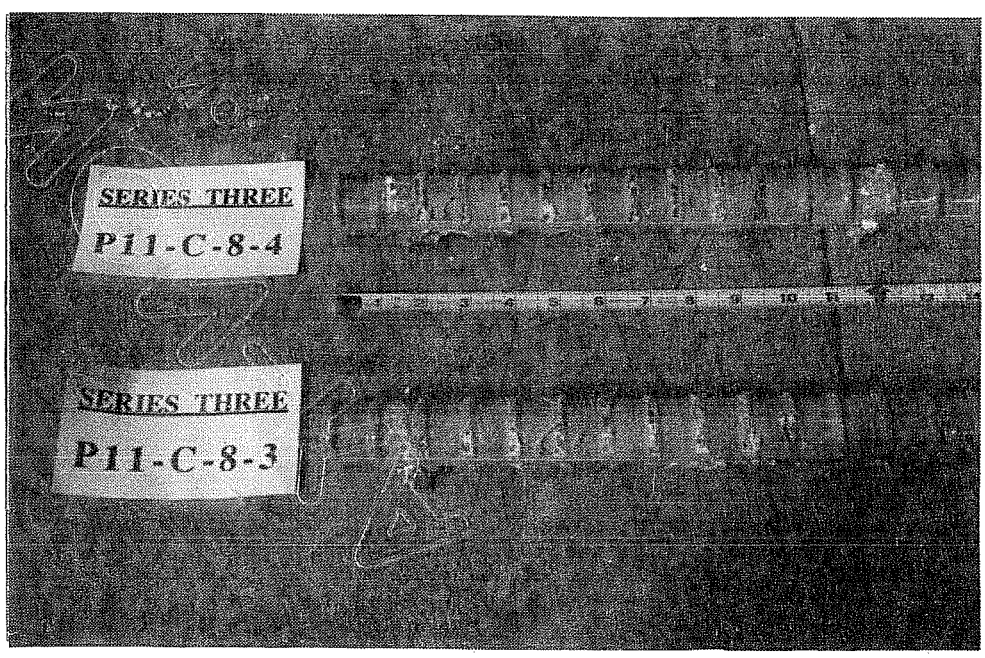

Figure 5.13 Epoxy-coating chipped off the deformations of #11 coated bars upon pullout.

the increased cracking intensity of some specimens had no impact on the bond strength or load-slip behavior.

(6) After failure, the epoxy-coating was found to have chipped off the bar deformations of all coated bars (see Figure 5.13). More epoxy was removed with higher levels of top load.

The cracking pattern of all six specimens in the series with manufactured bars (rib face angles 30, 45 and 60 degrees), was identical to that of other Type A pullout specimens. It is interesting to note that for the uncoated bar with a rib face angle of 60 degrees, virtually all the concrete between bar deformations was sheared off as shown in Figure 5.14. The reason is that with larger rib face angles, the horizontal (longitudinal) component of the bearing force against the concrete keys will be larger and the radial splitting component will be smaller (see Figure 5.15). Hence, the failure will be more of a pullout failure where the concrete keys are sheared off.

5.3.2 Type B Pullout Specimens. All Type B specimens exhibited a sudden splitting mode of failure. Uncoated, epoxy-coated, and painted bar specimens with 1-in. cover to the anchored bar, showed more of a V-notch splitting mode of failure. One crack formed in the concrete cover along the length of the reinforcing bar and other cracks spread from the bar in a V-pattern into the 1-in. cover (see Figure 5.16).

Uncoated, epoxy-coated, and painted bar specimens with 2-in. cover to the reinforcing bar, exhibited more of a face-and-side splitting pattern (see Figures 5.17 and 5.18). Along with the longitudinal crack in the cover along the reinforcing bar, other cracks radiated from the bar to the sides of the concrete specimen. For the uncoated bar specimens, splitting broke the block into three pieces separated by the crack lines as shown in Figure 5.18(a). The presence of a #3 bar hooked over the bar at the middle of the anchorage length, was intended to confine the anchored bar but did not change the load-slip behavior nor the mode of failure.

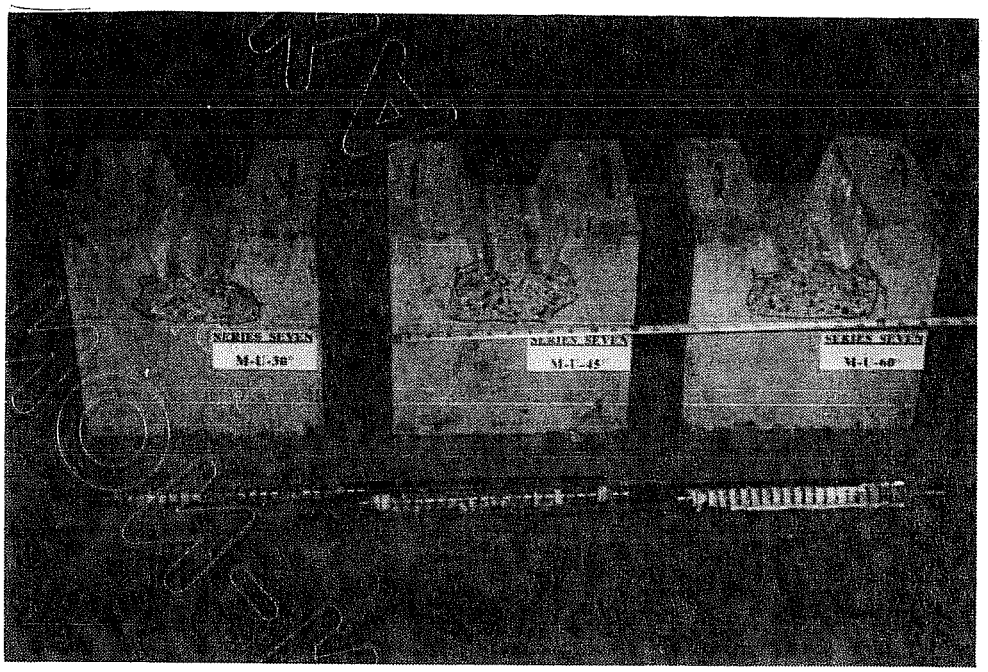

Figure 5.14 Uncoated manufactured bar Type A pullout specimens after failure, top load = 10 kips, concrete strength = 4750 psi.

5.4 Test Results

It is important to note that the pullout specimens used in this phase of the test program do not represent actual beam or column conditions in reinforced concrete structures. Therefore, the test results are only used to indicate and study the effect of the different variables on the relative performance of epoxy-coated bars and uncoated bars. Absolute values of bond stresses and free-end slip are not useful for design.

In all tests, failure took place in pullout or splitting before the bar yielded. The bond strength could be determined directly from the stress developed in the steel. The bond strength was based on an average stress along the embedment length. To evaluate the bond stress, u, the total force developed in the bar, $A_b f_s$, was divided by the embedded surface area of the bar over the 10-in. anchorage length, $C\ell_d$:

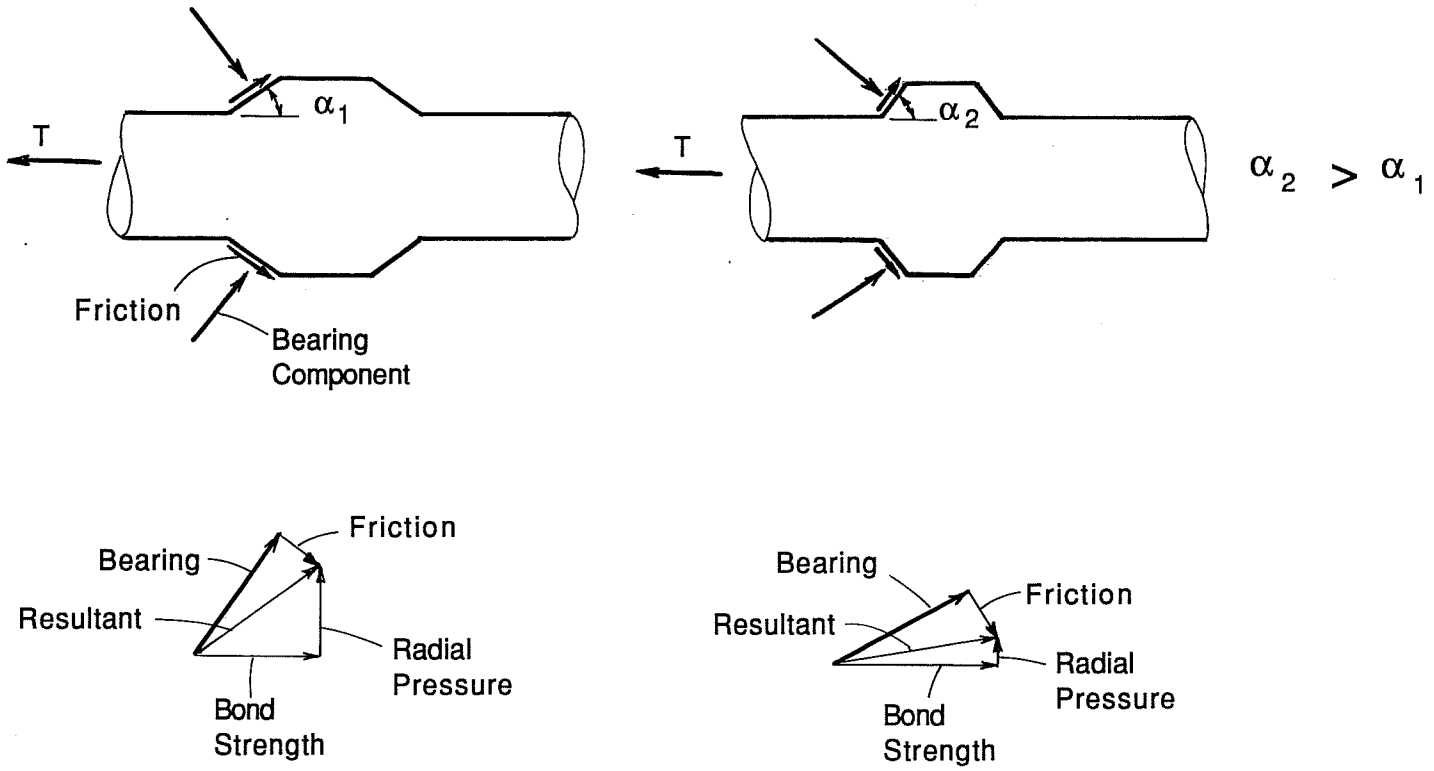

Figure 5.15 Comparison of bond strength components for different rib face angles.

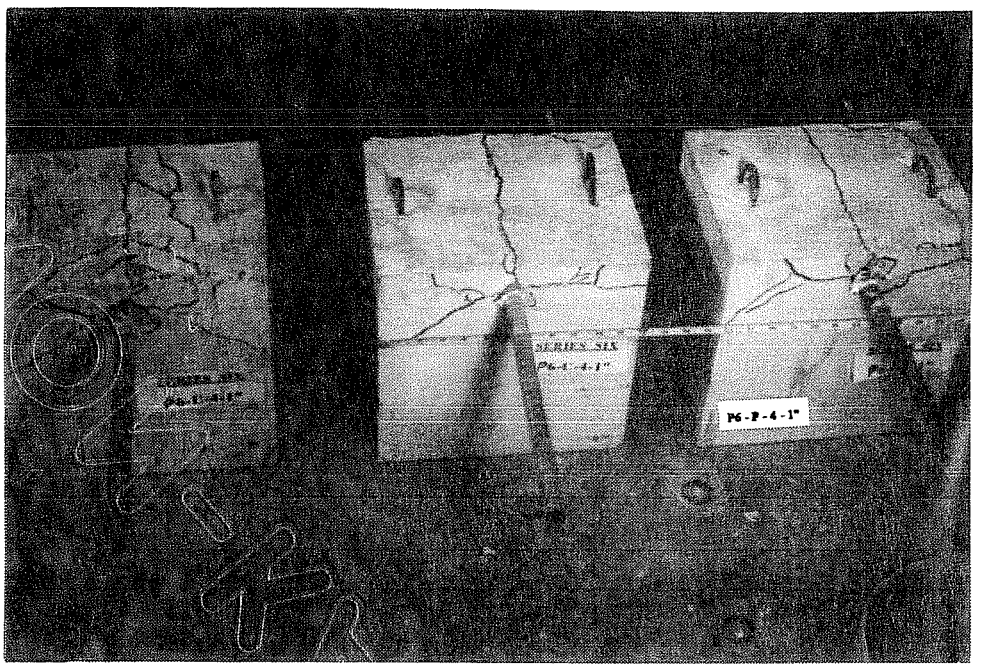

Figure 5.16 V-notch failure of #6 bar type B pullout specimens with 1-in. clear cover, series SIX, f'_c = 4500 psi.

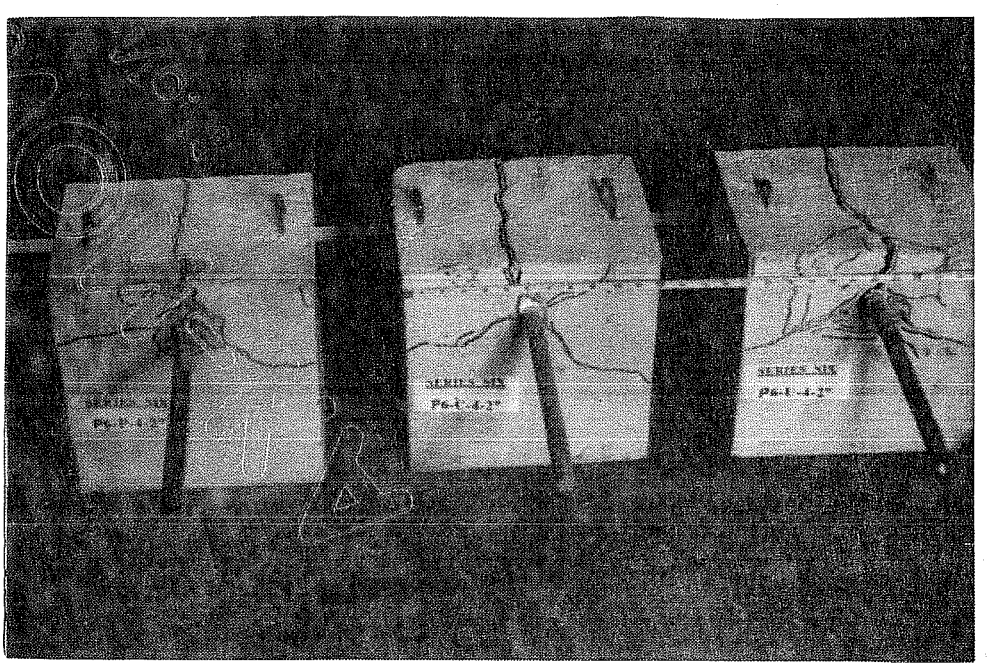

Figure 5.17 Face-and-side splitting of #6 bar Type B pullout specimens with 2-in. clear cover, series SIX, f'_c = 4500 psi.

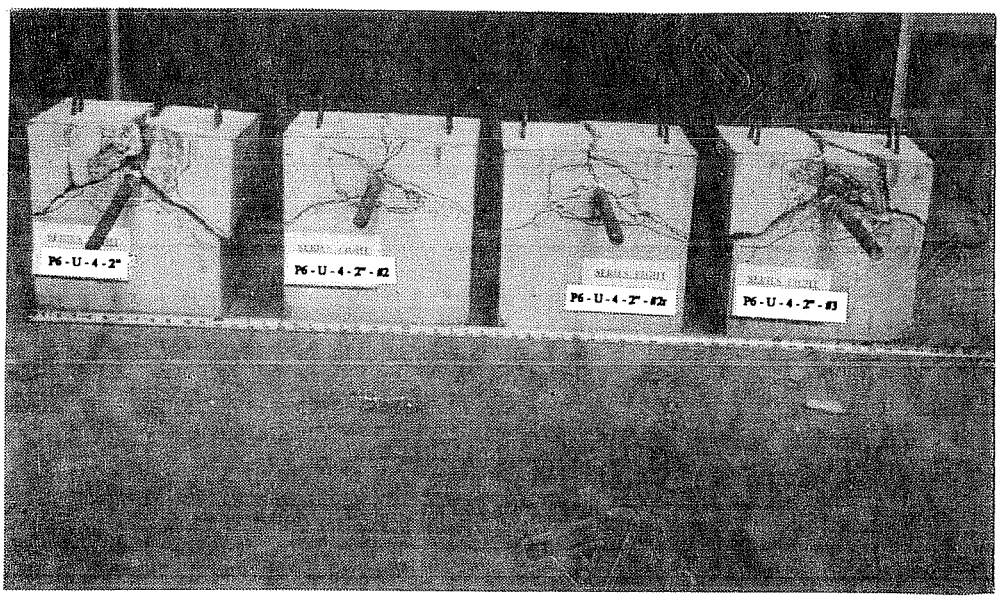

(a) Uncoated bar specimens

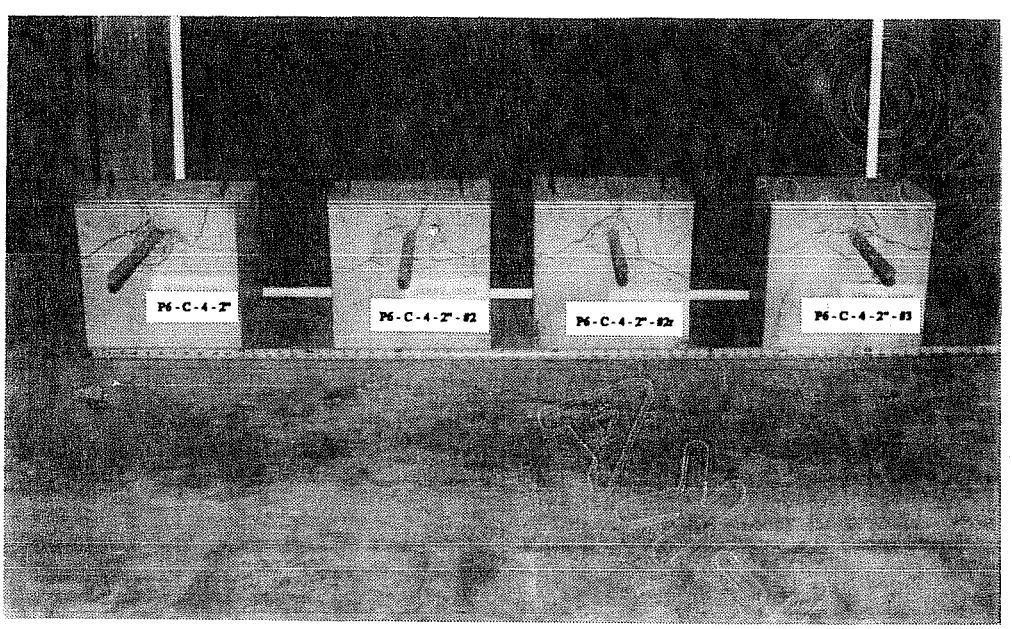

(b) Epoxy-coated bar specimens

Figure 5.18 Face-and-side splitting of #6 bar Type B pullout specimens of series EIGHT, concrete strength = 4900 psi.

$$u = A_b f_s/(C\ell_d)$$

$C = \pi d_b/2$ Type A Specimens

$C = \pi d_b$ Type B Specimens

The effect of each variable on the relative bond strength and load-slip behavior of uncoated and epoxy-coated bars in Type A and B of pullout specimens, will be discussed in Sections 5.5 and 5.6. However, the test results of all eighty specimens are shown in Appendix Tables A1 to A8. The following data is listed for each bar specimen:

(1) The ultimate bond stress and corresponding free-end slip

(2) The bond stress at 0.002-in. free-end slip

(3) The bond ratio (coated to uncoated) at ultimate

(4) The bond ratio at 0.002-in. free-end slip

Also, load-slip curves for all bars are shown in Figures A1 to A28.

In general, the results show that epoxy-coated bars developed lower ultimate bond strengths and larger slip at similar load levels (i.e. lower load-slip stiffness) than uncoated bars. These trends are independent of the variables investigated.

5.5 Relative Bond Performance of Uncoated and Epoxy-Coated Bars - Type A Specimens

In Table 5.1, the bond ratios (coated and uncoated) for Type A specimens of the first five series are summarized. Each listed ratio is the average of bond ratios corresponding to the four different levels of top load (5, 10, 15 and 20 kips). Average bond ratios vary from 0.84 to 0.92 for different bar sizes, coating thicknesses, bar deformation patterns, and concrete strengths. A comparison of steel stresses and free-end slip between uncoated and epoxy-coated bars for the first five series, is shown using bar charts in Figures 5.19 up to 5.23.

Table 5.1 Summary of bond ratio test results for Type A pullout specimens tested in the first five series.

Epoxy-Coated Bar Type			Average Bond Ratio* u(coated)/u(uncoated)	
Bar Size	Deformation Pattern	Nominal Coating Thickness (mils)	Normal-Strength Concrete	High-Strength Concrete
#11	Diamond	5	**0.92**(5300 psi)**	-
#11	Diamond	12	**0.91**(5300 psi)	-
#11	Parallel	8	**0.92**(5200 psi)	**0.84**(9400 psi)
#11	Crescent	8	-	**0.92**+(9400 psi)
# 6	Parallel	8	**0.87**(5400 psi)	**0.84**(8700 psi)
# 6	Crescent	8	-	**0.88**+(8700 psi)

* This ratio is the average of four bond ratios corresponding to the different investigated levels of the confining top load: 5, 10, 15, and 20 Kips.

**The number in parenthesis is the average concrete strength corresponding to the tabulated bond ratio.

\+ This value corresponds to one level of top load, 15 Kips.

The effect of each variable on the bond strength and load-slip behavior of uncoated and epoxy-coated reinforcing bars in the first five series of Type A specimens (Figures 5.19-5.23, Table 5.1, and Appendix A), can be summarized as follows:

5.5.1 Effect of Top Load. The ultimate bond stress of an uncoated or epoxy-coated bar increased as the confining load increased. If the ultimate bond stress at 10-, 15-, and 20-kip top load is compared with that at 5 kips, average increases of 33, 64, and 93% were observed. With larger confining loads, the bar tends to behave in a pullout rather than a splitting mode of failure.

In Table 5.2, the bond ratios (coated to uncoated) at different levels of top load are listed for the various bar sizes, bar deformation patterns, and concrete strengths. These ratios are plotted in Figure 5.24. The largest range of bond ratios, 0.65 to 1.00, occurs at the lowest level of top load, 5 kips. At higher values of top load (10, 15 and 20 kips), the scatter of bond ratios is smaller, 0.79 to 0.92. Variation of top load above 5 kips had no clear effect on the bond ratio. The reason could

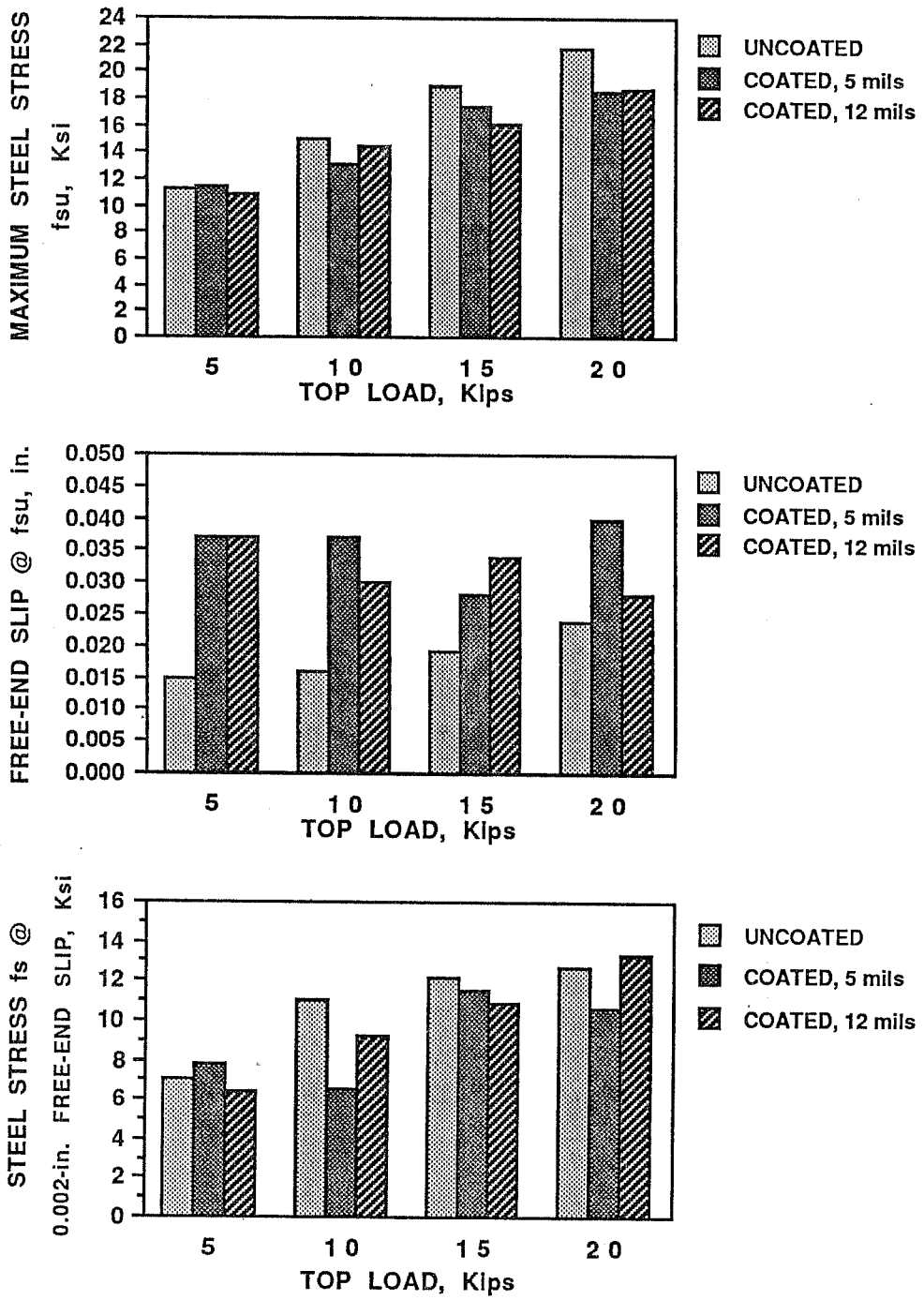

Figure 5.19 Comparison of stresses and free-end slip for series ONE of Type A pullout specimens, #11 bars, diamond deformation pattern, f'_c = 5300 psi.

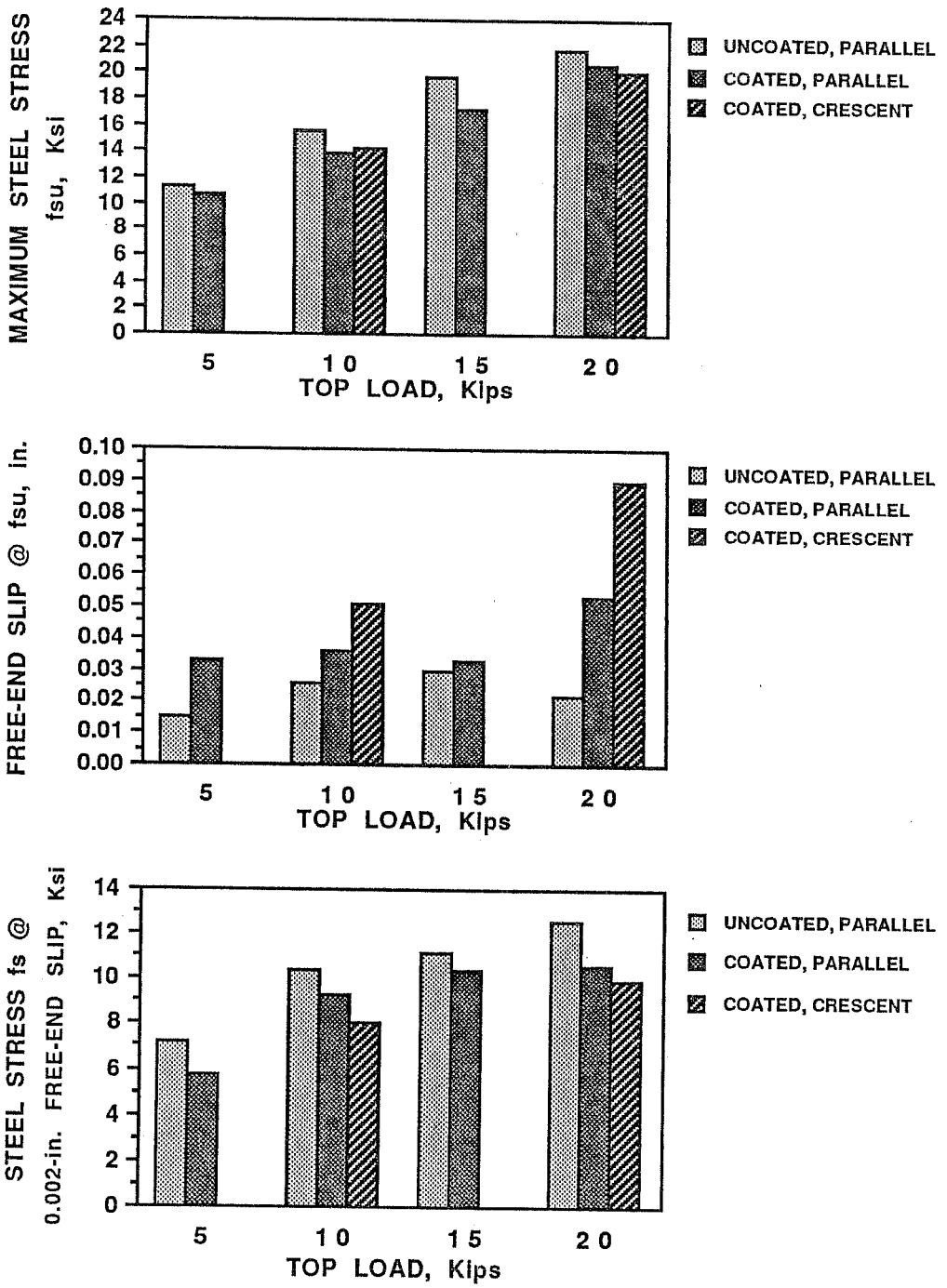

Figure 5.20 Comparison of stresses and free-end slip for series TWO of Type A pullout specimens, #11 bars, f'_c = 5200 psi.

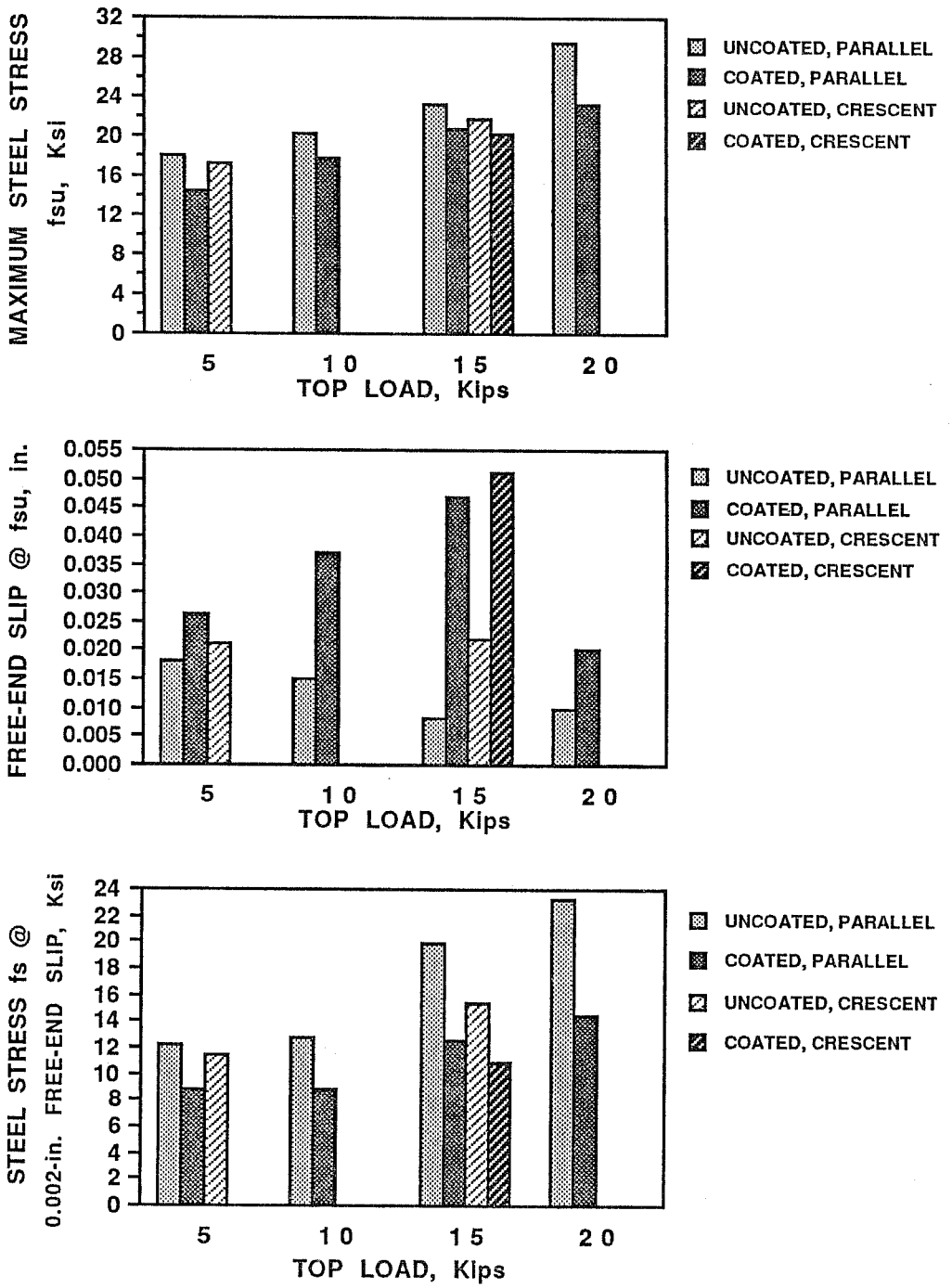

Figure 5.21 Comparison of stresses and free-end slip for series THREE of Type A pullout specimens, #11 bars, f'_c = 9400 psi.

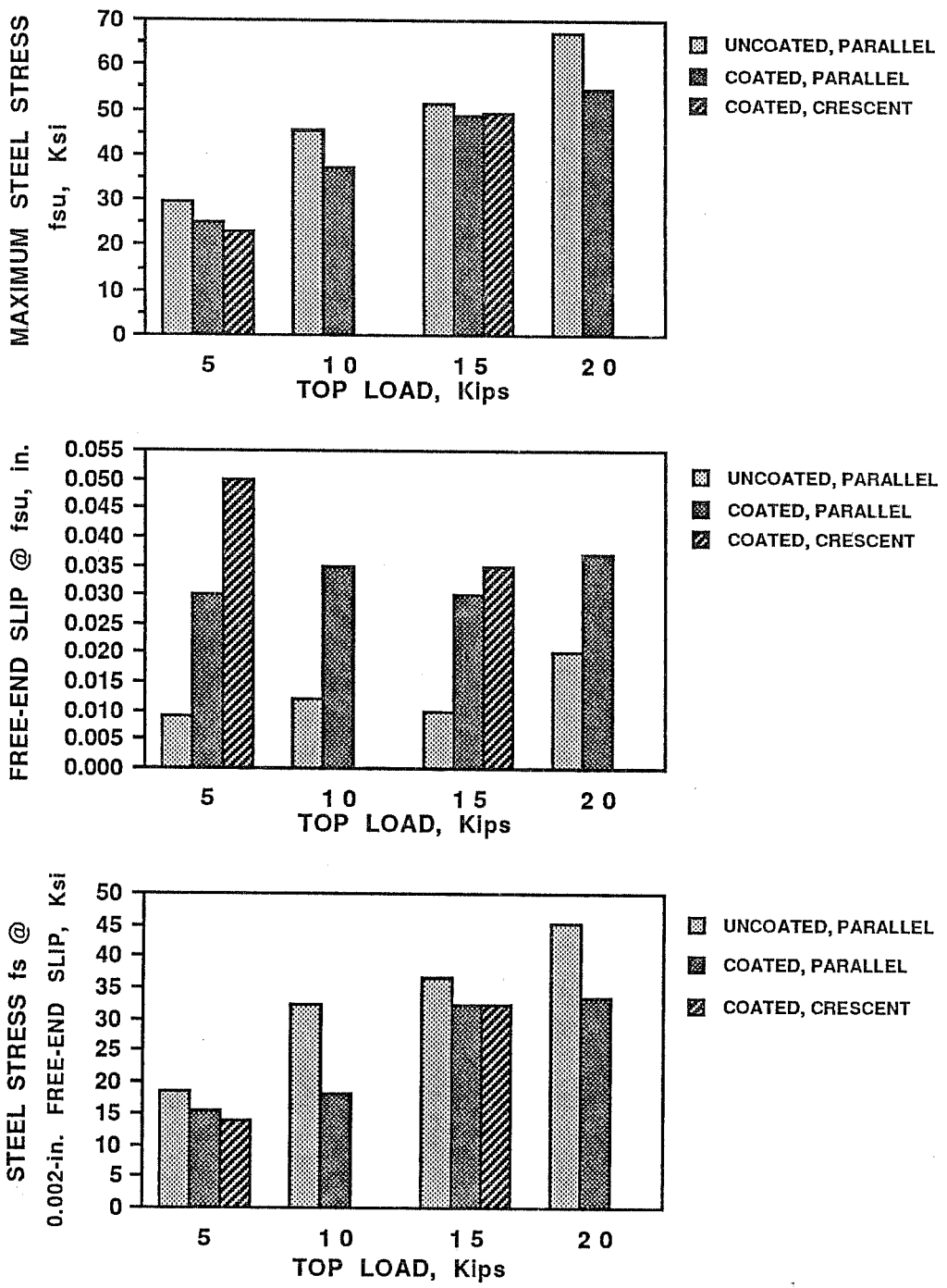

Figure 5.22 Comparison of stresses and free-end slip for series FOUR of Type A pullout specimens, #6 bars, f'_c = 5400 psi.

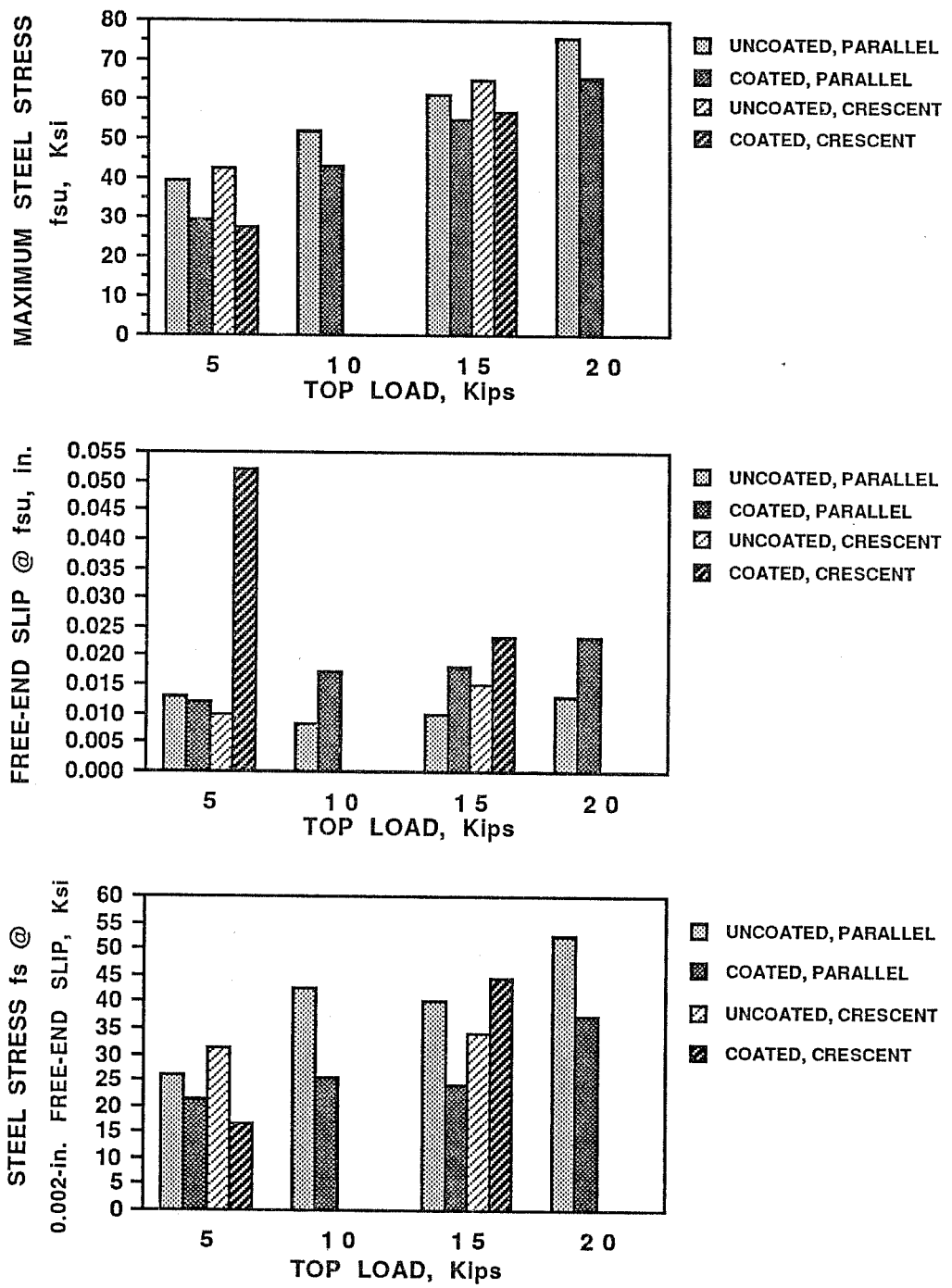

Figure 5.23 Comparison of stresses and free-end slip for series FIVE of Type A pullout specimens, #6 bars, f'_c = 8700 psi.

Table 5.2 Variation of bond ratio with the level of confining top load for the various bar sizes, deformation patterns, and concrete strengths investigated in the first five series of Type A pullout specimens.

Bar Size	Deformation Pattern	Concrete Strength (psi)	Bond Ratio : u(coated)/u(uncoated) Top Load 5 Kips	Top Load 10 Kips	Top Load 15 Kips	Top Load 20 Kips
#11	Diamond	5300	1.00	0.92	0.89	0.86
#11	Parallel	5200	0.95	0.90	0.87	0.91
#11	Parallel	9400	0.80	0.88	0.90	0.79
#11	Crescent	9400	-	-	0.92	-
# 6	Parallel	5400	0.86	0.83	0.95	0.82
# 6	Parallel	8700	0.75	0.83	0.90	0.87
# 6	Crescent	8700	0.65	-	0.88	-

be that at a top load of 5 kips, the resistance of concrete at the interface with the bar against splitting is small, resulting in a splitting mode of failure. Whereas higher levels of top load (10, 15, and 20 kips) provide adequate confinement to the concrete resulting in a pullout mode of failure.

In Figures 5.25 and 5.26, load-slip curves of uncoated and epoxy-coated bars are shown at two levels of top load (5 and 10 kips) for two bar sizes (#6 and #11) with parallel deformation patterns. The reduction in bond strength and in load-slip stiffness of epoxy-coated bars relative to uncoated bars is similar for the two levels of top load.

5.5.2 Effect of Bar Size. The reduction in bond strength of epoxy-coated bars relative to uncoated bars was not influenced by bar size. the average bond ratios for #6 and #11 bars are similar for a given bar deformation pattern and comparable concrete strengths.

5.5.3 Effect of Coating Thickness. The average bond ratios are 0.92 for 5-mil and 0.91 for 12-mil coating thicknesses. In Figures 5.27 and 5.28, load-slip curves of 5-mil and 12-mil epoxy-coated #11 bars are compared with those of uncoated bars at two levels of top loads, 10 and 15

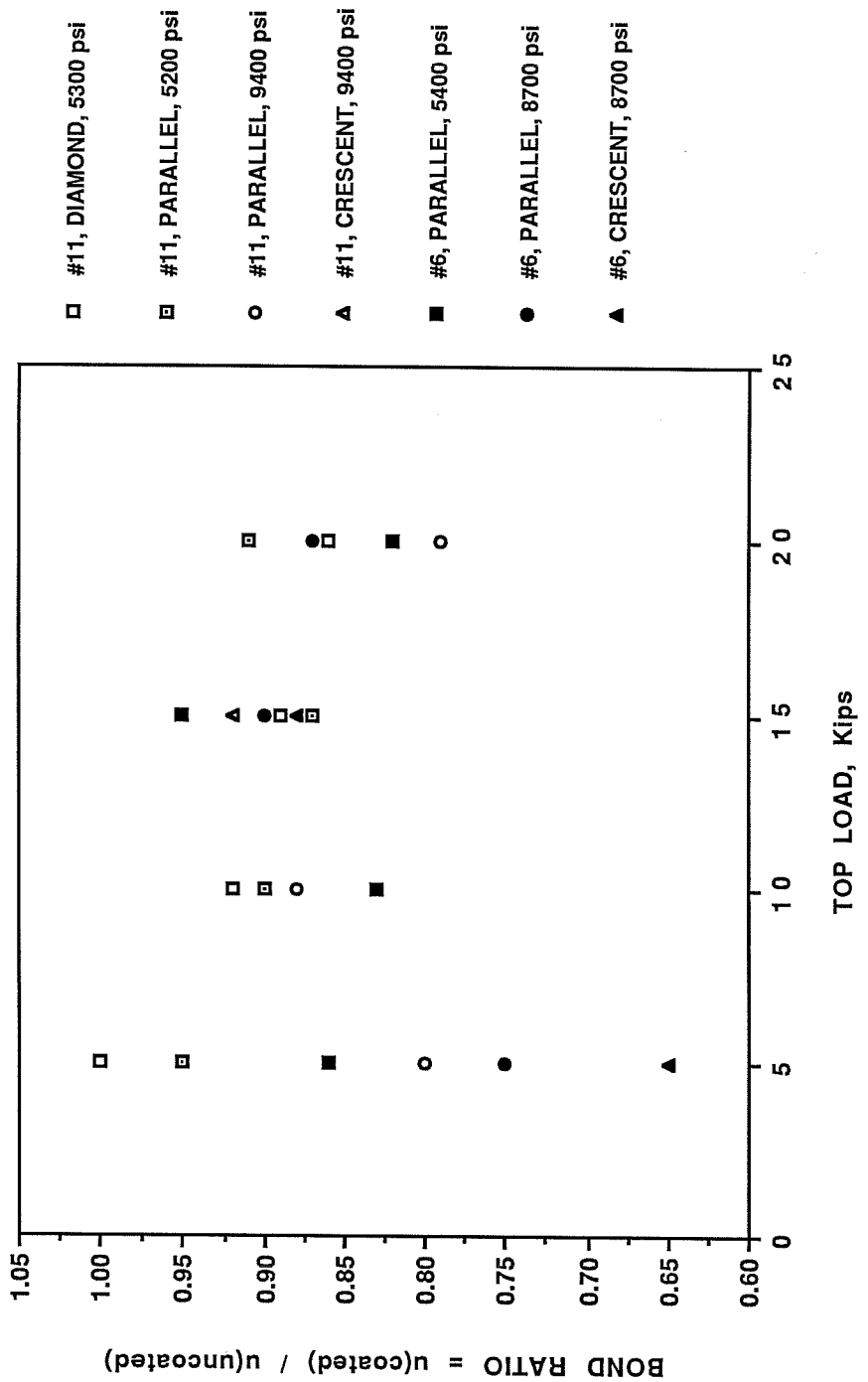

Figure 5.24 Variation of bond ratio with top load for Type A pullout specimens.

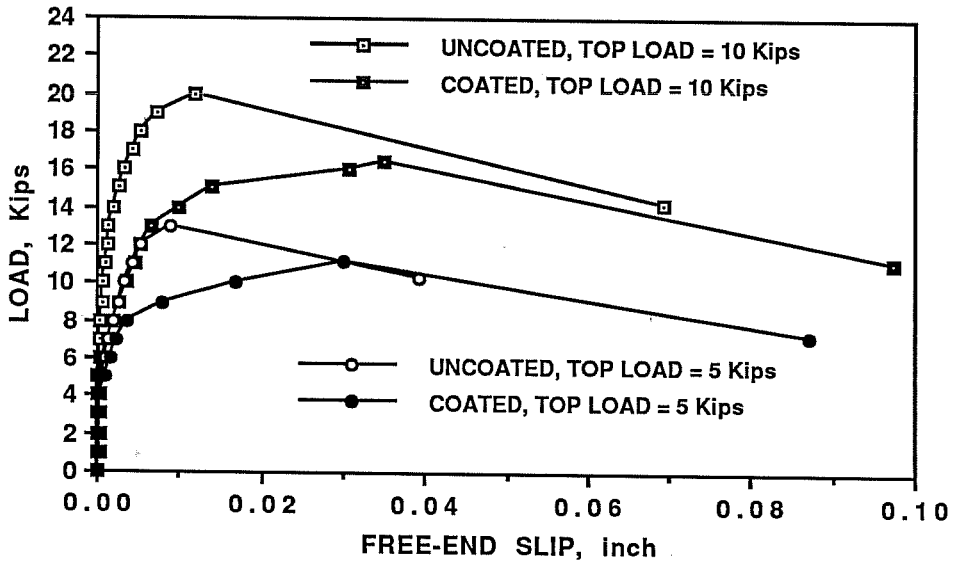

Figure 5.25 Effect of top load on load-slip behavior of #6 uncoated and epoxy-coated bars, parallel deformation pattern, f'_c = 5400 psi.

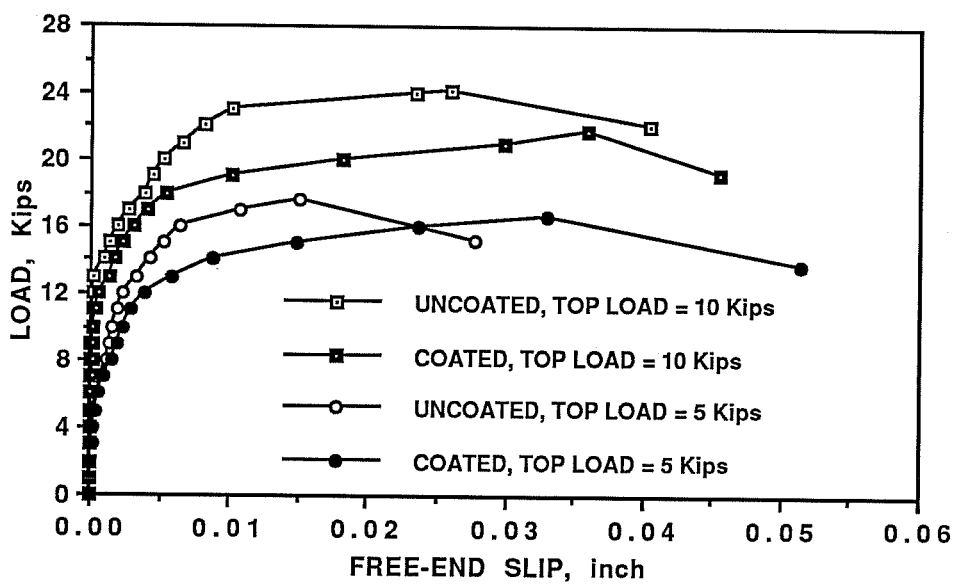

Figure 5.26 Effect of top load on load-slip behavior of #11 uncoated and epoxy-coated bars, parallel deformation pattern, f'_c = 5200 psi.

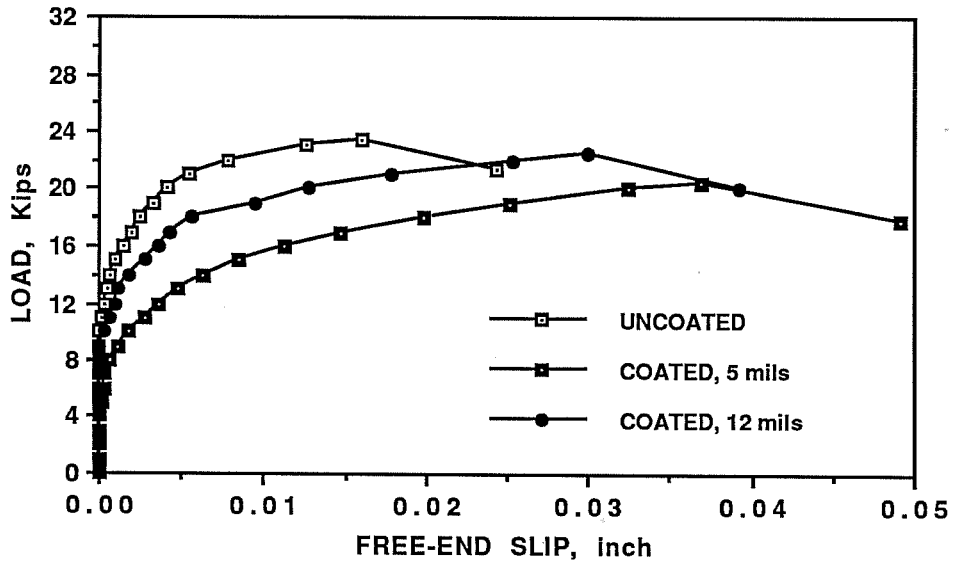

Figure 5.27 Effect of coating thickness on load-slip behavior of #11 epoxy-coated bars, diamond deformation pattern, top load = 10 kips, f'_c = 5300 psi.

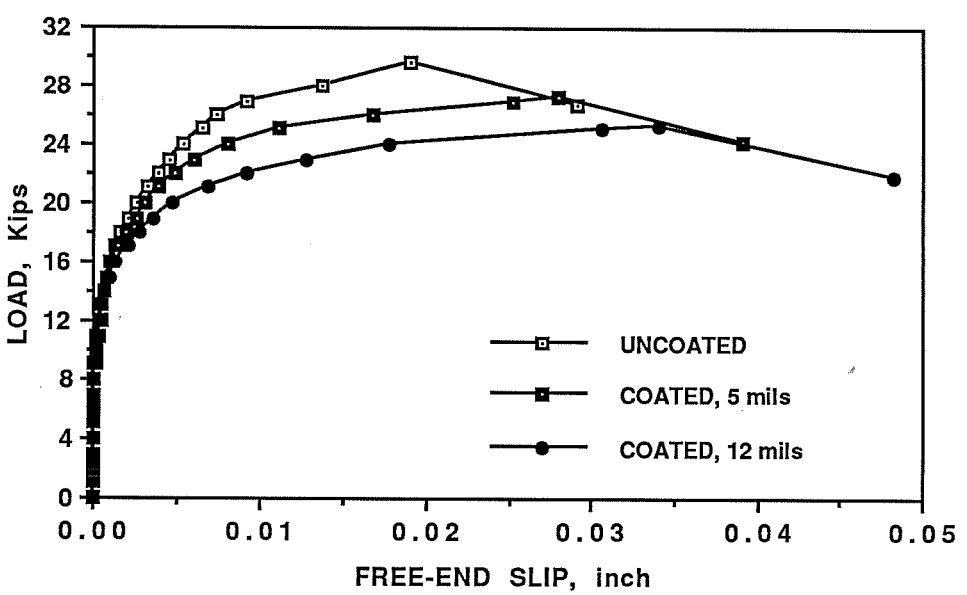

Figure 5.28 Effect of coating thickness on load-slip behavior of #11 epoxy-coated bars, diamond deformation pattern, top load = 15 kips, f'_c = 5300 psi.

kips. These results show that the reduction in bond strength and in load-slip stiffness of epoxy-coated bars relative to uncoated bars is independent of coating thickness.

5.5.4 Effect of Bar Deformation Pattern. Three bar deformation patterns were investigated: diamond, parallel, and crescent. The bond strength of epoxy-coated bars relative to uncoated bars was independent of bar deformation pattern, regardless of bar size, concrete strength, or level of top load.

Load-slip curves of #11 uncoated and epoxy-coated bars with different deformation patterns are shown in Figures 5.29 and 5.30. There was no major difference in load-slip behavior of parallel and diamond deformation pattern bars. However, the curves indicate that regardless of concrete strength or top load, crescent deformations tended to slip more than other coated bars at a given level of top load. Larger slips of crescent pattern bars relative to parallel pattern bars at comparable load levels, are also evident in the load-slip curves of #6 bars in Figures 5.31 and 5.32.

5.5.5 Effect of Concrete Strength. Results of series THREE (#11, 9400 psi) relative to series TWO (#11, 5200 psi), and results of series FIVE (#6, 8700 psi) relative to series FOUR (#6, 5400 psi), indicate that the ultimate bond strength of a reinforcing bar, uncoated or epoxy-coated, increases as the concrete strength increases. However, the results do not indicate a major influence of concrete strength on the bond strength of epoxy-coated bars relative to uncoated bars. As shown in Table 5.1, the average bond ratios (coated to uncoated) of #11 parallel deformation pattern bars are 0.92 at 5200 psi and 0.84 at 9400 psi. For #6 bars, the ratios are 0.87 at 5400 psi and 0.84 at 8700 psi.

Load-slip curves shown in Figures 5.33 and 5.34, indicate that the load-slip stiffness of #6 and #11 reinforcing bars increases as the concrete strength increases. However, the load-slip behavior of epoxy-coated bars relative to uncoated bars was not affected by the change in concrete strength.

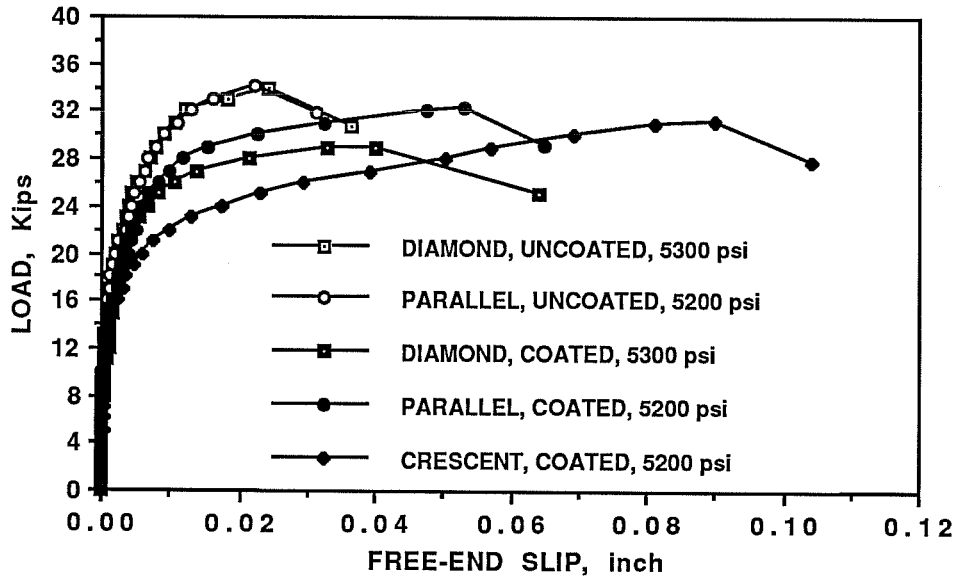

Figure 5.29 Effect of deformation pattern on load-slip behavior of #11 uncoated and epoxy-coated bars, top load = 20 kips, f'_c = 5200-5300 psi.

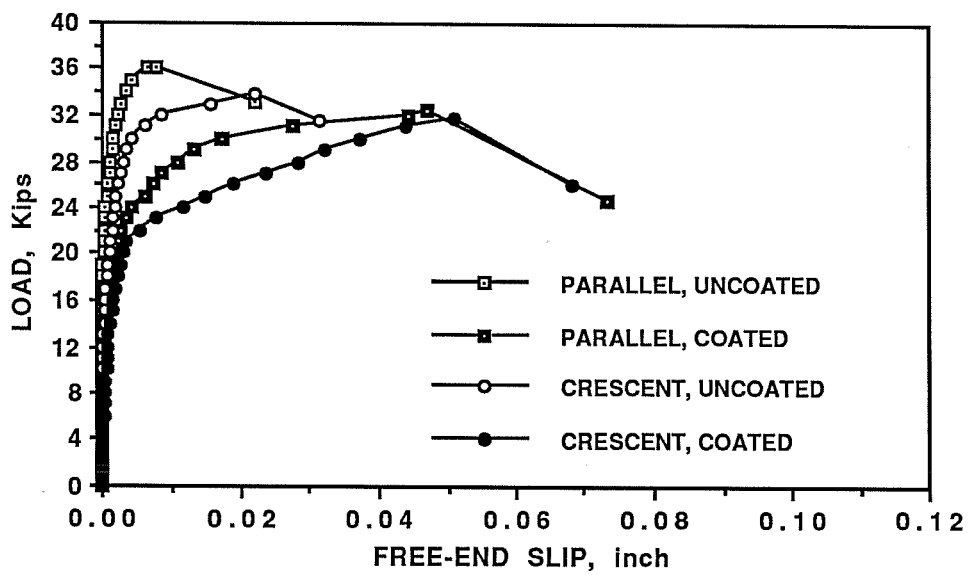

Figure 5.30 Effect of deformation pattern on load-slip behavior of #11 uncoated and epoxy-coated bars, top load = 15 kips, f'_c = 9400 psi.

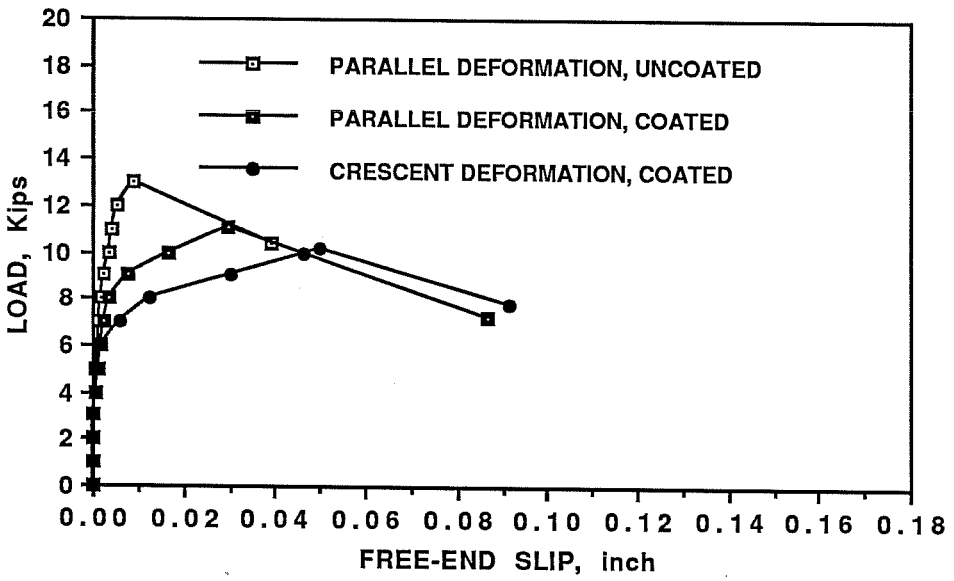

Figure 5.31 Effect of deformation pattern on load-slip behavior of #6 uncoated and epoxy-coated bars, top load = 5 kips, f'_c = 5400 psi.

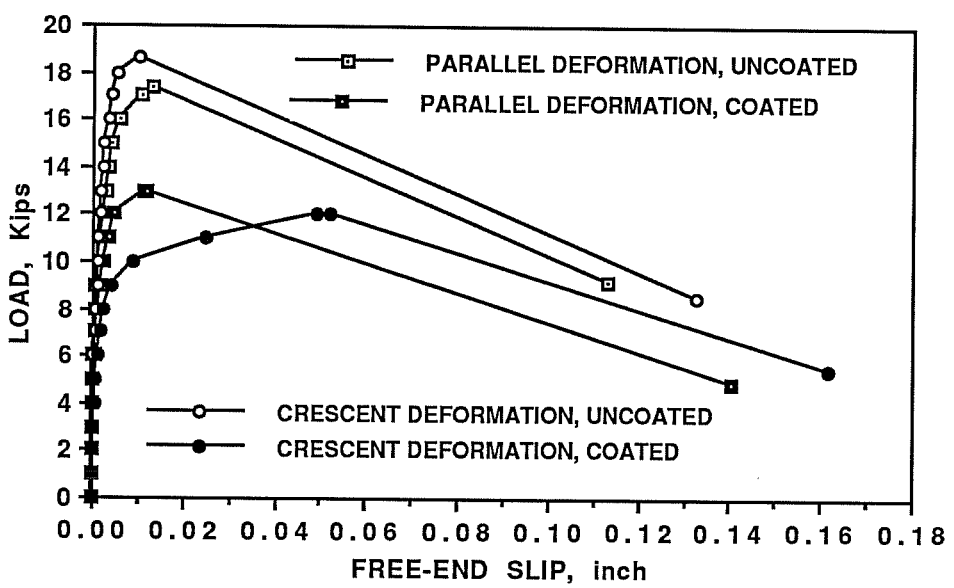

Figure 5.32 Effect of deformation pattern on load-slip behavior of #6 uncoated and epoxy-coated bars, top load = 5 kips, f'_c = 8700 psi.

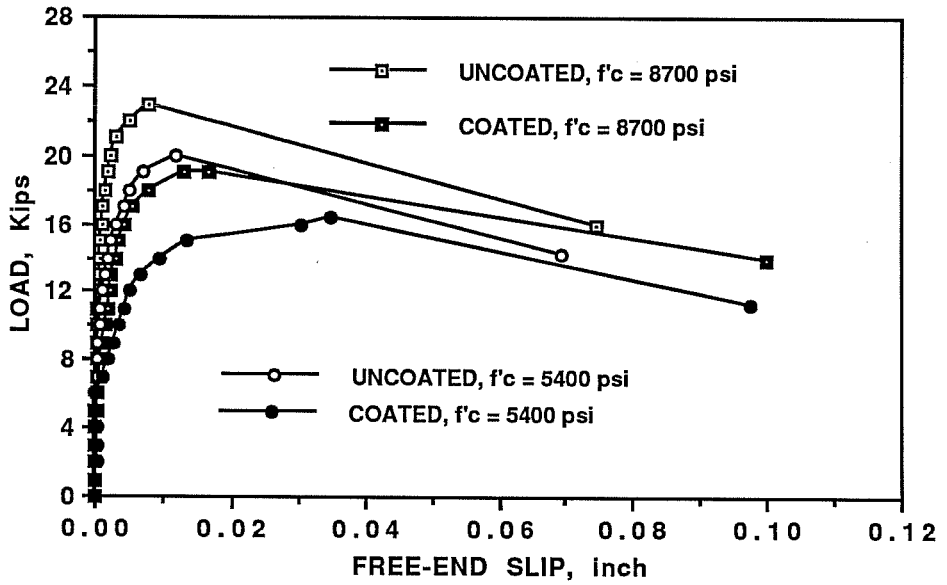

Figure 5.33 Effect of concrete strength on load-slip behavior of #6 uncoated and epoxy-coated bars, parallel deformation pattern, top load = 10 kips.

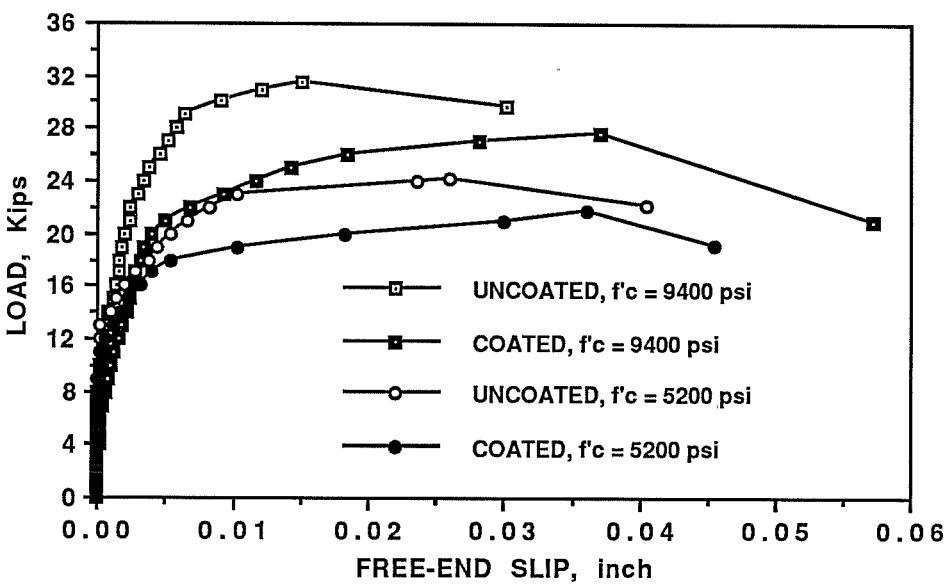

Figure 5.34 Effect of concrete strength on load-slip behavior of #11 uncoated and epoxy-coated bars, parallel deformation pattern, top load = 10 kips.

5.5.6 Effect of Rib Face Angle. Test results of series SEVEN, shown in Figure 5.35 (and in Table A7), indicate that the bond strength of a reinforcing bar, uncoated or epoxy-coated, increases slightly as the rib face angle increases. For uncoated bars, the increase in ultimate bond stress relative to that of the 30-degree rib face angle was 1% for 45 degrees and 10% for 60 degrees. The corresponding percentages for the coated bars were 16 and 18. In Figure 5.36, load-slip curves of uncoated reinforcing bars manufactured with different rib face angles, are compared. The curves indicate that as the rib face angle increases, the load at which the slip increases significantly is greater, and the slip corresponding to a given load decreases. The bar with the 60-degree angle started to slip significantly just before reaching ultimate. As discussed in Section 5.3.1 and illustrated in Figure 5.14, the failure is more of a pullout failure with slip corresponding to shearing of the concrete keys.

Bond ratios of coated to uncoated for series SEVEN (shown in Figure 5.35 and in Table A7), indicate that the bond performance of epoxy-coated bars relative to uncoated bars tends to improve with increase in rib face angle above 30 degrees. The ratios corresponding to rib face angles of 30, 45 and 60 degrees are 0.77, 0.90 and 0.83. However, within the scope of the few tests conducted, there is no clear trend of the effect of rib face angle on bond strength of epoxy-coated bars relative to uncoated bars. The bond ratios at ultimate are similar to the average bond ratios of the first five series (Table 5.1).

In Figure 5.37, load-slip curves of uncoated and epoxy-coated manufactured bars for two rib face angles (30 and 60 angles) are compared. Although epoxy-coated bars slipped more than uncoated bars at comparable load levels, the overall shape of the load-slip curves of coated and uncoated bars is similar regardless of the rib face angle. The curves for 30-degree rib face angles are similar to the curves of #6 and #11 bars tested in the first five series in which the rib face angles of the commercial #6 and #11 bars included in the test program range from 26.5 to 36 degrees (Table 4.4).

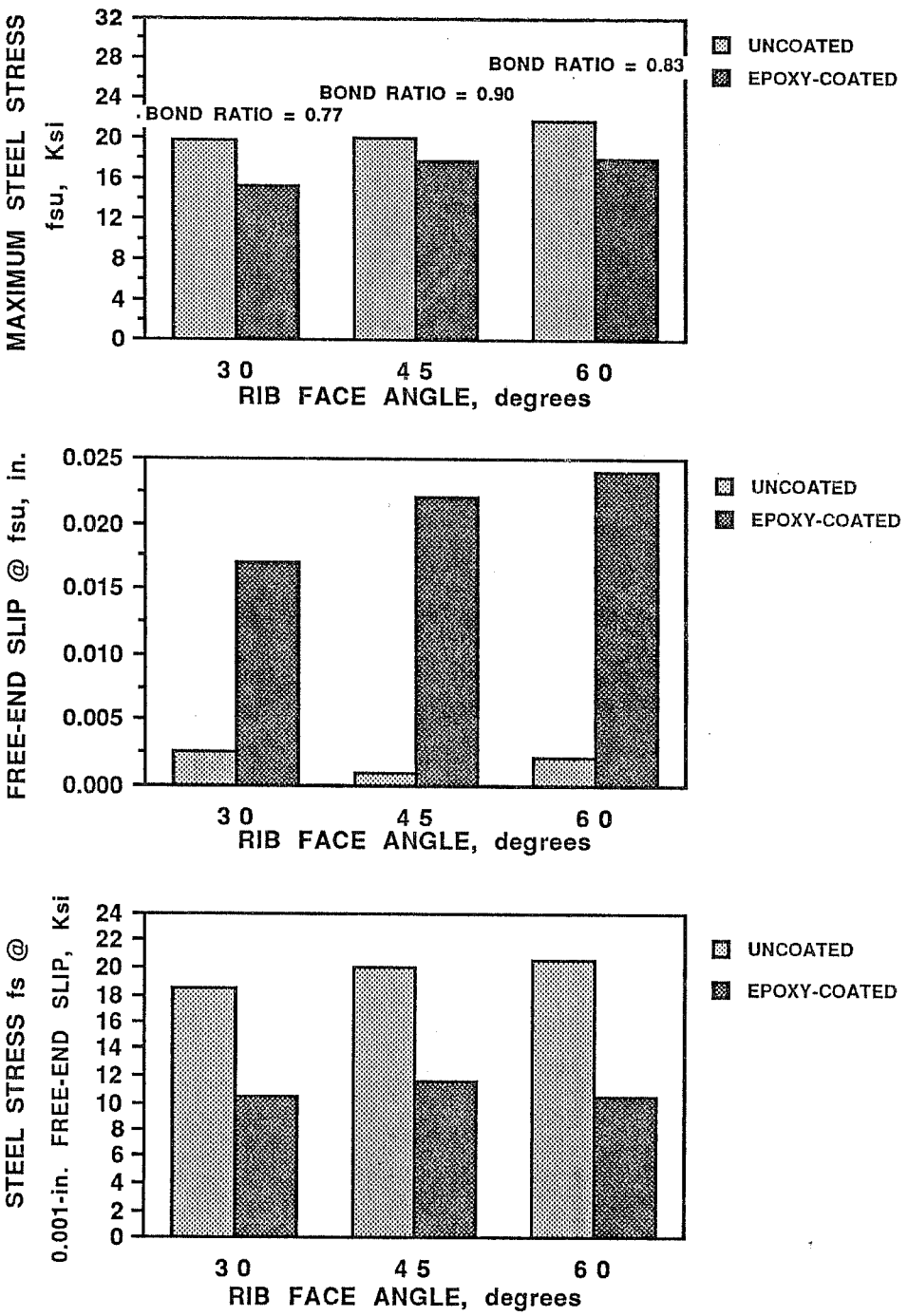

Figure 5.35 Comparison of stresses and free-end slip for series SEVEN of Type A pullout specimens, top load = 10 kips, concrete strength = 4750 psi.

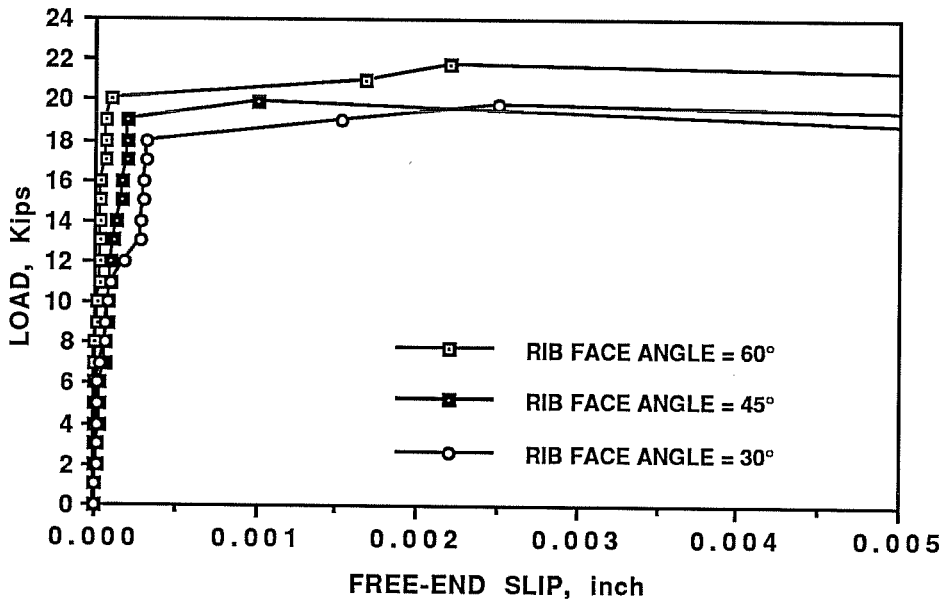

Figure 5.36 Effect of rib face angle on load-slip behavior of deformed bars, top load = 10 kips, concrete strength = 4750 kips.

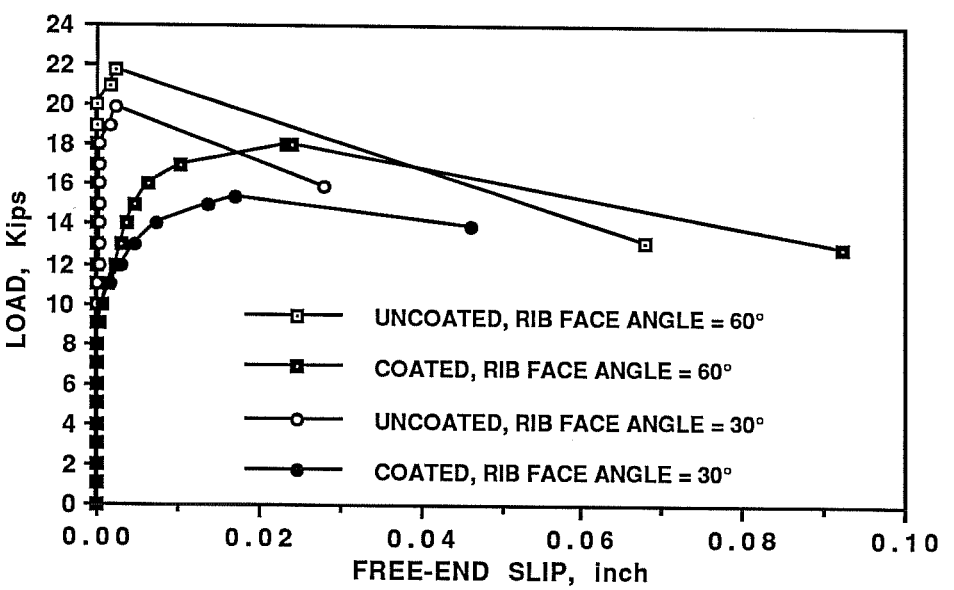

Figure 5.37 Effect of rib face angle on load-slip behavior of uncoated and epoxy-coated bars, top load = 10 kips, concrete strength = 4750 psi.

5.6 Relative Bond Performance of Uncoated and Epoxy-Coated Bars - Type B Specimens

In Table 5.3, the bond ratios (coated to uncoated) for Type B specimens (#6 bars with parallel deformation pattern) of the sixth and eighth series, are summarized. Concrete strengths of the two series were comparable. As shown in Table 5.3, bond ratios vary from 0.72 to 0.79 for the range of variables investigated. Variables included the amount of concrete cover to the bar, transverse reinforcement in the form of one #2 or one #3 uncoated bar hooked over the anchored bar at the middle of the anchorage length, and painting versus epoxy-coating.

Steel stresses and free-end slip of uncoated and epoxy-coated bars of the sixth and eighth series, are compared using bar charts in Figures 5.38 and 5.39. The effect of each variable on the performance of uncoated and epoxy-coated bars in Type B pullout specimens is summarized as follows:

5.6.1 Effect of Concrete Cover. Test results of the sixth series, shown in Figure 5.38 (and in Table A6), indicate that the bond strength of a reinforcing bar (uncoated, epoxy-coated, or painted) increases as the amount of concrete cover over the bar increases from 1 in. to 2 in. The increases are 5% for the uncoated bar, 7% for the epoxy-coated bar, and 10% for the painted bar. The amount of slip at ultimate, for the three bar types, is comparable for the two covers. Larger cover provided larger resistance to splitting at the interface between the concrete and steel.

Bond ratios listed in Table 5.3 and load-slip curves shown in Figure 5.40, indicate that the relative bond strength and load-slip behavior of uncoated and epoxy-coated bars are not affected by the change in concrete cover from 1 in. to 2 in. The bond ratios are 0.72 for a cover of 1 in. and 0.74 for the cover of 2 in.

5.6.2 Effect of Bar Painting. In the sixth series, two latex-painted bars were tested to compare their bond performance with that of epoxy-coated bars under similar conditions. The bond ratios (painted to uncoated), listed in Table 5.3, are 0.75 for a cover of 1 in. and 0.79 for a cover of 2 in. The values for epoxy-coated bars are 0.72 and 0.74, respectively. This shows that the

Table 5.3 Summary of bond ratio test results for Type B pullout specimens tested in the sixth and eighth series with #6 parallel deformation bars.

Type of Bar	Concrete Strength (psi)	Concrete Cover (inch)	Transverse Reinforcement*	Bond Ratio u(coated)/u(uncoated)
Epoxy-Coated	4500	1	-	0.72
Painted	4500	1	-	0.75
Epoxy-Coated	4500	2	-	0.74
Painted	4500	2	-	0.79
Epoxy-Coated	4900	2	-	0.76
Epoxy-Coated	4900	2	#2@10	0.75
Epoxy-Coated	4900	2	#3@10	0.77

*Transverse reinforcement, if provided, consisted of one Grade 60 deformed bar hooked over the anchored bar at the middle of the 10-in. anchorage length.

application of any coating on the surface of a reinforcing bar, whether it is epoxy coating or latex painting, destroys the adhesion between the bar and the surrounding concrete leading to a reduction in bond strength.

As shown in Figure 5.40, the load-slip stiffness of painted bars was much less than that of epoxy-coated bars. At the same load level painted bars slipped much more than epoxy-coated bars due to the softness of the latex painting as compared to the hard fusion-bonded epoxy coating.

5.6.3 Effect of Transverse Reinforcement. In the eighth series, the concrete cover to the anchored bar was 2 in. The addition of one #2 or one #3 tie at the middle of the embedment length, increased the bond strength of both uncoated and epoxy-coated bars. Results listed in Table A8 show that the bond strength of the uncoated bar improved 7% by adding a #2 tie and 11% by adding a #3 tie. The percentages for the epoxy-coated bar were 8 and 13, respectively. The additional tie hooked over the anchored bar provided the concrete at the interface with the bar with additional splitting and shearing resistance. Bond ratios, listed in Table 5.3, and load-slip curves

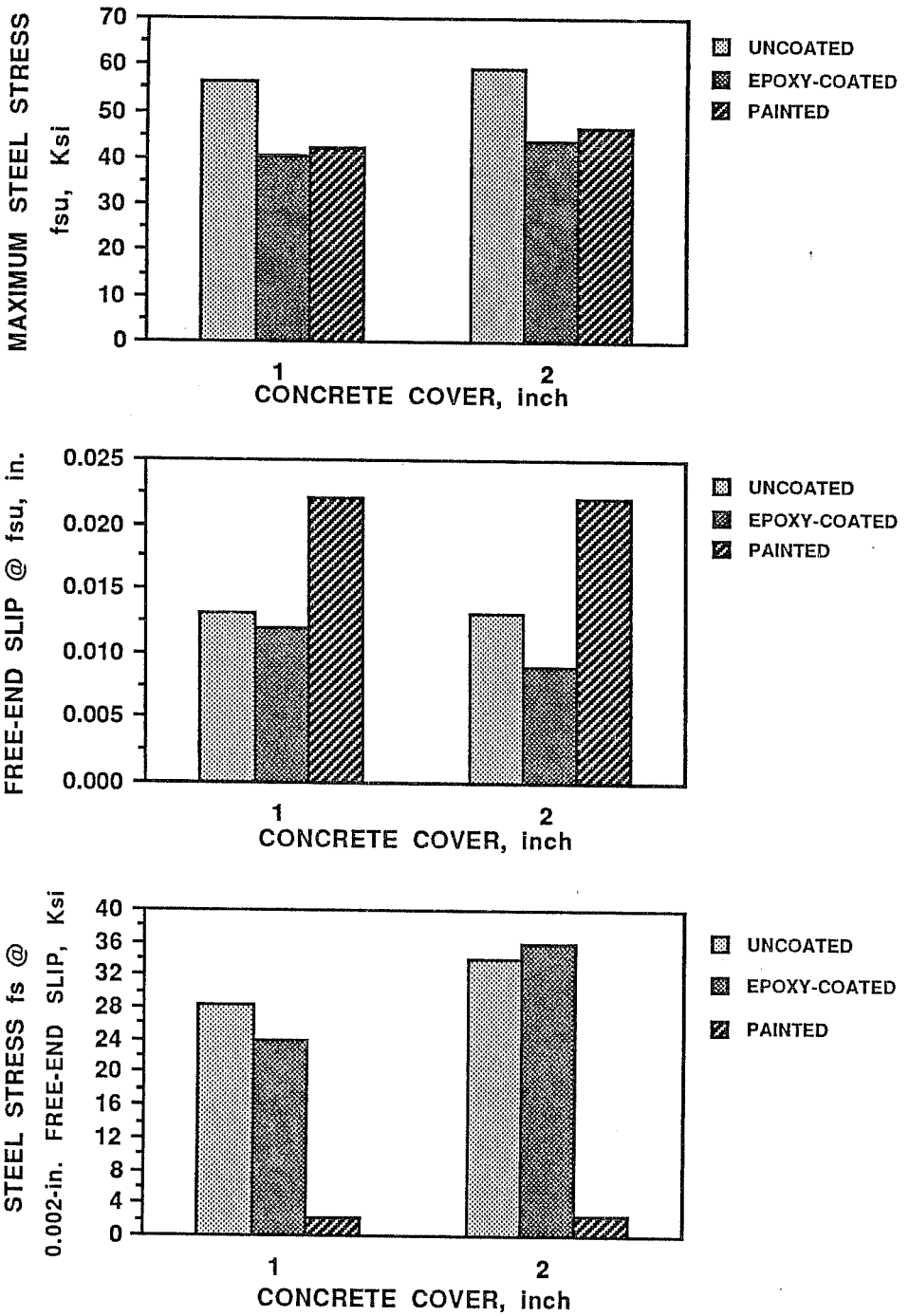

Figure 5.38 Comparison of stresses and free-end slip for series SIX of Type B pullout specimens, #6 bars, parallel deformation pattern, f'_c = 4500 psi.

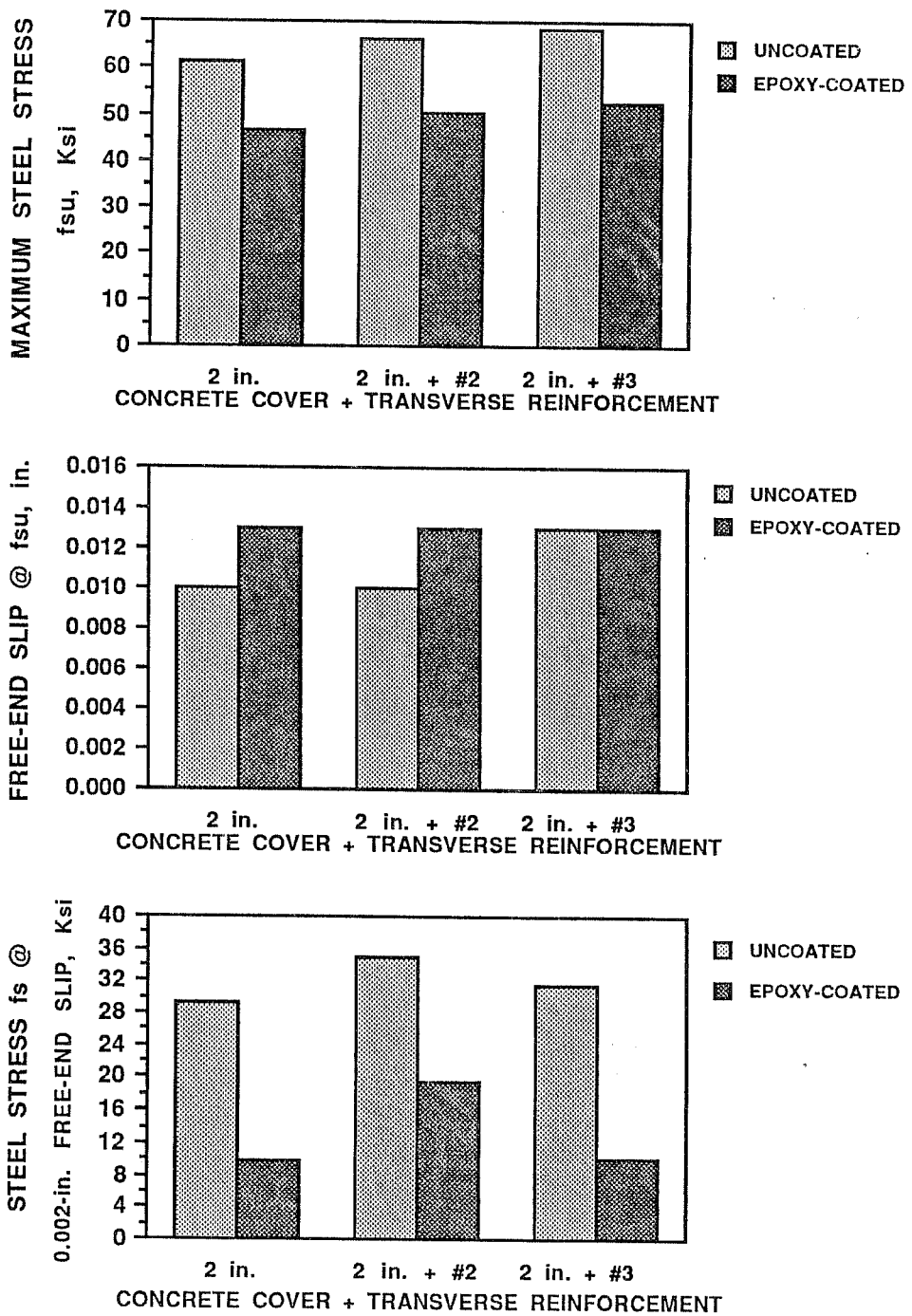

Figure 5.39 Comparison of stresses and free-end slip for series EIGHT of Type B pullout specimens, #6 bars, parallel deformation pattern, concrete strength = 4900 psi.

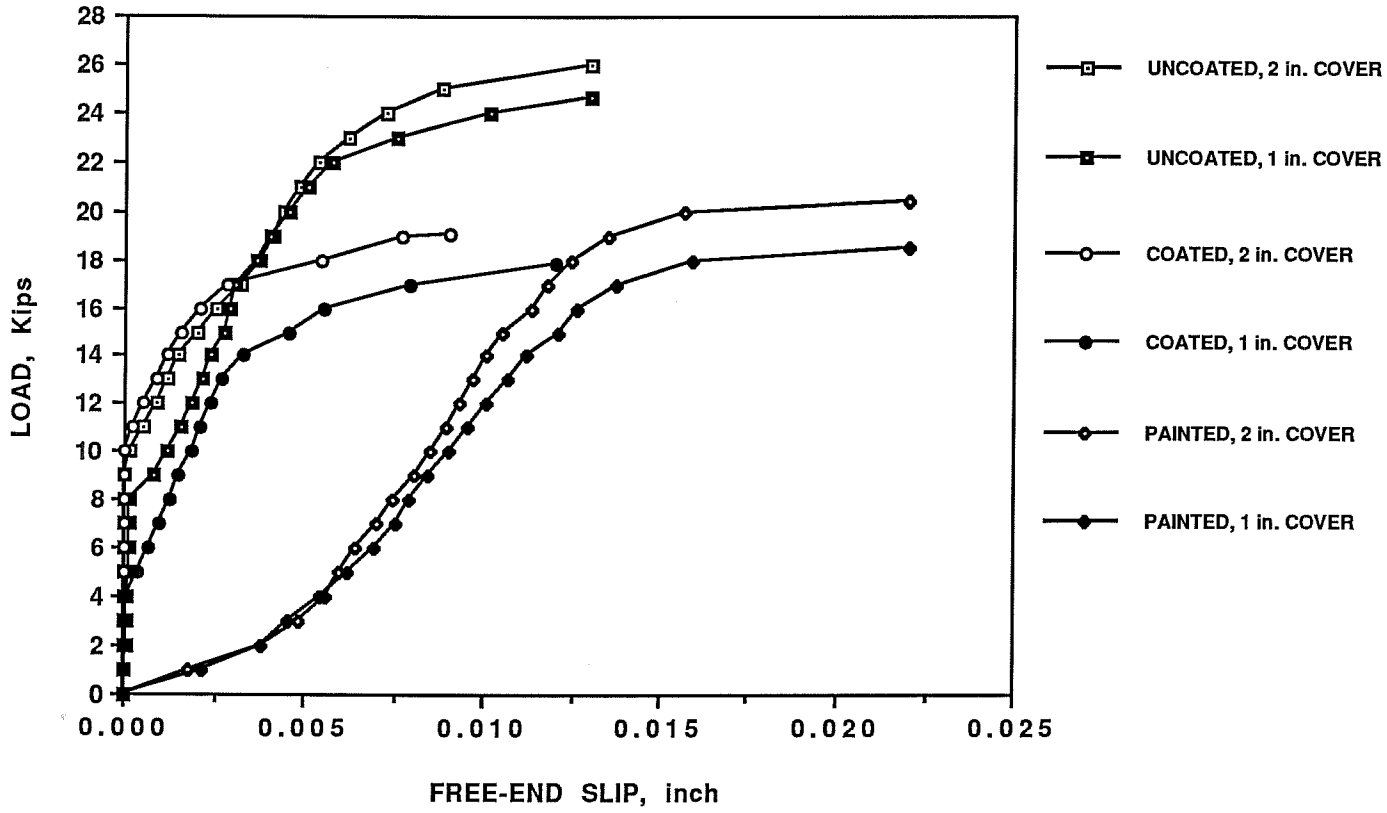

Figure 5.40 Effect of concrete cover on load-slip behavior of #6 bars, parallel deformation pattern, f'_c = 4500 psi.

shown in Figure 5.41, indicate that the bond performance of epoxy-coated bars relative to uncoated bars was not affected by the additional tie.

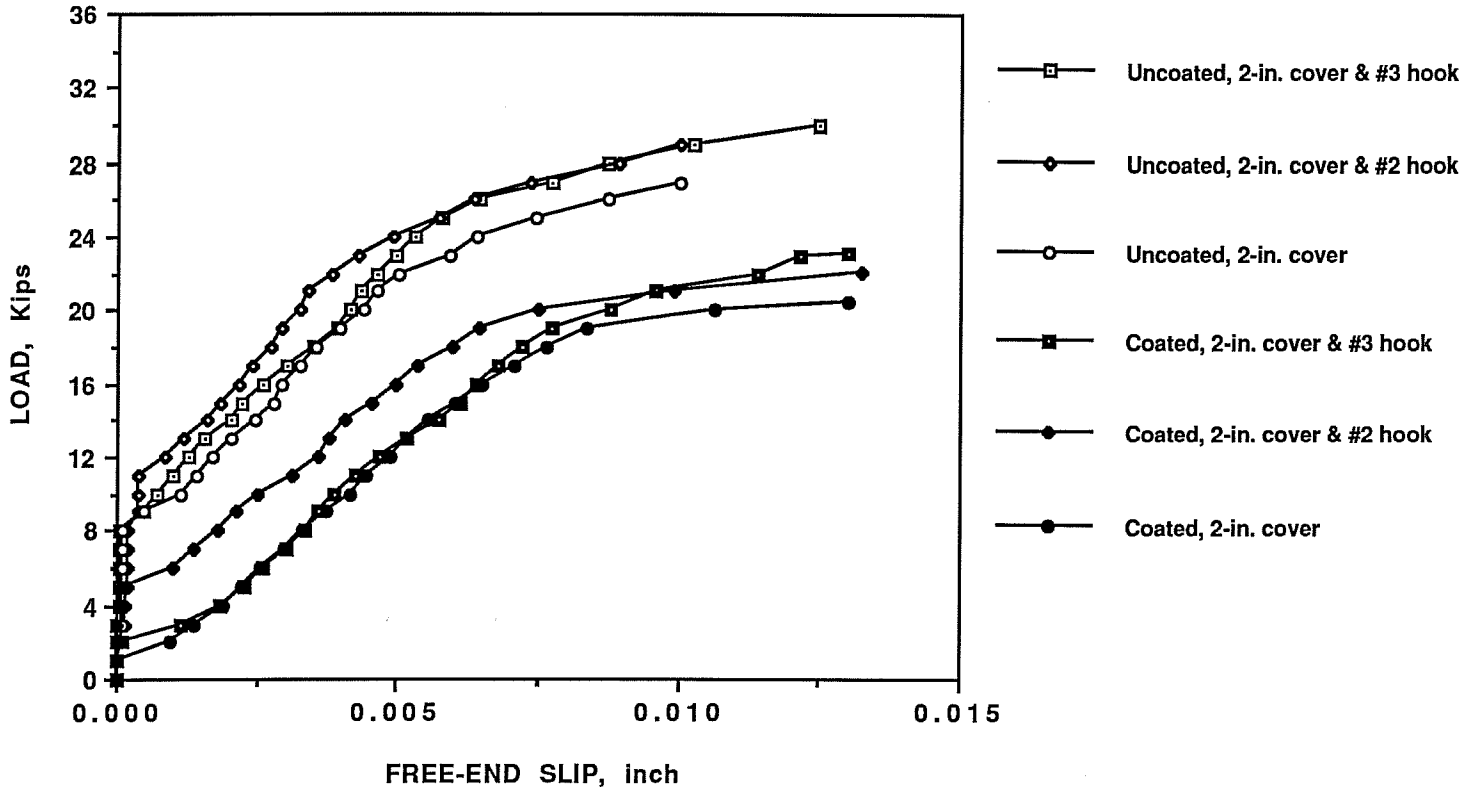

Figure 5.41 Effect of transverse reinforcement on load-slip behavior of #6 bars, parallel deformation pattern, 2-in. cover, concrete strength = 4900 psi.

CHAPTER 6

ROLE OF EPOXY-COATED TRANSVERSE REINFORCEMENT - EXPERIMENTAL PROGRAM

6.1 Design of Specimens

Twelve beams (three series) were tested in negative bending to determine the effect of coated transverse reinforcement on the bond strength of epoxy-coated bar splices. The specimens were cast with the bars in a "top" position; that is, more than 12 in. of fresh concrete was cast below the bars.

The test specimens are identified in Table 6.1. A five-part notation system was used to identify the variables of each beam. First, the beam is identified in the sequence it was tested. Second, the bar size (#6 or #11) is noted. Third, the nominal concrete strength (4 ksi) is identified. Fourth, uncoated (U) or epoxy-coated (C) bars are noted. The digit "3", following the letter U or C, refers to the presence of three splices instead of two splices as in the first six beams. The fifth portion indicates the presence of transverse reinforcement in the splice region where U represents uncoated ties and C epoxy-coated ties. The number in parenthesis is the average spacing of the ties along the splice length. The absence of a fifth portion in the notation of a beam indicates that transverse reinforcement was not present in the splice region. As an example of the notation system, B3-11-4-U-U(10") indicates that the third beam tested included #11 uncoated splices, had a 4000-psi nominal concrete strength, and included uncoated transverse reinforcement at an average spacing of 10 in. in the splice region.

The loading system was designed to produce a constant moment region in the middle of the specimen. The reinforcing bars were spliced at midspan so that the bond strength could be determined. The applied loading system produced the most severe splice condition and allowed for

Table 6.1 Test parameters of the beam specimens.

SERIES NUMBER	Specimen Notation	Bar Size	Splice Length (inch)	Nominal Concrete Strength f'_c (psi)	Transverse Reinforcement in Splice Region: Type	Transverse Reinforcement in Splice Region: Average spacing (inch)
	B1-11-4-U*	#11	30	4000	-	-
	B2-11-4-C**	#11	30	4000	-	-
SERIES	B3-11-4-U-U(10")	#11	30	4000	U*	10
ONE	B4-11-4-C-C(10")	#11	30	4000	C**	10
	B5-11-4-U-U(5")	#11	30	4000	U	5
	B6-11-4-C-C(5")	#11	30	4000	C	5
SERIES	B7-11-4-U3-U(5")	#11	30	4000	U	5
TWO	B8-11-4-C3-C(5")	#11	30	4000	C	5
	B9-6-4-U3	#6	18	4000	-	-
SERIES	B10-6-4-C3	#6	18	4000	-	-
THREE	B11-6-4-U3-U(6")	#6	18	4000	U	6
	B12-6-4-C3-C(6")	#6	18	4000	C	6

* U = Uncoated bars.
** C = Coated bars.

random formation of cracks. Applying negative bending to the specimens was convenient for observation and measurement of crack widths on the top surface of the beam.

The splice length of the deformed bars, used in the beam specimens, was selected to develop a steel stress, f_s, less than yield. The bars had a specified yield strength of 60 ksi. A yielding mode of failure provides little or no information regarding average bond strength or stress along the bar. Since the objective was to predict relative bond strengths of epoxy-coated and uncoated splices and not ductilities of those splices, f_s was set less than yield to ensure a splitting mode of failure in all beam specimens.

Equation (3-3), developed by Orangun, Jirsa and Breen[20] and described in Section 3.1.3, was used in designing the splices.

$$\ell_s = \frac{d_b\left[\frac{f_s}{4\sqrt{f'_c}} - 50\right]}{1.2 + 3\frac{c}{d_b} + K_{tr}}, \qquad K_{tr} = \frac{a_{tr} f_{yt}}{500 s d_b}$$

$$\frac{c}{d_b} \le 2.5 \, , \; K_{tr} \le 3.0$$

The above equation is the basis of the current development length provisions in the 1989 ACI Code (ACI 318-85)[1].

As an example, for specimen B1-11-4-U-U(10"), to develop a steel stress of 45,000 psi:

with d_b = 1.41 in.

f_s = 45000 psi

f'_c = 4000 psi

c = 2 in.

$$K_{tr} = \frac{0.11 \times 60{,}000}{500 \times 10 \times 1.41} = 0.94$$

then $\ell_s \cong 28$ in.

The splice length was set at 30 in. for all #11 bar specimens and 18 in. for the #6 bar specimens.

A concrete cover of 2 in. to the reinforcing bars was chosen as a typical side and top cover for all the beam specimens. This corresponds to the minimum cover for bridge decks specified by the American Association of State Highway and Traffic Officials (AASHTO) standards[32].

In the six beams of the first series, two #11 bar splices were designed so that the side cover, 2 in., was one-half the clear spacing between splices, 4 in., and equal to the top cover, 2 in. This allowed identical confinement for both splices by concrete and by any ties crossing the splitting plane in the splice region. This meant that the failure could occur as either a side split failure or a face-and-side split failure. With 2-in. cover and 4-in. clear spacing, the beam width was 13.5 in.

The two beams of the second series were designed with three #11 bar splices and the four beams of the third series had three #6 bar splices. The clear spacing between the splices was one bar diameter (1.41 in.) in the second series and 1.25 in. in the third series. With close spacing between splices, a splitting crack is likely to form in the plane between bars. The clear spacings were at or near the minimum values allowed in codes. The beam widths were 15.5 in. and 11 in. in the second and third series, respectively.

The cross-section details of all beams tested are shown in Figure 6.1. The depth was 16 in. for all beams.

After the section properties were chosen, the lengths of the test specimens were determined. Since determining the spacing and width of cracks was also an objective, it was desired

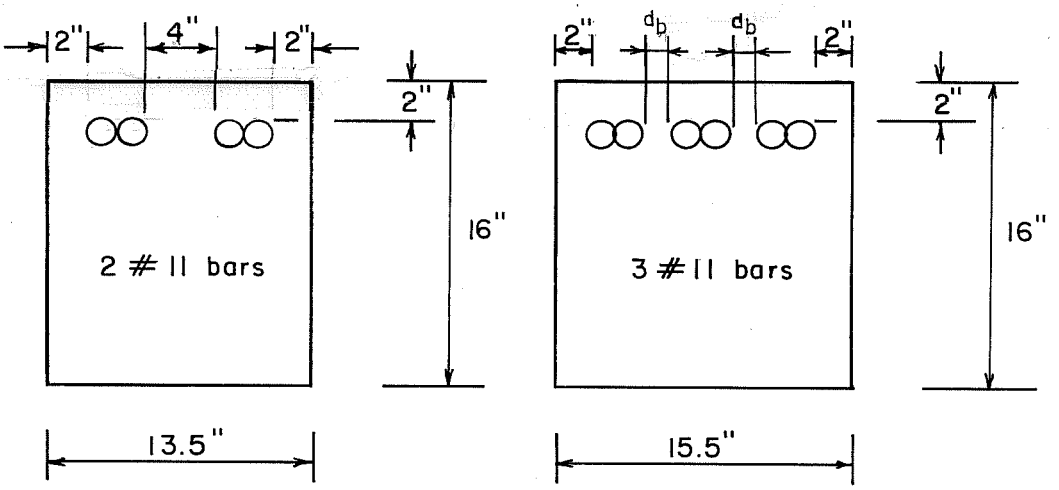

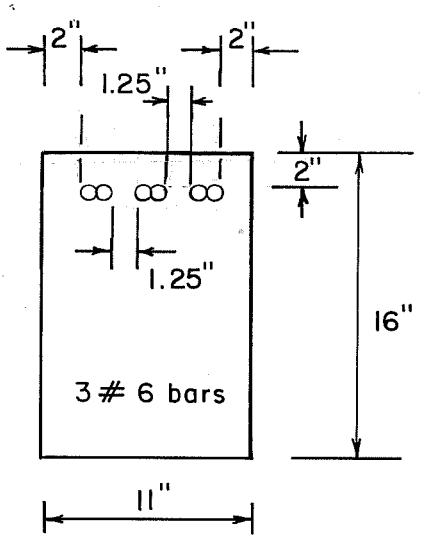

Figure 6.1 Cross-section details of the beam specimens.

to have a constant moment region long enough to allow random distribution of cracks outside of the splice. Flexural cracks usually form at or near each end of the splice. Also, cracks tend to form directly over or near the supports. The length of the constant moment region was selected so that the location and spacing of cracks was not influenced by these discontinuities.

In order for the beam to fail at the splice, the remaining portion of the beam was designed to develop yield in the steel. Therefore, the length of the bars outside the constant moment region was at least equal to the required development length.

Two practical considerations controlled the final lengths of the specimens. The tie-down anchors in the reaction floor at the Ferguson Structural Engineering Laboratory are spaced four feet in each direction. The length of each specimen had to be a multiple of 4 ft. It was also desired to cast only two sizes of specimens: one for the #6 bar specimens and another for the #11 bar specimens.

A length of 12 ft. between loading points with a 4 ft. constant moment region was chosen for the #6 bar specimens. A length of 20 ft. between loading points with a 9 ft. constant moment region was chosen for the #11 bar specimens. These lengths provided adequate constant moment regions and shear spans long enough to develop yield in the steel. Six inches were added to each end of the specimens to allow area for a loading beam. This resulted in overall lengths of 13 ft. for the #6 bar specimens and 21 ft. for the #11 bar specimens (see Figure 6.2).

6.2 Materials

6.2.1 Reinforcing Steel. Bars of each size, #6 and #11, were from the same heat of steel and had a parallel deformation pattern. This ensured that both uncoated and epoxy-coated bars in companion specimens had identical rib geometry and mechanical properties. The bars met ASTM A615-87a[30] and were Grade 60. Samples of the bars were shown in Figure 4.2, and a listing of their physical and mechanical properties was given in Table 4.4. The stress-strain history

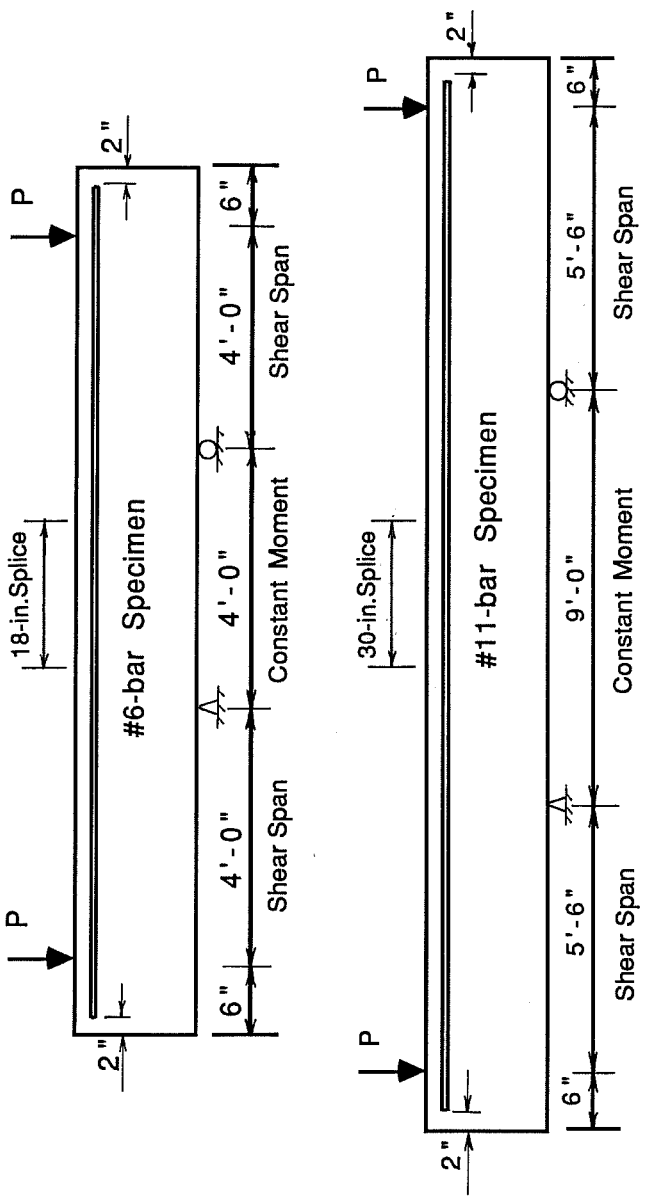

Figure 6.2 Dimensions and test setup of the beam specimens.

for the #6 parallel deformation bar was shown in Figure 4.5, and that of the #11 parallel deformation bar was shown in Figure 4.6. The transverse reinforcement used in the beams was #3 Grade 60 deformed bars. Two coupon tests were done in the laboratory to confirm the mill test report of the #3 ties. The corresponding stress-strain curve is shown in Figure 6.3.

All epoxy-coated bars used were coated at the same fabrication plant including the bars used for transverse reinforcement. The nominal coating thickness was 8 mils. The stirrups were bent after coating and damage at the bent regions was touched up by the fabricator.

Prior to casting, the thickness of the epoxy coating was measured with a Microtest Thickness Gage. The gage and the measuring procedure were shown in Figures 4.7 and 4.8. Each bar in the beam specimen was measured in six places along the marked splice length on each side of the bar, a side being considered the area between longitudinal ribs. The average coating thickness for the longitudinal bars in each epoxy-coated bar specimen, is shown in Table 6.2. Also, the distribution of measured coating values for the bars in each beam specimen are shown in Figures 6.4, 6.5, and 6.6. The average coating thickness for the epoxy-coated transverse reinforcement was approximately 9 mils.

6.2.2 Concrete. In phase one, the 28-day concrete compression strength was more than 1000 psi above the design value of 4000 psi. Based on that a mix was proportioned for 3000 psi to be provided by the same supplier in order to obtain a nominal concrete strength of 4000 psi for the beam specimens. The mix was non air-entrained and had a maximum size aggregate of 3/4 in. Assuming saturated surface dry conditions for the aggregates, the mix proportions per cubic yard were:

Cement (Type I)	360 lb.
Coarse Aggregate	1881 lb.
Sand	1435 lb.
Water	266 lb.
Water reducer-retarder	10.5 oz.

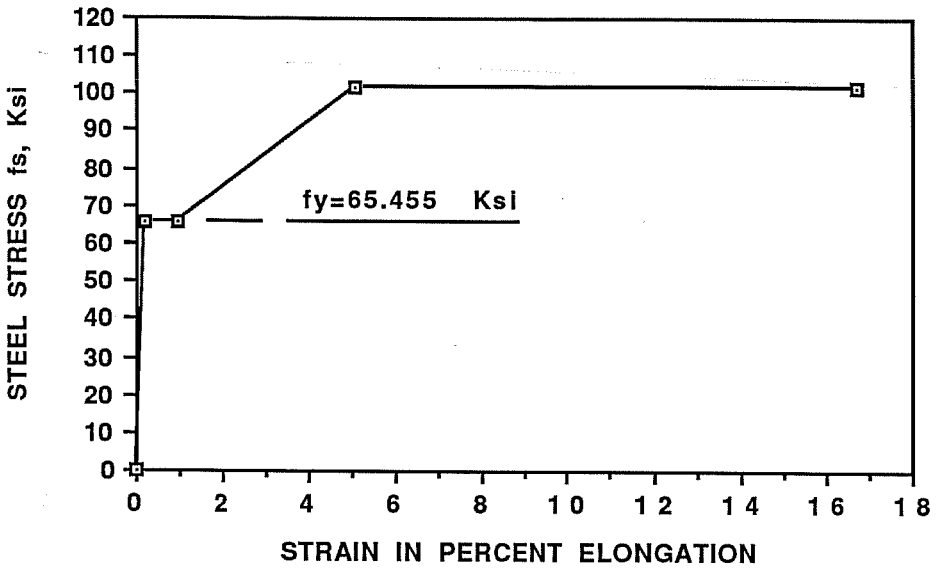

Figure 6.3 Stress-strain curve for the #3 ties used in the beam specimens, parallel deformation pattern.

Table 6.2 Epoxy coating thickness in the beam specimens.

Specimen Notation	Average Coating Thickness (mils)	Standard Deviation (mils)
B2-11-4-C	8.0	1.2
B4-11-4-C-C(10")	8.6	1.2
B6-11-4-C-C(5")	8.8	1.1
B8-11-4-C3-C(5")	8.6	1.0
B10-6-4-C3	6.8	1.1
B12-6-4-C3-C(6")	6.7	1.0

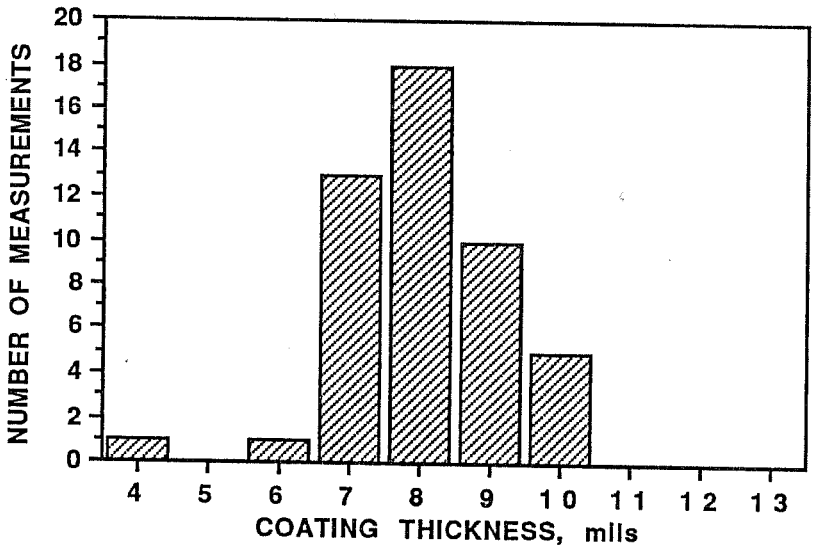

(a) Beam B2-11-4-C

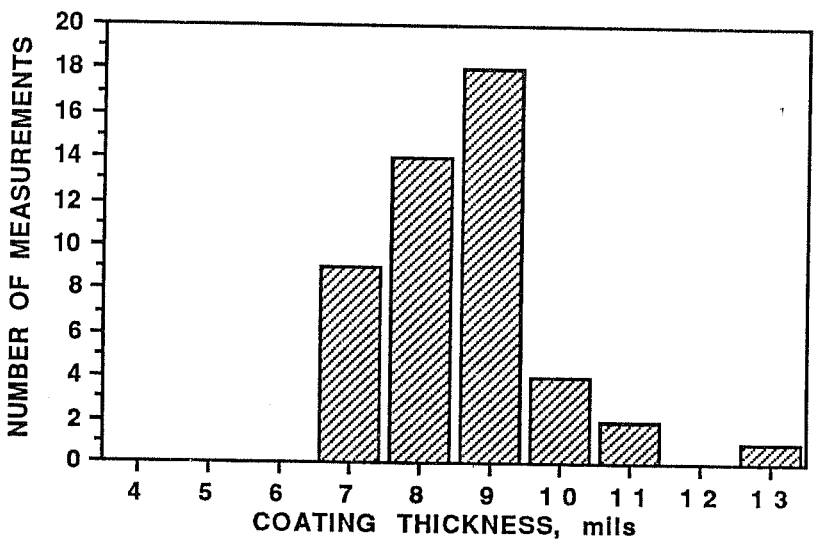

(b) Beam B4-11-4-C-C(10")

Figure 6.4 Distribution of coating thickness measurements for the epoxy-coated bars in beams B2 and B4.

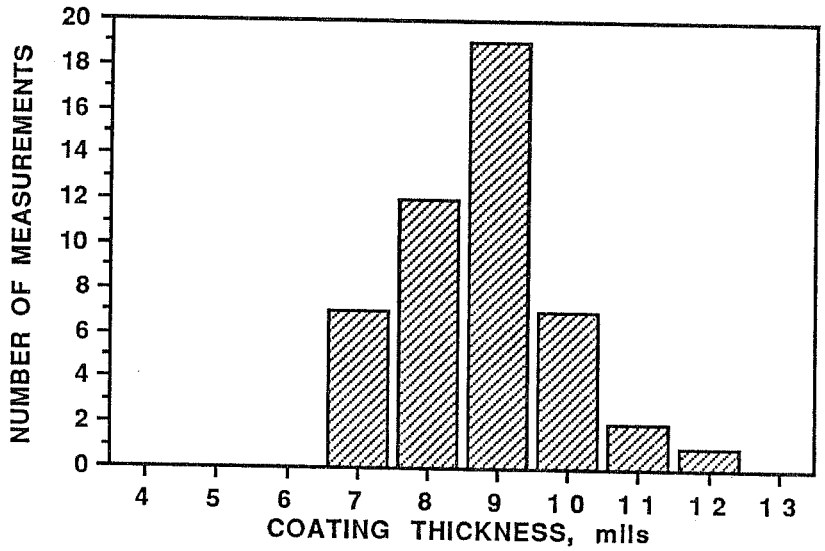

(a) Beam B6-11-4-C-C(5")

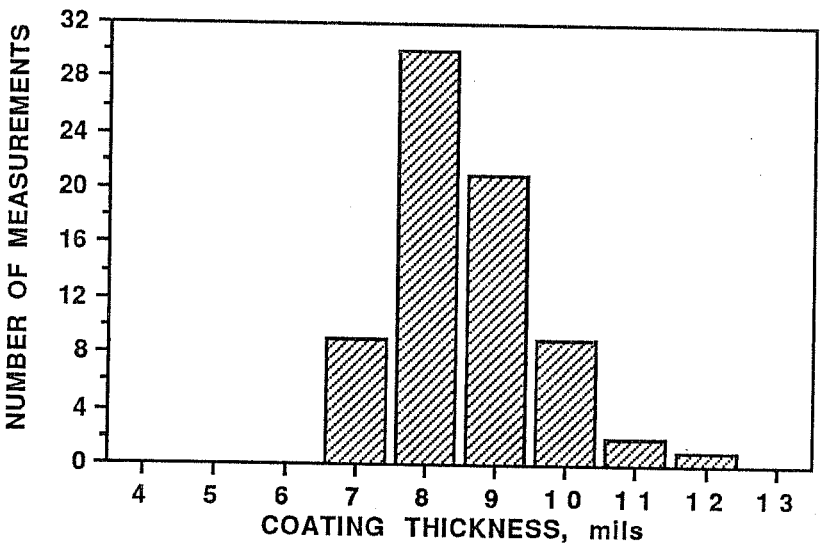

(b) Beam B8-11-4-C3-C(5")

Figure 6.5 Distribution of coating thickness measurements for the epoxy-coated bars in beams B6 and B8.

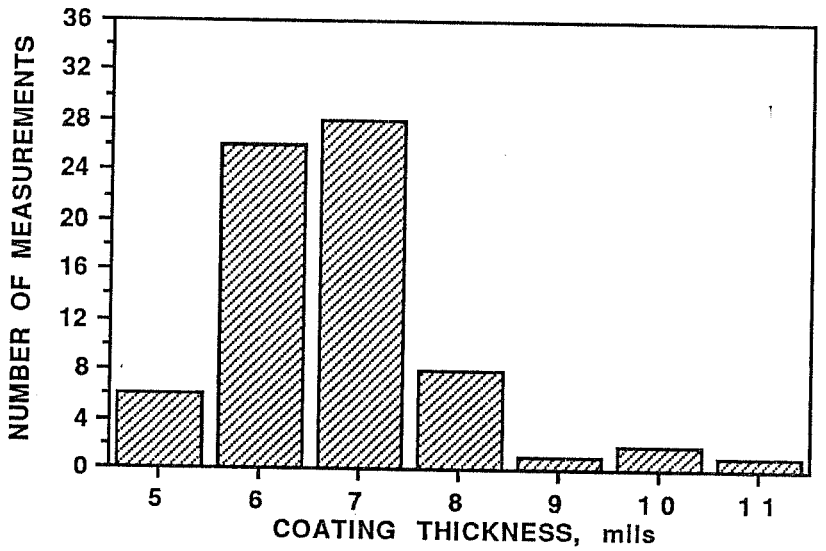

(a) Beam B10-6-4-C3

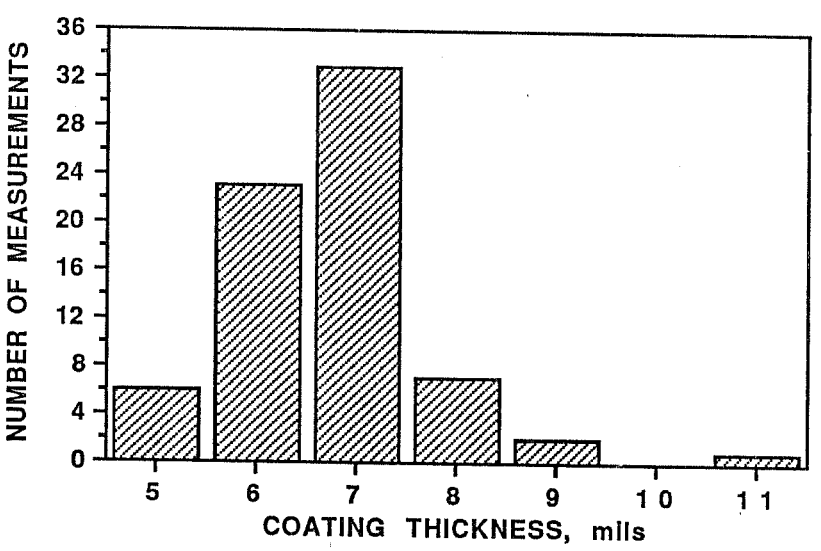

(b) Beam B12-6-4-C3-C(6")

Figure 6.6 Distribution of coating thickness measurements for the epoxy-coated bars in beams B10 and B12.

However, the proportions of the mixes delivered varied from the above design according to the moisture content of the aggregates. The amount of water added was always less than the specification. Upon arrival of the truck carrying the concrete, and before casting, additional water was added in small increments until the desired slump of about 3.0 in. was reached. While the slump of the concrete cast in the two series of #11 bar beams was around 3.5 in., the slump of the concrete cast in the #6 bar series was only 2.0 in. The variations of the concrete compression strength with time for all beam specimens are shown in Figure 6.7.

6.3 Construction of Specimens

6.3.1 Formwork. The formwork was designed so that four beams would be cast simultaneously from the same batch of concrete. Two formwork bases were built each with the capacity of holding two #6 or #11 beam specimens. The side forms were first designed for the longer #11 bar beams of the first two series. The side forms were later modified to cast the third series of #6 bar beams. The end forms were sandwiched between the two side forms in positions that gave the specimen its desired length. The side forms and the end forms were bolted to the base of the formwork. To maintain a constant width of the beam along its length and to ensure the rigidity of the form, bracing was provided for the side forms. The lines of contact between the side forms and the end forms and between any side or end form and the base form, were sealed with tape to ensure the water-tightness of the formwork. The intersections of any two pieces of one form were sealed. A side view of the formwork is shown in Figure 6.8 prior to casting beams B1, B2, B3 and B4.

6.3.2 Fabrication of Cages. The steel cages were fabricated and placed in the formwork. The bars were cut to provide the correct splice length and overall length of the beams. The bars were spliced with the longitudinal rib up as shown in Figure 6.9.

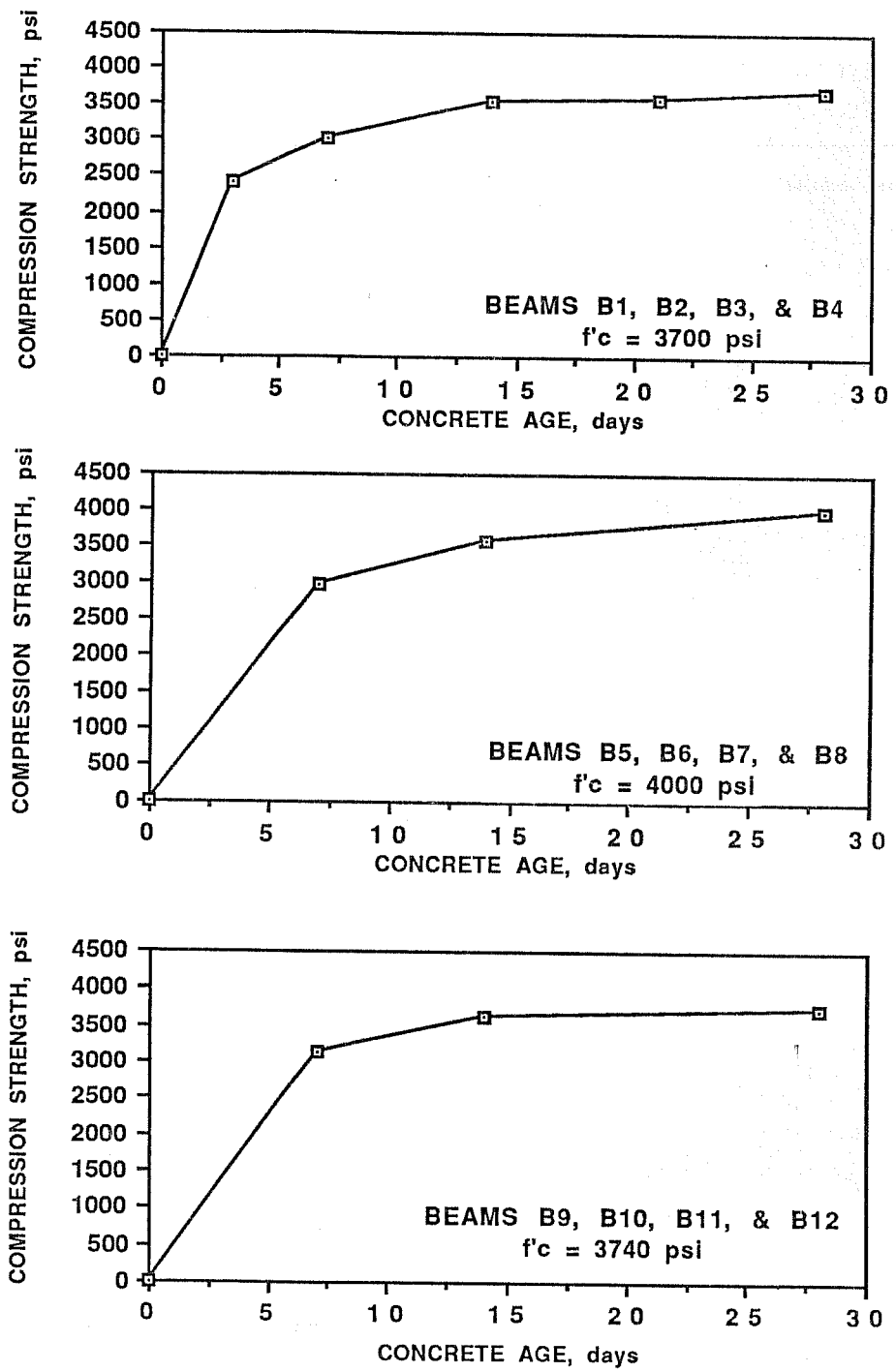

Figure 6.7 Variation of concrete compression strength with age for the beam specimens.

Coated bars tend to have a thicker coating at the cut end because the ends are coated manually after they are cut to length by the coating fabricator. Therefore, the coated ends of the bars, as received from the supplier, were not placed in the splice to avoid large changes in coating thickness over the length of the splice.

Hoop stirrups were tied to the longitudinal bars over the length of each shear span. In all the beams a few hoop stirrups were also added in the constant moment region outside the splice to help hold the cages in the form. Two #3 bottom bars extended along the entire beam length. In Figures 6.10, 6.11, and 6.12, the layouts of the steel cages in all beam specimens tested, are shown.

To maintain the correct top cover for the reinforcing bars in the splice region, chairs were placed under the cages. In beams with no stirrups in the splice region, additional help was needed to hold the splices in the correct location. A method was used where after the cages were placed in the formwork, two bars were placed across the top of the formwork in the splice region. Each splice was held in the correct position by wires from the two bars placed across the forms as shown in Figure 6.13.

6.3.3 Casting. Four beam specimens were cast simultaneously. The casting procedure was the same for all beam specimens. The concrete was placed in two lifts from a bucket using the overhead crane. The bottom lift was placed in each form and compacted. Then the final lift was placed and compacted. At least two persons did the compacting using mechanical vibrators. One person vibrated the concrete in the splice region of all beam specimens to make sure that concrete was compacted similarly around the splices. Concrete was also placed in 6x12 cylinder molds while the beams were being cast. At the end of the casting procedure, the top surface of each beam specimen was screeded and trowelled smooth. The casting procedure is shown in Figure 6.14. A few days after casting, the forms for beams in the first and second series were stripped. In the case of the beams with #6 bars in the third series, the side forms were stripped three days after casting

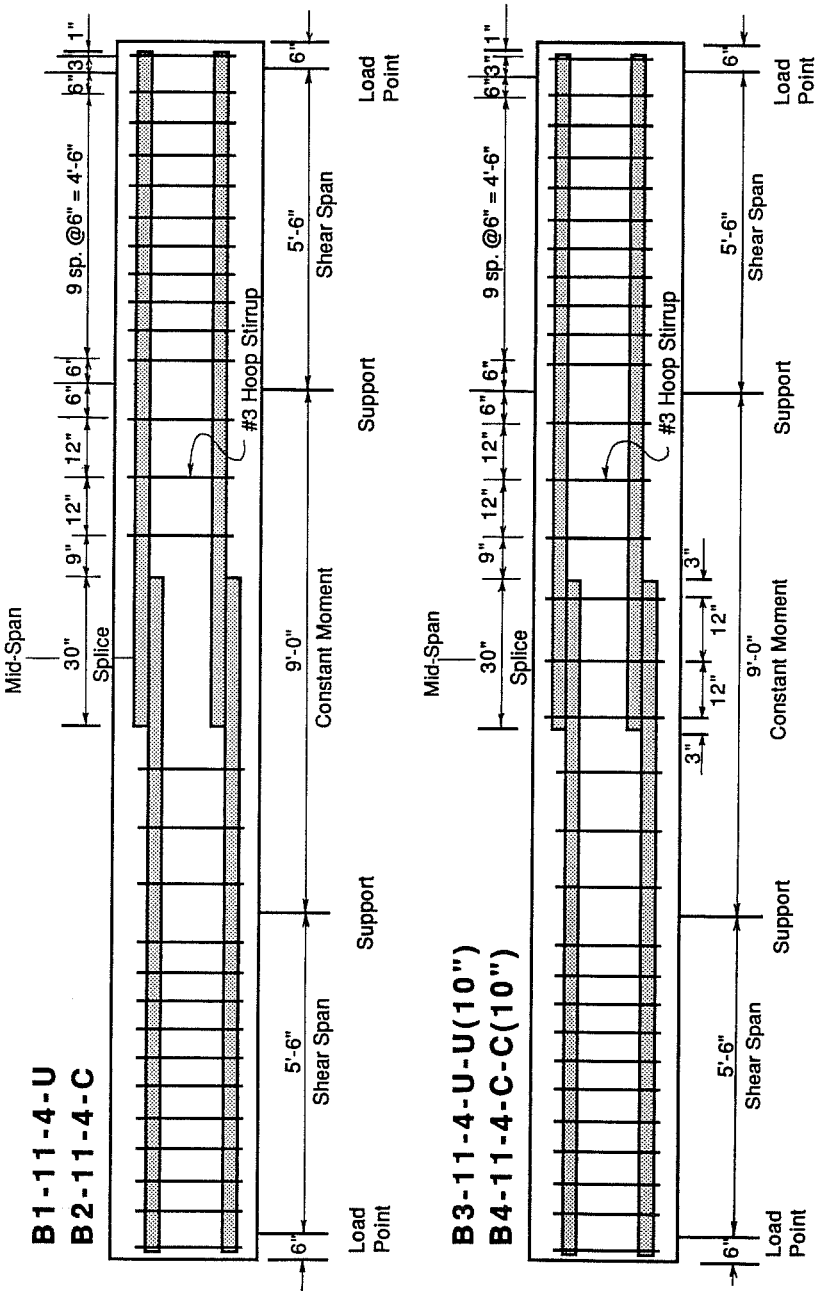

Figure 6.10 Steel layout of beams B1, B2, B3 and B4.

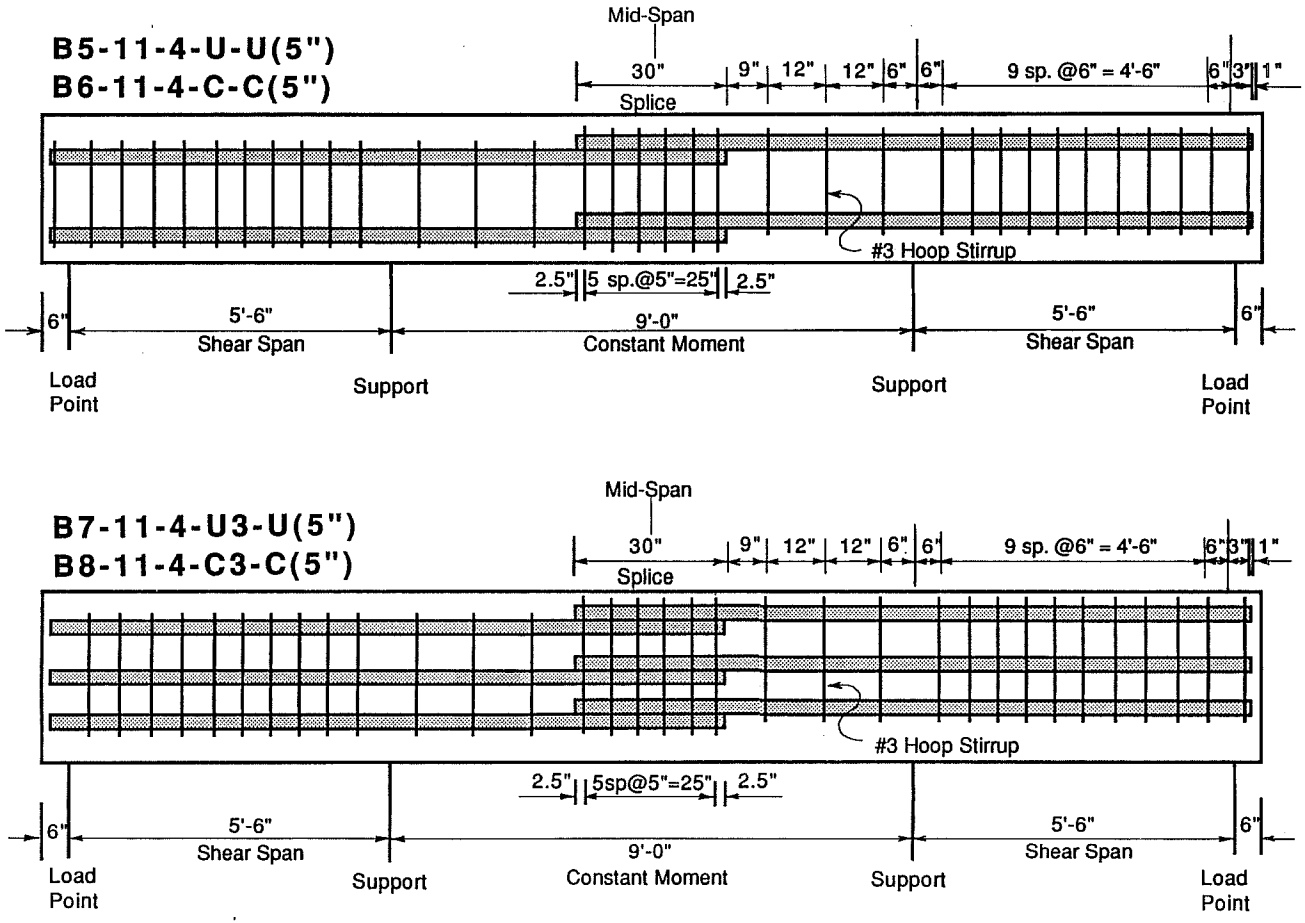

Figure 6.11 Steel layout of beams B5, B6, B7 and B8.

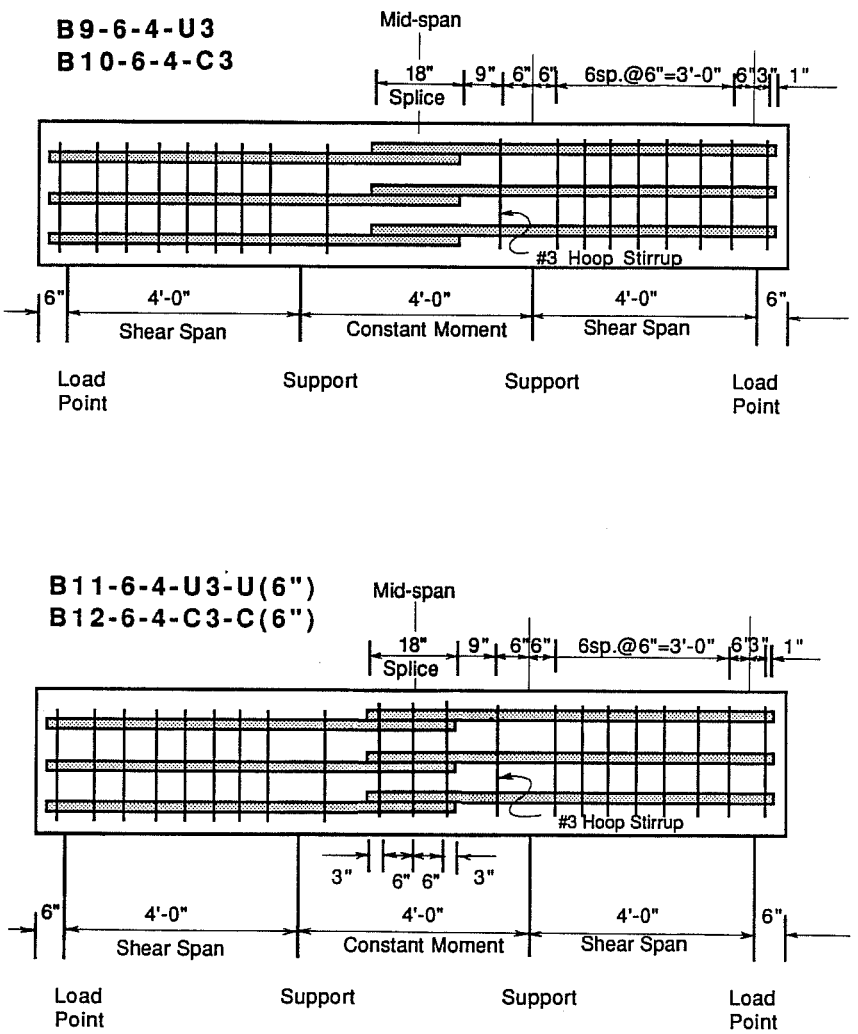

Figure 6.12 Steel layout of beams B9, B10, B11 and B12.

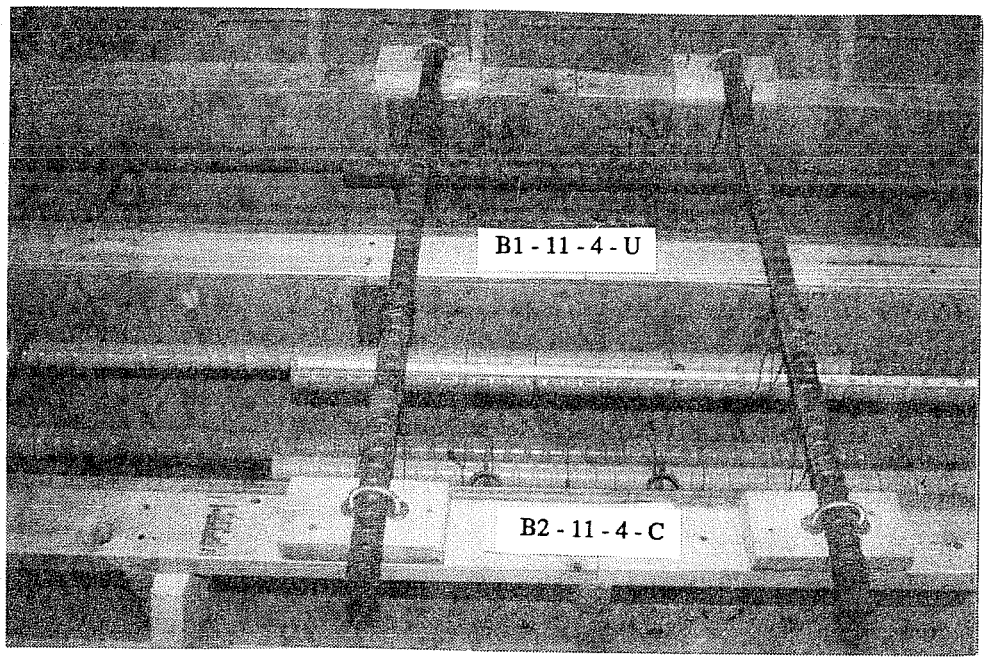

(a) Overall view

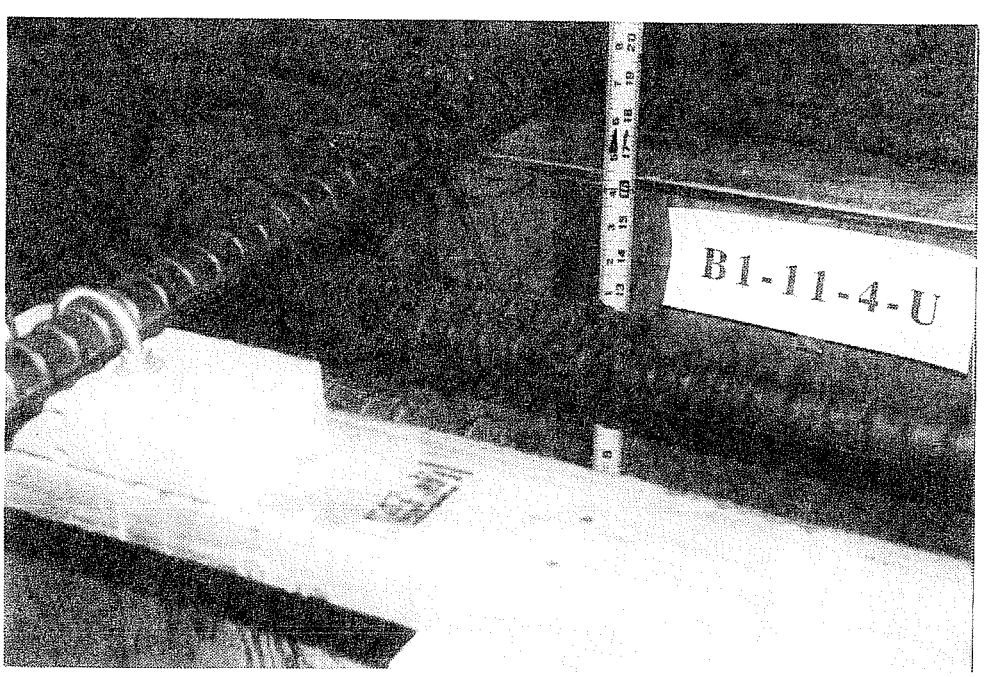

(b) Closer detail

Figure 6.13 Splice support bars used in beams with no stirrups in the splice region.

(a) Concrete placement and compaction

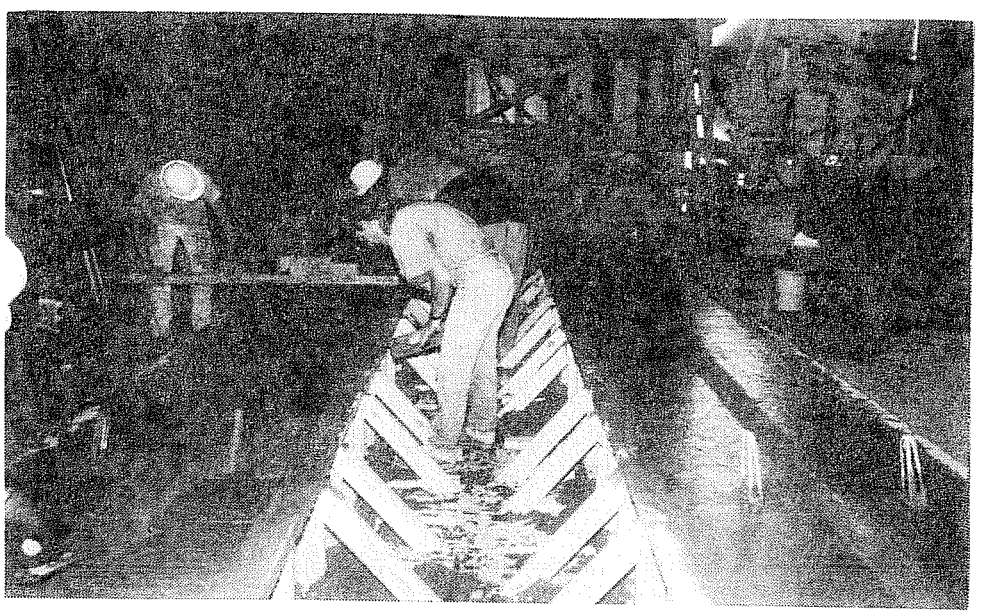

(b) Screeding and trowelling the beam surface

Figure 6.14 Casting of the beam specimens.

but the beams were left on the form-base until they were tested. The 6x12 cylinders were also removed from the forms when the beam forms were stripped.

6.4 Test Procedure

The test setup is shown in Figure 6.15. Each specimen was supported by 7/8-in. diameter bars on concrete blocks. A 1-in. thick steel plate was grouted to the support block and a similar plate was grouted to the bottom of the beam at each support and the 7/8-in. bar was placed between the two plates. At one support, the bar was welded to the support block steel plate to simulate a pin connection. At the other support, the round bar was free to translate simulating a roller connection.

Load was applied to the beam by means of two 30-ton double-action rams at each end. All four rams were operated by one hydraulic pump. The rams had a 6.0-in. stroke and a 6.53-sq. in. effective area. Long tie-down anchor rods transferred the reaction from the rams to the reaction floor. A closer view of the loading system is shown in Figure 6.16. Load was gradually applied in 1.0-kip increments until failure occurred. The load was monitored by a 5000 psi pressure transducer. Hydraulic hose pressure was also measured at the pump by a calibrated 5000 psi pressure gage.

At each load stage the maximum load was read. After reaching a desired load, the pressure line was closed. However, the load dropped slightly while reading deflections and crack widths. The highest load at each stage was recorded.

At each load stage, deflection readings were taken and flexural cracks were marked and measured. The crack widths were measured with a crack width comparator. Since the width of a flexural crack varied only slightly along its length, each crack was measured at only one location. Deflection readings were taken with dial gages at one end (at the point of loading) and at the center of the beam.

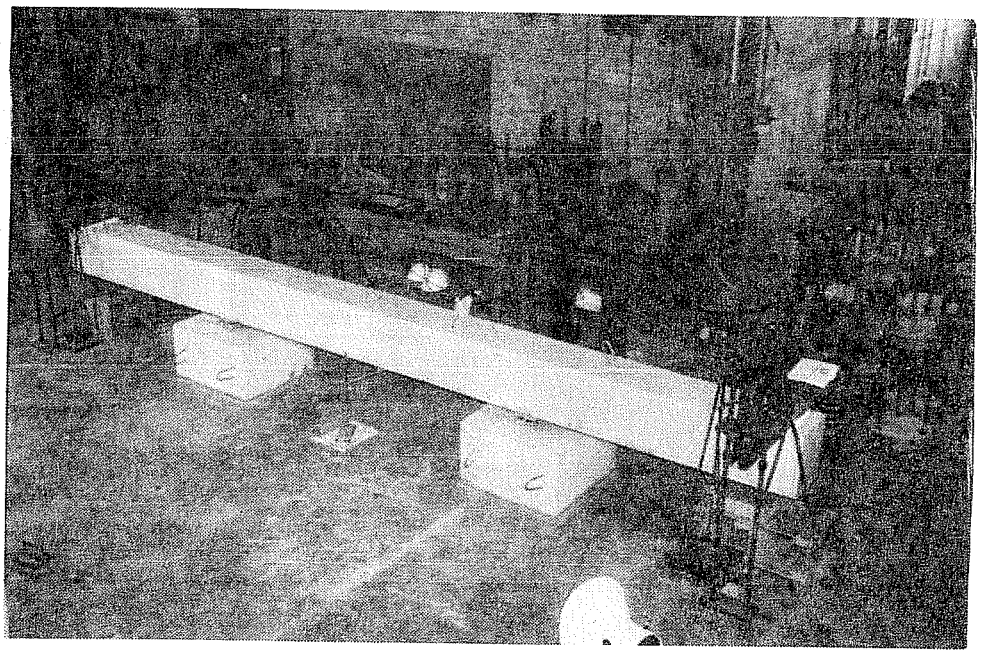

Figure 6.15 Test setup of the beam specimens.

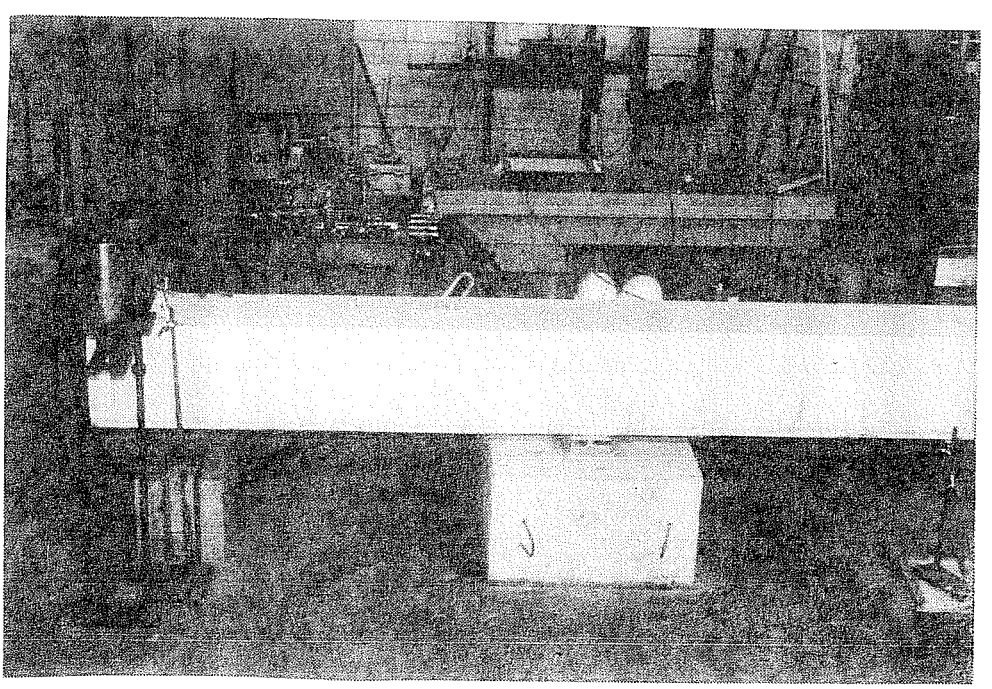

Figure 6.16 Loading system of the beam specimens.

During each test the variation of the end load versus the end deflection was plotted using an X-Y plotter. The load and deflection instrumentation connected to the plotter were independent of the previously mentioned instrumentation. The load was monitored by a calibrated electronic 10,000 psi pressure transducer connected to the pressure line. A plunger-type potentiometer was used to measure the end deflection. The shaft of the potentiometer rested against a 1.5-in. x 1.5-in. piece of plexi-glass glued to the end of the beam.

CHAPTER 7

ROLE OF EPOXY-COATED TRANSVERSE REINFORCEMENT - SPECIMEN BEHAVIOR AND ANALYSIS OF TEST RESULTS

7.1 Introduction

The general behavior of the specimens is discussed in terms of flexural cracking and longitudinal cracking comparing epoxy-coated and uncoated bar specimens. The effect of varying the amount of transverse reinforcement in the splice region on the behavior is discussed. Based on the test results the performance of epoxy-coated bars is compared with that of uncoated bars in terms of ultimate bond strength, cracking and stiffness.

7.2 General Behavior

7.2.1 Cracking and Failure Patterns. The first flexural cracks in all the beams occurred randomly in the constant moment region on the tension side of the beams outside the splice. As loading continued, cracks formed along the entire length of the constant moment region including the splice. Most of the flexural cracks on the tension side of the beam extended into the side faces.

Flexural cracks in the splice region formed randomly in uncoated and epoxy-coated beam specimens B1, B2, B9 and B10 where there were no sitrrups crossing the splitting plane. However, in beams with stirrups provided in the splice region, flexural cracks formed only at the stirrup locations with the exception of uncoated bar specimen B3. Specimen B3 had three widely spaced stirrups, 12 in. on centers, in a 30-in. splice length. Six flexural cracks formed in the splice region of B3; three of which developed along the stirrups.

Before failure, and throughout loading, the depth and width of flexural cracks in the splice region of all the beams were noticeably less than the depth and width of cracks outside the splice region. The reason is that at load levels below failure, the bond stress in the splice is below capacity and there is effectively twice as much steel in the splice region as outside the splice. The largest cracks in width and depth formed on the tension face along the edges of the splice region.

In each of the Appendix B Figures B1 to B6, a steel layout and the crack pattern on the tension face of the corresponding uncoated and epoxy-coated bar beam specimens, are shown.

In the #11 uncoated and epoxy-coated specimens, respectively B1 and B2, which had two 30-in. splices and no stirrups in the splice region, failure occurred just after longitudinal splitting cracks started to form. The longitudinal cracks formed in the top cover directly over the splices and in the side cover adjacent to the bars. The final mode of failure was a face-and-side split failure. The failure was sudden. After failure, the beams carried virtually no load. The crack pattern in the splice region of beam B2, is shown in Figure 7.1. Numbers along each crack indiate the load levels at which extensions were observed. Cracks marked with the letter "F" formed at failure.

The reinforcement in beams B3 and B4 was identical to that in beams B1 and B2 respectively with one exception. Beams B3 and B4 had three #3 ties spaced 12 in. on centers along the 30-in. splice length. The ties were uncoated in Beam B3 and epoxy-coated in Beam B4. In the uncoated bar specimen B3, longitudinal cracks started to form in the top cover over the two splices at about 70% of the maximum load. The crack pattern in the splice region of beam B3 is shown in Figure 7.2. In the coated bar beam B4, longitudinal cracks began forming at about the same load

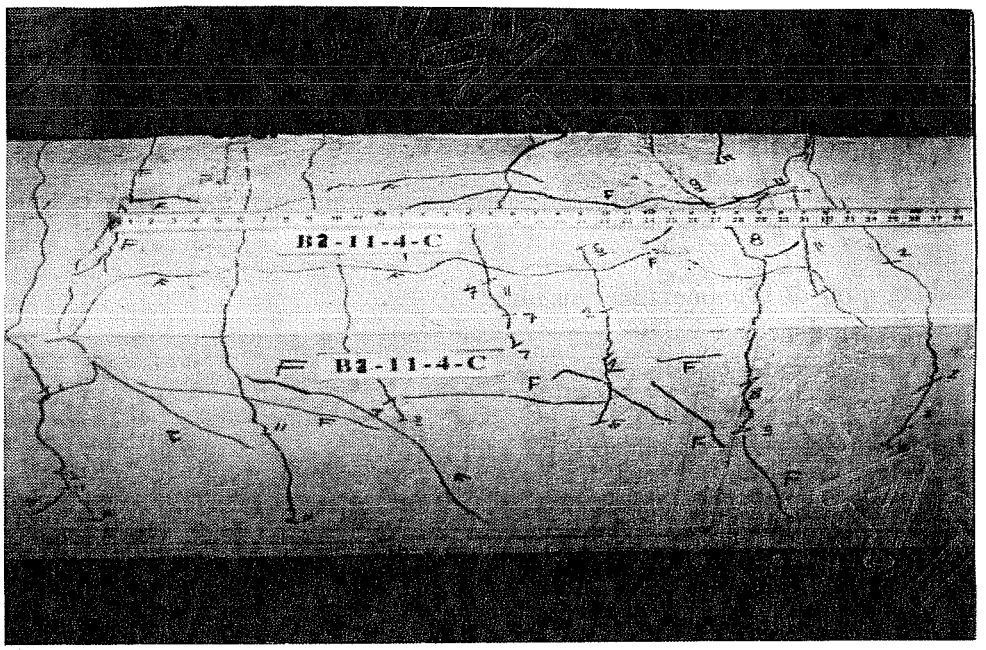

Figure 7.1 Face-and-side split failure of the epoxy-coated bar Specimen B2-11-4-C.

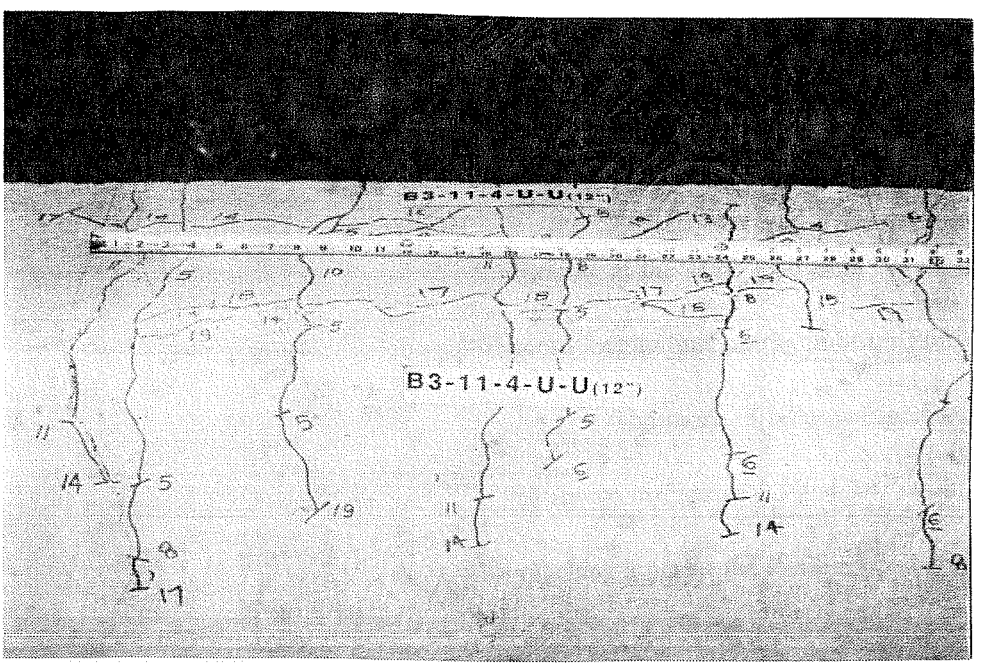

Figure 7.2 Splitting failure of the uncoated bar Specimen B3-11-4-U-U(10").

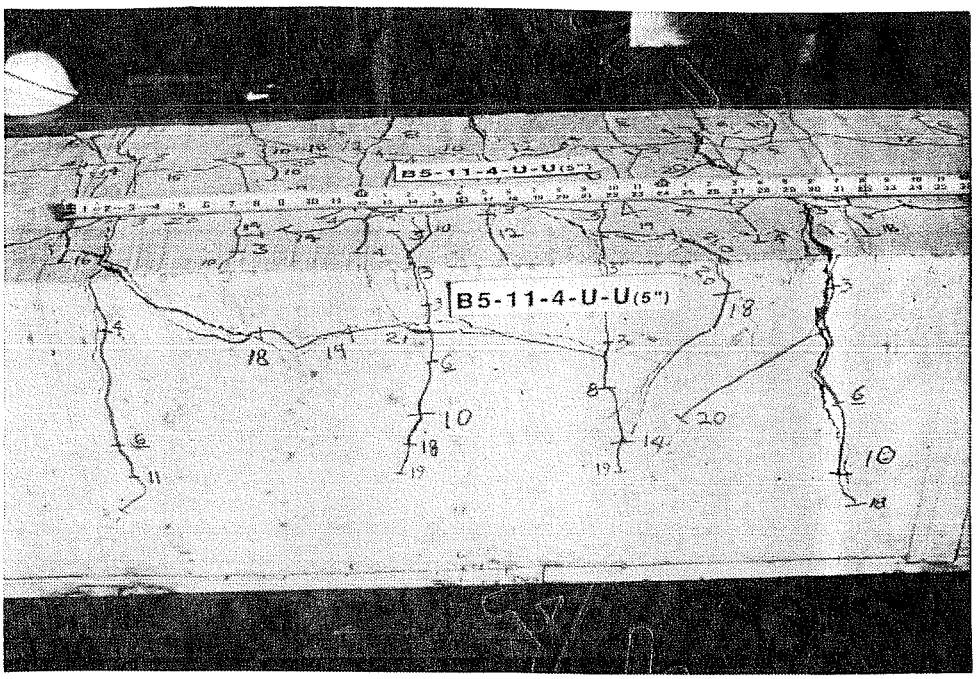

Figure 7.3 Face-and-side split failure of the uncoated bar specimen B5-11-4-U-U(5").

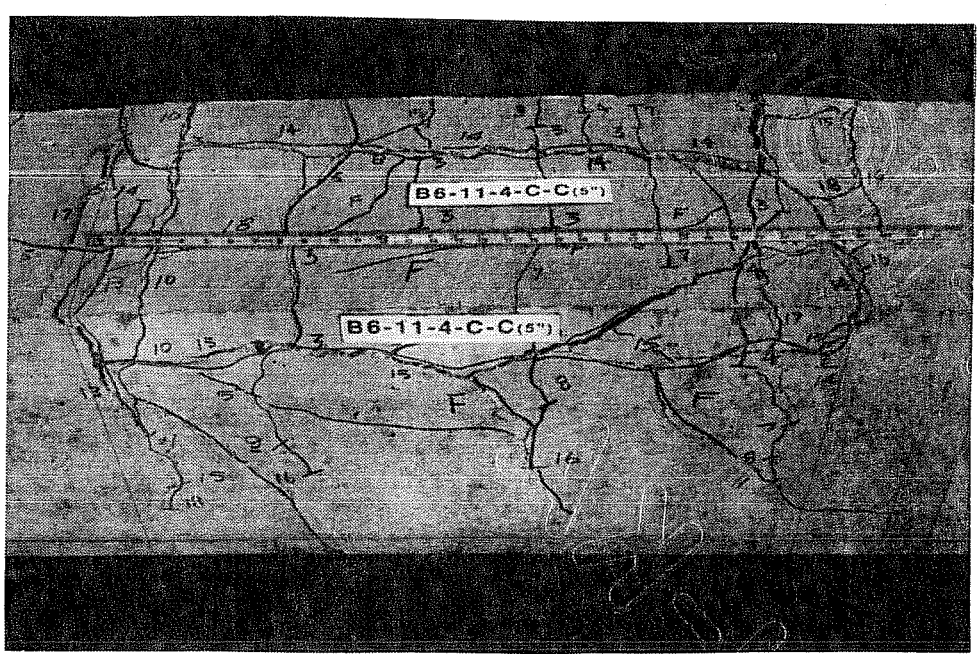

Figure 7.4 Face-and-side split failure of the epoxy-coated bar specimen B6-11-4-C-C(5").

load, the deflection was very large and the concrete top and side covers started to split off in the splice region.

The uncoated and the epoxy-coated specimens, respectively B7 and B8, had three 30-in. splices with six #3 ties spaced 5 in. on centers along the splice length. The ties were uncoated in B7 and epoxy-coated in B8. The clear spacing between adjacent splices was one bar diameter whereas the top and side clear concrete covers were 2 in. each. In both beams, B7 and B8, a single longitudinal crack started forming on the tension face over the middle splice at about 85% of the maximum load in B7 and about 70% of the maximum load in B8. The reason is that the middle splice was confined less than the two exterior splices. Moreover, the exterior splices were tied to the corners of the hoop stirrups in the splice region and hence were provided with more resistance against splitting than the middle splice. Along with the single top cover longitudinal crack, and at the same time, longitudinal cracks began to develop in the side cover adjacent to the bars. The two exterior splices did not show any sign of distress until failure when a few scattered longitudinal cracks formed at random along those splices.

The mode of failure of beams B7 and B8 could be characterized as a face-and-side split failure as shown in Figures 7.5 and 7.6. The failure was gradual and the behavior after reaching ultimate load was similar to the behavior of beams B5 and B6.

Specimens B9, B10, B11 and B12 with #6 bars, were designed with three 18-in. splices. The clear spacing between adjacent splices was 1.25 in. and the 2-in. concrete top and side covers were maintained. The uncoated specimen B9 and the epoxy-coated specimen B10 had no ties in

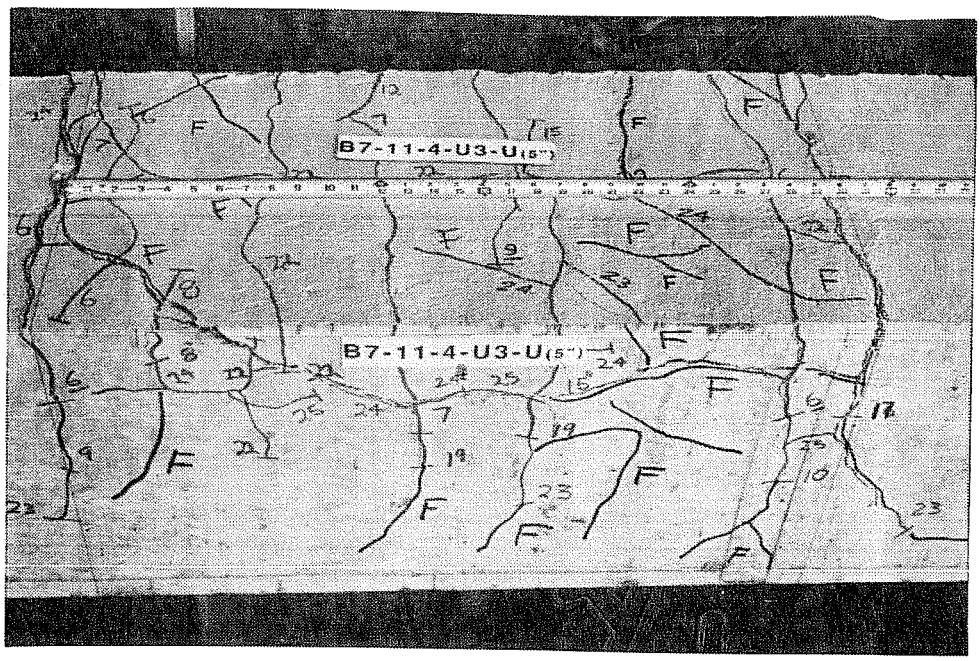

Figure 7.5 Face-and-side split failure of the uncoated bar specimen B7-11-4-U3-U(5").

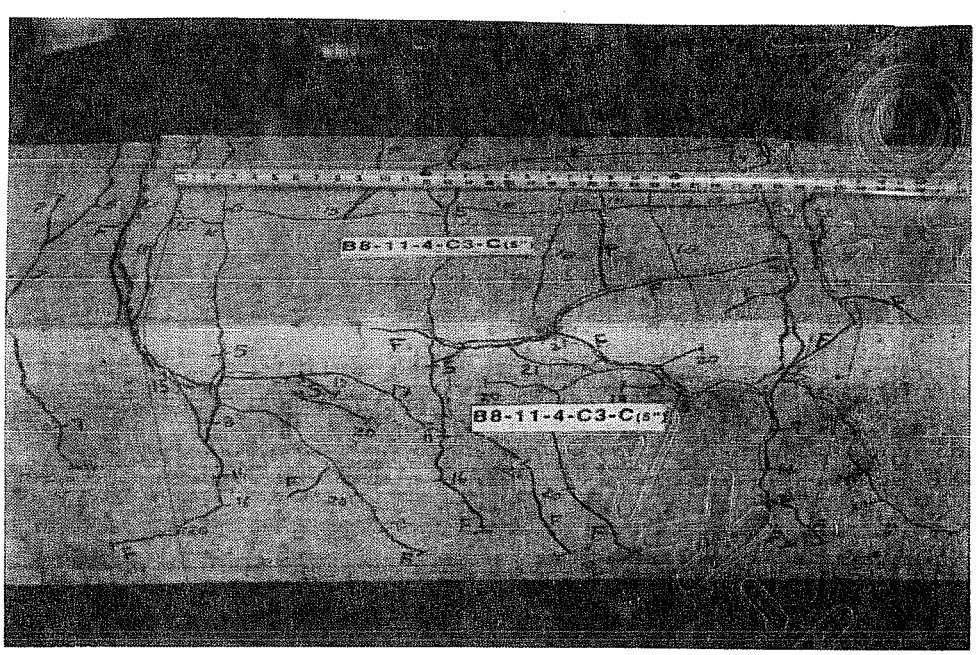

Figure 7.6 Face-and-side split failure of the epoxy-coated bar specimen B8-11-4-C3-C(5").

the splice region. No longitudinal cracks were observed in the splice region until sudden failure took place. After failure, longitudinal cracks formed in the side cover adjacent to the bars and few scattered longitudinal cracks developed on the tension face. The mode of failure could be considered a face-and-side split failure in B9 and a side-split failure in B10 where side splitting was much more pronounced than face splitting. The crack pattern in the splice region of beam B9 is shown in Figure 7.7.

The uncoated specimen B11 and the epoxy-coated specimen B12 had three #3 ties spaced 6 in. on centers along the 18-in. splice length. The ties were uncoated in B11 and epoxy-coated in B12. In beam B11 longitudinal cracks in the side cover, adjacent to the bars in the splice region,

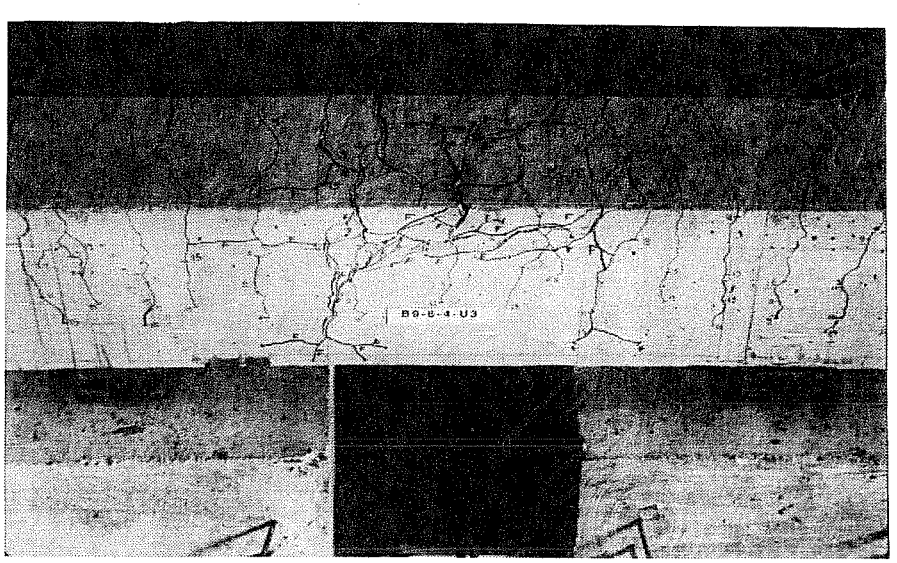

Figure 7.7 Face-and-side split failure of the uncoated bar specimen B9-6-4-U3.

started to form at about 80% of the maximum load. At failure a single longitudinal crack formed on the tension face over an exterior splice. The failure of B11 was sudden in comparison to other beams which had stirrups in the splice region. After failure, the load dropped at a faster rate than other beams with ties in the splice region.

On the other hand, a single longitudinal crack began forming in the top cover over the middle splice of beam B12 at about 55% of the maximum load. With futher loading longitudinal cracks developed in the side cover at about 65% of the maximum load. The behavior after failure of beam B12 was similar to beam B11. The load dropped quickly with increasing deflection until it held steady at about 20% of the maximum load.

7.2.2 Appearance After Failure. After the beams reached ultimate, additional deflections were imposed to increase the severity of the splitting in the splice region while the load continued to drop. The added splitting permitted easy removal of the top and side concrete cover to reveal the failure plane in the splice region. In general, it was more difficult to remove the cover in the uncoated than in the epoxy-coated beams.

In Figures 7.8 and 7.9, an uncoated splice and an epoxy-coated splice are shown after the concrete cover was removed. Also, the appearances of the concrete covers of beams B9 and B10 after splice failure are shown in Figures 7.10 and 7.11.

The uncoated bars adhered to the surrounding concrete. Large concrete particles were firmly attached to the shaft of the bar. After the cover was removed, concrete deposits were left

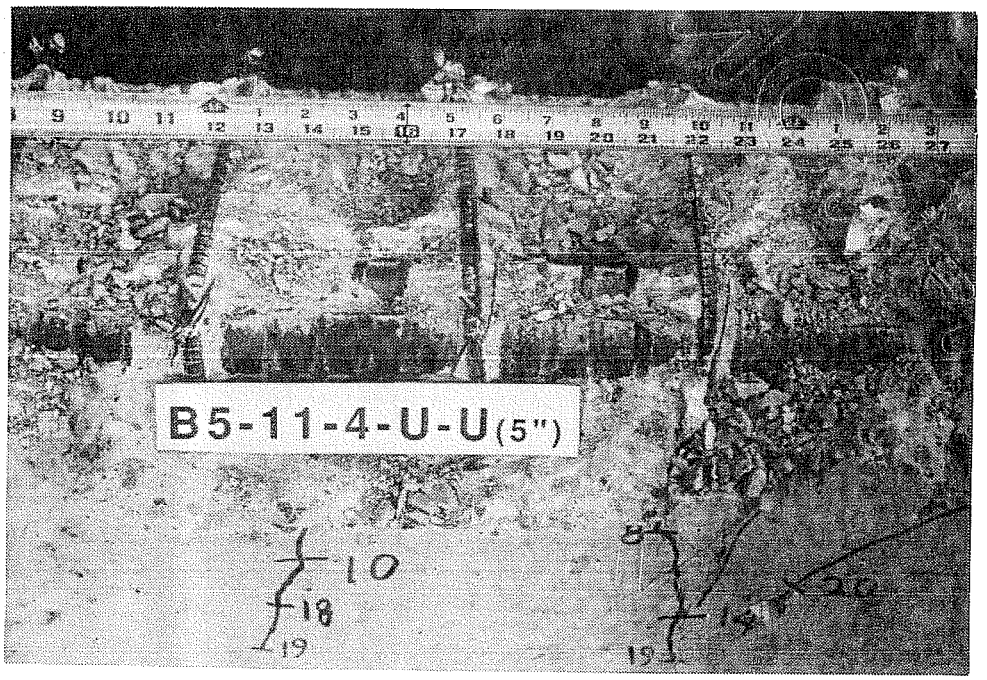

Figure 7.8 Uncoated reinforcing bars after splice failure.

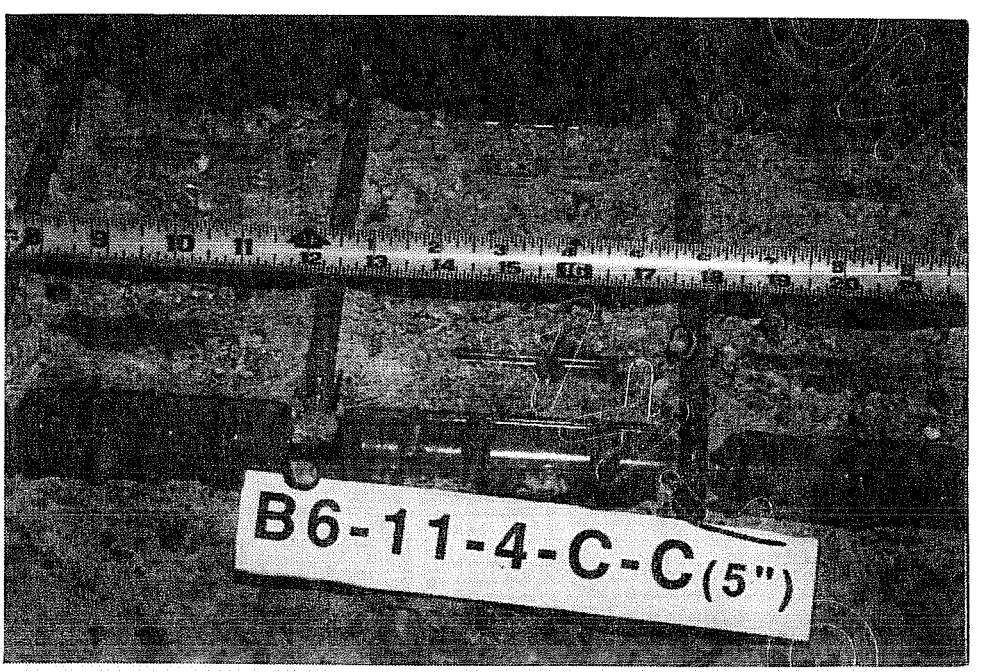

Figure 7.9 Epoxy-coated reinforcing bars after splice failure.

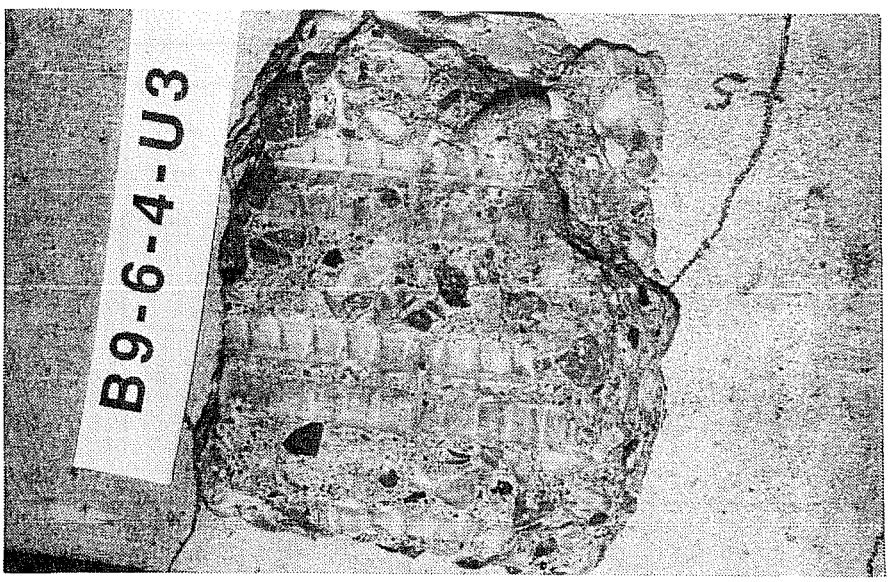

Figure 7.10 Concrete cover after splice failure, uncoated bars.

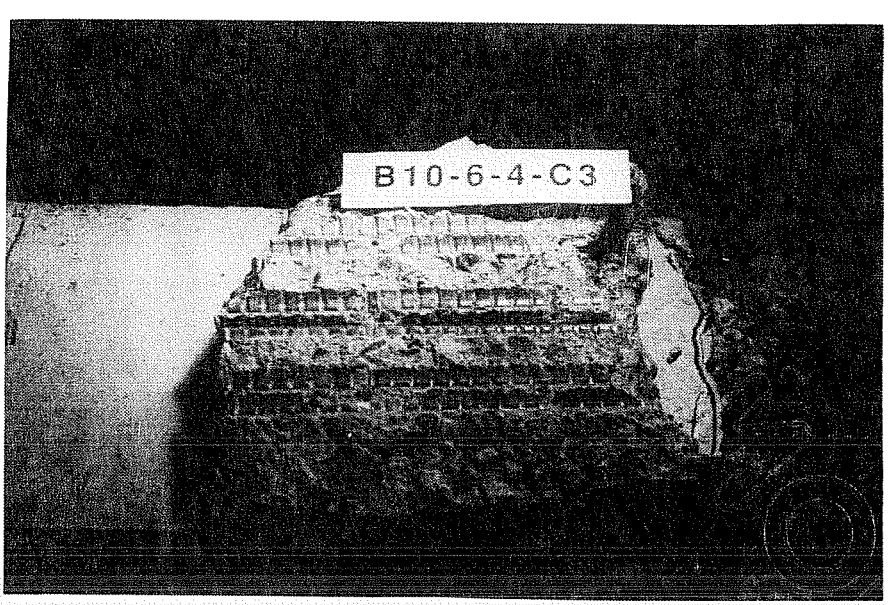

Figure 7.11 Concrete cover after splice failure, epoxy-coated bars.

on the sides of the deformations (see Figure 7.8). The grooves left in the concrete cover by the uncoated bars were dull, rough and worn in appearance (see Figure 7.10).

On the other hand, the epoxy-coated bars in the splice region were very clean and had no concrete residue left on the deformations or on the shaft of the bar (see Figure 7.9). The concrete in contact with the epoxy-coated bars had a smooth glassy surface as if a bond-breaker had been applied. The patterns left in the concrete by the deformations of the bars were in perfect condition. There were no signs of the concrete being crushed against the bar deformations (see Figure 7.11).

7.3 Test Results

The characteristics of each specimen and the ultimate steel stresses developed during the tests are shown in Table 7.1. The test results show that the epoxy-coated bars reached lower ultimate stresses than the uncoated bars. The steel stress developed by each beam specimen was determined by analyzing the section based on cracked elastic behavior. The analysis ignored the tensile stresses in the concrete above the neutral axis and assumed a linear stress-strain diagram. This approach to measure steel stresses was used previously by Treece[25].

In Section 7.4, the effect of epoxy coating on the width and spacing of flexural cracks will be discussed. Also, the effect of transverse reinforcement in the splice region on crack width will be considered. In Section 7.5, the effect of epoxy coating and splice region transverse reinforcement on the beam stiffness will be examined. In Section 7.6, the bond strengths of the beam specimens within each series will be evaluated and compared. The effect of epoxy coating and the variation of transverse reinforcement in the splice region on the bond strength will be discussed. Measured

Table 7.1 Parameters and results of the beam tests.

SERIES NUMBER	Specimen Notation	d_b (inch)	f'_c (psi)	ℓ_s (inch)	c_b (inch)	2 x c_s (inch)	Splice Region Stirrups	P_{max} (Kips)	f_{su} (Ksi)
	B1-11-4-U	1.41	3700	30	2	4.00	-	18.0	34.84
	B2-11-4-C	1.41	3700	30	2	4.00	-	13.0	25.61
SERIES ONE	B3-11-4-U-U(10")	1.41	3700	30	2	4.00	3 #3 @ 10 in.*	19.6	37.74
	B4-11-4-C-C(10")	1.41	3700	30	2	4.00	3 #3 @ 10 in.	15.6	30.48
	B5-11-4-U-U(5")	1.41	4000	30	2	4.00	6 #3 @ 5 in.	21.7	41.55
	B6-11-4-C-C(5")	1.41	4000	30	2	4.00	6 #3 @ 5 in.	18.0	34.75
SERIES TWO	B7-11-4-U3-U(5")	1.41	4000	30	2	1.41	6 #3 @ 5 in.	25.5	32.98
	B8-11-4-C3-C(5")	1.41	4000	30	2	1.41	6 #3 @ 5 in.	21.6	28.17
	B9-6-4-U3	0.75	3740	18	2	1.25	-	20.2	62.24
SERIES THREE	B10-6-4-C3	0.75	3740	18	2	1.25	-	13.3	41.73
	B11-6-4-U3-U(6")	0.75	3740	18	2	1.25	3 #3 @ 6 in.	22.4	68.76
	B12-6-4-C3-C(6")	0.75	3740	18	2	1.25	3 #3 @ 6 in.	16.5	51.06

*There are three #3 hoop stirrups in the splice region with an average spacing of 10 in. along the splice.

bond strengths will be compared with the predicted values using the empirical equation of Orangun, et. al.[20], and the current ACI Building Code (ACI 318-89) bond specifications[1].

7.4 Crack Width and Spacing

The constant moment region outside the splice length was used to study the effect of epoxy-coating on the spacing and width of flexural cracks due to three reasons:

(1) The region is longer than the splice length. Therefore, more cracks formed and gave a more representative sample for comparing crack spacing.

(2) The cracks outside the splice were much larger than the cracks within the splice which resulted in better accuracy in measuring crack widths.

(3) Usually in a structure, flexural cracking outside the splice region is of prime concern because the area of steel is greater and the stresses are smaller along the splice than outside.

The variation of the steel stress versus the average width of the flexural cracks in the constant moment region outside the splice length of each beam specimen is shown in Figures 7.12, 7.13 and 7.14. The cracks which formed at the edge of the splice were included in the average. In general, the results indicate that the average crack width of an epoxy-coated bar spcimen was larger than that of a companion uncoated bar specimen at the same level of stress.

Beams B7 and B8 with #11 bars, and beams B11 and B12 with #6 bars, had three closely spaced splices each with relatively closely spaced hoop stirrups crossing the splitting plane in the splice region ($K_{tr} > 2$). The steel stress versus average crack width plots for beams B7, B8, B11

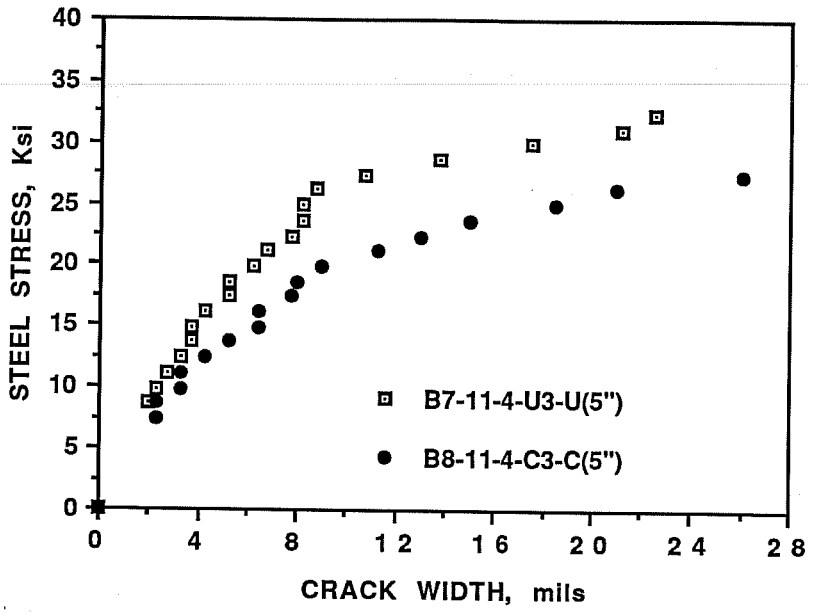

Figure 7.13 Variation of steel stress versus average crack width, series TWO of the beam tests.

and B12 indicate larger crack widths near the ultimate steel stress than in other beam tests with larger spacing between bars. The presence of closely spaced hoop stirrups provided confinement in the splice region, and prevented splice bond failure until large slips occurred. The large slips opened the flexural cracks, especially at the end of the splice larger. Moreover, the plots for B7, B8, B11 and B12 show the largest increase in average crack width of epoxy-coated bar beams relative to uncoated bar beams.

In Table 7.2, the average crack widths of every pair of uncoated and epoxy-coated bar beams, which were otherwise identical, are compared. The steel stress, at which the comparison is done, is close to the level at which the epoxy-coated bars failed. This steel stress is around 30 ksi except for beams B1 and B2 because B2 developed an ultimate steel stress of 25.61 ksi only.

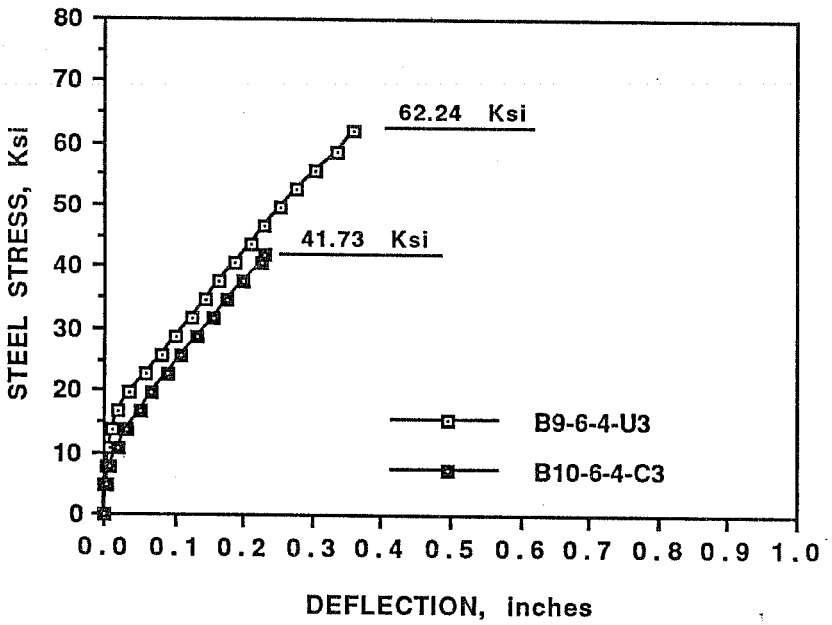

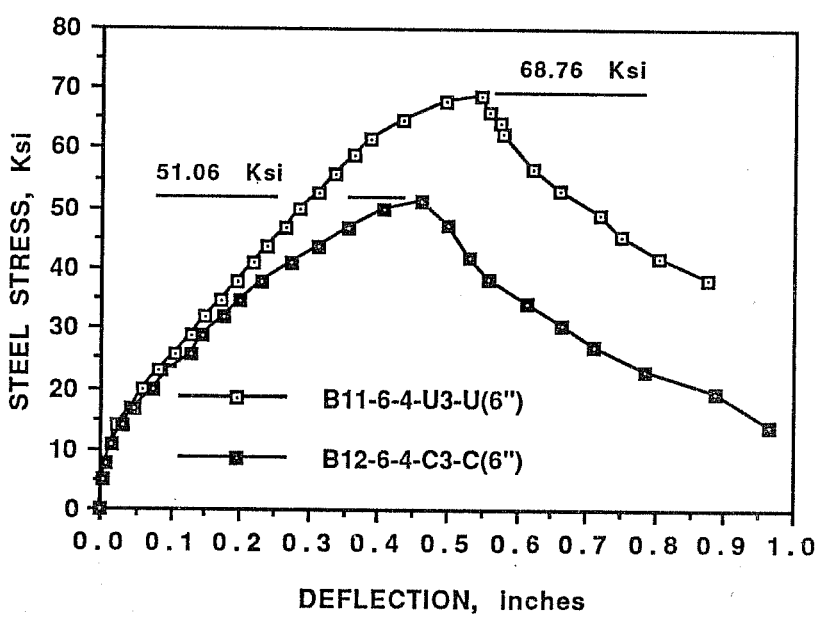

Figure 7.18 Variation of steel stress versus end deflection, series THREE of the beam tests.

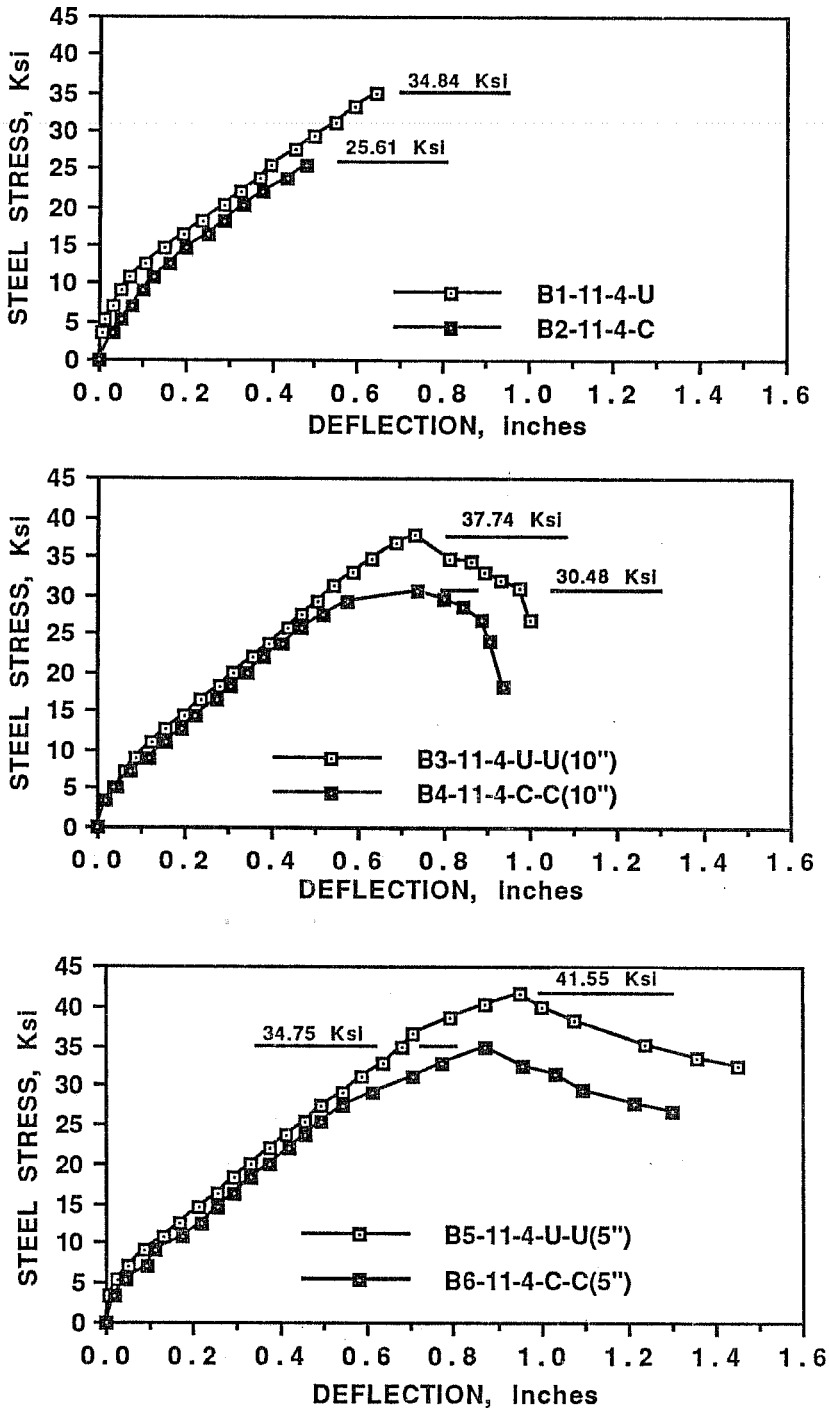

Figure 7.16 Variation of steel stress versus end deflection, series ONE of the beam tests.

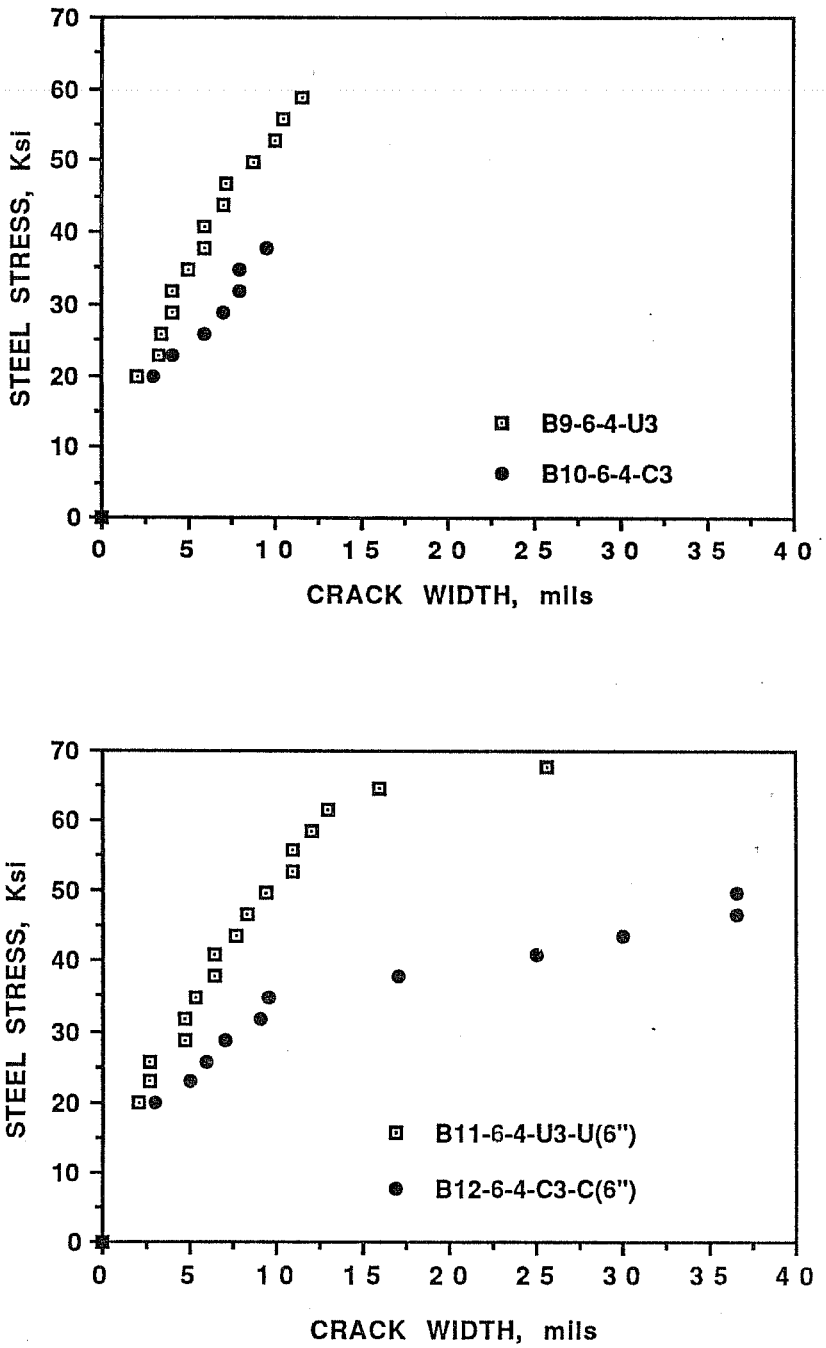

Figure 7.14 Variation of steel stress versus average crack width, series THREE of the beam tests.

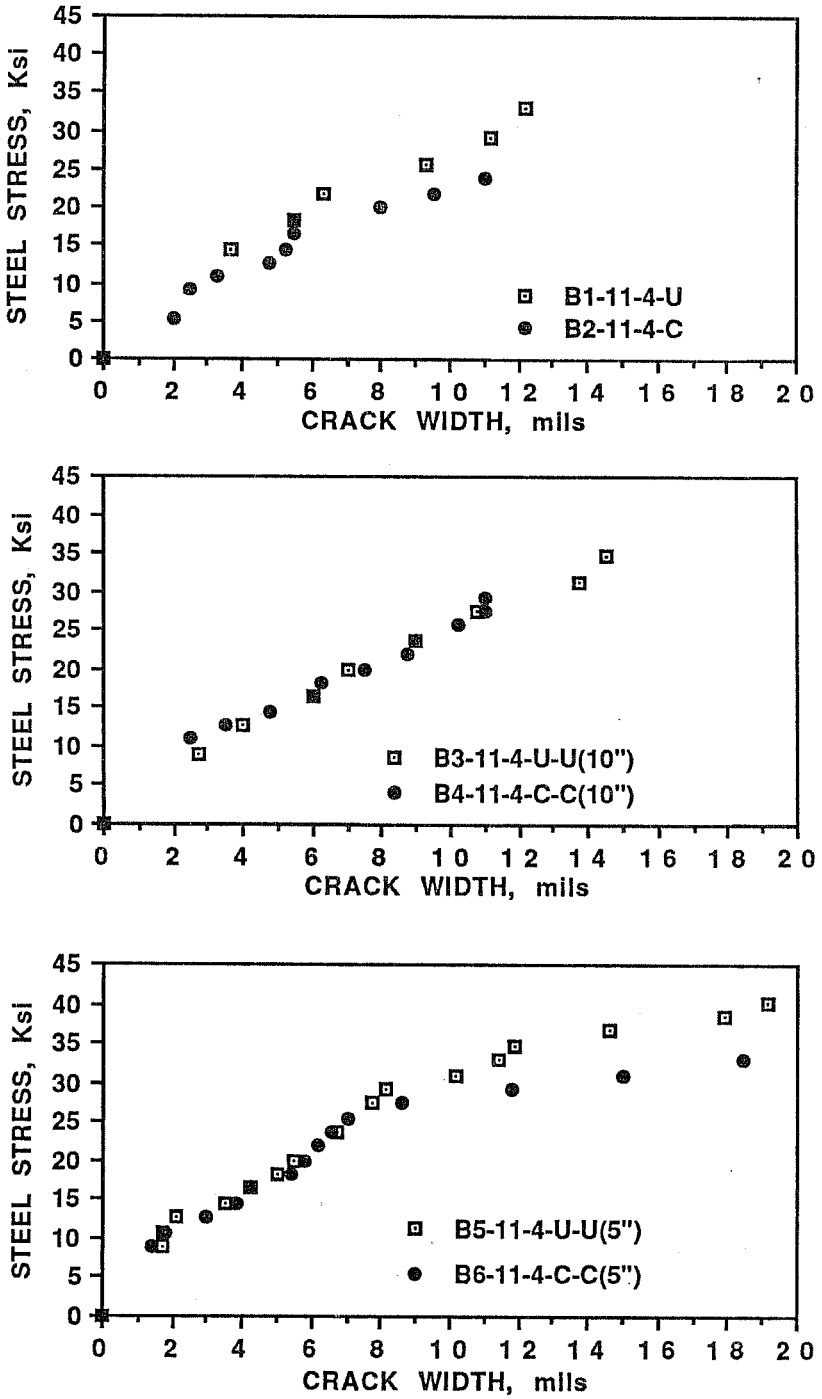

Figure 7.12 Variation of steel stress versus average crack width, series ONE of the beam tests.

Table 7.2 Comparison of the average crack widths of the beam specimens.

SERIES NUMBER	Specimen Notation	Number of Cracks	Number Ratio coated/uncoated	K_{tr} +	CRACK WIDTH COMPARISON		
					Steel Stress Level (Ksi)	Average Crack Width (mils)	Crack Width Ratio coated/uncoated
	B1-11-4-U	6	-	0	23	7.2	-
	B2-11-4-C	4	0.67	0	23	10.4	1.44
SERIES ONE	B3-11-4-U-U(10")	4	-	1.02	29	12.0	-
	B4-11-4-C-C(10")	4	1.00	1.02	29	11.0	0.92
	B5-11-4-U-U(5")	8	-	2.04	33	11.4	-
	B6-11-4-C-C(5")	5	0.63	2.04	33	18.4	1.61
SERIES TWO	B7-11-4-U3-U(5")	4	-	1.36	27	10.1	-
	B8-11-4-C3-C(5")	4	1.00	1.36	27	24.5	2.43
	B9-6-4-U3	4	-	0	30 (37)	4.0 (5.7)*	-
SERIES THREE	B10-6-4-C3	2	0.50	0	30 (37)	7.4 (9.1)	1.85 (1.6)**
	B11-6-4-U3-U(6")	3	-	2.13	30 (49)	4.7 (9.1)	-
	B12-6-4-C3-C(6")	2	0.67	2.13	30 (49)	7.8 (36.5)	1.70 (4.0)

+ $K_{tr} = a_{tr}f_{yt}/(500sd_b)$.

* The crack width in parenthesis corresponds to the steel stress in parenthesis.

** The number in parenthesis is the ratio of the average crack widths in parentheses of the corresponding epoxy-coated bar and uncoated bar specimens.

In addition, the specimens of the third series were compared at two levels of stresses because they developed relatively larger steel stresses.

The following quantities are listed in Table 7.2 for each beam test: the number of cracks included in the average, the number ratio, K_{tr}, the steel stress level at which the comparison is performed, the average crack width, and the crack width ratio. The number ratio is the number of cracks in the epoxy-coated bar specimen, included in the average, divided by the corresponding number of cracks in the companion uncoated bar specimen. The crack width ratio is the average crack width of the epoxy-coated bar specimen divided by the average crack width of the corresponding uncoated bar specimen.

In general epoxy-coated bar specimens had fewer or larger spaced flexural cracks yet the width of the cracks was larger than in uncoated bar specimens. As shown in Figure 7.15, a larger number of flexural cracks at failure existed in the uncoated bar specimen B11-6-4-U3-U(6") than in the epoxy-coated bar specimen B12-6-4-C3-C(6"). Although larger cracks allow more corrosive material like chlorides to enter the reinforced concrete number, the epoxy coating will prevent the chlorides from reaching the surface of the steel bars to cause corrosion. Moreover, as shown in Table 7.2, for most of the beams the crack width ratio is approximately the reciprocal of the crack number ratio. This implies that the total width of all cracks is approximately equal. However, the #11 bar beams B7 and B8 and the #6 bar beams B11 and B12 did not show the above property. The total width of all cracks was larger in the epoxy-coated bar beams B8 and B12 than in the corresponding uncoated bar beams B7 and B11. This indicates a reduction in the stiffness of epoxy-

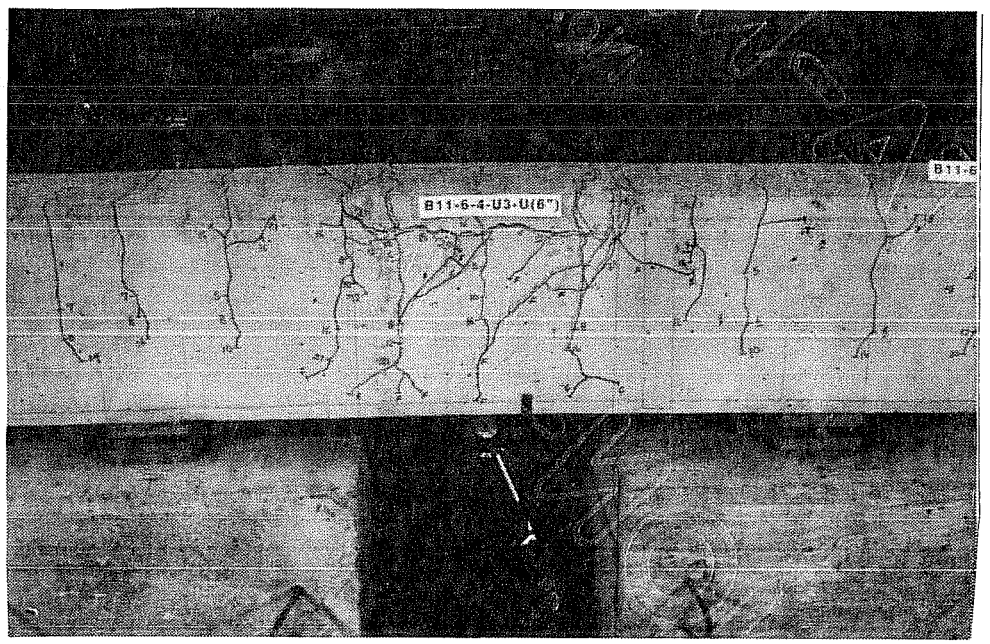

(a) Uncoated bar specimen

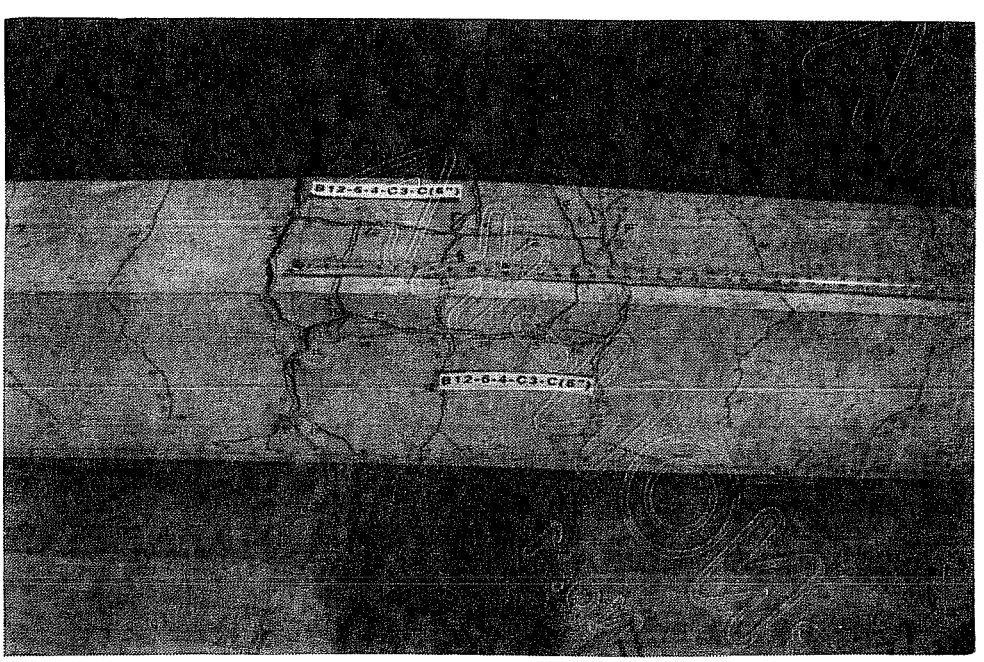

(b) Epoxy-coated bar specimen

Figure 7.15 Comparison of the number of flexural cracks in the constant moment region of two companion uncoated and epoxy-coated bar specimens.

coated bar specimens, with closely spaced splices and closely spaced stirrups in the splice region, relative to the corresponding uncoated bar specimens at high level of stress.

In Table 7.3, the width of the flexural crack at the edge of the splice region of an uncoated bar beam and that of the companion epoxy-coated bar beam, corresponding to a steel stress close to the level at which the coated bar beam failed, are listed and compared. Also, listed for each uncoated bar specimen are the splice edge crack width just before failure and the corresponding steel stress. If the comparison is performed at the stress just before the coated bar specimen failed then the following conclusions could be made:

(1) For beams with no ties (B1 and B2, B9 and B10) or with widely spaced ties in the splice region (B3 and B4), the crack widths at the edge of the splice region of uncoated and comparison epoxy-coated bar beams are comparable.

(2) For beams with closely spaced ties in the splice region (B5 and B6, B7 and B8, B11 and B12), the crack width at the edge of the splice region of an expoy-coated bar beam is much larger than that of the companion uncoated bar beam.

On the other hand, if the comparison is performed between an uncoated bar beam before its failure and the companion coated bar beam before its failure, then the crack widths at the edge of the splice region are comparable for beams with ties in the splice region and not comparable for beams with no ties.

Table 7.3 Comparison of crack width at the edge of the splice region.

SERIES NUMBER	Specimen Notation	K_{tr}	Splice Edge Steel Stress (Ksi)	Crack+ Crack Width (mils)
	B1-11-4-U	0	23 (32.99)*	10.9 (20)**
	B2-11-4-C	0	23	9.6
SERIES ONE	B3-11-4-U-U(10")	1.02	29 (34.84)	11.3 (13)
	B4-11-4-C-C(10")	1.02	29	10.0
	B5-11-4-U-U(5")	2.04	33 (40.28)	16.2 (60)
	B6-11-4-C-C(5")	2.04	33	40.0
SERIES TWO	B7-11-4-U3-U(5")	1.36	28 (32.37)	16.0 (50)
	B8-11-4-C3-C(5")	1.36	28	50.0
	B9-6-4-U3	0	37 (58.68)	6.5 (20)
SERIES THREE	B10-6-4-C3	0	37	8.5
	B11-6-4-U3-U(6")	2.13	49 (67.65)	10.0 (50)
	B12-6-4-C3-C(6")	2.13	49	60.0

+ In absence of a flexural crack at the end of the splice region, the crack closest to the edge was used for comparison.

* The number in parenthesis is the steel stress at which the last measurement of crack width for the uncoated bar specimen was made.

** The number in parenthesis is the crack width corresponding to the steel stress in parenthesis.

7.5 Beam Stiffness

The stiffness of beams with epoxy-coated bars was compared to the stiffness of beams with uncoated bars by plotting the steel stress versus the end deflection for each beam specimen. The steel stress-deflection curves for every pair of uncoated and epoxy-coated bar specimens, which were otherwise identical, are plotted on the same graph. Graphs for each series are shown in the same figure using the same scale to help visualize the effect of varying the amount of transverse reinforcement in the splice region on the performance of epoxy-coated bar specimens relative to uncoated bar specimens.

The steel stress-end deflection curves, presented in Figures 7.16, 7.17 and 7.18, show little difference in stiffness between the uncoated and the companion epoxy-coated bar specimens which had no stirrups in the splice region. When such reinforcement was provided, the two otherwise identical uncoated and coated bar specimens show almost identical stiffnesses at low levels of loading. However, the two curves start to separate with the coated bar specimen showing a gradual decrease in stiffness relative to the uncoated bar specimen as the load level gets closer to the failure load and as the amount of transverse reinforcement in the splice region increases. The separation between the curves of the uncoated bar specimen and the corresponding epoxy-coated bar specimen starts at a relatively earlier stage in beams B7 and B8 of the second series and beams B11 and B12 of the third series. These beams had three closely spaced splices confined with relatively closely spaced stirrups ($K_{tr} > 2$). The total width of all the cracks was larger in the epoxy-coated bar

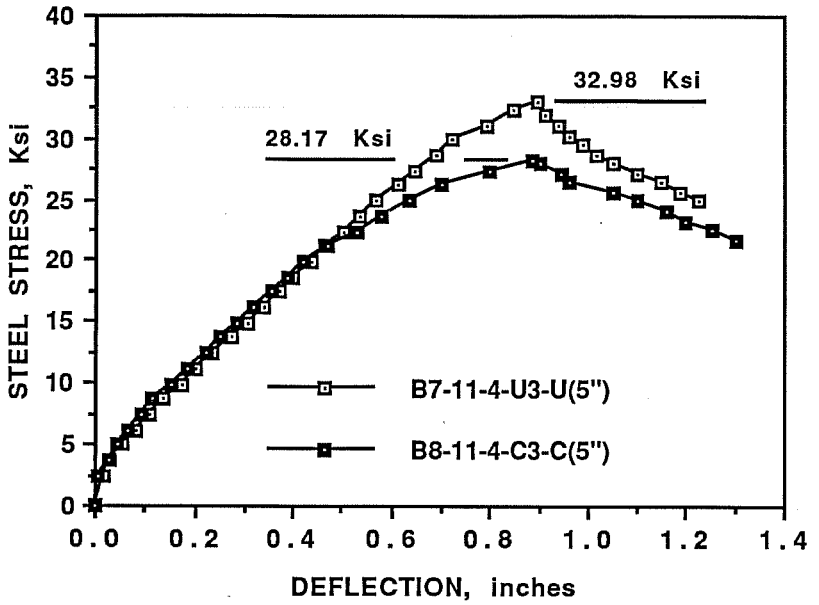

Figure 7.17 Variation of steel stress versus end deflection, series TWO of the beam tests.

specimens B8 and B12 than in the corresponding uncoated bar specimens B7 and B11 at load levels close to the failure loads of the coated bar specimens.

The negligible difference in the stiffnesses of an epoxy-coated bar beam and the corresponding uncoated bar beam at relatively low levels of loading, regardless of the amount of transverse reinforcement, proves that epoxy coating does not significantly affect the flexural cracking load. This was also observed by Treece[25] and Cleary and Ramirez[26].

7.6 Bond Strength

In all beam specimens, the mode of failure was splitting of the top concrete cover at the tension face of the splice region, or the side concrete cover in the plane of the splices (side split failure), or both the top and side covers (face-and-side split failure). The splitting mode of failure indicates that the splice reached its maximum capacity. Therefore, the bond strength could be determined directly from the stress developed in the steel. The bond strength was based on an average stress along the length of the splice. To evaluate the bond stress, u, the total force developed in the bar, $A_b f_s$, was divided by the surface area of the bar over the splice length, $\pi d_b \ell_s$:

$$u = \frac{A_b f_s}{\pi d_b \ell_s} = \frac{f_s d_b}{4\ell_s}$$

The steel stress, f_s, was determined from the maximum load, as discussed in Section 7.3, using statics and fully-cracked elastic transformed section theory.

The concrete strength of beams B5 and B6 was 4000 psi whereas the concrete strength of the other four beams in series ONE was 3700 psi. To allow comparison of the results of all beams in the first series, an adjustment was made for the difference in concrete strength. The bond stresses of beams B5 and B6, calculated using $u = f_s d_b / (4\ell_s)$, were multiplied by $\sqrt{\frac{3700}{4000}}$.

In Table 7.4, the maximum bond stress and the corresponding bond ratio are listed for each beam. The bond ratio is the bond stress of the epoxy-coated bar specimen divided by that of the companion uncoated bar specimen.

Table 7.4 Bond stresses and bond efficiencies of the beam specimens.

Specimen Notation	c/d_b	ℓ_s/d_b	K_{tr}*	Measured Bond Stress		Predicted Bond Stress		Bond Efficiency	
				u_t (psi)	Bond Ratio**	Orangun Eq. (7.1) (psi)	ACI (318-89) Eq. (7.2) (psi)	$\frac{u_t}{u(\text{Orangun})}$	$\frac{u_t}{u(\text{ACI})}$
B1-11-4-U	1.42	21.28	0	409	-	365	145	1.12	2.82
B2-11-4-C	1.42	21.28	0	301	**0.74**	365	111	0.83	2.71
B3-11-4-U-U(10")	1.42	21.28	1.02	443	-	413	145	1.07	3.06
B4-11-4-C-C(10")	1.42	21.28	1.02	358	**0.81**	413	111	0.87	3.23
B5-11-4-U-U(5")	1.42	21.28	2.04	470	-	461	145	1.02	3.24
B6-11-4-C-C(5")	1.42	21.28	2.04	393	**0.84**	461	111	0.85	3.54
B7-11-4-U3-U(5")	0.50	21.28	1.36	388	-	312	151	1.24	2.57
B8-11-4-C3-C(5")	0.50	21.28	1.36	331	**0.85**	312	115	1.06	2.88
B9-6-4-U3	0.83	24.00	0	648	-	272	274	2.38	2.36
B10-6-4-C3	0.83	24.00	0	435	**0.67**	272	210	1.60	2.07
B11-6-4-U3-U(6")	0.83	24.00	2.13	716	-	372	274	1.93	2.61
B12-6-4-C3-C(6")	0.83	24.00	2.13	532	**0.74**	372	210	1.43	2.53

* $K_{tr} = a_{tr}f_{yt}/(500sd_b)$.

**Bond Ratio = u_t(coated)/u_t(uncoated).

7.6.1 Relative bond strength of uncoated and coated bar splices. For beams with no stirrups in the splice region, the bond ratios were 0.74 for the #11 bars and 0.67 for the #6 bars. These ratios fit within the scatter of the bond ratios of Treece's tests[25]. The average bond ratio for Treece's beam tests was 0.67 with a standard deviation of 0.09.

The bond capacity of #6 and #11 bar splices improved as the amount of transverse reinforcement crossing the splitting plane in the splice region increased. Such reinforcement provides the concrete in the plane of the splices with more confinement and tensile resistance against splitting. The improvement in bond strength was greater for epoxy-coated bar splices than uncoated bar splices. Results listed in Table 7.4 indicate that the bond strength of the #11 uncoated bar splices, relative to the case with no transverse reinforcement in the 30-in. splice region, increased by 8% when three #3 ties were provided and by 15% when six #3 ties were provided. For the #11 epoxy-coated bar splices the increases were 19 and 31%, respectively. As a result the bond ratio (coated to uncoated) increased from 0.74 in the absence of splice region ties to 0.81 with K_{tr} = 1.02 and to 0.84 with K_{tr} = 2.04. On the other hand, the bond strength of the #6 uncoated bar splcies, relative to the case with no transverse reinforcement in the 18-in. splice region, increased by 10% when three #3 ties were placed in the splice region. The increase was 22% for the #6 epoxy-coated bar splices. The bond ratio improved from 0.67 in the absence of splice region ties to 0.74 with ties provided.

The improvement in the bond capacity of epoxy-coated bar splices relative to uncoated bar splices, in the presence of ties in the splice region, was independent of the number of splices, bar

size, or bar spacing. The average bond ratio for beams with ties in the splice region was 0.81 with a 0.05 standard deviation.

7.6.2 Comparison with Orangun and ACI 318-89. The measured bond strength of each beam was compared with the theoretical value computed using the empirical equation developed by Orangun, Jirsa, and Breen[20]:

For bottom casting:
$$u = (1.2 + 3\frac{c}{d_b} + 50\frac{d_b}{\ell_s} + K_{tr})\sqrt{f'_c}$$

For top casting:
$$u = \frac{1}{1.3}\left(1.2 + 3\frac{c}{d_b} + 50\frac{d_b}{\ell_s} + K_{tr}\right)\sqrt{f'_c} \qquad (7.1)$$

$$K_{tr} = \frac{a_{tr} f_{yt}}{500 s d_b}, \quad \frac{c}{d_b} \le 2.5, \; K_{tr} \le 3$$

No modification factor for epoxy-coated bars was included in the above equation.

Comparison was also made with the current ACI Code (ACI 318-89)[1] bond specifications using $\ell_s = 1.3\ell_{db}$ according to Section 12.15 of the code:

$$\ell_s = 1.3\ell_{db}, \; \ell_{db} = \frac{0.04 A_b f_y}{\sqrt{f'_c}} \ge 0.03\frac{d_b f_y}{\sqrt{f'_c}}, \quad \sqrt{f'_c} \le 100 \text{ psi}$$

Combining the above equations with $\pi d_b \ell_s = A_b f_y$:

$$u = 6.12\frac{\sqrt{f'_c}}{d_b} \le 6.41\sqrt{f'_c}, \quad \sqrt{f'_c} \le 100 \text{ psi}$$

The modification factor for top cast bars is 1.3 according to Section 12.2.4.1. Also, the factor for epoxy coating is 1.5 according to Section 12.2.4.3. However, the product of the factors for top

reinforcement and for epoxy coating is taken as 1.7 according to Section 12.2.4.3. If the modification factor for bar spacing, cover, and transverse rienforcement from Section 1.2.2.3 is 1.0 then:

For uncoated bars:	Bottom casting	$u = 6.12\sqrt{f'_c}/d_b$	
	Top casting	$u = 4.71\sqrt{f'_c}/d_b$	
For epoxy-coated bars:	Bottom casting	$u = 4.08\sqrt{f'_c}/d_b$	
	Top casting	$u = 3.60\sqrt{f'_c}/d_b$	[7.2(a)]

On the other hand, if the modification factor for bar spacing, cover, and transverse reinforcement is 1.4, then:

For uncoated bars:	Bottom casting	$u = 4.37\sqrt{f'_c}/d_b$	
	Top casting	$u = 3.36\sqrt{f'_c}/d_b$	
For epoxy-coated bars:	Bottom casting	$u = 2.91\sqrt{f'_c}/d_b$	
	Top casting	$u = 2.57\sqrt{f'_c}/d_b$	[7.2(b)]

The upper limit on u in any case is $6.41\sqrt{f'_c}$ with $\sqrt{f'_c} \leq 100$ psi.

The predicted bond stresses computed using equations (7.1) and (7.2) are listed in Table 7.4. The measured bond stress for each specimen was divided by the predicted values to obtain the bond efficiencies listed in Table 7.4. The mean bond efficiency for the uncoated bar splices using Eq. (7.1) of Orangun, et al., is 1.46 with a standard deviation of 0.56. Using Eq. (7.2) derived from the current ACI Code, the mean bond efficiency for the uncoated bars is 2.78 with a standard deviation of 0.33. The results imply that for the uncoated bar splices tested, Eq. (7.1) of Orangun,

et al., provides a better estimate of bond strength than Eq. (7.2). Also, using Eq. (7.2), the mean bond efficiency for all uncoated and epoxy-coated bar splices is 2.80 with a standard deviation of 0.42. The current ACI bond strength specifications are consistently overly conservative regardless of bar size, bar spacing, or presence of transverse reinforcement in the splice region.

7.7 Evaluation of Bond Data of Splice Tests

7.7.1 Beams with no stirrups in the splice region. Four beams were tested with no ties in the splice region, namely B1, B2, B3 and B4. All the beams included in Treece's study[25] had no ties in the splice region. Recently, Choi, Hadje-Ghaffari, Darwin and McCabe[33] reported a series of fifteen beams tested in negative bending with splices in the middle and no stirrups in the splice region. The specimens of Choi, et. al., were similar to Treece's tests, but the bars were bottom cast. The objective was to study the effect of bar size (#5, #8 and #11) and bar deformation pattern (parallel and crescent) on the bond strength of epoxy-coated splices relative to uncoated splices.

A summary of the test data of beams with no ties in the splice region, including the tests of Treece[25] and Choi, et al.[33] is shown in Table 7.5. The cover over the bars was less than $3d_b$ in all the beams included in this evaluation, and the mode of failure was splitting of the concrete cover in the splice region. The bond ratios (coated to uncoated) vary from 0.54 to 0.94 with an average value of 0.83 and a standard deviation of 0.1. These results indicate that Treece's recommendation of a 50% increase in the development or splice length of epoxy-coated bars relative

Table 7.5 Summary of test data for beams with no stirrups in the splice region.

Beam Notation	Bar Type	Casting Position	f'_c (psi)	Bar Size	c/d_b	f_s/d_b	u_t (psi)	Bond Ratio	Bond Efficiency Relative Eq. (7.1)	Bond Efficiency To Eq.(7.2)
B1-11-4-U	U*	Top	3700	#11	1.42	21.28	409	-	1.12	2.82
B2-11-4-C	C**	Top	3700	#11	1.42	21.28	301	**0.74**	0.83	2.71
B9-6-4-U3	U	Top	3740	#6	0.83	24.00	648	-	2.38	2.36
B10-6-4-C3	C	Top	3740	#6	0.83	24.00	435	**0.67**	1.60	2.07
Treece [25]										
0-11-4	U	Top	5030	#11	1.42	25.53	420	-	1.05	2.49
12-11-4	C	Top	5030	#11	1.42	25.53	280	**0.65**	0.69	2.17
5-11-4	C	Top	5030	#11	1.42	25.53	300	**0.70**	0.74	2.32
0-11-4b	U	Bot.	4290	#11	1.42	25.53	450	-	0.93	2.22
12-11-4b	C	Bot.	4290	#11	1.42	25.53	240	**0.54**	0.50	1.78
0-11-8	U	Top	8280	#11	1.42	12.77	790	-	1.21	3.64
12-11-8	C	Top	8280	#11	1.42	12.77	500	**0.63**	0.77	3.01
0-11-12	U	Top	10510	#11	1.42	12.77	920	-	1.25	3.86
12-11-12	C	Top	10510	#11	1.42	12.77	660	**0.72**	0.90	3.62
0-11-12b	U	Bot.	9600	#11	1.42	12.77	840	-	0.92	2.77
12-11-12b	C	Bot.	9600	#11	1.42	12.77	540	**0.64**	0.59	2.67
Choi, et al. [33]										
GROUP SP1	U	Bot.	5360	#5	1.60	19.20	797	-	1.27	1.70
	C	Bot.	5360	#5	1.60	19.20	592	**0.74**	0.94	1.74
GROUP SP2	U	Bot.	6010	#6	1.33	16.00	675	-	1.05	1.49
	C	Bot.	6010	#6	1.33	16.00	634	**0.94**	0.98	2.11
	U	Bot.	6010	#6	1.33	16.00	761	-	1.18	1.68
	C	Bot.	6010	#6	1.33	16.00	577	**0.76**	0.89	1.92
GROUP SP3	U	Bot.	5980	#8	1.50	16.00	627	-	0.92	1.86
	C	Bot.	5980	#8	1.50	16.00	561	**0.90**	0.82	2.49
	U	Bot.	5980	#8	1.50	16.00	630	-	0.92	1.86
	C	Bot.	5980	#8	1.50	16.00	538	**0.85**	0.79	2.39
GROUP SP4	U	Bot.	5850	#11	1.42	17.02	552	-	0.86	2.33
	C	Bot.	5850	#11	1.42	17.02	391	**0.67**	0.61	2.48
	U	Bot.	5850	#11	1.42	17.02	517	-	0.81	2.18
	C	Bot.	5850	#11	1.42	17.02	420	**0.67**	0.65	2.66

* U = Uncoated.
**C = Coated.

to uncoated bars, with a cover less than $3d_b$ or spacing less than $6d_b$ and with no ties crossing the splitting plane, is appropriate.

The bond efficiencies listed for each beam test in Table 7.5 are computed relative to Eq. (7.1) of Orangun, et. al., and Eq. (7.2) derived from the 1989 ACI Code Specifications. Using Eq. (7.1), the mean bond efficiency for the uncoated bars is 1.13 with a standard deviation of 0.39. On the other hand, using Eq. (7.2), the mean bond efficiency for the uncoated bars is 2.38 with a standard deviation of 0.71, and the mean bond efficiency for the coated bars is 2.41 with a standard deviation of 0.49. The current ACI provisions are overly conservative for all the beams included in Table 7.5.

7.7.2 Beams with stirrups in the splice region. Eight beams were tested with ties in the splice region in this program. DeVries and Moehle[27] reported a series of beams that included #3 ties in the splice region. DeVries and Moehle did not comment on the effectiveness of the ties because their test program did not include companion beams without ties.

A summary of the test data of beams with ties in the splice region, including the beams tested by DeVries and Moehle[27], is shown in Table 7.6. The mode of failure of all beams included in this evaluation, was splitting of the concrete cover in the splice region. The transverse reinforcement parameter, K_{tr}, defined by Orangun, et. al.[20], is larger than 1.0 for all the beams. The bond ratios (coated to uncoated) vary from 0.71 to 0.99 with an average value of 0.84 and a standard deviation of 0.10. The wide scatter of the bond ratios shows that there is no general trend based on concrete strength, bar size, $\frac{c}{d_b}$, $\frac{\ell_s}{d_b}$, or K_{tr} values exceeding 1.0. A plot of the bond

Table 7.6 Summary of test data for beams with stirrups in the splice region.

Beam Notation	Casting Position	f'_c (psi)	Bar Size	c/d_b	ℓ_s/d_b	K_{tr}	u_t (psi)	Bond Ratio	Bond Efficiency Relative To Eq. (7.1)	Bond Efficiency Relative To Eq. (7.2)
B3-11-4-U-U(10")	Top	3700	#11	1.42	21.28	1.02	443	-	1.07	3.06
B4-11-4-C-C(10")	Top	3700	#11	1.42	21.28	1.02	358	**0.81**	0.87	3.23
B5-11-4-U-U(5")	Top	3700	#11	1.42	21.28	2.04	470	-	1.02	3.24
B6-11-4-C-C(5")	Top	3700	#11	1.42	21.28	2.04	393	**0.84**	0.85	3.54
B7-11-4-U3-U(5")	Top	4000	#11	0.50	21.28	1.36	388	-	1.24	2.57
B8-11-4-C3-C(5")	Top	4000	#11	0.50	21.28	1.36	331	**0.85**	1.06	2.88
B11-6-4-U3-U(6")	Top	3740	#6	0.83	24.00	2.13	716	-	1.93	2.61
B12-6-4-C3-C(6")	Top	3740	#6	0.83	24.00	2.13	532	**0.74**	1.43	2.53
DeVries and Moehle [27]										
8G-18B-P9	Bot.	8610	#9	1.00	15.96	2.55	826	-	0.90	2.30
8G-18B-E9	Bot.	8610	#9	1.00	15.96	2.55	628	**0.76**	0.69	2.63
8G-18T-P9	Top	8610	#9	1.00	15.96	2.55	758	-	1.08	2.75
8G-18T-E9	Top	8610	#9	1.00	15.96	2.55	663	**0.87**	0.94	3.14
8N-18B-P9	Bot.	7660	#9	1.00	15.96	2.55	814	-	0.94	2.40
8N-18B-E9	Bot.	7660	#9	1.00	15.96	2.55	607	**0.75**	0.70	2.69
8N-18T-P9	Top	7660	#9	1.00	15.96	2.55	652	-	0.98	2.50
8N-18T-E9	Top	7660	#9	1.00	15.96	2.55	647	**0.99**	0.98	3.25
8G-9B-P6	Bot.	8850	#6	1.50	12.00	7.68	1458	-	1.20	2.66
8G-9B-E6	Bot.	8850	#6	1.50	12.00	7.68	1057	**0.72**	0.87	2.90
8G-9T-P6	Top	8850	#6	1.50	12.00	7.68	1339	-	1.44	3.18
8G-9T-E6	Top	8850	#6	1.50	12.00	7.68	1019	**0.76**	1.09	3.16
8N-9B-P6	Bot.	8300	#6	1.50	12.00	7.68	1167	-	1.00	2.20
8N-9B-E6	Bot.	8300	#6	1.50	12.00	7.68	896	**0.77**	0.76	2.54
8N-9T-P6	Top	8300	#6	1.50	12.00	7.68	1026	-	1.14	2.51
8N-9T-E6	Top	8300	#6	1.50	12.00	7.68	814	**0.79**	0.90	2.61
10G-12B-P9	Bot.	9680	#9	1.00	10.64	3.83	887	-	0.76	2.33
10G-12B-E9	Bot.	9680	#9	1.00	10.64	3.83	732	**0.83**	0.63	2.88
10G-12T-P9	Top	9680	#9	1.00	10.64	3.83	771	-	0.86	2.63
10G-12T-E9	Top	9680	#9	1.00	10.64	3.83	747	**0.97**	0.83	3.33
10N-12B-P9	Bot.	9780	#9	1.00	10.64	3.83	885	-	0.75	2.31
10N-12B-E9	Bot.	9780	#9	1.00	10.64	3.83	806	**0.91**	0.69	3.16
10N-12T-P9	Top	9780	#9	1.00	10.64	3.83	729	-	0.81	2.47
10N-12T-E9	Top	9780	#9	1.00	10.64	3.83	682	**0.94**	0.75	3.03

Table 7.6 (continued)

Beam Notation	Casting Position	f'_c (psi)	Bar Size	c/d_b	f_s/d_b	K_{tr}	u_t (psi)	Bond Ratio	Bond Efficiency Relative To Eq. (7.1)	Bond Efficiency Relative To Eq. (7.2)
15G-12B-P9	Bot.	16100	#9	1.00	10.64	3.83	1155	-	0.77	2.98
15G-12B-E9	Bot.	16100	#9	1.00	10.64	3.83	897	**0.78**	0.59	3.48
15G-12T-P9	Top	16100	#9	1.00	10.64	3.83	1062	-	0.91	3.56
15G-12T-E9	Top	16100	#9	1.00	10.64	3.83	939	**0.88**	0.81	4.12
15N-12B-P9	Bot.	13440	#9	1.00	10.64	3.83	1191	-	0.86	3.08
15N-12B-E9	Bot.	13440	#9	1.00	10.64	3.83	850	**0.71**	0.62	3.29
15N-12T-P9	Top	13440	#9	1.00	10.64	3.83	1044	-	0.99	3.50
15N-12T-E9	Top	13440	#9	1.00	10.64	3.83	1021	**0.98**	0.96	4.48

ratios versus K_{tr}, for the beams listed in Table 7.6 and Treece's beams, is shown in Figure 7.19. Because of the wide scatter of the bond ratios, a value of 0.83 (very close to the average) is recommended for design purposes for cases where K_{tr} exceeds 1.0. In other words, a 20% increase in anchorage length of epoxy-coated reinforcing bars relative to uncoated bars, is recommended for cases where the bars are confined by transverse reinforcement with a $K_{tr} = \frac{a_{tr} f_{yt}}{500 s d_b}$ exceeding 1.0 regardless of spacing between bars or amount of cover.

In Table 7.6, the bond efficiencies relative to Eq. (7.1) of Orangun, et al., and Eq. (7.2) derived from the 1989 ACI Code Specifications, are listed for each beam. Using Eq. (7.1), the mean bond efficiency for the uncoated bars is 1.03 with a standard deviation of 0.27. On the other hand, using Eq. (7.2), the mean bond efficiency for the uncoated bars is 2.74 with a standard deviation of 0.41, and the mean bond efficiency for the coated bars is 3.14 with a standard deviation of 0.50. As was the case with beams with no ties in the splice region, the current ACI provisions are overly conservative for all the beams included in Table 7.6.

7.7.3 Assessment of the 1989 ACI Code bond specifications. The results of all splice tests, with and without ties in the splice region, show that the current ACI Code (ACI-318-89)[1] bond specifications are overly conservative and could be modified to provide a better and more reasonable estimate of the bond strength of bar splices.

In Section 12.1.2 of the ACI Code, a limit of 100 psi is imposed on the value of $\sqrt{f'_c}$ used in the development length equations. In the Commentary to Section 12.2.2, the ACI Code states that research on anchorage capacity of bars in high strength concretes is not sufficient to allow using

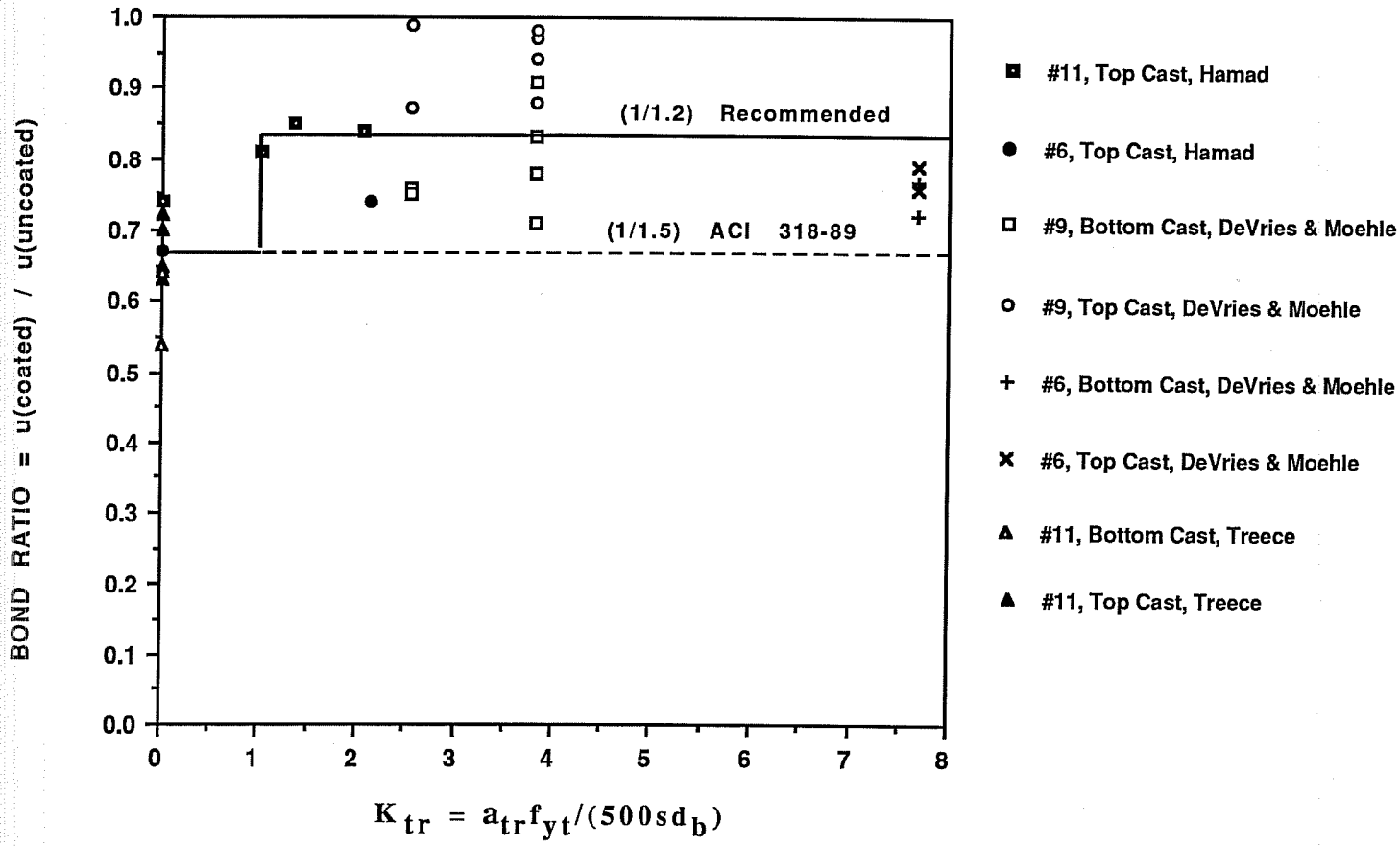

Figure 7.19 Variation of bond ratio (coated to uncoated) with the amount of transverse reinforcement crossing the splitting plane.

a value higher than 100 psi for $\sqrt{f'_c}$. However, test results listed in Tables 7.5 and 7.6 show that for bars in beams with high strength concrete (above 10,000 psi), the ACI 318-89 provisions are more conservative than in other cases. For beams (0-11-12) and (12-11-12) tested by Treece[25], the bond efficiencies relative to Eq. (7.2) are 3.86 and 3.62. For the two series 15G9 and 15N9 tested by DeVries and Moehle[27] with concrete strengths of 16100 and 13400 psi (the last eight beams in Table 7.6), the bond efficiencies relative to Eq. (7.2) vary from 2.98 to 4.48. The results indicate that the 100 psi limit on the value of $\sqrt{f'_c}$ set by ACI 318-89 could be increased.

In Section 12.2.3.1(b) of ACI 318-89, a modification factor of 1.0 is applied to the basic development length to account for bar spacing, amount of cover, and enclosing transverse reinforcement. The conditions are that the cover must not be less than the minimum cover requirements of Section 7.7.1 and the bars must be enclosed with transverse reinforcement A_{tr} (A_{tr} = Na_{tr}), along the development length with $A_{tr} \geq \left(\frac{d_b s N}{40}\right)$. Most of the beams tested by DeVries and Moehle and listed in Table 7.6, satisfied the transverse reinforcement requirement and still could not benefit from the above provision. The reason is that the cover in all the beams was 1.125 in. whereas the minimum cover requirement set for beams in Section 7.7.1 of the ACI Code is 1.5 in. Based on the available test data, it would be more appropriate to change the limit set on the cover in Section 12.2.3.1(b) from the requirements of Section 7.7.1 to one bar diameter (d_b).

In Section 12.2.4.3 of the ACI Code, a 1.5 modification factor is applied to the basic development length to account for epoxy-coated bars with cover less than $3d_b$ or clear spacing between bars less than $6d_b$. The factor is 1.2 for all other conditions. Based on bond ratios (coated

to uncoated) of beams with ties in the splice region, it was recommended earlier that the 1.2 modification factor be also applied to epoxy-coated bars enclosed by ties satisfying $\left(\frac{a_{tr}f_{yt}}{500sd_b}\right) \geq 1.0$. Also, Section 12.2.4.3 of ACI 318-89 states that the product of the factor for top bars, 1.3, and the factor for epoxy-coated reinforcement should not exceed 1.7. However, the size of available data on epoxy-coated top cast bars and the corresponding test results strengthen the argument made previously by DeVries and Moehle[27] that the effects of top casting and epoxy coating are not cumulative. The computed bond efficiencies of epoxy-coated top cast bars relative to Equation (7.2) listed in Tables 7.5 and 7.6, indicate that the 1.7 factor recommended by ACI 318-89 for the combined effect of top casting and epoxy coating is very high. Top bars included in this phase of the research program and top bars included in Treece's study and in DeVries and Moehle's study, had approximately 12.5 to 14.5 in. of fresh concrete cast below the bars. This is closed to the minimum amount of fresh concrete below the bar (12 in.) set by the ACI Code in the definition of a top cast bar. However, tests done at the University of Texas on the effect of casting position on the bond strength of reinforcing bars[34], indicated that bars cast with 1 to 6 ft. of fresh concrete below the bars developed more than 80% of the bond strength of bottom cast bars ($\frac{1}{0.8} = 1.25 < 1.3$, top bar factor of ACI 318-89).

Based on the available test data, it is suggested that when the factors for top casting and epoxy coating are both applicable, the larger of the two factors should control. For example, in the case of an epoxy-coated top cast bar with a cover less than $3d_b$ and with no transverse reinforcement along the anchorage length, the factor for epoxy coating is 1.5 and the factor for top

casting is 1.3. In this case the 1.5 factor controls. On the other hand, in the case of an epoxy-coated top cast bar which is well confined by transverse reinforcement along the development or splice length with $K_{tr} > 1.0$, the factor for epoxy coating is 1.2 and the factor for top casting is 1.3. In this case the 1.3 factor controls.

Moreover, based on the comparison of all available splice data with the current ACI Code bond specifications, it is evident that the factors for splices, top casting, epoxy coating, and cover and spacing and transverse reinforcement, are not all cumulative. In cases where all the above factors are applicable, the ACI specifications with the inclusion of the recommended modifications are still highly conservative. Therefore, it is recommended that an upper factor of 2.0 be set on the product of the modification factors for all cases of uncoated and epoxy-coated reinforcing bars.

Using all the above recommended modifications to the 1989 ACI Code bond provisions, the bond efficiencies of all available splice tests were reevaluated. The new values are shown in Table 7.7 and 7.8. For beams with no ties in the splice region, the mean bond efficiency dropped from 2.38 to 2.20 for the uncoated bars and from 2.41 to 1.67 for the coated bars. The standard deviation dropped from 0.71 to 0.51 for the uncoated bars and from 0.49 to 0.30 for the coated bars. The probability is 95% that the bond efficiency for the uncoated bars exceeds 1.36 and the bond efficiency for the coated bars exceeds 1.18. The two values, 1.36 and 1.18, are above 1.00 and are comparable. Also, the probability is 99% that both bond efficiencies exceed 1.00. On the other hand, for beams with ties in the splice region, the mean bond efficiency dropped from 2.74 to 2.10 for the uncoated bars and from 3.14 to 1.82 for the coated bars. The standard deviation dropped

Table 7.7 Effect of the proposed modifications to ACI 318-89 on bond efficiencies, beams with no stirrups in the splice region.

Beam Notation	Bar Type	u_t (psi)	Predicted Bond Stress: ACI 318-89 Eq.(7.2) (psi)	Predicted Bond Stress: ACI 318-89 + Modifications (psi)	Bond Efficiency Relative To: ACI 318-89 Eq.(7.2)	Bond Efficiency Relative To: ACI 318-89 + Modifications
B1-11-4-U	U	409	145	172	2.82	2.38
B2-11-4-C	C	301	111	172	2.71	1.75
B9-6-4-U3	U	648	274	325	2.36	1.99
B10-6-4-C3	C	435	210	325	2.07	1.34
Treece [25]						
0-11-4	U	420	169	200	2.49	2.10
12-11-4	C	280	129	200	2.17	1.40
5-11-4	C	300	129	200	2.32	1.50
0-11-4b	U	450	203	203	2.22	2.22
12-11-4b	C	240	135	184	1.78	1.30
0-11-8	U	790	217	257	3.64	3.07
12-11-8	C	500	166	257	3.01	1.95
0-11-12	U	920	238	289	3.86	3.18
12-11-12	C	660	182	289	3.62	2.28
0-11-12b	U	840	304	304	2.76	2.76
12-11-12b	C	540	202	276	2.67	1.96
Choi, et al. [33]						
GROUP SP1	U	797	469	469	1.70	1.70
	C	592	341	465	1.74	1.27
GROUP SP2	U	675	452	452	1.49	1.49
	C	634	301	411	2.11	1.54
	U	761	452	452	1.68	1.68
	C	577	301	411	1.92	1.40
GROUP SP3	U	627	338	338	1.86	1.86
	C	561	225	307	2.49	1.83
	U	630	338	338	1.86	1.86
	C	538	225	307	2.39	1.75
GROUP SP4	U	552	237	237	2.33	2.33
	C	391	158	216	2.48	1.81
	U	517	237	237	2.18	2.18
	C	420	158	216	2.66	1.94
		Uncoated (U) Bars:				
		Mean Bond Efficiency =			**2.38**	**2.20**
		Standard Deviation =			**0.71**	**0.51**
		Epoxy-Coated (C) Bars:				
		Mean Bond Efficiency =			**2.41**	**1.67**
		Standard Deviation =			**0.49**	**0.30**

Table 7.8 Effect of the proposed modifications to ACI 318-89 on bond efficiencies, beams with stirrups in the splice region.

Beam Notation	Bar Type	u_t (psi)	Predicted Bond Stress: ACI 318-89 Eq.(7.2) (psi)	Predicted Bond Stress: ACI 318-89 + Modifications (psi)	Bond Efficiency Relative To: ACI 318-89 Eq.(7.2)	Bond Efficiency Relative To: ACI 318-89 + Modifications
B3-11-4-U-U(10")	U	443	145	172	3.06	2.58
B4-11-4-C-C(10")	C	358	111	172	3.23	2.08
B5-11-4-U-U(5")	U	470	145	172	3.24	2.73
B6-11-4-C-C(5")	C	393	111	172	3.54	2.28
B7-11-4-U3-U(5")	U	388	151	179	2.57	2.17
B8-11-4-C3-C(5")	C	331	115	179	2.88	1.85
B11-6-4-U3-U(6")	U	716	274	324	2.61	2.21
B12-6-4-C3-C(6")	C	532	210	324	2.53	1.64
DeVries and Moehle [27]						
8G-18B-P9	U	826	359	359	2.30	2.30
8G-18B-E9	C	628	239	326	2.63	1.93
8G-18T-P9	U	758	276	327	2.75	2.31
8G-18T-E9	C	663	211	327	3.14	2.03
8N-18B-P9	U	814	339	339	2.40	2.40
8N-18B-E9	C	607	226	308	2.69	1.97
8N-18T-P9	U	652	261	309	2.50	2.11
8N-18T-E9	C	647	199	309	3.25	2.09
8G-9B-P6	U	1458	548	603	2.66	2.42
8G-9B-E6	C	1057	365	603	2.90	1.75
8G-9T-P6	U	1339	421	589	3.18	2.27
8G-9T-E6	C	1019	322	589	3.16	1.73
8N-9B-P6	U	1167	531	584	2.20	2.00
8N-9B-E6	C	896	353	584	2.54	1.53
8N-9T-P6	U	1026	408	571	2.51	1.80
8N-9T-E6	C	814	312	571	2.61	1.43
10G-12B-P9	U	887	381	533	2.33	1.66
10G-12B-E9	C	732	254	445	2.88	1.64
10G-12T-P9	U	771	293	410	2.63	1.88
10G-12T-E9	C	747	224	410	3.33	1.82
10N-12B-P9	U	885	383	536	2.31	1.65
10N-12B-E9	C	806	255	446	3.16	1.81
10N-12T-P9	U	729	295	413	2.47	1.77
10N-12T-E9	C	682	225	413	3.03	1.65

Table 7.8 (continued)

Beam Notation	Bar Type	u_t (psi)	Predicted Bond Stress: ACI 318-89 Eq.(7.2) (psi)	Predicted Bond Stress: ACI 318-89 + Modifications (psi)	Bond Efficiency Relative To: ACI 318-89 Eq.(7.2)	Bond Efficiency Relative To: ACI 318-89 + Modifications
15G-12B-P9	U	1155	387	687	2.98	1.68
15G-12B-E9	C	897	258	573	3.48	1.57
15G-12T-P9	U	1062	298	530	3.56	2.00
15G-12T-E9	C	939	228	530	4.12	1.77
15N-12B-P9	U	1191	387	628	3.08	1.90
15N-12B-E9	C	850	258	523	3.29	1.63
15N-12T-P9	U	1044	298	484	3.50	2.16
15N-12T-E9	C	1021	228	484	4.48	2.11
			Uncoated (U) Bars:			
			Mean Bond Efficiency =		**2.74**	**2.10**
			Standard Deviation =		**0.41**	**0.31**
			Epoxy-Coated (C) Bars:			
			Mean Bond Efficiency =		**3.14**	**1.82**
			Standard Deviation =		**0.50**	**0.22**

from 0.41 to 0.31 for the uncoated bars and from 0.50 to 0.22 for the coated bars. The probability is 95% that the bond efficiency for the uncoated bars exceed 1.59 and the bond efficiency for the coated bars exceeds 1.46. Again, the two values, 1.59 and 1.46, are above 1.00 and are comparable. Also, the probability is 100% that both bond efficiencies exceed 1.00.

The bond efficiencies computed relative to the 1989 ACI Code provisions, after applying the recommended modifications, are still conservative but appear to be much more realistic. It is important to note that Eq. (7.1) of Orangun, et. al., is still a much better approach especially after applying the recommended modification factors for epoxy coating and for the combined effect of top casting and epoxy coating.

7.8 Design Recommendations

Based on the test results and on the analysis of the available data on splice tests, the following recommendations are proposed:

(1) The upper limit of 100 psi set on the value of $\sqrt{f'_c}$ in Section 12.1.2 of ACI 318-89[1], could be raised to a value of 130 to 140.

(2) Section 12.2.3.1(b) of the 1989 ACI Code provides conditions which, if satisfied, would allow the use of a 1.0 modification factor to account for bar spacing, amount of cover, and enclosing transverse reinforcement. Section 12.2.3.1(b) needs to be changed to read as follows:

"Bars in beams or columns with (1) minimum cover not less than d_b and (2) enclosed within transverse reinforcement A_{tr}, along the development length satisfying Eq. (12-1)

$$A_{tr} \geq \frac{d_b sN}{40} \qquad (12\text{-}1)$$

where d_b is the diameter of the bar being developed."

(3) Section 12.2.3.2 which specifies a 2.0 modification factor to account for bar spacing, amount of cover, and enclosing transverse reinforcement, needs to be changed to read as follows:

"For bars with cover of d_b or less and with clear spacing of $2d_b$ or less, and without any transverse reinforcement along the development length . . . . . 2.0"

(4) To account for epoxy-coated bars enclosed or not enclosed by transverse reinforcement and to account for the combined effect of top casting and epoxy coating, Section 12.2.4.3 of the 1989 ACI Code needs to be changed to read as follows:

"Bars with cover less than $3d_b$ or clear spacing between bars less than $6d_b$ 1.5

Bars with cover larger than $3d_b$ amd clear spacing betweem bars larger than $6d_b$ 1.2

Bars enclosed with transverse reinforcement A_{tr}, along the development length satisfying $A_{tr} \geq \frac{d_b s N}{120}$, regardless of the amount of cover or clear spacing between bars 1.2

For epoxy-coated top reinforcement the larger of the factor for top reinforcement of 12.2.4.1 and the applicable factor for epoxy-coated reinforcement of Section 12.2.4.3 shall be used."

(5) An upper limit of 2.0 is to be imposed on the product of the splice class factor and the factors for bar spacing, amount of cover, enclosing transverse reinforcement, top reinforcement, and epoxy-coated reinforcement.

CHAPTER 8
EPOXY-COATED HOOKED BARS

8.1 Background

Up to date there has been no research work done to study the anchorage performance of epoxy-coated hooked bars. However, in 1972, Jirsa and Marques[35] reported a series of tests to determine the capacity of uncoated hooked bars. Nineteen specimens simulating exterior beam-column joints in a frame structure were tested to evaluate the capacity of uncoated anchored beam reinforcement subjected to varying degrees of confinement at the joint. The types of confinement included vertical column reinforcement, lateral reinforcement through the joint, side concrete cover, and column axial load.

The properties of the nineteen specimens are summarized in Table 8.1. The dimensions and reinforcement details are shown in Figures 8.1, 8.2 and 8.3. The tests were conducted using either two #7 (J7 series) or two #11 (J11 series) beam bars anchored in 50-in. long columns. Standard 90- or 180-degree hooks conforming to ACI 318-63 standard hook details [17] were used throughout. The column cross-section was either 12-in. x 12-in. or 12-in. x 15-in. By varying the size of the column, the lead embedment before the hook portion of the anchored bar was also varied. In the 12-in. x 15-in. columns, the column reinforcement consisted of six #8 longitudinal bars and #3 ties at 5 in. outside the joint. The 12-in. x 12-in. columns were reinforced with four #8 longitudinal bars and #3 ties at 5 in. outside the joint. The clear cover over the ties was 1-1/2 in. Four types of confinement were considered:

(1) Longitudinal column bars: To determine the influence of column bars, tests were run with column bars placed outside the anchored beam bars and comparison tests were run with the column bars placed inside the beam bars. In both cases, the concrete cover over the beam bars was 2-7/8 in.

Table 8.1 Parameters and results of Marques and Jirsa hooked bar tests [35].

Specimen Notation*	Column Size	Column Axial Load (Kips)	Angle of Bend (degrees)	f'c (Ksi)	Lead Embed. (inch)	Lateral Confinement Type**	P_{max} (Kips)
J7-90-15-1-H	12x15	545	90	4.60	9.5	1	55
J7-90-15-1-M	12x15	269	90	5.05	9.5	1	60
J7-90-15-1-L	12x15	145	90	4.80	9.5	1	58
J7-90-12-1-H	12x12	420	90	4.15	6.5	1	37
J7-180-15-1-H	12x15	545	180	4.00	9.5	1	52
J7-180-12-1-H	12x12	425	180	4.35	6.5	1	37
J7-90-15-2-H	12x15	545	90	4.75	9.5	2	59
J7-90-15-2-M	12x15	274	90	4.75	9.5	2	57
J7-90-15-3-H	12x15	555	90	4.65	9.5	3	62
J7-90-15-3a-H	12x15	535	90	3.75	9.5	3a	59
J7-90-15-4-H	12x15	548	90	4.50	9.5	4	44
J11-90-15-1-H	12x15	540	90	4.90	6.0	1	75
J11-90-15-1-L	12x15	154	90	4.75	6.0	1	81
J11-90-12-1-H	12x12	437	90	4.60	3.0	1	66
J11-180-15-1-H	12x15	540	180	4.40	6.0	1	70
J11-90-15-2-H	12x15	540	90	5.00	6.0	2	76
J11-90-15-2-L	12x15	125	90	4.50	6.0	2	83
J11-90-15-3-L	12x15	150	90	4.85	6.0	3	97
J11-90-15-3a-L	12x15	175	90	5.00	6.0	3a	108

* For example J7-90-15-1-H implies: #7 bars, 90-degree hook, 12x15 column, confinement type = 1, and high level of column axial load.

**Lateral confinement types are:
1 = Column bars + 2-7/8 in. cover
2 = Only 2-7/8 in. cover
3 = 2-7/8 in. cover + #3 ties @ 5" through the joint
3a = 2-7/8 in. cover + #3 ties @ 2.5" through the joint
4 = Only 1-1/2 in. cover

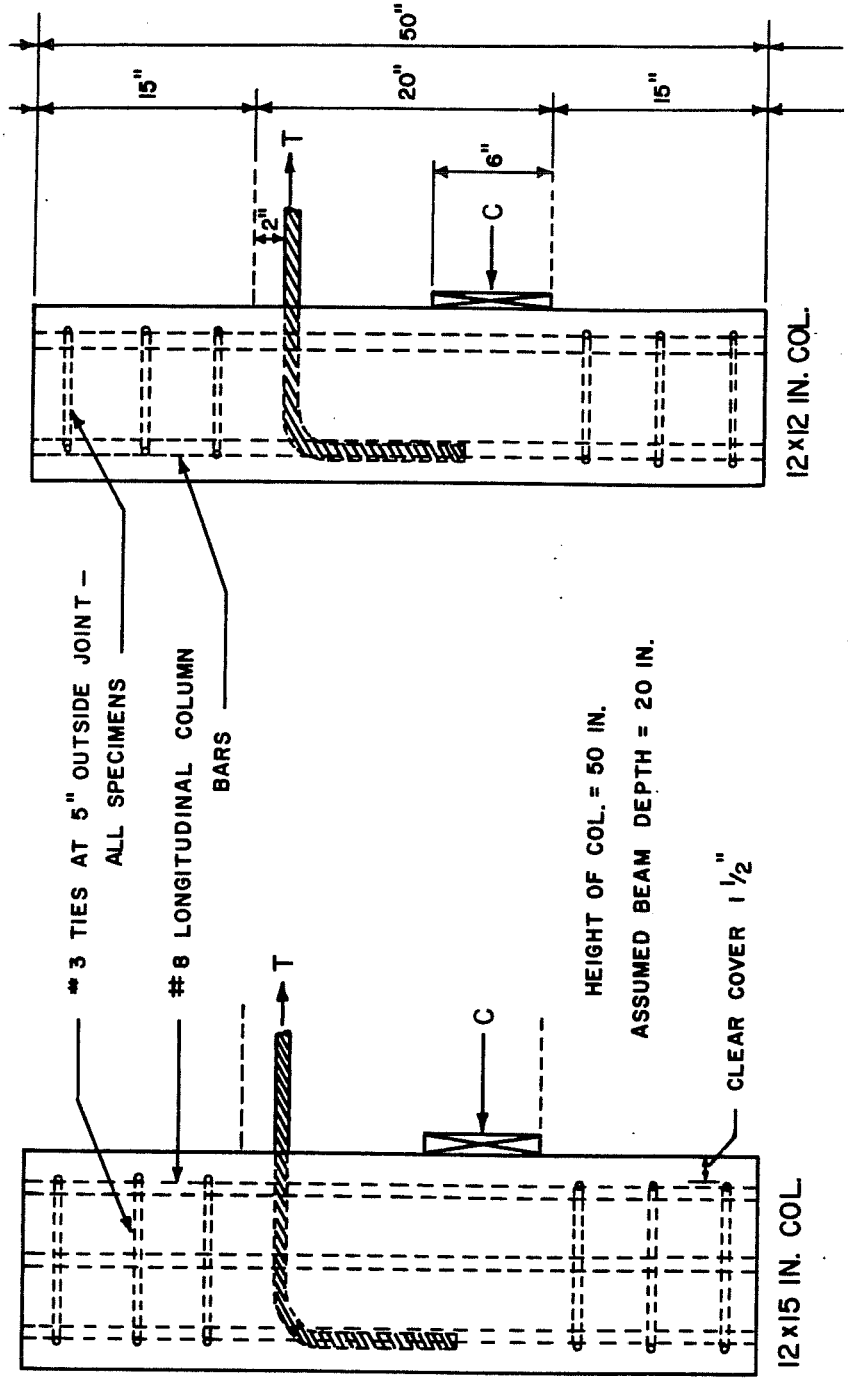

Figure 8.1 Details of hooked bar specimens, Marques and Jirsa[35].

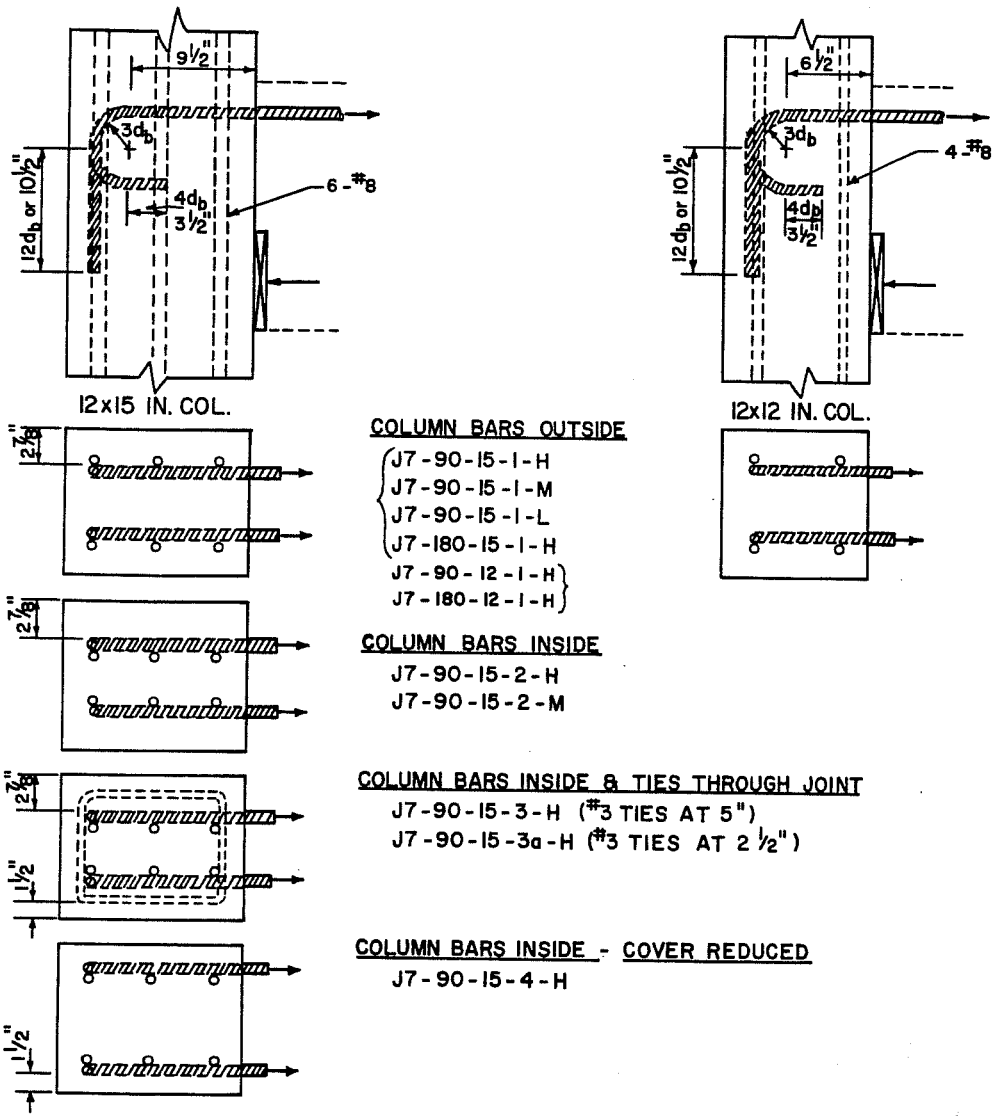

Figure 8.2 Joint details of the J7 series of #7 hooked bar specimens, Marques and Jirsa[35].

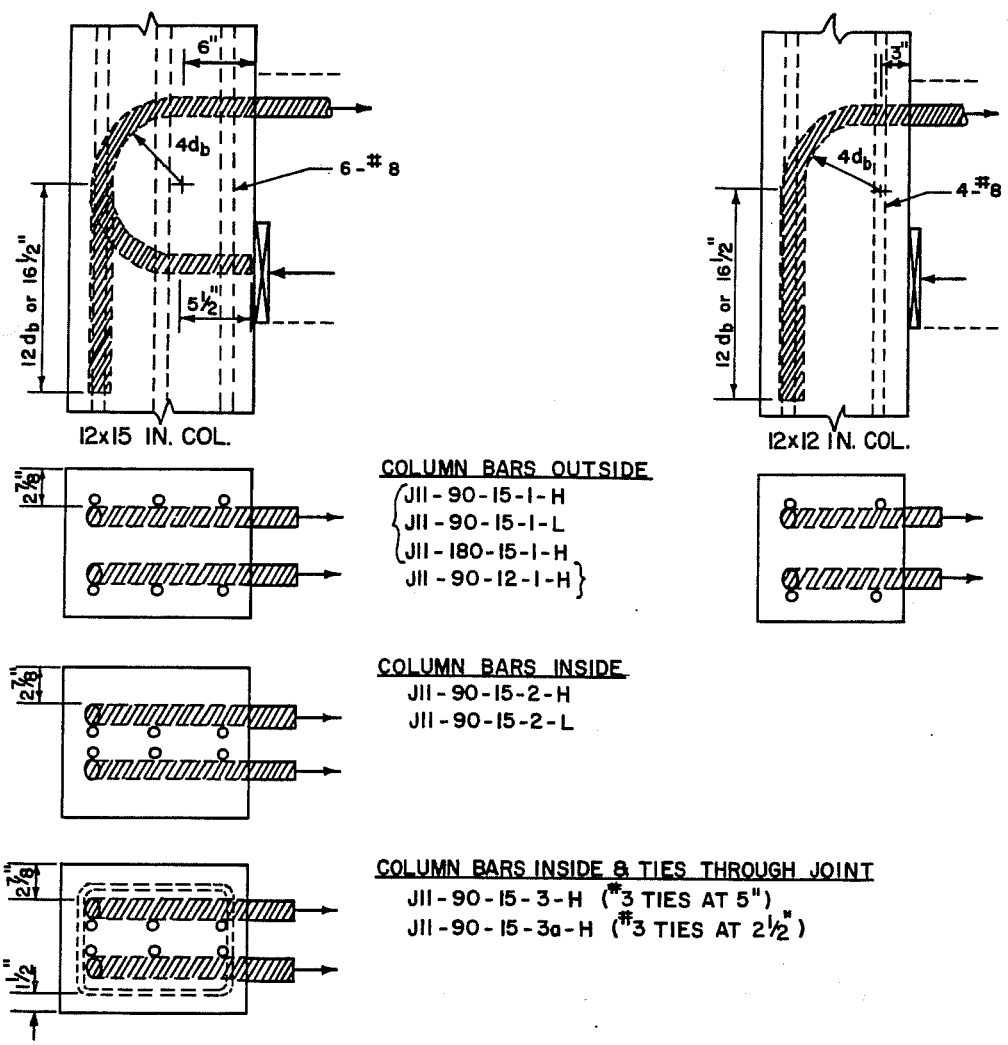

Figure 8.3 Joint details of the J11 series of #11 hooked bar specimens, Marques and Jirsa[35].

(2) Lateral ties through the joint: The effect of the ties was isolated by retaining the same column steel, placing the column bars inside the beam bars, and carrying ties through the joint. In this case the confinement consisted of a concrete cover of 2-7/8-in. plus #3 ties at a spacing of 5 in. or 2-1/2 in. through the joint.

(3) Concrete cover (normal to plane of hook): The effect of concrete cover was determined by conducting one test in the J7 series (#7 bars) with the concrete cover reduced from 2-7/8 in. to 1-1/2 in. and placing the column bars inside the beam bars so that only clear concrete cover confined the anchored beam bars.

(4) Column axial load: Three nominal levels of axial load were considered: 135 kips (designated by L in Table 8.1), 270 kips (designated by M) and 540 kips (designated by H). The actual levels of axial load measured during testing are listed in Table 8.1.

In each test, the column axial load was applied and maintained constant throughout the loading sequence. This load represented the dead loads in a structure which would remain constant with increasing moment on the beam. To simulate moment action, tension was applied to the two anchored bars by hydraulic rams operated by hand pumps and a reaction steel column transferred compression load to the specimen. In all tests slip was measured at five points along the length of the anchored bar.

The reinforcing bars of the assumed beam were loaded in increments of roughly 2000 psi. Crack patterns were marked at all load stages. A test was terminated when one of the anchored bars pulled out of the column. In general, failure in most tests was sudden and complete and resulted in the entire side cover of the column spalling away to the level of the hooked anchorage. The ultimate loads of the test specimens are listed in Table 8.1.

Based on slip and strain measurements and observations of failure, Marques and Jirsa[35] made the following conclusions:

(1) The level of column axial load did not significantly influence the behavior of hooked bar anchorages.

(2) The embedment length between the beginning of a standard hook and the critical section at the face of the column was the prime factor in determining the capacity of the hooked bar anchorages.

(3) Placement of the column bars inside or outside the anchored beam bars did not influence stress or slip characteristics of the anchored bars.

(4) Ties through the joint reduced slip and increased capacity but only if the tie spacing was small relative to the diameter of the bend of the anchored beam bar.

(5) Concrete cover did not appear to influence the stress-slip characteristics provided that the cover was sufficient to prevent a local failure in the vicinity of the bent portion of the hooked anchorage.

(6) There was very little difference between the capacity of 90- and 180-degree hooks; however, the slip at a given stress was greater for 180-degree hooks.

8.2 Experimental Program

The objective of this part of the project was to study the behavior and anchorage capacity of epoxy-coated hooked bars relative to uncoated bars. Twenty-four specimens, simulating exterior beam-column joints in a structure, were tested in six series. The effects of bar size, concrete strength, concrete cover, lateral reinforcement through the joint, and hook geometry on the relative performance of uncoated and epoxy-coated hooked bars were evaluated.

8.2.1 Design of Specimens. The test specimens are identified in Table 8.2 A four-term notation system was used to identify the variables of each specimen. The first term is the bar size: #7 or #11. The second term is hook geometry: 90 or 180 degrees. The third term indicates whether the bar is uncoated (U) or epoxy-coated (C). The fourth term of the notation, if present,

Table 8.2 Test parameters of the hooked bar tests.

SERIES NUMBER	Specimen Notation	f'_c (psi)	Bar Size	Angle of Bend (degrees)	Ties in Joint Region
ONE	7-90-U*	5400	#7	90	-
	7-90-C*	5400	#7	90	-
	11-90-U*	5400	#11	90	-
	11-90-C*	5400	#11	90	-
TWO	7-90-U-T4	3700	#7	90	#3 @ 4"
	7-90-C-T4	3700	#7	90	#3 @ 4"
	11-90-U-T6	3700	#11	90	#3 @ 6"
	11-90-C-T6	3700	#11	90	#3 @ 6"
THREE	7-180-U-T4	3900	#7	180	#3 @ 4"
	7-180-C-T4	3900	#7	180	#3 @ 4"
	11-180-U-T6	3900	#11	180	#3 @ 6"
	11-180-C-T6	3900	#11	180	#3 @ 6
FOUR	7-90-U	2570	#7	90	-
	7-90-C	2570	#7	90	-
	11-90-U	2570	#11	90	-
	11-90-C	2570	#11	90	-
FIVE	7-90-U-SC+	4225	#7	90	-
	7-90-C-SC+	4225	#7	90	-
	11-90-U-T4	4225	#11	90	#3 @ 4"
	11-90-C-T4	4225	#11	90	#3 @ 4"
SIX	11-90-U-HS	7200	#11	90	-
	11-90-C-HS	7200	#11	90	-
	11-180-U-HS	7200	#11	180	-
	11-180-C-HS	7200	#11	180	

* Slip measurements of the four specimens of the first series were not reliable.

+The nominal side concrete cover over the hooked bars was 1-7/8 in. with the column bars placed inside the beam bars. In all other test specimens the nominal side cover was 2-7/8 in. with the beam bars placed inside the column bars.

is used for three indications: T4 or T6 indicates the presence of #3 ties in the hook region spaced at 4 or 6 in.; an SC indicates small concrete cover to the anchored bars; and an HS indicates high strength concrete. Ties placed in the hook region of an epoxy-coated hooked bar specimen were also epoxy-coated.

The specimens simulated full-scale beam-column joints. To determine the influence of epoxy coating on hooked bar anchorages, coating application was the only variable in each pair of tests. The design of the specimens was similar to the design used by Marques and Jirsa[35] to allow comparison of test results. In each specimen, two #7 or #11 beam bars were anchored in a 48-in. long column. Standard 90- or 180-degree hooks conforming to ACI 318-89 standard hook details[1] were used. Geometrical and reinforcement details of the #7 and #11 hooked bar specimens of all six series, are shown in Figures 8.4 to 8.8.

The 48-in. height of the column was chosen to permit the embedment of the hooked bars and to allow some additional column length above and below an assumed beam depth of 20 in. The width of the beam was 12 in. and was equal to the width of the column. This would allow a spacing of about 3-1/2 in. between two #11 hooked bars anchored inside the column bars. The column dimension in the plane of the hook was 12 in. for the #7 bars and 15 in. for the #11 bars.

The 12-in. x 12-in. column was reinforced with four #8 longitudinal bars and #3 ties at 6 in. outside the joint. The 12-in. x 15-in. column was reinforced with six #8 longitudinal bars and #3 ties at 6 in. outside the joint. In series ONE, where the tie spacing outside the joint noted above was adopted, there were signs of anchorage failure of the column bars. Therefore, in the next five series, the spacing of #3 column ties below the joint was reduced (3 to 4 in.), and prior to casting, the column bars in the back face were welded to 3-in. x 3-in. x 1/2-in. anchor plates at the base of the specimen. It is important to note that in all epoxy-coated hooked bar specimens, the column longitudinal bars were also coated. The only exceptions were specimens 7-90-C* and 11-90-C* where the column bars were uncoated.

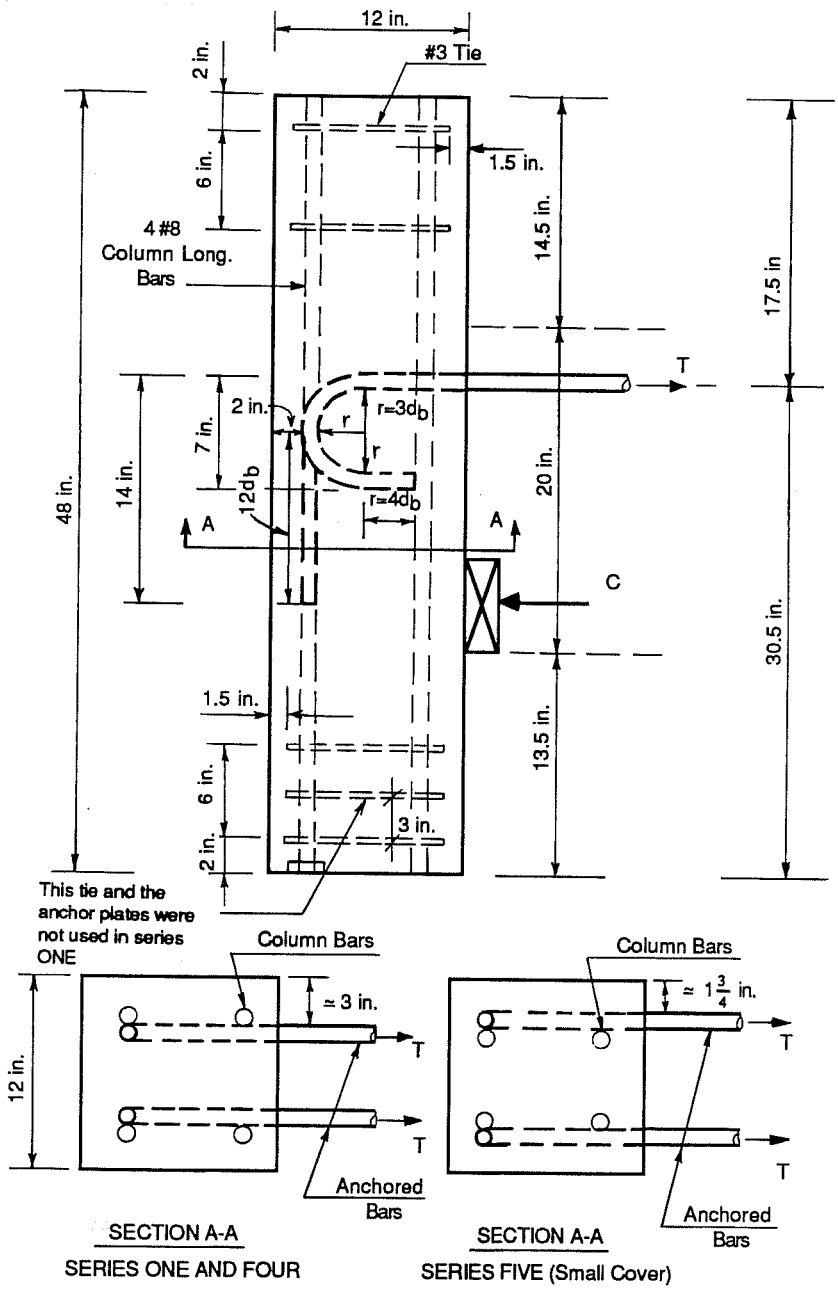

Figure 8.4 Specimens with #7 hooked bars, no ties in the joint region.

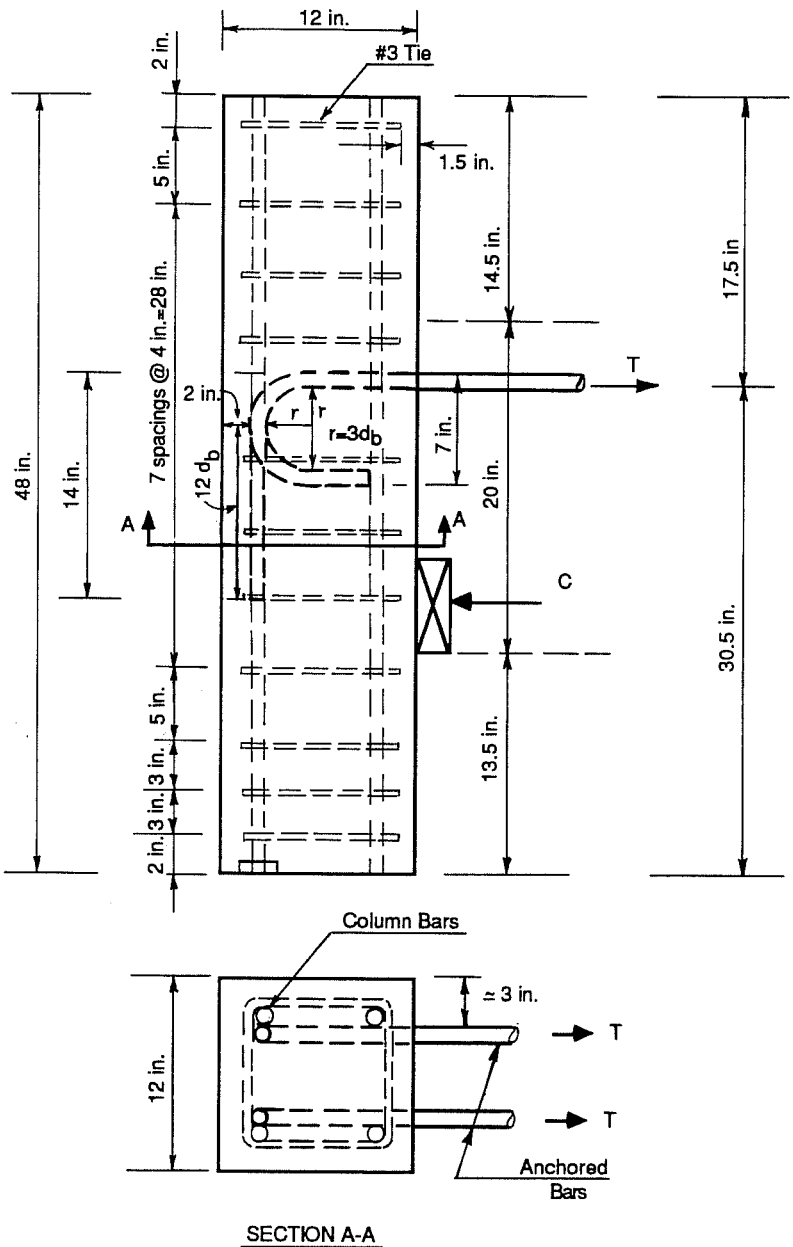

Figure 8.5 Specimens with #7 hooked bars, #3 ties at 4 in. in the joint region.

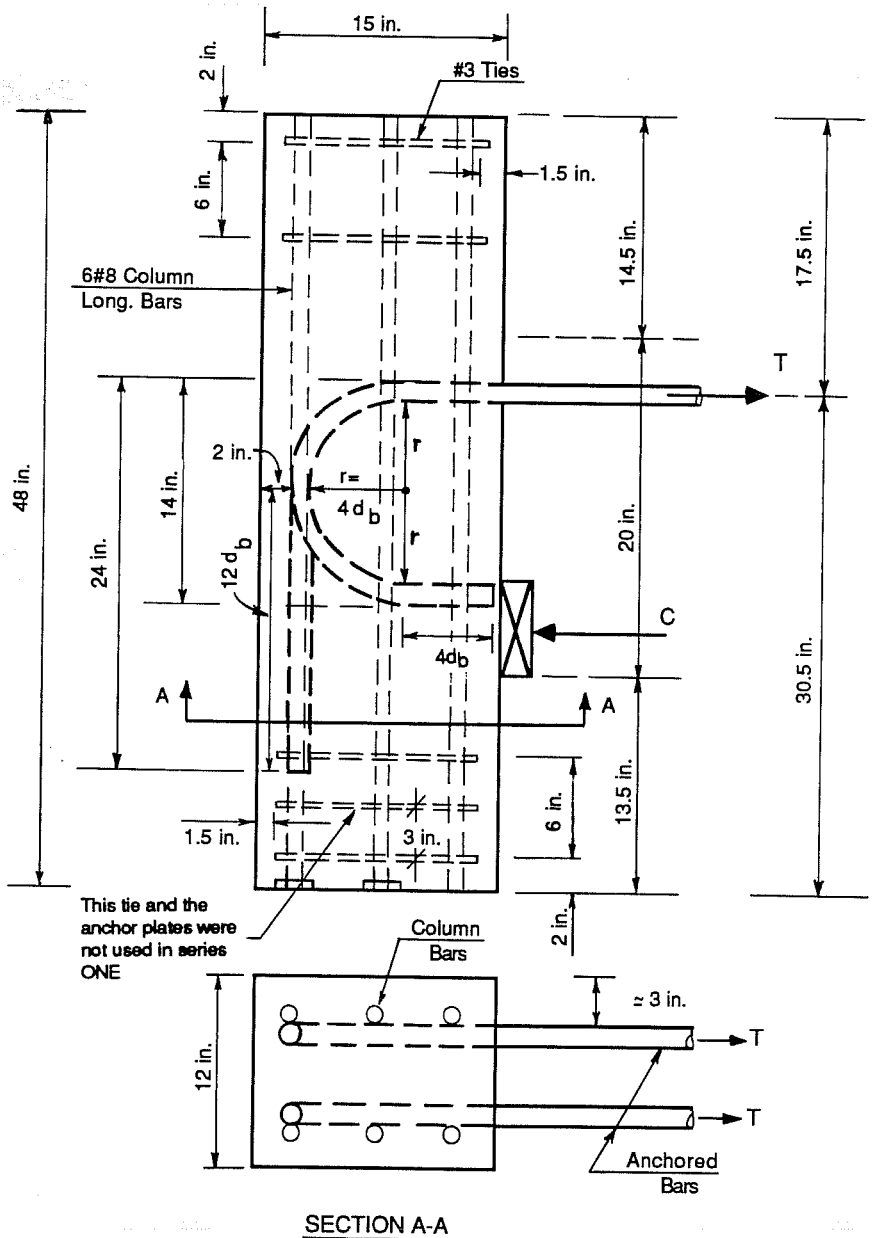

Figure 8.6 Specimens with #11 hooked bars, no ties in the joint region.

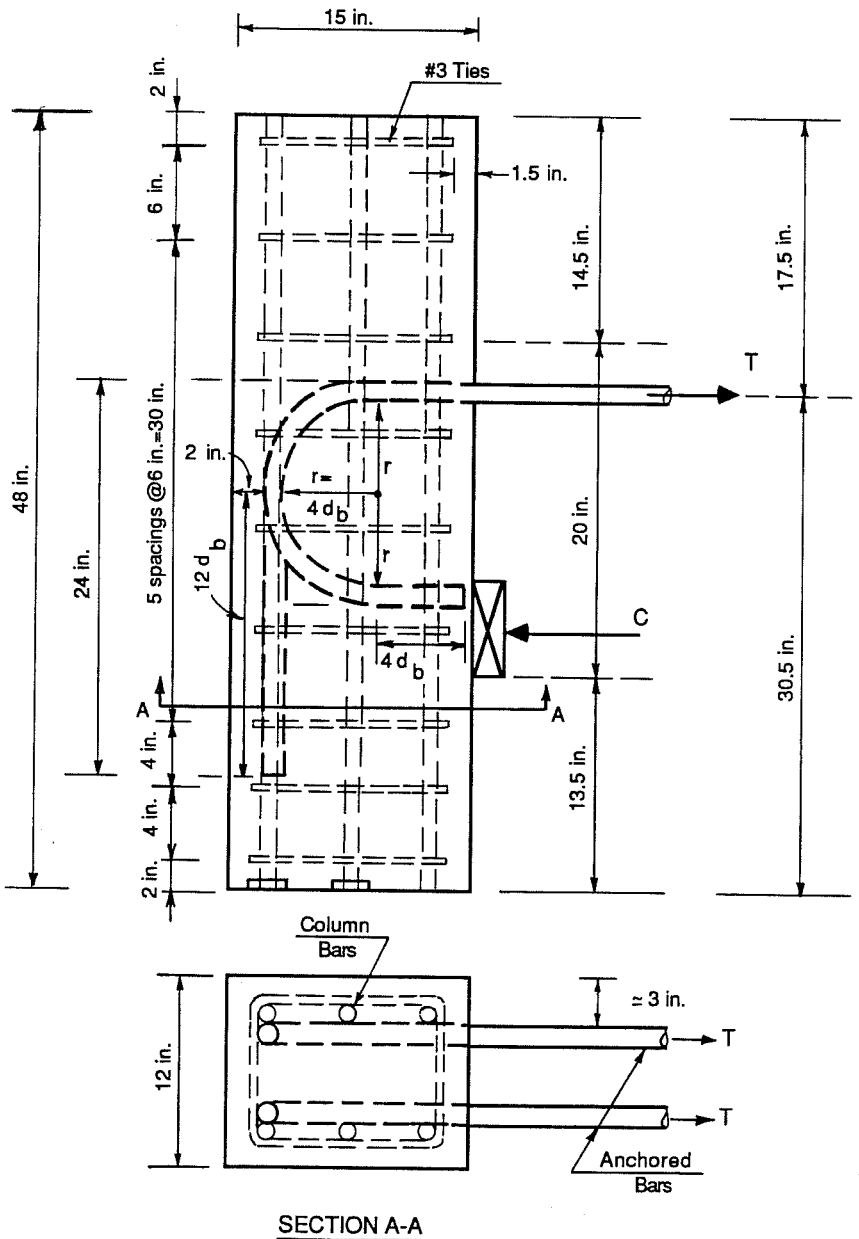

Figure 8.7 Specimens with #11 hooked bars, #3 ties at 6 in. in the joint region.

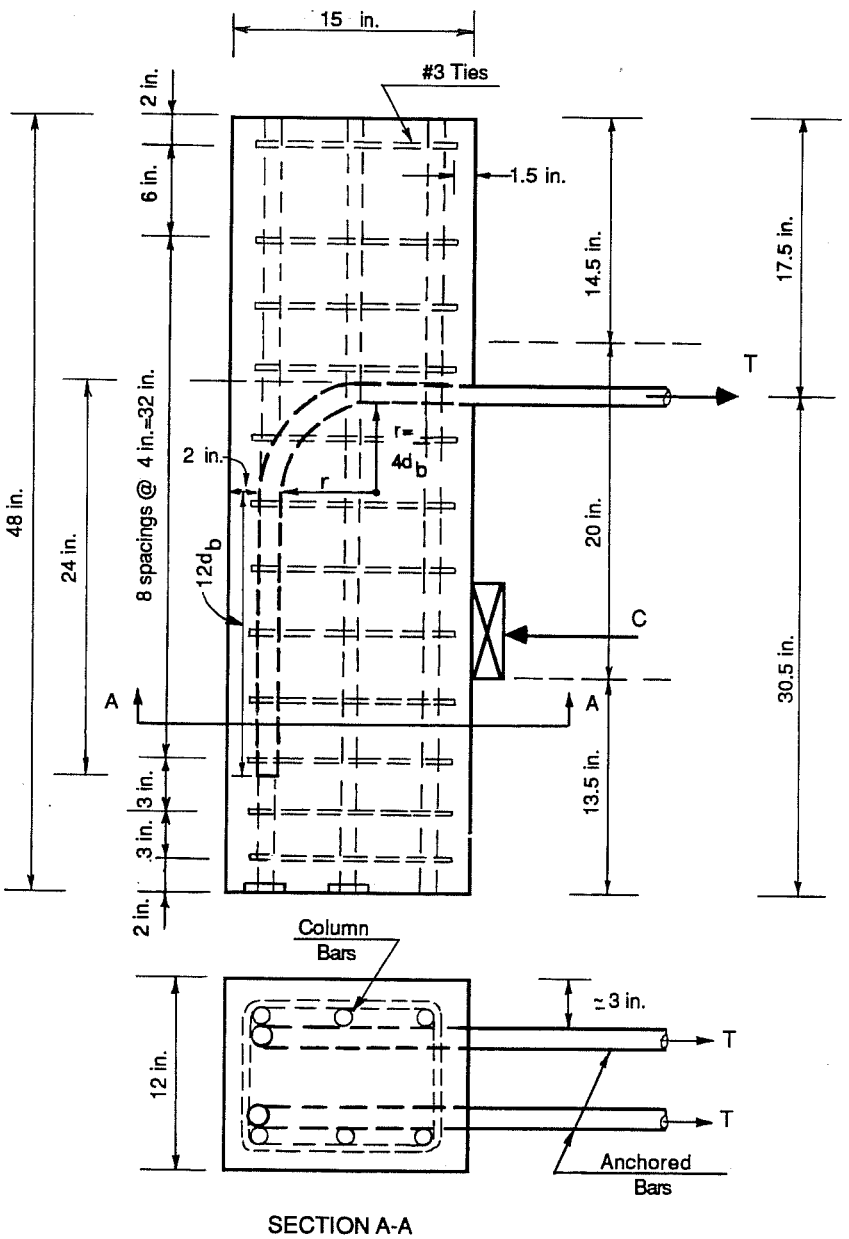

Figure 8.8 Specimens with #11 hooked bars, #3 ties at 4 in. in the joint region.

In all specimens, the concrete cover over the ties was 1-1/2 in. The cover in the plane of the hooks over the tail extension of the anchored beam bars, was 2 in.

The column dimension in the plane of the hook was chosen so that the development length provided for the #7 or #11 hooked bars would be shorter than required by Section 12.5.1 of the ACI Building Code (ACI 318-89)[1]. This would ensure bond failure before the steel yielded. According to ACI 318-89, the basic development length for a Grade 60 hooked bar is: $\ell_{hb} = 1200\ d_b\ /\sqrt{f'_c}$. For #11 bars and smaller with side cover not less than 2-1/2 in. and for a 90-degree hook with cover on bar extension beyond the hook not less than 2 in., the ACI modifies ℓ_{hb} by a factor of 0.7 ($\ell_{dh} = 0.7\ \ell_{hb}$). The modified development length should not be less than $8d_b$ nor less than 6 in.

Assuming the 0.7 modification factor applies and considering a nominal concrete strength of 4000 psi:

$$\ell_{dh} = 11.6 \text{ in. for } \#7 \text{ bars}$$

and

$$\ell_{dh} = 18.7 \text{ in. for } \#11 \text{ bars}$$

The provided ℓ_{dh} is 10 in. for the #7 bars and 13 in. for the #11 bars (see Figure 8.9).

The anchored bars extended past the face of the column to accommodate placing the hydraulic rams. The length of the #7 and #11 reinforcing bars, measured to the outside end of the hook, was 50 in. (see Figure 8.9). The loading setup simulated flexure.

8.2.2 Materials. In all six series, reinforcing bars of each size were from the same heat of steel and had a parallel deformation pattern. The beam bars: #7 and #11, and the column bars: #3 and #8, were all Grade 60 and met ASTM A615-87a[30]. The stress-strain diagrams of the #11 and #3 bars were shown in Figures 4.5(a) and 6.3, respectively. The measured properties of the

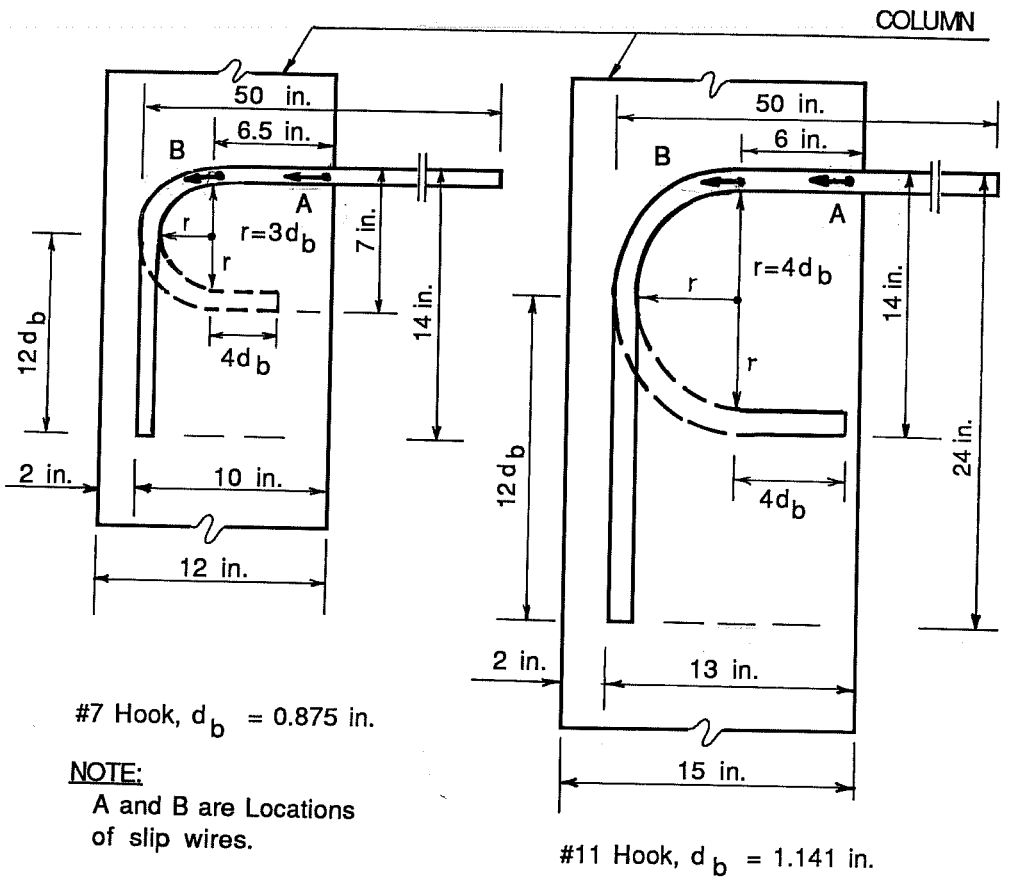

Figure 8.9 Details of anchored beam reinforcement in the hooked bar specimens.

#7 and #8 bars are shown in Table 8.3. The average coating thickness for all epoxy-coated hooked bars was 8 mils. The average coating thickness for the epoxy-coated transverse reinforcement was approximately 9 mils.

Three non air-entrained concrete mix designs were ordered from a ready-mix company, and were proportioned to yield a compression strength of 3000, 4000, and 8000 psi. Assuming saturated surface dry conditions for the aggregates, the mix proportions per cubic yard are shown in Table

Table 8.3 Measured properties of #7 and #8 parallel deformation pattern reinforcing bars compared with ASTM A615-87a specifications.

Deformation Properties	**#7 Deformed Bar**	**#8 Deformed Bar**
Average Spacing (inch)	0.583(≤0.612)*	0.663(≤0.700)
Average Height (inch)	0.058(≥0.044)	0.063(≥0.050)
Gap (inch)	0.219(≤0.334)	0.219(≤0.383)
Strength Properties	**#7 Deformed Bar**	**#8 Deformed Bar**
Yield Strength (Ksi)	68.8(≥60)	64.7(≥60)
Ultimate Strength (Ksi)	106.7(≥90)	106.6(≥90)

*Number in parenthesis is ASTM A615-87a specification.

Table 8.4 Concrete mix proportions per cubic yard for the hooked bar specimens.

	Nominal Concrete Strength 3000 psi	4000 psi	8000 psi
Max. Size Aggregate, in.	3/4	3/8	3/8
Cement(Type 1), lb.	360	470	525
Fly Ash, lb.	-	-	225
Coarse Aggregate, lb.	1881	1625	1790
Sand, lb.	1435	1655	1131
Water, lb.	266	250	295
Water Reducer Retarder, oz.	10.5	20.0	22.5
Measured Concrete Strength, psi	2570-4225	5400	7200

8.4. However, the proportions of the mixes delivered varied from the design according to the moisture content of the aggregates. For the 3000 and 4000 psi batches, water was added in small amounts to obtain a slump of 5.0 to 6.0 in. For the 8000 psi batch, 55 oz. per cubic yard of superplasticizer admixture were added to achieve a slump of 7 in. The measured concrete compression strengths for all twenty-four specimens are shown in Table 8.2.

8.2.3 Construction of Specimens. Four formwork units were built so that four specimens could be cast from the same batch of concrete. The front and back forms of each unit were sandwiched between the two side forms using form ties designed to ensure that the form was rigid and reasonably water-tight. The front form had holes of slightly larger diameter than the diameter of the test bars. The front form was fabricated in two pieces (one below and one above the anchored beam bars) to facilitate placing the bars and stripping the forms. In Figure 8.10, a formwork unit is shown before placing the side form and the top front form. Since the two anchored bars extended 37 to 40 in. past the face of the column, a wood frame was connected to the formwork base to support the extended beam bars (see Figure 8.11).

Each specimen was cast in two lifts using a bucket operated by an overhead crane. Compaction was done using mechanical vibrators. Standard 6 x 12 cylinders were cast as concrete was placed in the form. After casting, the top surface of the specimen was screeded and trowelled smooth. Figure 8.11 shows the casting procedure.

8.2.4 Slip Instrumentation. Slip of the anchored reinforcing bar relative to the concrete was measured using a procedure developed by Minor[36] and used by Marques and Jirsa[35]. A 0.059-in. diameter piano wire was attached to the anchored bars at selected locations by making a short 90-degree bend at the end of the wire and inserting it into a 1/2-in. deep hole of equal diameter drilled in the anchored bar. The wire was oriented parallel to the bar axis in the expected direction of slip. For one of the two anchored bars, slip was measured at two points representing the loaded-end position and the beginning of the standard hook part of the anchored bar (points

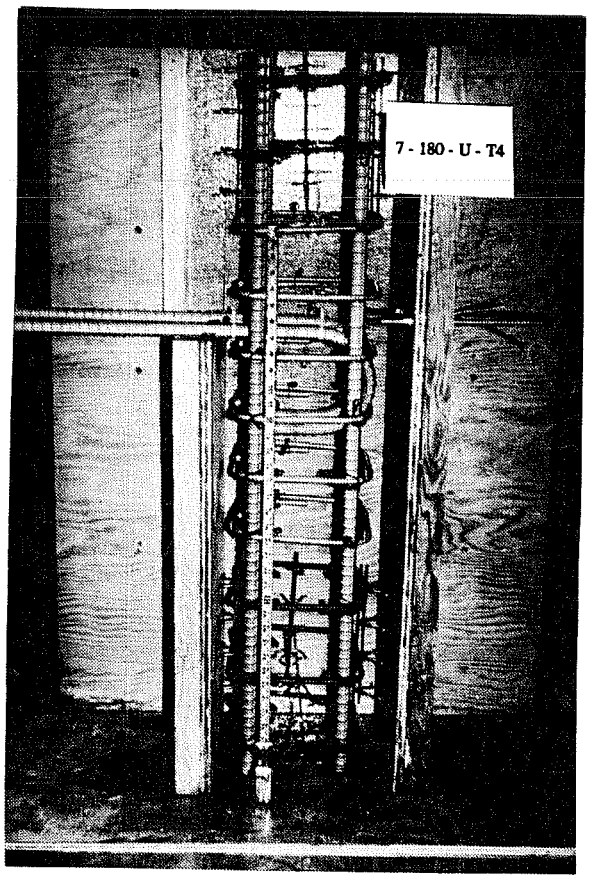

Figure 8.10 Formwork details of a hooked bar specimen.

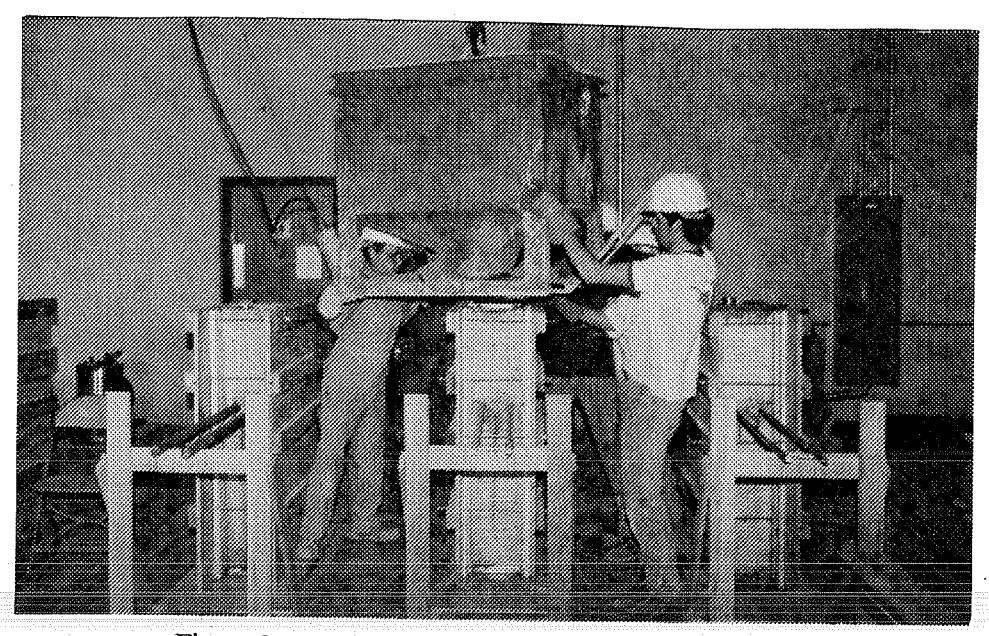

Figure 8.11 Casting of the hooked bar specimens.

A and B in Figure 8.9). For the second bar, slip was measured only at the loaded-end position.

After the wire was placed in the bar, a plastic tube was placed over the entire length of the wire to prevent bonding and to allow free movement of the piano wire. The plastic tube was sealed at the bar to prevent cement from entering the tube. The amount of sealer was small and the loss of bond surface area was kept to a minimum.

It was necessary to ensure that slip was measured relative to a stable reference point. The slip wires extended from the anchored bars to the back surface of the specimen behind the hook.

To reduce the wobble of the slip wire in the plastic tube, the wire was placed in tension using a spring between the concrete surface and a small brass plug fastened to the wire with a set-screw. Dial gages were used to measure the movement of wires connected to points A and B (Figure 8.9) of one bar, and a potentiometer hooked to an X-Y plotter was used to measure the movement of the wire connected to the loaded-end position of the other bar. The dial gages and the potentiometer rested against the brass plugs at the ends of the slip wires.

8.2.5 Test Frame. The method of loading simulated the reaction conditions at a joint in a frame structure. Schematic elevation and top views of the test frame are shown in Figures 8.12 and 8.13. A bending moment was applied at the face of the test specimen by a couple consisting of a tensile force in the test bars and a compressive force concentrated at a distance of 14 in. below the centerline of the bars. The compression force was applied by a 2-in. thick plate welded to the reaction column simulating a 6-in. deep compression zone of the assumed beam. To provide uniform compression on the face of the test specimen, a layer of hydrostone was placed between the face of the specimen and the compression plate. Tension was applied by means of two center-hole hydraulic rams, of the single-action spring-return type, operated by a hand pump. The rams used to test the #7 bars had a 30-ton capacity whereas the rams used to test the #11 bars had a 60-ton capacity. The forces were transferred to the bars by means of wedge grip assemblies similar to those used in the first phase of the test program (Figures 4.16 and 4.17). Because of limited

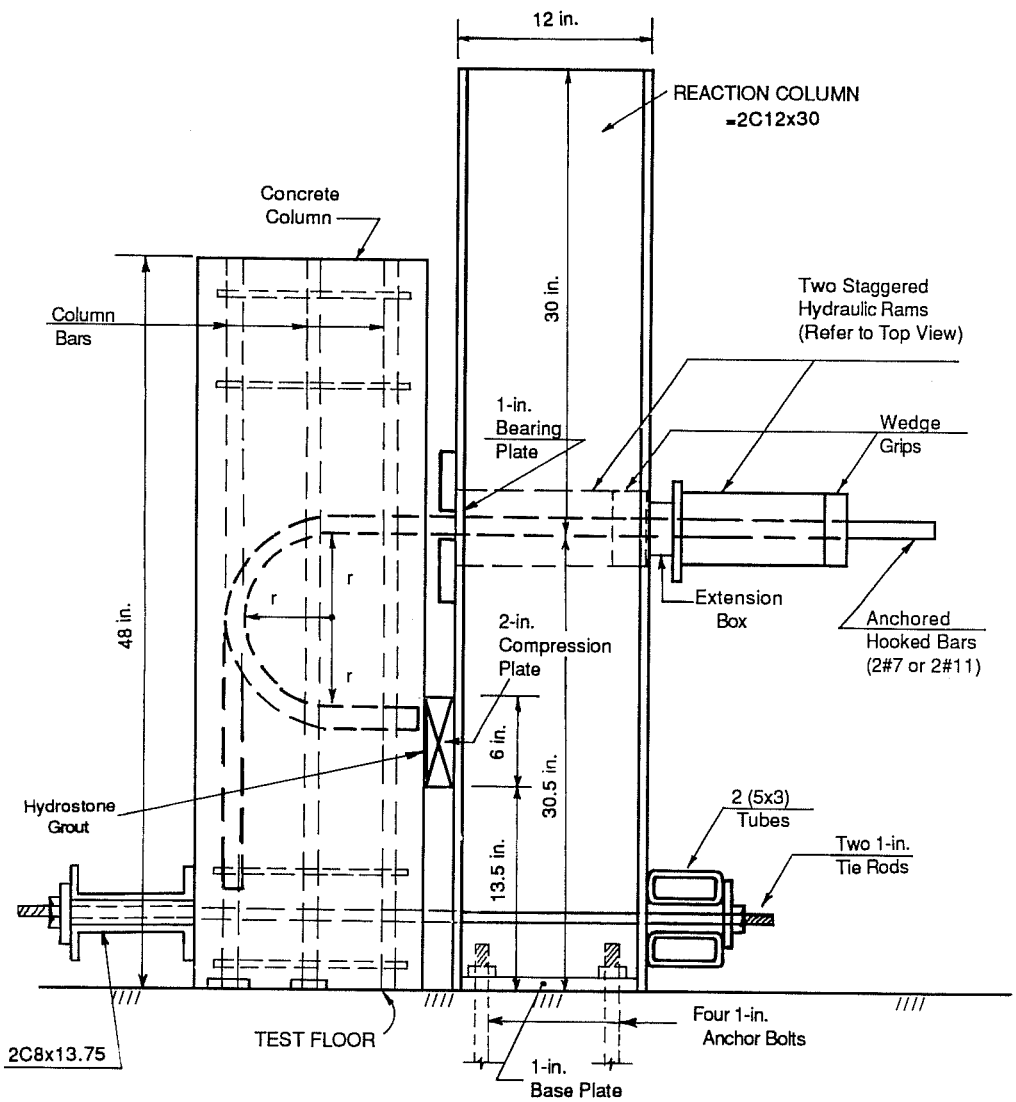

Figure 8.12 Schematic of the test setup of the hooked bar specimens, elevation view.

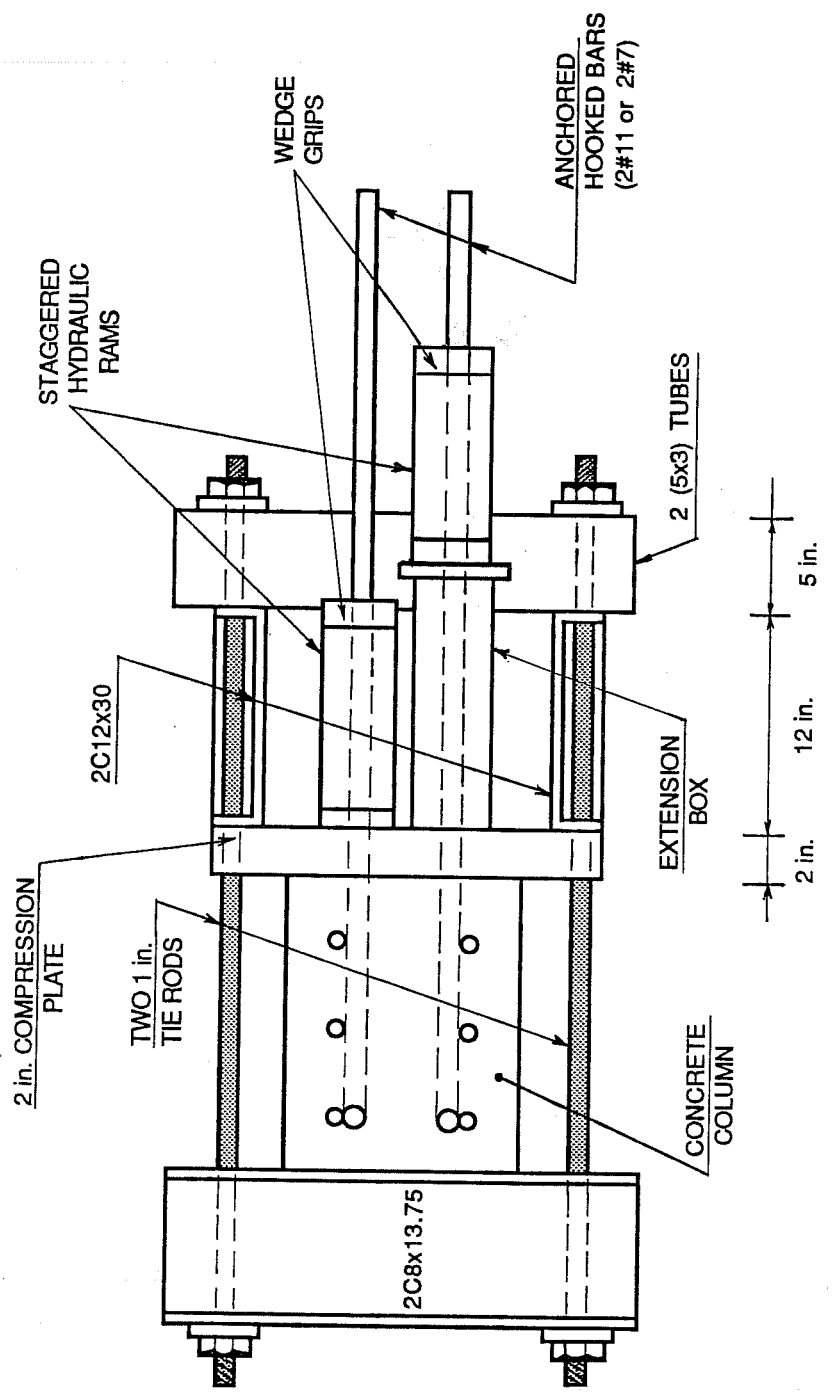

Figure 8.13 Schematic of the test setup of the hooked bar specimens, top view.

space between the two anchored bars, the hydraulic rams were staggered using an extension (4 x 4) structural tube as shown in Figure 8.13.

The reaction column consisted of 2 C12 x 30 structural shapes connected and stiffened by 1-in. thick plates. The steel column was welded to a 1-in. thick base plate and bolted down to the test floor by two 1-in. anchor bolts. To balance the moment imposed by the simulated beam, a horizontal reaction was provided through 1-in. threaded tie rods near the bottom of the reaction column (refer to Figure 8.12). In the first series, there was a tendency for the column specimen to rotate under moment action (and anchorage failure of the column bars) and bend towards the reaction column. Therefore, in the next five series, the column bars in the back face were welded to small anchor plates at the base of the column, and a plate was placed between the top of the test specimen and the reaction column to prevent excessive rotation of the specimen. Although the plate changed the reactions on the specimen, it did not appear to influence either the strength or mode of failure of the anchored bars. An overall view of the test setup is shown in Figure 8.14.

8.2.5 Test Procedure. The tensile load, applied by the hydraulic rams, was monitored by an electronic pressure transducer and was measured at the pump by a pressure gage. The tensile load was generally applied in 1.0- or 2.0-kip increments for the #7 bar specimens and in 2.0- or 4.0-kip increments for the #11 bar specimens until bond failure or bar yield occurred.

The pressure transducer measuring the load and the potentiometer measuring the loaded-end slip of one anchored bar, were hooked to an X-Y plotter. At each load stage, the maximum load was read, the potentiometer voltage and the two dial gages were read, and crack patterns were marked.

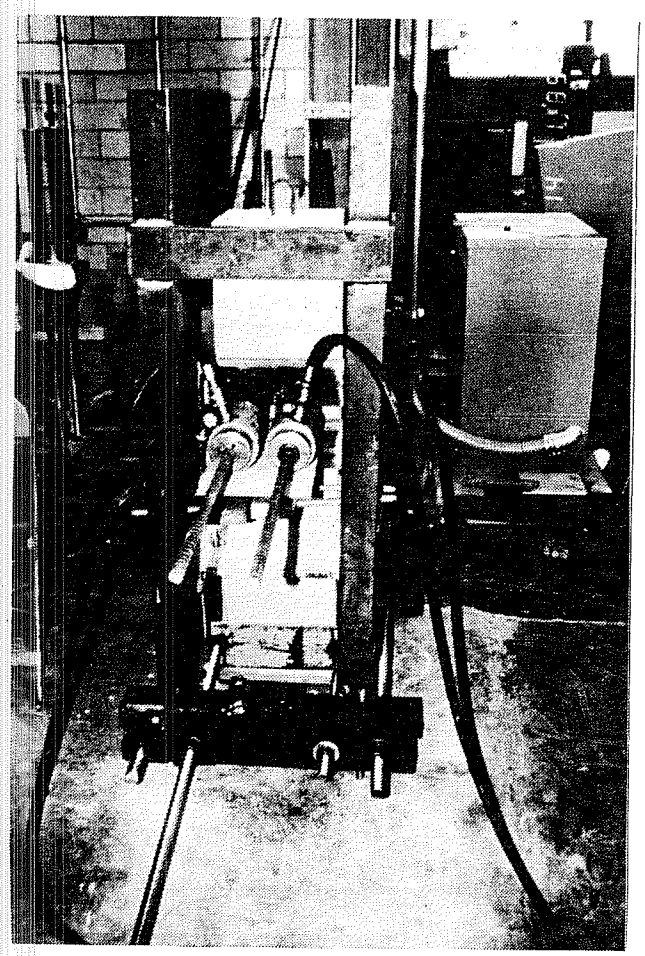

(a) Front view

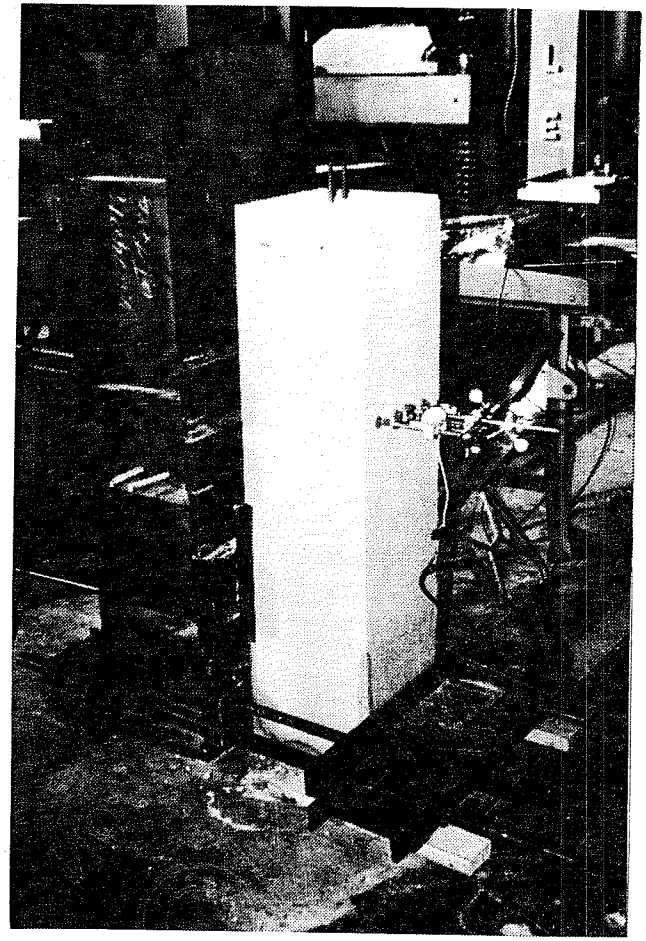

(b) Side view

Figure 8.14 Test frame used to test the hooked bar specimens.

8.3 Mode of Failure

In nearly all twenty-four tests, the cracking sequence and resulting failure followed similar patterns. It was difficult to check and mark the cracks on the front face of the column because the spacing between the specimen and the reaction column was only 2 in.

On the sides of the specimen, cracks first appeared in the vicinity of the assumed compression zone and spread downward and upward at about 45-degree angles. Cracks also appeared almost at the same time in the side concrete cover near the bent portion of the hooked bar. There was a tendency for these cracks along with the cracks radiating upward from the compression zone to propagate upward along the longitudinal column reinforcement near the back face of the specimen. Almost before failure, the cracks discussed above widened and increased in number indicating more concrete crushing in the side cover. Cracks could also be seen on the front face of the column spreading horizontally and vertically from the two anchored bars. The crack pattern on the side of specimen 11-90-U* is shown in Figure 8.15.

With the exception of the #7 bar specimens of the second series which yielded, failure was sudden and the load dropped immediately to a fraction of the maximum level. Slip increased rapidly until spalling of the side cover was observed.

After testing, the spalled side cover was removed from a few specimens to examine the cracking and crushing of the concrete in the vicinity of the hook. The following observations were made:

(1) In general, less effort was needed to remove the cover over the epoxy-coated hooked bars than the uncoated bars because of the lack of adhesion between the concrete and the epoxy coating.

(2) A large portion of the side cover was easily removed in specimens with a small cover (7-90-U-SC and 7-90-C-SC), and in normal strength concrete specimens with no ties in the joint region (see Figures 8.16 and 8.17).

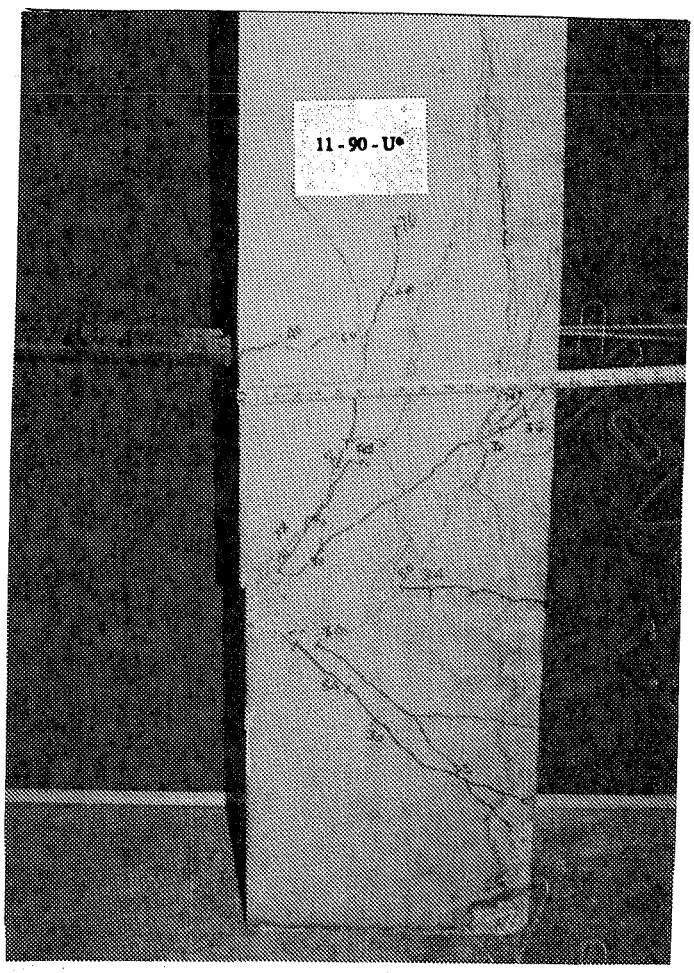

Figure 8.15 Crack pattern of the #11 hooked bar specimen 11-90-U*.

(3) The soundness of the concrete in the hook regions of specimens with ties in the joint or with high strength concrete, was evident when trying to remove the side covers. The presence of ties in the joint region was almost as effective in providing lateral restraint to side splitting as using high strength concrete. Figures

(a) Uncoated bar specimen

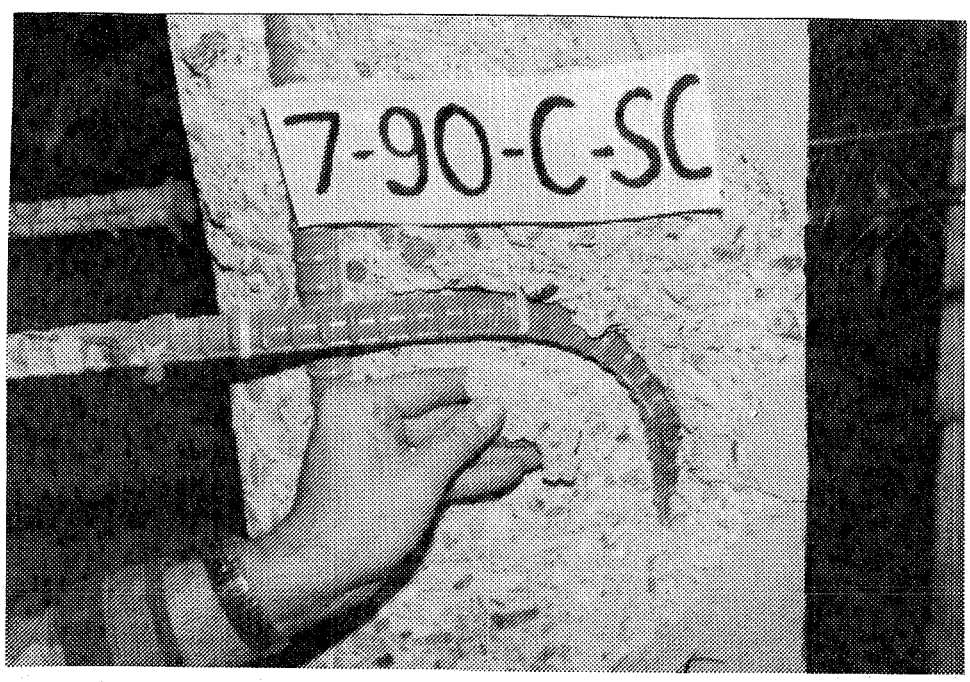

(b) Epoxy-coated bar specimen

Figure 8.16 Joint regions of the #7 hooked bar specimens of the fifth series after failure, small cover, f'_c = 4225 psi.

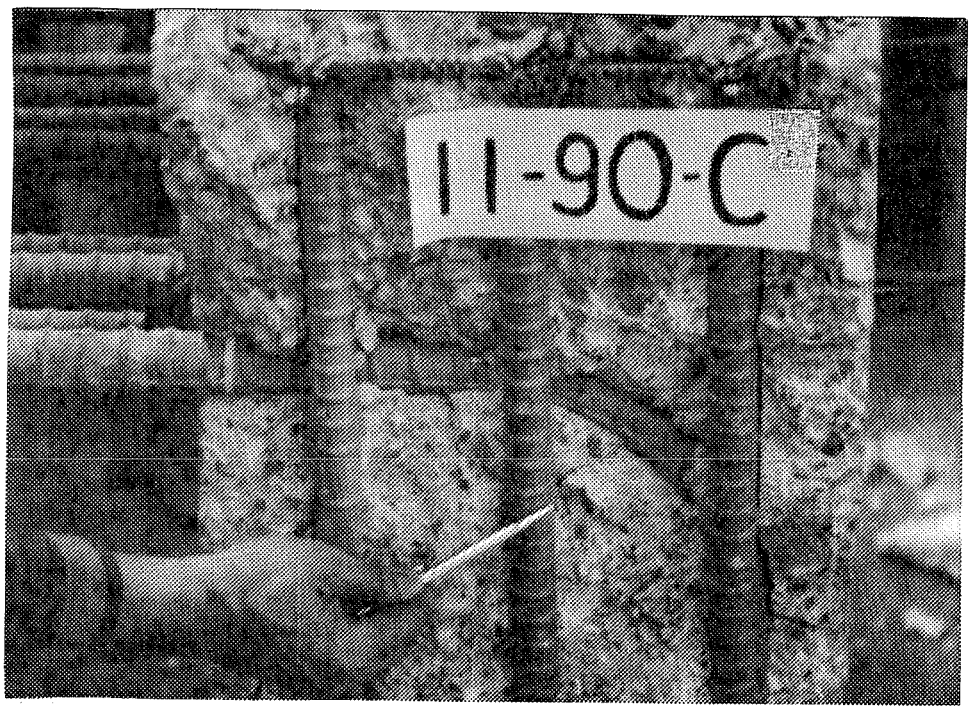

Figure 8.17 Joint region of the #11 epoxy-coated hooked bar specimen of the fourth series after failure, f'_c = 2570 psi.

8.18 and 8.19 show parts of the joint region of two specimens, one with ties in the joint region and one with high strength concrete. It was extremely difficult to remove any more of the concrete in the joint region without using power tools.

(4) As in the pullout and beam tests, after removing the concrete cover, concrete deposits were seen left on the sides of the deformations of the uncoated bars (see Figure 8.16a). However, epoxy-coated bars were clean and had no concrete residue left on the bar (see Figures 8.16(b) and 8.17).

(5) Close examination of the hook regions showed crushing of the concrete at the inside radius of the bend (see Figures 8.16 and 8.17). This behavior is consistent with the failures observed in the hook tests reported by Minor and Jirsa[36] and by Marques and Jirsa[35]. The bent portion of a hooked bar subjected to tension,

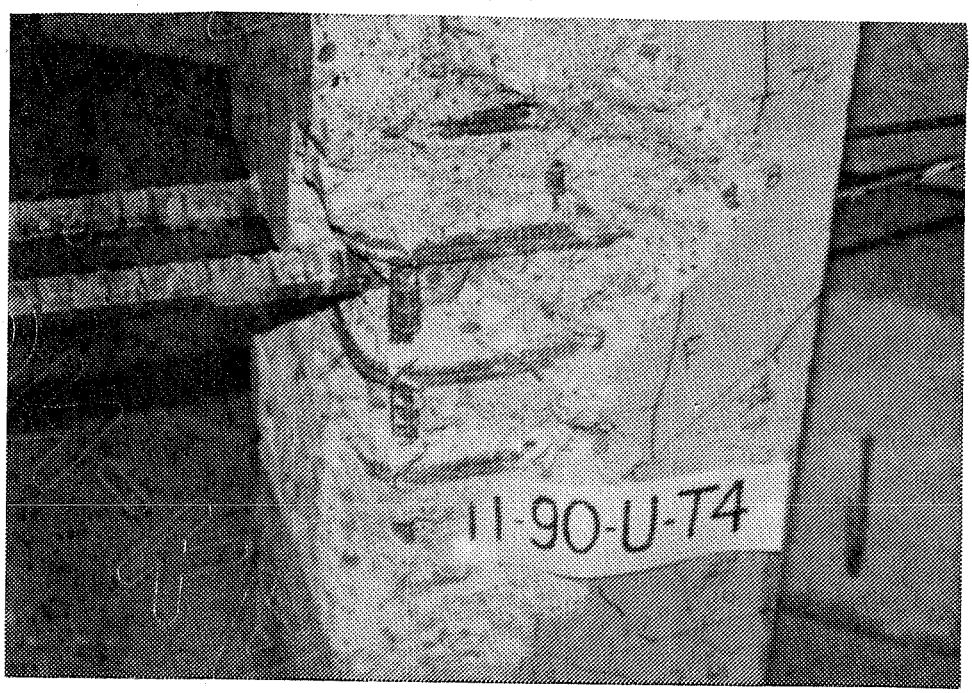

Figure 8.18 Joint region of the #11 uncoated hooked bar specimen of the fifth series, #3 at 4 in., f'_c = 4225 psi.

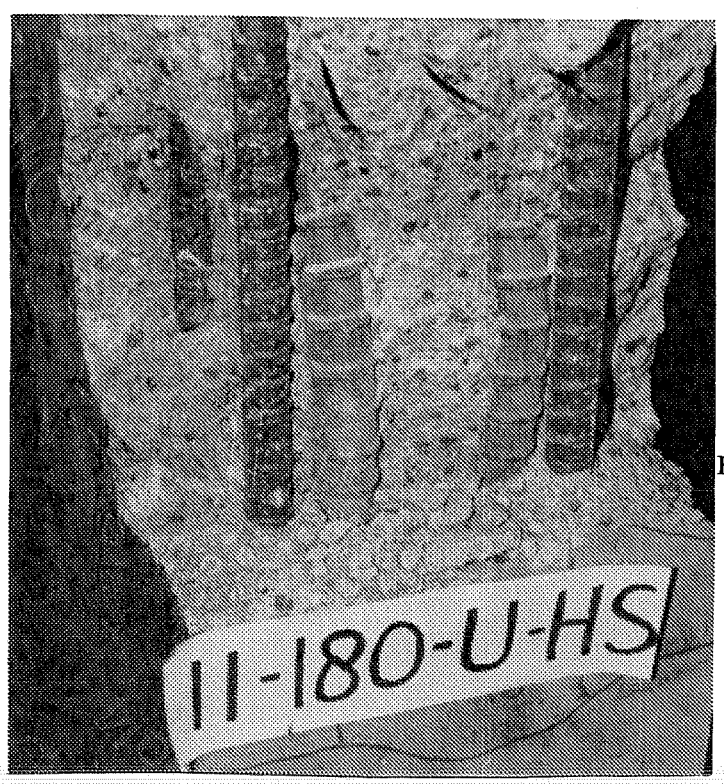

Figure 8.19 Joint region of the #11 uncoated hooked bar specimen of the sixth series, 180-degree bend, f'_c = 7200 psi.

tends to straighten, thus pulling the bar towards the center of the bend and reducing the arc distance between the horizontal and vertical bar segments of the anchorage. This produces intense lateral compressive stresses at the bend which in effect "punch out" the side cover at the bend and force the entire side cover to spall away[35].

(6) In all test specimens with 90-degree hooks, horizontal cracks appeared on the back face of the specimen near the tail of the hook at high levels of loading. With large slips and with the tendency of the bar to straighten under tension, the tail end of the hook would tend to kick out (or pry against the concrete), thus splitting the concrete cover behind the hook. However, these cracks were very small, implying that a cover of 2 in. over the tail extension as used in all test specimens should be sufficient for design purposes.

8.4 Test Results

The results of the twenty-four hooked bar specimens are presented and analyzed in terms of the effect of each variable on the ultimate capacity, load-slip behavior, and relative performance of uncoated and epoxy-coated hooked bars. Also, results of a few uncoated bar specimens will be compared with results of similar tests done by Marques and Jirsa[35].

The four specimens of each series, cast together, were tested within a few days of the 28-day curing period. Therefore, variation of concrete strength between different specimens of one series was negligible.

The maximum load of each specimen, the corresponding loaded-end slip (potentiometer reading), and the bond ratios (coated to uncoated), are listed in Table 8.5. The value of each maximum load is normalized for f'_c = 4000 psi by multiplying it by the ratio of the square root of 4000 to the square root of the specimen's concrete strength. The normalized capacities are listed

Table 8.5 Test results of the hooked bar tests.

Specimen Notation	f'_c (psi)	P_{max} (Kips)	f_{su} (Ksi)	Lead Slip (inch)	P_{max} Normalized @ f'c = 4000 psi (Kips)	Bond Ratio u(coated)/u(uncoated)
7-90-U*	5400	36.73	61.22	.033	31.61	-
7-90-C*	5400	28.32	47.20	.020	24.37	**0.77**
11-90-U*	5400	75.00	48.08	.012	64.55	-
11-90-C*	5400	66.30	42.50	.017	57.06	**0.88**
7-90-U-T4	3700	39.23	Y**	.075	-	-
7-90-C-T4	3700	36.00	Y**	.090	-	-
11-90-U-T6	3700	71.80	46.03	.120	74.65	-
11-90-C-T6	3700	68.40	43.85	.132	70.08	**0.94**
7-180-U-T4	3900	34.60	57.67	.060	35.04	-
7-180-C-T4	3900	30.20	50.33	.082	30.58	**0.87**
11-180-U-T6	3900	X++	-	-	-	-
11-180-C-T6	3900	66.30	42.50	.120	67.15	-
7-90-U	2570	26.00	43.33	.024	32.44	-
7-90-C	2570	21.00	35.00	.050	26.20	**0.81**
11-90-U	2570	48.00	30.77	.030	59.88	-
11-90-C	2570	40.60	26.03	.038	50.65	**0.85**
11-90-U-SC+	4225	29.96	49.93	.029	29.15	-
11-90-C-SC+	4225	23.11	38.52	.033	22.49	**0.77**
11-90-U-T4	4225	83.20	53.33	.110	80.95	-
11-90-C-T4	4225	66.30	42.50	.074	64.51	**0.80**
11-90-U-HS	7200	73.75	47.28	.040	-	-
11-90-C-HS	7200	55.74	35.73	.046	-	**0.76**
11-180-U-HS	7200	58.85	37.72	.027	-	-
11-180-C-HS	7200	54.11	34.69	.075	-	**0.92**

* Slip measurements of the four specimens of the first series were not reliable.

**Y = The bar yielded.

\+ The measured side concrete cover over the hooked bar was 1.75 in. In all other test specimens the measured side cover was approximately 3 in.

++X = The specimen could not be tested.

in Table 8.5. Load-slip curves of the four specimens of each series are shown in Figures C1-C6 in Appendix C. In general, the results show that epoxy-coated hooked bars developed lower anchorage capacities and larger slips at the same load levels than uncoated hooked bars. Bond ratios varied from 0.76 to 0.94 with an average of 0.84 and a standard deviation of 0.06.

In all tests, it was found that the loaded-end slips of the two anchored beam bars, one measured by a dial gage and the other measured by a potentiometer, were comparable. Also, the slip measured at the beginning of the bend was almost equal to the loaded-end slip of the same bar due to the short straight embedment length: 6.5 in. for the #7 bars and 6.0 in. for the #11 bars (see Figure 8.9). Therefore, it was decided to use only one slip value, the potentiometer reading, for evaluation of the test results.

In all four tests of series ONE, anchorage failure of the longitudinal column bars and the tendency of the specimen to rotate in the direction of the applied beam moment changed the slip of the anchored bars relative to the concrete column. In subsequent tests, the anchorage problem was solved by reducing the spacing of the #3 column ties below the beam column joint level and by welding the longitudinal bars to anchor plates at the bottom of the specimen. The rotation problem was solved by placing a 2-in. plate between the top of the specimen and the reaction column to prevent excessive column deformation. The load-slip curves of series ONE specimens in Appendix C can be compared with one another but not with load-slip curves of specimens of other series.

It is important to note that the #7 90-degree hooked bars of the second series, with ties at 4 in. in the joint region, yielded. The mode of failure in all other tests was splitting of the concrete in the joint region.

8.4.1 Effect of Bar Size. Test results listed in Table 8.5 show that for the range of variables investigated, bond ratios (coated to uncoated) varied from 0.77 to 0.87 for the #7 hooked bar specimens and from 0.76 to 0.94 for the #11 hooked bar specimens. As was found for straight

anchored bars in the first phase of the study, bar size had no effect on the bond performance of epoxy-coated hooked bars relative to uncoated bars.

Provided all other conditions are identical, the stiffness of the #11 bars, calculated from a steel stress-slip curve, was consistently smaller than that of the #7 bars. Number 11 bars slipped more than #7 bars at the same level of stress. This trend was also identified by Marques and Jirsa[35] in their uncoated hooked bar tests. Stress-slip curves of #7 and #11 uncoated and epoxy-coated hooked bars are shown in Figure 8.20.

8.4.2 Effect of Concrete Strength. The only difference between series ONE and series FOUR was concrete strength. As shown in Figure 8.21, the anchorage strength of a #7 or #11 hooked bar, uncoated or epoxy-coated, increased as the concrete strength increased. However, the reduction in anchorage strength of epoxy-coated hooked bars relative to uncoated bars was not greatly affected. Bond ratios (coated to uncoated) for #7 hooked bars varied from 0.81 at 2570 psi to 0.77 at 5400 psi. For the #11 hooked bars, the ratios were 0.85 and 0.88, respectively.

The stiffness of uncoated and epoxy-coated hooked bars, measured from a load-slip curve, increased as the concrete strength increased (see Figure 8.22). However, the load-slip behavior of epoxy-coated hooked bars relative to uncoated bars was not affected. The same trends were indicated for straight embedded bars in the first phase of the study.

8.4.3 Effect of Concrete Cover. The effect of side concrete cover over the hooked bars, in a direction normal to the plane of the hook, was assessed by designing the two #7 bar specimens of the fifth series with the column bars inside the anchored beam bars. This resulted in a nominal concrete cover of 1-7/8 in. In all other specimens the column bars were placed outside the beam bars and the nominal side concrete cover was 2-7/8 in.

In Figure 8.23, the capacities of #7 hooked bar specimens of the first and fifth series with measured side concrete covers of 3 in. and 1-3/4 in., respectively, are compared. In both cases

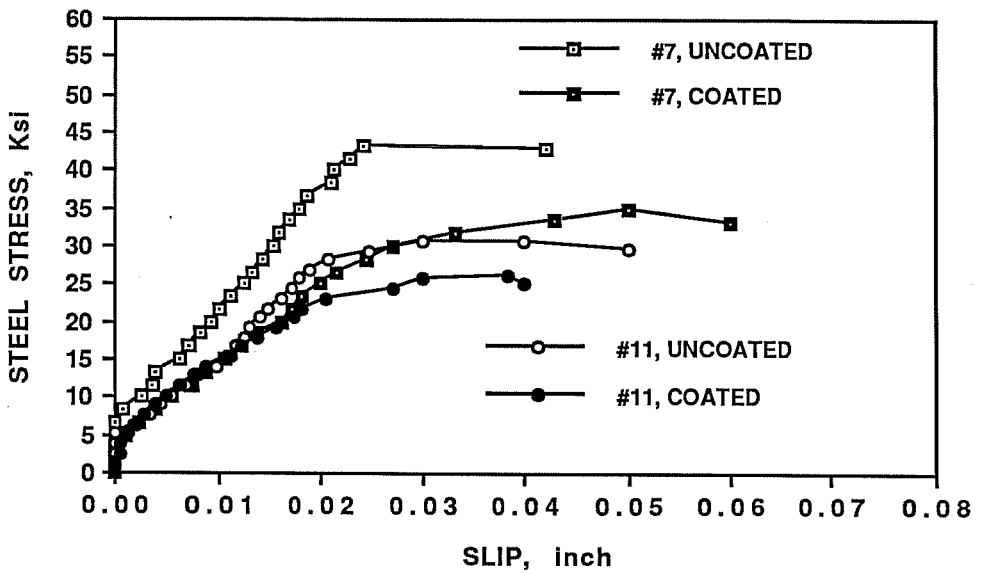

Figure 8.20 Effect of bar size on steel stress-slip behavior of uncoated and epoxy-coated 90-degree hooked bars, f'_c = 2570 psi.

there were no #3 ties in the joint region. The bar charts of Figure 8.23 show that the anchorage strength of a #7 hooked bar, uncoated or epoxy-coated, decreased about 8% as the cover decreased from 3 in to 1-3/4 in. The reduced concrete cover caused a reduction in the lateral confinement of the joint region and its restraint against splitting. It is important to note that the lateral restraint of the joint was not affected by the location of the column bars relative to the beam bars because the lateral stiffness of #8 longitudinal bars, unsupported by ties over a 30-in. height, is quite low.

However, the variation of the level of confinement, provided by concrete cover, did not affect the amount of reduction of anchorage strength of epoxy-coated bars relative to uncoated bars. Bond ratios (coated to uncoated) for both covers were the same, 0.77.

8.4.4 Effect of Joint Ties. Test results normalized at f'_c = 4000 psi and listed in Table 8.5, show that in general the presence of ties in the region of the beam-column joint increased the ultimate load at failure of uncoated and epoxy-coated #7 and #11 hooked bars. As shown in

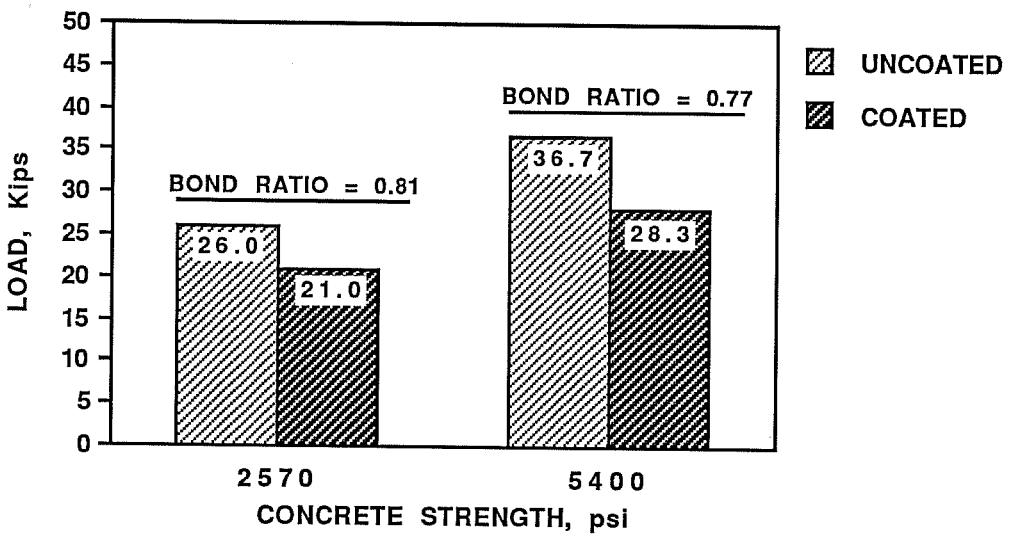

(a) Number 7 hooked bars

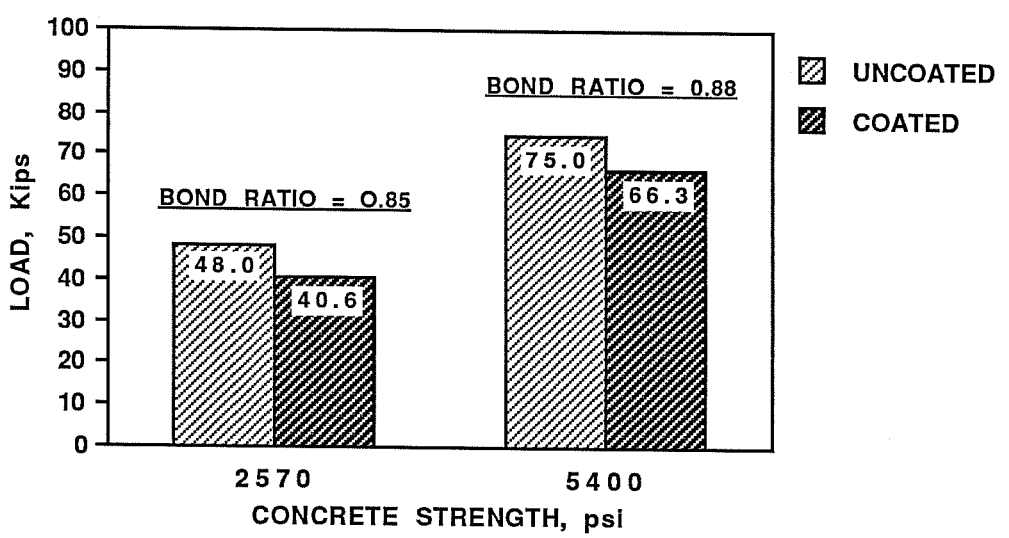

(b) Number 11 hooked bars

Figure 8.21 Effect of concrete strength on anchorage capacities of uncoated and epoxy-coated 90-degree hooked bars.

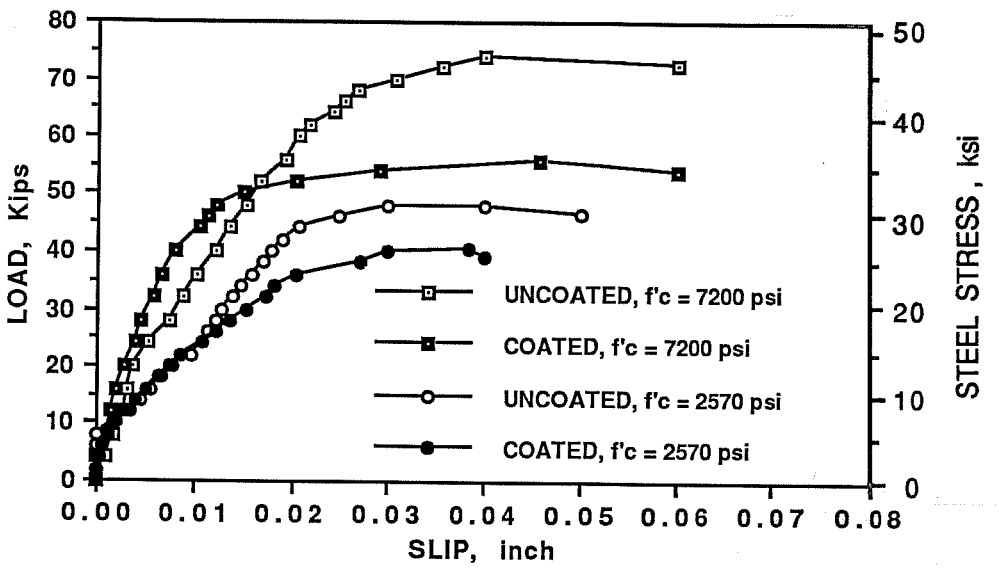

Figure 8.22 Effect of concrete strength on load-slip behavior of #11 uncoated and epoxy-coated 90-degree hooked bars.

Figure 8.24, the anchorage strength of #11 hooked bars increased as the spacing of the #3 ties in the joint region decreased, all other conditions (concrete strength, concrete cover, and hook geometry) identical. With the loads normalized at a concrete strength of 4000 psi, the anchorage capacity of #11 uncoated 90-degree hooked bars, relative to the case with no joint ties, increased approximately by 25% with #3 ties at 6 in. ($\cong 4d_b$) and 36% with #3 ties at 4 in. ($\cong 3d_b$) in the joint region. As for the #11 epoxy-coated hooked bars, the increases in anchorage capacity were approximately 38% and 27%, respectively.

The anchorage capacity of the #11 uncoated 90-degree hooked bars of series SIX with high strength concrete, improved by about 23% over the same reference case mentioned above. This implies that adding #3 ties at $4d_b$ in the joint region improved the anchorage capacity of an

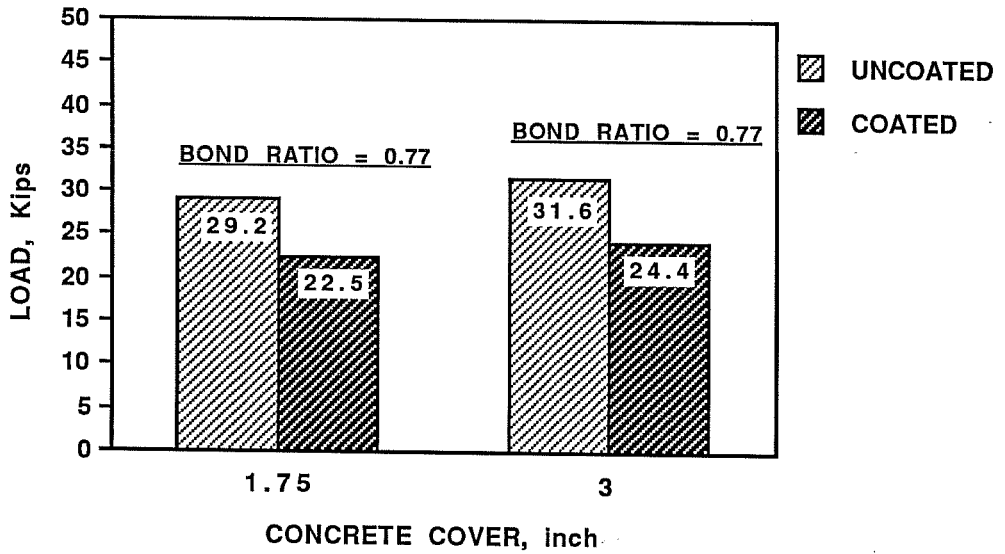

Figure 8.23 Effect of concrete cover on anchorage capacities of #7 uncoated and epoxy-coated 90-degree hooked bars, loads are normalized at f'_c = 4000 psi.

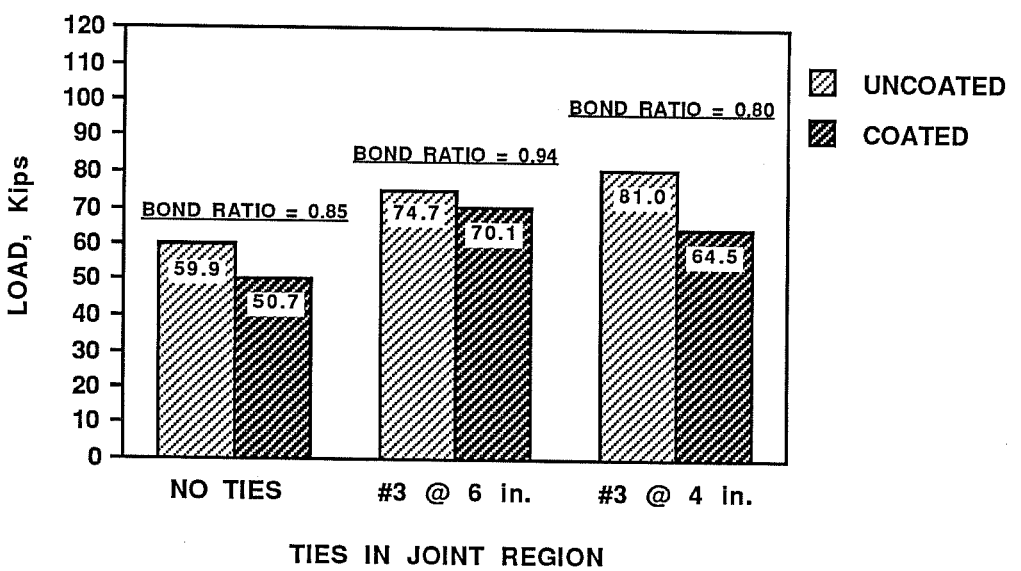

Figure 8.24 Effect of joint ties on anchorage capacities of #11 uncoated and epoxy-coated 90-degree hooked bars, loads are normalized at f'_c = 4000 psi.

uncoated hooked bar by approximately an equivalent percentage as increasing the concrete strength from 4000 to 7200 psi ($\sqrt{\frac{7200}{4000}} = 1.34$).

As for the #7 hooked bars, the inclusion of #3 ties at 4 in. in the joint region in the second series resulted in yielding of the bars. Because the capacity was not governed by anchorage, the increase in strength over other cases could not be identified.

Section 12.5.3.3 of the 1989 ACI Code (ACI 318-83)[1] modifies the basic development length of a hooked bar, #11 or smaller, by a factor of 0.8 if the hook is enclosed with ties at a spacing not greater than $3d_b$. This reflects an assumed increase in anchorage strength of 25% (1/0.8 = 1.25). The test results of the #11 hooked bars indicate a similar increase in strength with a tie spacing of about $4d_b$ in the joint region. Taking into consideration the small number of tests included in this study and the wide scatter of bond results, the ACI recommendation seems appropriate.

Test results listed in Table 8.5 show that the bond ratios (coated or uncoated) varied from 0.76 to 0.92 when no ties were present in the joint region and from 0.8 to 0.94 when ties were present. The scatter of the results with and without ties are comparable.

The presence of ties in the joint region improved the load-slip behavior of uncoated and epoxy-coated hooked bars. As shown in Figures 8.25 and 8.26, the presence of joint ties improved both the strength and deformation at failure of #7 and #11 hooked bars. The coating application had no negative effect on the deformation imposed prior to failure. Slips at failure of uncoated and coated bars were more than twice the slips when no ties were present in the joint region. It is interesting to note that although the increase in concrete strength improved the strength of hooked bars, the deformations reached at failure were not improved much (refer to Figure 8.22).

8.4.5 Effect of Hook Geometry. Designs of the second and third series were identical except for the bend angle: 90 degrees for series TWO and 180 degrees for series THREE.

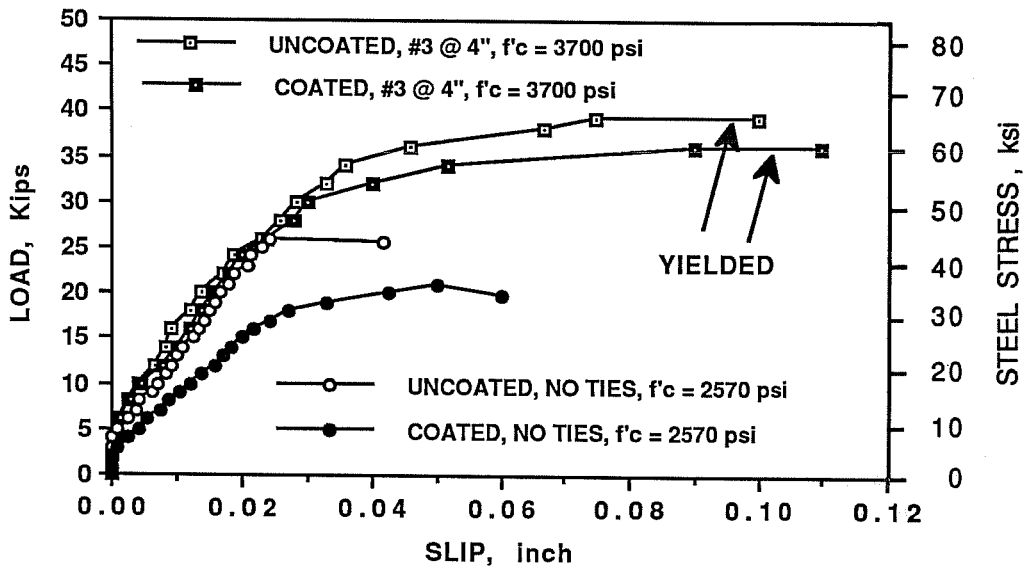

Figure 8.25 Effect of lateral reinforcement through the joint region on load-slip behavior of #7 uncoated and epoxy-coated 90-degree hooked bars.

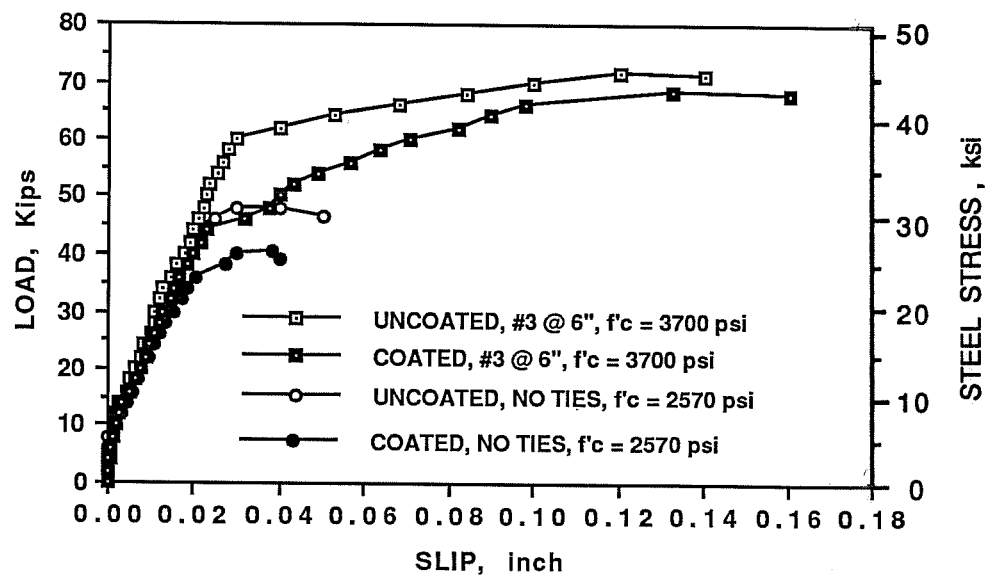

Figure 8.26 Effect of lateral reinforcement through the joint region on load-slip behavior of #11 uncoated and epoxy-coated 90-degree hooked bars.

Specimens of both series had #3 ties in the joint region spaced at 4 in. for the #7 bars and at 6 in. for the #11 bars.

The failure of the uncoated #11 180-degree hooked bar specimen of the third series due to instrumentation problems, did not allow comparison with the corresponding 90-degree bar specimen of the second series. On the other hand, test results listed in Table 8.5 show that the epoxy-coated #11 180-degree hooked bar specimen of the third series developed around 96% of the anchorage capacity of the corresponding 90-degree hooked bar of the second series. As for the #7 bars, both the uncoated and epoxy-coated 90-degree hooked bars of the second series yielded and their anchorage capacities could not be determined. However, the corresponding 180-degree hooked bars developed capacities lower than yield. Load-slip curves of the #7 hooked bars of the second and third series, shown in Figure 8.27, indicate that the hook geometry had no effect on the amount of deformation at failure.

Moreover, test results of the sixth series with high strength concrete show that #11 uncoated and epoxy-coated 180-degree hooked bars developed lower capacities than companion 90-degree hooked bars. The reduction was 20% for the uncoated bars and 8% for the coated bars.

Bond ratios (coated to uncoated), listed in Table 8.5, do not indicate a major influence of hook geometry on the relative capacities of uncoated and epoxy-coated bars. For 180-degree hooked bars, bond ratios were 0.87 and 0.92 for two different cases. These ratios fit within the scatter of bond ratios for the 90-degree hooked bars: 0.76 to 0.94.

Examination of the load-slip curves of the #7 bars of the second and third series with different bend angles, shown in Figure 8.27, and the load-slip curves of the #11 bars of the sixth series, shown in Figure 8.28, lead to the following remarks applicable to the two bar sizes:

(1) For either bend angle, 90 and 180 degrees, epoxy-coated bars developed lower capacities and slipped more than uncoated bars at the same level of load.

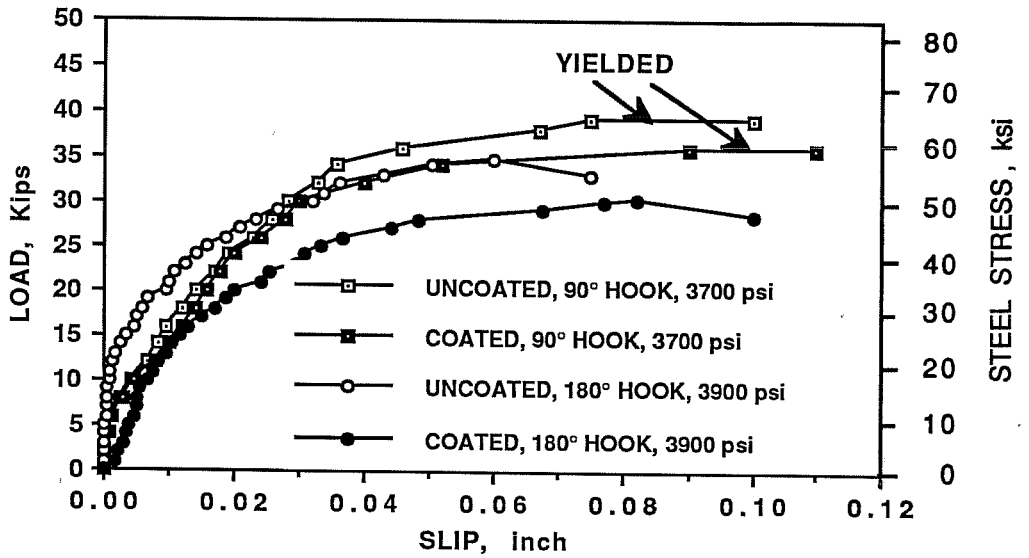

Figure 8.27 Effect of hook geometry on load-slip behavior of #7 uncoated and epoxy-coated hooked bars with #3 ties at 4 in. in the joint region.

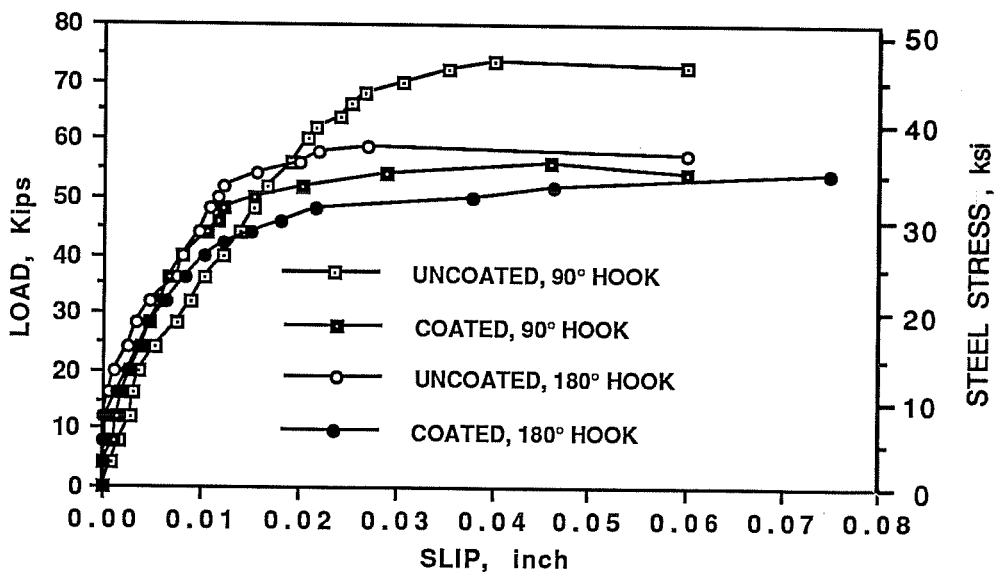

Figure 8.28 Effect of hook geometry on load-slip behavior of #11 uncoated and epoxy-coated hooked bars, f'_c = 7200 psi.

(2) For the uncoated bars, the 180-degree hooked bar was initially stiffer than the 90-degree hooked bar at lower levels of loading. However, at high level of loading prior to failure, slip of the 180-degree hooked bar out-paced the slip of the corresponding 90-degree hooked bar at the same stress.

(3) For the epoxy-coated bars, the 90-degree hooked bar was stiffer than the corresponding 180-degree hooked bar, with smaller slip at the same stress, throughout the load-slip history.

8.5 Comparison with Marques and Jirsa Test Results

In Table 8.6, results of some of the uncoated hooked bar tests are compared with results of similar tests done by Marques and Jirsa[35]. The only difference between the two sets of tests is the applied column axial load in Marques and Jirsa's tests. However, it should be noted that Marques and Jirsa concluded, based on stress and slip measurements for tests in which axial loads were varied, that the influence of column axial load on load-slip behavior was negligible.

The loads at failure for the different tests are normalized at f'_c = 4000 psi and listed in Table 8.6. The differences between the results of comparative tests are within 15%. Taking into consideration the scatter of bond data and the presence of applied axial loads in one set of tests, the differences are minimal.

In Figure 8.29, stress-slip curves of #11 90-degree hooked bars are compared. The difference in the curves is mostly due to the difference in concrete strength. On the other hand, with comparable values of concrete strength, the stress-slip curves of two #7 180-degree hooked bars, shown in Figure 8.30, indicate very good similarity of behavior.

The current ACI Building Code (ACI 318-89)[1] hooked bar specifications were based on Marques and Jirsa's tests. Therefore, the similarity of the hooked bar test results to Marques and

Table 8.6 Comparison of hooked bar test results with results of Marques and Jirsa [35].

Specimen Notation	Bar Size	Angle of Bend (degrees)	Ties in Joint Region	Column Size	Column Axial Load (Kips)	P_{max} Normalized @ f'c = 4000 psi (Kips)
7-90-U	#7	90	-	12x12	0	31.6
J7-90-12-1-H*	#7	90	-	12x12	420	36.5
7-180-U-T4	#7	180	#3 @ 4"	12x12	0	35.0
J7-180-12-1-H*	#7	180	-	12x12	425	35.1
11-90-U	#11	90	-	12x15	0	64.6
J11-90-15-1-L*	#11	90	-	12x15	154	74.7
J11-90-15-1-H*	#11	90	-	12x15	540	67.7
11-90-U-T6	#11	90	#3 @ 6"	12x15	0	74.7
J11-90-15-3-L*	#11	90	#3 @ 5"	12x15	150	87.8
11-90-U-T4	#11	90	#3 @ 4"	12x15	0	81.0
J11-90-15-3a-L*	#11	90	#3 @ 2.5"	12x15	175	96.3

* Marques and Jirsa tests.

NOTE : The nominal side concrete cover over the hooked bars in all tests included in this comparison was 2-7/8 in.

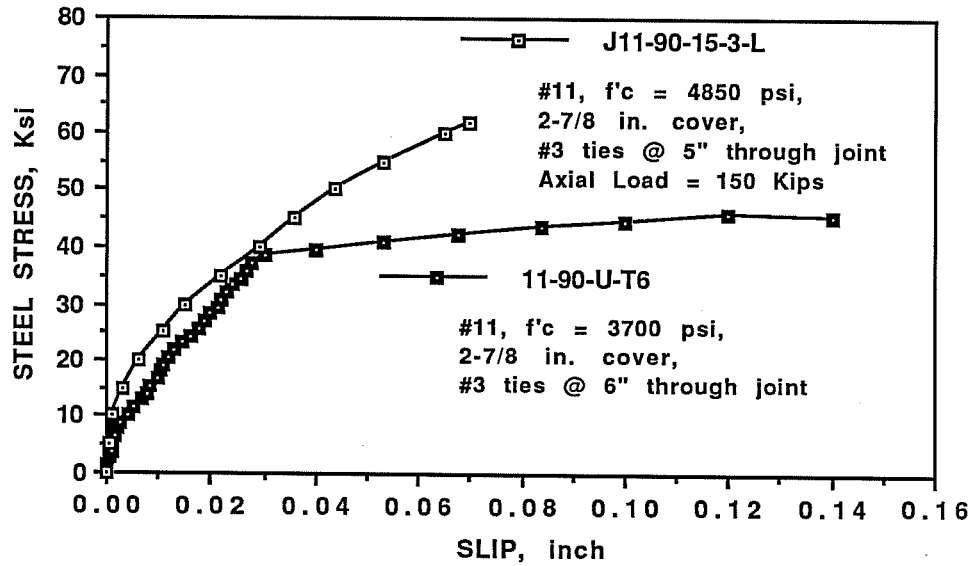

Figure 8.29 Comparison of the stress-slip curves of specimen 11-90-U-T6 and specimen J11-90-15-3-L from Marques and Jirsa tests[35].

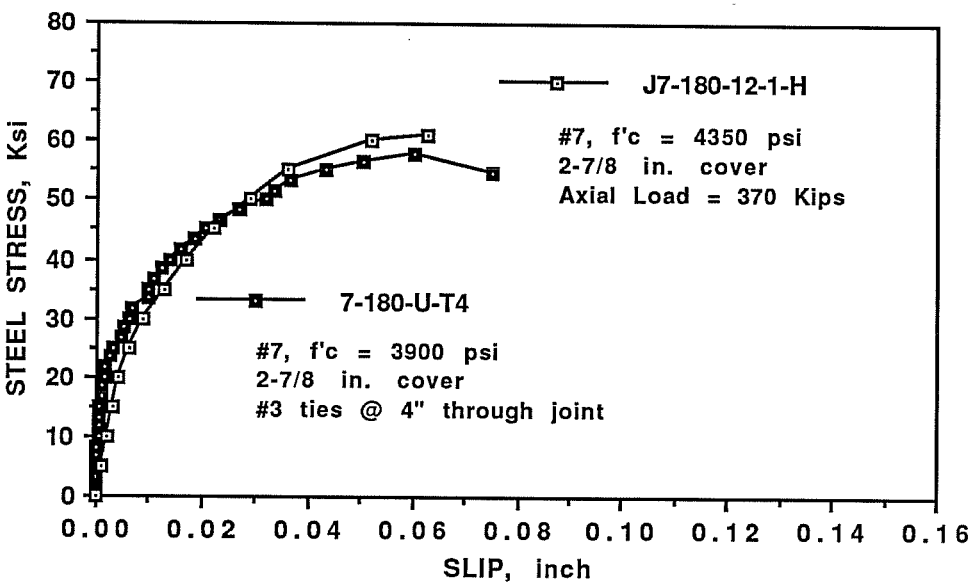

Figure 8.30 Comparison of the stress-slip curves of specimen 7-180-U-T4 and specimen J7-180-12-1-H from Marques and Jirsa tests[35].

Jirsa's results, can be used to validate the tests performed and the design recommendations that will be suggested.

8.6 Conclusions and Design Implications

Based on the mode of failure of the twenty-four hooked bar specimens, the anchorage capacities, and the load-slip characteristics, the following conclusions are drawn:

(1) Number 11 hooked bars consistently showed lower stress-slip stiffness than #7 hooked bars.

(2) Anchorage capacities and load-slip stiffnesses of #7 and #11 hooked bars, increased with increase in concrete strength. However, the load-slip behavior was not improved.

(3) The reduction of side concrete cover over the hooked bars caused a reduction in the anchorage strength of #7 hooked bars.

(4) The presence of #3 ties in the beam-column joint region improved both the anchorage capacity and the load-slip behavior with bars failing at greater loads and undergoing larger slips.

(5) Ninety-degree hooked bars developed slightly larger anchorage capacities than 180-degree hooked bars. Also, 90-degree hooked bars showed greater load-slip stiffness than 180-degree hooked bars at a high level of loading prior to failure.

(6) Epoxy-coated hooked bars consistently developed lower anchorage capacities and load-slip stiffnesses than companion uncoated hooked bars (see Figure 8.31).

(7) Relative anchorage strength and load-slip behavior of uncoated and epoxy-coated hooked bars were independent of bar size, concrete strength, side concrete cover, or hook geometry.

(8) The presence of #3 ties in the joint region did not improve the relative anchorage strength of uncoated and epoxy-coated hooked bars significantly. The average bond ratio for specimens with ties in the joint region was 0.87 with a standard deviation of 0.07. For all the tested hooked bar specimens the average bond ratio was 0.84 with a standard deviation of 0.06.

(9) Based on the test results, a 20% increase in the basic development length ℓ_{hb} of an uncoated hooked bar is recommended for epoxy-coated hooked bars (see Figure 8.31).

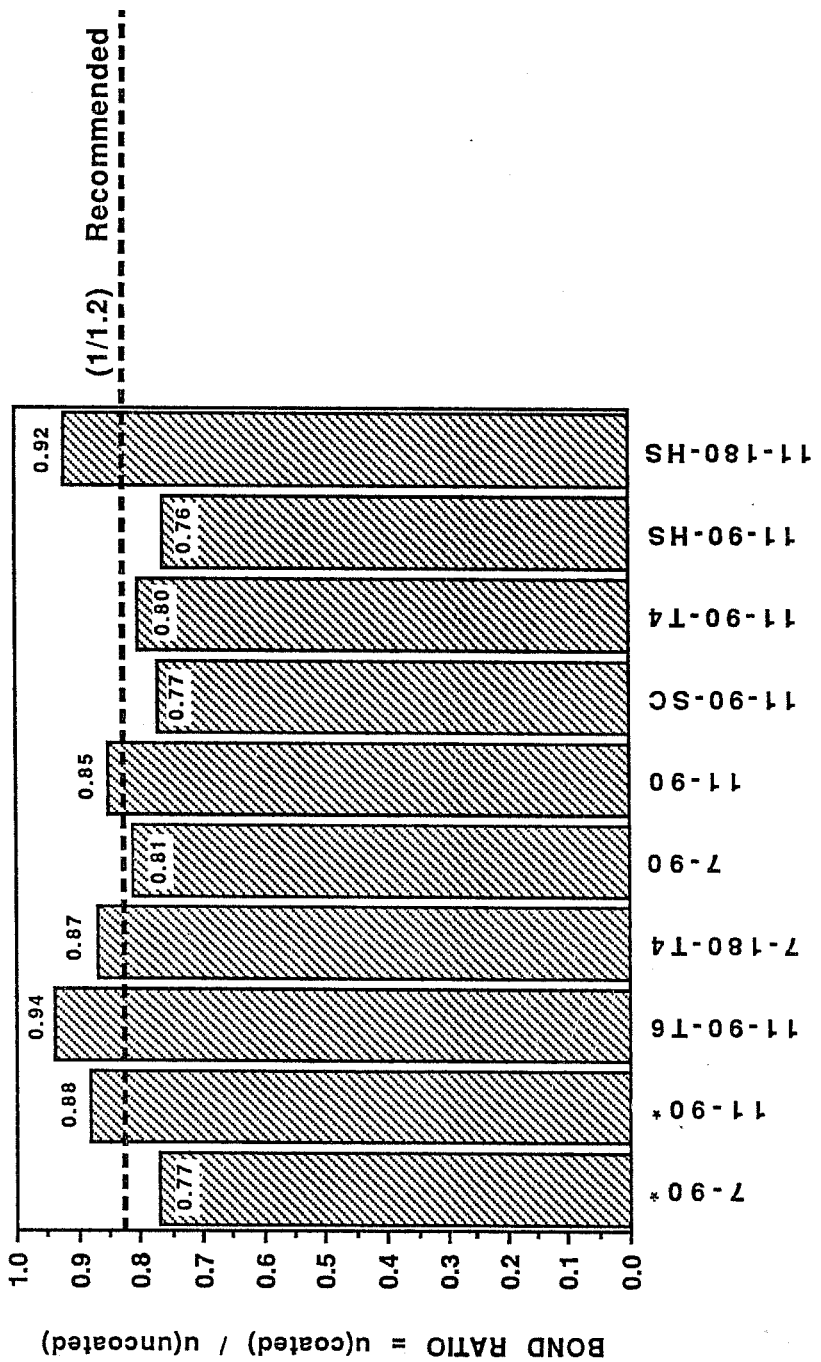

Figure 8.31 Variation of bond ratios (coated to uncoated) for the hooked bar specimens.

CHAPTER 9

SUMMARY AND CONCLUSIONS

9.1 Objective

Corrosion of reinforcing steel in concrete is the most common cause of premature deterioration of reinforced concrete structures. Of all the methods of corrosion protection possible, fusion-bonded epoxy coating often offers the best combination of protection, ease of use, and economy. Since 1973 the use of epoxy-coated reinforcing bars in the United States and Canada has spread to nearly all types of structures where concrete is exposed to a corrosive environment.

A very important consideration in the use of epoxy-coated reinforcing bars is the effect of epoxy coating on the strength of bond between reinforcing bars and concrete. The available test data, on which the current ACI Code epoxy-coated bar bond specifications are based, are limited. The objective of the research program was to provide a better and more complete understanding of the bond problem of epoxy-coated bars, and to develop or revise the existing recommendations for the design of straight and hooked epoxy-coated reinforcement.

The study was divided into three parts: fundamental bond studies, beam splice tests, and hooked bar tests.

9.2 Fundamental Bond Studies

Eighty pullout specimens of two types were tested to examine the influence of factors including bar size, coating thickness, bar deformation pattern, rib face angle, concrete strength and

level of confinement, on the relative bond characteristics of normal mill scale uncoated and epoxy-coated reinforcing bars. In sixty-six specimens only the bottom surface of the bar was embedded and a vertical confining load was directly applied to the exposed upper surface. In fourteen other specimens the bar was fully embedded in the concrete.

The following conclusions were made:

(1) Bond strength of an uncoated or an epoxy-coated bar increased with increase in concrete strength, rib face angle, and level of confinement. Epoxy-coated bars consistently developed lower bond strength than companion uncoated bars. The reduction in bond strength ranged from about 10% to about 25%.

(2) Relative bond strength of uncoated and epoxy-coated bars was not affected by the level of the different variables investigated.

(3) Bars with crescent deformation pattern slipped more than bars with parallel or diamond deformation pattern at a given load level regardless of bar size, concrete strength, or level of confinement.

Future research is needed to investigate the effect of the various mechanical properties of a reinforcing bar including deformation pattern, rib face angle, and height and spacing of deformations, on the bond characteristics of the bar.

9.3 Beam Splice Tests

Twelve beams, with multiple splices in a constant moment region at the center of the beam, were tested in negative bending to assess the effectiveness of epoxy-coated transverse reinforcement

crossing the splitting plane in the splice region. The variables were bar size, bar spacing and amount of transverse reinforcement in the splice region. All bars were cast in a top position with more than 12 in. of concrete below the bars. The mode of failure in all test specimens was splitting of the concrete cover in the splice region.

The measured bond stresses of the splices in the current study, along with the results of all previous splice tests with and without stirrups in the splice region, were compared with the empirical equation developed by Orangun, Jirsa and Breen[20], and with the 1989 ACI Building Code (ACI 318-89)[1] bond provisions. Based on the analysis of the test results and the evaluation of the ACI Code bond provisions, the following conclusions were made:

(1) The bond strength of epoxy-coated #11 bar splices relative to uncoated bar splices improved from 74%, in the absence of transverse reinforcement crossing the splitting plane in the splice region, to around 80 to 85% when the transverse reinforcement was provided. The improvement was independent of the number of splices or bar spacing. For #6 bar splices the improvement was from 67% to 74%.

(2) The empirical equation (7.1) developed by Orangun, Jirsa, and Breen[20] provides the best available approach to estimate the bond strength of reinforcing bars.

(3) The ACI Building Code (ACI 318-89)[1] bond specifications for uncoated and epoxy-coated bars are overly conservative when compared to the results of all available splice tests with and without ties in the splice region. Modifications of

the ACI bond specifications were recommended to better estimate the bond strength of bottom cast and top cast uncoated and epoxy-coated reinforcing bars. One recommendation suggested raising the upper limit of 100 psi set on the value of $\sqrt{f'_c}$ in Section 12.1.2 to a value of 130 to 140. Another recommendation suggested modifying Section 12.2.3.1(b) to change the lower limit set on the cover from the requirements of Section 7.7.1 to one bar diameter. A third recommendation suggested changing the disjunction: "or" between the cover and clear spacing requirements in Section 12.2.3.2 to a conjunction: "and". A fourth recommendation suggested modifying Section 12.2.4.3 specifying the use of a 1.2 factor for epoxy-coated bars enclosed with transverse reinforcement A_{tr}, along the development length satisfying $A_{tr} \geq \frac{d_b s N}{120}$, regardless of the amount of cover or clear spacing between bars. For epoxy-coated top reinforcement, the recommendation suggested using the larger of the factor for top reinforcement and the factor for epoxy-coated reinforcement. A final recommendation suggested imposing a 2.0 upper limit on the product of the splice class factor and the factors for bar spacing, amount of cover, enclosing transverse reinforcement, top reinforcement, and epoxy-coated reinforcement.

9.4 Hooked Bar Tests

Twenty-four specimens simulating beam-column joints in a structure were tested to assess the effect of several variables on the relative bond characteristics of uncoated and epoxy-coated

bars. Variables included bar size, concrete strength, concrete cover, hook geometry, and amount of transverse reinforcement (column ties) in the beam-column joint. The test specimens were designed to simulate the anchorage of two hooked bars in a reinforced concrete column.

The following conclusions were made:

(1) Anchorage capacities and load-slip stiffnesses of #7 and #11 hooked bars increased with increase in concrete strength. However, the load slip behavior was not improved. Epoxy-coated hooked bars consistently developed lower anchorage capacities and greater slips than companion uncoated bars.

(2) Relative anchorage capacity and load-slip behavior of uncoated and epoxy-coated hooked bars were independent of bar size, concrete strength, side concrete cover, or hook geometry.

(3) The reduction of side concrete cover to the hooked bar caused a reduction in the anchorage strength.

(4) The presence of #3 ties in the beam-column joint improved both the anchorage capacity and the load-slip behavior with bars failing at greater loads and undergoing larger slips.

(5) Ninety-degree hooked bars developed slightly larger loads than 180-degree hooked bars. Also, 90-degree hooked bars showed less slip than 180-degree hooked bars at high levels of loading prior to failure.

Based on the test results, a 20% increase in the basic development length of an uncoated hooked bar was recommended for epoxy-coated hooked bars.

9.5 Further Research

The results and design recommendations of this study provide a better and more complete understanding of the bond and anchorage characteristics of epoxy-coated straight and hooked reinforcement.

The extensive use of epoxy-coated bars in nearly all types of structures where concrete is exposed to a corrosive environment raises the question whether the design equations are applicable to the use of epoxy-coated reinforcement in lightweight concrete structures or in moment resisting frames in seismic zones. Future research is needed to investigate the effects of lightweight aggregate concrete and cyclic loading on the bond and anchorage capacities of epoxy-coated bar splices and hooked reinforcement.